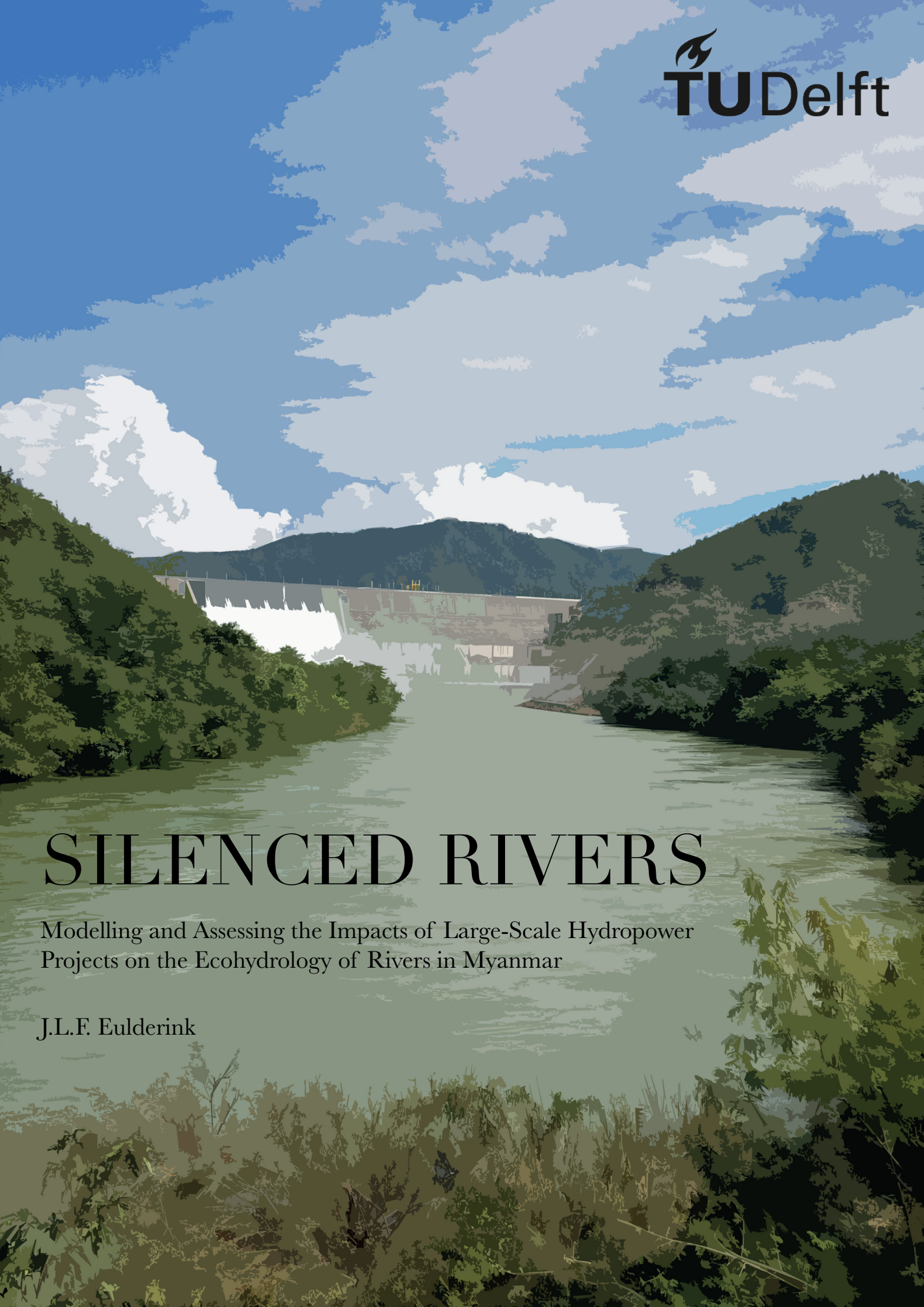

SILENCED RIVERS

Modelling and Assessing the Impacts of Large-Scale Hydropower Projects on the Ecohydrology of Rivers in Myanmar

J.L.F. Eulderink

The cover of this report shows an edited photo of the Yeywa dam on the Myitnge river in Myanmar. I visited the hydropower plant during October of 2018, where I took this picture from a bridge.

Silenced rivers

Modelling and assessing the impacts of large-scale hydropower projects on the ecohydrology of the Myitnge and Myittha rivers in Myanmar

by

J.L.F. Eulderink

to obtain the degree of Master of Science
at the Delft University of Technology,
to be defended publicly on Tuesday April 2, 2019 at 15:30 PM.

Student number:	4206711	
Project duration:	August 1, 2018 - April 2, 2019	
Thesis committee:	Dr. T. Bogaard,	TU Delft, supervisor
	Dr. Ir. H. Winsemius,	TU Delft, Deltares
	Dr. Ir. K. Sloff,	TU Delft, Deltares

An electronic version of this thesis is available at `http://repository.tudelft.nl/`.

TU Delft

Abstract

Hydrological modifications to the natural flow regime through the regulation of a river threaten the integrity of river ecosystems. In Myanmar, the exponentially growing hydropower sector poses a threat to the ecohydrology of some of the last large free-flowing rivers in the world. This study investigates to what extent the natural flow regime of the Myitnge in Myanmar has been hydrologically altered by the Yeywa dam, which is currently the largest hydropower dam in Myanmar. The study furthermore examines which ecological processes have been or could potentially be most affected by these hydrological modifications. This is done by modelling the natural flow regime of the dammed Myitnge river in Myanmar using the distributed hydrological rainfall-runoff Wflow_sbm model, which consists of a set of python programs to perform hydrological simulations. The suitability of this model as a tool for environmental flow management in Myanmar is simultaneously investigated. The model uses PCRaster, which in turn makes use of a dynamic modelling language within a GIS framework. It was forced using static and dynamic data which is mostly globally available from different satellites, and derivatives of this, and calibrated and validated on data collected during field visits in 2018 as well as some secondary data sources. The field data collection focused on river bathymetry and soil properties such as infiltration capacity. Furthermore, scenarios were developed and simulated that varied in dam operational capacity (29% and 80%), reservoir management (for flood mitigation), and irrigation demand. Using modelled discharge results, multiple environmental flow assessments were carried out, comparing pre- and post-dam scenarios. The results demonstrated that different elements of the flow regime can be altered slightly depending on the Yeywa operational scenario. For the irrigation scenario, the high water uptake to meet the crop demand alters the magnitudes and duration to the largest extent of all the scenarios. According to the results, the dam alone does not alter most of the components of the natural flow regime (and hence presumably the associated ecological factors) to a very large extent, regardless of the capacity it is operated at. This is because the attainable operational capacity is limited by inflow: raising the capacity at which the dam is operated can only be done for a limited amount of time due to the extreme seasonality. For the current operation and in the simulated scenarios, habitat availability for different species of plants and animals, as well as the river's ability to structure the channel morphology are the elements most at risk due to the Yeywa dam. This is mostly because the occurrence of large floods has significantly reduced or completely disappeared from the flow regime, as also demonstrated by a habitat inundation analysis for the Myitnge. There is potential for the optimisation of the operation of the Yeywa reservoir, but it remains limited to the availability of inflows, which in turn is dependent on the natural seasonality and the size of the reservoir. Therefore, one of the main recommendations is to avoid keeping the outflow below the natural inflow in the dry season, and to run the turbines at maximum capacity during the monsoon period. This is advised in order to protect the downstream channel area from dewatering in the dry season, and to maximize the electricity generation during the wet season, while simultaneously keeping the released discharge very close to the natural flow regime.

What I love most about rivers is
You can't step in the same river twice
The water's always changing, always flowing

But people, I guess, can't live like that
We all must pay a price
To be safe, we lose our chance of ever knowing
What's around the river bend
Waiting just around the river bend

- Pocahontas

Acknowledgements

Some chickens stumble into a pot of rice
- Myanmar proverb

Before you lies the finished product of my master thesis project. It has been quite the journey, literally. I had the pleasure of travelling to Myanmar from October until the beginning of December of 2018. This period of research and travel taught me so much about who I am and what I want to become. Besides the exquisite landscapes and wonderful food, I was inspired by the attentive, knowledgeable and compassionate people of Myanmar. The unique experience of travelling along the Myittha and Myitnge rivers and taking measurements from tiny fisherman's boats, was one I will never forget. I started this preface with a Myanmar proverb which I was taught upon my arrival in Myanmar. It means that some people find happiness and success by pure chance, and it reminds me of the way I stumbled into this project, which ended up being a great pot of rice.

There are many people to whom I am very grateful. Firstly, I would like to acknowledge the insights and advice provided by my daily supervisor. Thank you, Thom, for believing in this project, and believing in me. Without your constant enthusiasm and inspiration, I would not have gotten this far. Thank you to Hessel Winsemius and Kees Sloff for your insightful comments and encouragement. My trip and fieldwork was partially made possible by the Partners for Water and Niche projects, to whom I owe many thanks. I also want to acknowledge the support from several people at Deltares that helped me with the modelling. I am grateful to the loving and open community in Myanmar, with whom I shared some of my most beautiful memories of my educative life. A special thanks to May Ei, Su Su, Esther, Afia, Van Van and the students from KTU who helped me in the field.

I have had the privilege of belonging to a family which stimulates personal development and adventure, and that has been willing and able to support my endeavours over the past years. Therefore, I am deeply grateful for the different efforts made by my mother, father, and my sisters Sophie, Leonie and Nicole. A special mention goes to my father, who kept me sharp throughout this thesis period and asked the questions that I needed to answer, and to my mother, who never stopped admiring me, and made sure I stayed sane throughout. During my studies, I have also been surrounded by exceptionally talented, inspiring and fun friends, to whom I owe thanks. A special thanks to Charley, for your creative input, and to Swaen, Viet, Tych and Markus for moral support and an invaluable friendship throughout my master. And last but not least, a very special gratitude goes out to Friso, who never once complained while I could do nothing but, and who always pushes me to believe in myself.

It has been an amazing adventure, and I hope that this report sparks the reader's enthusiasm and interest on the subject of environmental flows, as well as the beautiful nation that is Myanmar.

J.L.F. Eulderink
Delft, March 2019

Contents

List of Figures

List of Tables

1 Introduction

River flow regimes are considered to be the primary force driving river ecosystems (Poff et al., 1997). Human-induced structures can pose a threat to ecosystems by altering these flow regimes. Water infrastructure such as hydropower dams have led to deteriorating riverine and wetland ecosystem conditions as well as loss of freshwater biodiversity across the globe (Forslund et al., 2009; Arthington et al., 2018). These threats have inspired the field of environmental flows. The Brisbane Declaration and Global Action Agenda on Environmental Flows 2018 defined environmental flows as *"the quantity, timing, and quality of freshwater flows and levels necessary to sustain aquatic ecosystems which, in turn, support human cultures, economies, sustainable livelihoods, and well-being"* (Arthington et al., 2018). Worldwide, 48% of the volume of rivers is moderately to severely impacted by flow regulation, fragmentation, or both. If all the dams that are planned and under construction are completed, this proportion will almost double (Grill et al., 2015). Therefore, The Brisbane Declaration presented an urgent call for action to protect and restore environmental flows across the globe (Arthington et al., 2018).

1.1. Research motivation

Sufficient quality and quantity of water largely determine a country's economic and human well-being, particularly in countries that are agriculture-dominated. Myanmar is such a nation as 65% of the population live in rural areas and work in the agricultural sector (Taft and Evers, 2016). The country as a whole is transforming on several fronts, with pressures emerging from internal reforms, economic liberalization and global trends, such as climate change. Besides the rising sea level and increasing temperatures, the climate change impacts in Myanmar are expected to include an increase in the magnitude and frequency of drought. Furthermore, rainfall variability including erratic and record-breaking intense rainfall events are expected, which is likely to increase floodings and storm surges (Myanmar Climate Change Alliance, 2012).

There is an increasing demand-supply electricity gap in Myanmar due to the expanding economy, which is one of the fastest growing in all of Asia (Asian Development Bank, 2018). To address the supply-demand gap caused by this, as well as aiming to make money through export of electricity, the Ministry of Electricity and Energy has turned to the exploitation of the hydropower potential of Myanmar's free flowing rivers. In 1960, the first large hydropower plant was completed in Myanmar, as part of the 168 megawatts (MW) Baluchaung II project. Development of large hydropower power continued over the following decades, accelerating after the year 2000, as shown in Figure 1.1. As of 2017, 29 hydropower plants have been completed with capacities ranging from 10 to 790 MW, totalling 3298 MW (IFC, 2017; IHA, 2015). This represents only a small fraction of the country's 100 GW of untapped hydropower potential, however (IHA, 2015).

The government of Myanmar finalized the National Electrification Plan in June of 2014. This plan aims to provide electricity to the entire nation by 2030, and therefore lays particular emphasis on the unexplored hydropower potential as a long-term energy solution. More specifically, the plan aims to triple the current installed hydropower capacity by 2030. This means that at least 50 large (greater than 30 MW) hydropower plants with a combined capacity of almost 6 GW are scheduled for development (IHA, 2015).

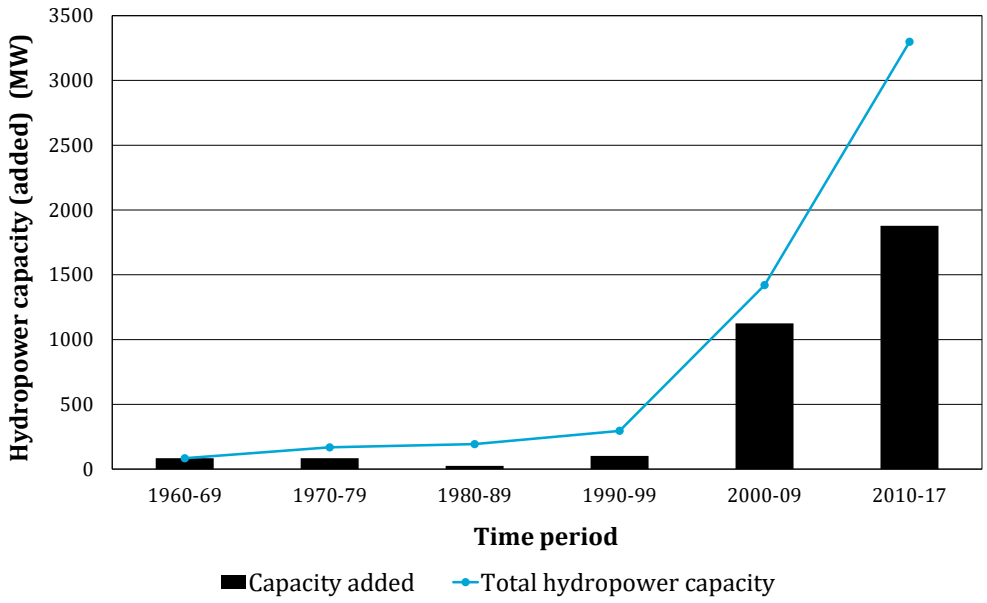

Figure 1.1: Hydropower capacity additions in Myanmar since 1960, adapted from (IFC, 2017)

Despite the benefits that hydropower has to offer, concerns have been raised by environmentalists and human rights groups related to these ambitious plans. The question they are asking is whether hydropower projects truly add to the overall socioeconomic development of the nation. Environmentalists are starting to warn the Myanmar government about the irreversible environmental impacts that hydropower can have by endangering water-related livelihoods, and increasing socioeconomic injustice and political discontent. The benefits and negative impacts from the dams in Myanmar are furthermore often asymmetrically distributed amongst the population (Kattelus et al., 2015).

1.2. Problem statement and knowledge gaps

As the previous section demonstrated, political and economic reforms in combination with growing climate change and environmental threats have caused Myanmar's society, economy, ecosystems and water resources to face major challenges. Therefore there is a urgent need for a deeper understanding of human–water system dynamics in place. Partly due to the complicated political history of Myanmar, many of the hydropower projects are being promoted and executed without appropriate planning nor public consultation, which can have irreversible effects on ecosystems (Spolum, 2017). Recognizing the values of ecosystems, however, and investing in them accordingly, could play a key role in achieving development as well as alleviating poverty in Myanmar.

Large hydropower projects reduce lateral and longitudinal connectivity of the river, have the potential to flatten flow peaks and troughs of the flow regime, and trap (nutrient-rich) sediments behind dams, which are critical for maintaining physical processes and habitats downstream. Furthermore, hydrodams often bring about changes in water quality indicators of a reservoir such as chemical composition and dissolved oxygen levels, and changes in the physical properties through, for example, temperature. The new environment created can become unsuitable to the aquatic plants and animals that evolved with a given river system, subjecting the system to the threat of invasion by non-native species that further disturb the river's natural communities of plants and animals (Efford, 1975; Young et al., 2004; Cullenward and Victor, 2006). The ecosystems that rely on the exploited rivers of Myanmar and their flow regime are essential for food and nutritional security throughout the nation. With the proper management of hydrodams in Myanmar, the introduction of environmental flows could help to go beyond simply meeting the water demands of water users, and take environmental impacts into account also. (Forslund et al., 2009).

The main agency for impact studies in Myanmar, the National Commission for Environmental Affairs (NCEA), currently does not have the authority required to commission environmental impact assessments (Nyunt, 2008). Furthermore, the expanding amount of foreign-owned hydropower development in Myanmar has a potential to threaten national control over water resources (Affeltranger, 2008). Even if the law of neigh-

bouring nations requires environmental impact assessment for domestic hydropower development, the legislation does not include cross-border projects, and hence it remains the responsibility of the host country (Magee and Kelley, 2009). This is especially important for countries like Myanmar, which lack appropriate laws and policies that would regulate the social and environmental impacts of dam projects (Thakkar, 2008). Furthermore, foreign-owned hydropower development in Myanmar has the potential to threaten national control over water resources, for example when choosing between hydropower and irrigation (Affeltranger, 2008). It is also often argued that hydropower operation can lead to better flood control in the wet season and benefit irrigation during the dry season. However, this is not a main concern when trying to optimize power production, and is unlikely to become a priority when a dam is owned or operated by foreign investors (Smith, 2011). In Myanmar, many people are directly dependent on land and water resources for their livelihoods, meaning that impacts on natural systems have a direct link to their well-being (Yu, 2003). Upstream changes, including hydropower development and (associated) land cover changes, are an important part of the downstream vulnerability. However, the potential socio-ecological impacts of hydropower projects are not yet appropriately addressed on a national nor regional level (Salmivaara et al., 2013). Only a few studies exist on Myanmar river basins at all, and many are dependent on the few data measured or provided by the government. The measurement techniques and the data quality of this data remains largely unknown (see Appendix A for more details). Therefore there is a need for an effective but resource non-intensive environmental flow assessment tool that can quantitatively evaluate dam operations in Myanmar.

1.3. Research objectives and scope

This study aims to quantify the hydrological alterations to the natural flow regime by the Yeywa dam and to assess the impact of these alterations on the ecohydrology in the Myitnge basin in Myanmar. A further aim of this research is to explore the suitability of the rainfall-runoff model (*WFlow_sbm*) as a tool for environmental flow management, for which two Myanmar case study areas are used: the Myitnge basin and the Myittha basin.

To provide structure in the research process the next three research questions form the basis of the assessment and together lead to the main research objective:

1. *How and to what extent has the natural flow regime of the Myitnge in Myanmar been hydrologically altered by the Yeywa dam?*
2. *Which ecological processes have been or could potentially be most affected by these hydrological modifications in the Myitnge?*
3. *To what extent is the Wflow_sbm model a suitable tool for environmental flow management in Myanmar?*

The research focuses on the hydrological aspects of the flow regime, and does not take water quality aspects into account, with the exception of some sediment parameters. Although water quality parameters are of vital importance to many ecological processes, previous fieldwork in the Myitnge showed the water quality and temperature to not be significantly different up- and downstream of the Yeywa dam, and hence these aspects are excluded from this research. It should also be noted that many ecological processes are impacted by sediment dynamics. By altering both bottom-up and top-down ecological processes and changing energy flow pathways, changed sediment loads alter biotic assemblage structure and ecological functioning significantly. This often results in in reduced biological diversity and productivity (Donohue and Garcia Molinos, 2009). These impacts are also excluded from this research, however, for analyzing the effects is highly data-demanding and not necessary for answering the research questions. Nevertheless, the expected effects of hydropower dams on sediment, and the associated impacts of this on ecology, are briefly explained in Appendix B. Furthermore, sediment transport is partially considered when analyzing the changes in geomorphic flow functions due to hydrodam operation.

1.4. Reader's guide

The remainder of this report is as follows. Following this introduction, this thesis continues with a theoretical background, which focuses on the functions of flow regime components and established effects of dams on ecohydrology from literature. The subsequent chapter is a description of the study locations in Myanmar: the Myitnge and the Myittha rivers. Chapter 4 describes the methodology of this research, followed by the results and a discussion of these results in Chapter 5. Finally, conclusions and recommendations are drawn in Chapter 6. This final chapter will also provide answers to the research questions posed in section 1.3.

At the end of the first few chapters, a summary box will be provided, as in the example below. The boxes highlight the essence and most important conclusions of the chapters. Reading these will help the reader understand the method and theory in concise way, as well as providing condensed answers to the research questions.

Summary of chapter

This is a chapter summary textbox

2

Theoretical background

This chapter aims to provide the theoretical background of the study. It starts with a section on some important definitions and concepts, after which the theory of the Natural Flow Regime will be explained, along with the functions of flow regarding ecology, and the river continuum concept. Section 2.4 briefly describes the hydropower technology, and subsequently examines the potential impacts of hydropower projects on the components of the hydrograph and sediment dynamics, depending on the operation. The final section, section 2.5, describes the links between ecosystems, the flow regime and human well-being, thereby reemphasizing the significance of this study.

2.1. Definitions and key concepts

2.1.1. Ecosystems and ecohydrology

The biosphere, which is the region of earth inhabited by living organisms, is comprised of smaller units, referred to as ecosystems. An **ecosystem** includes all of the living and non-living environment at a particular location. It is essentially a network that links organisms to other organisms and to the nonliving environment. This interconnectedness implies that a disturbance to or change in an ecosystem can spread through the network of interactions and thereby impact the ecosystem widespread and in unexpected ways (Postlethwait and Hopson, 2009). **Ecohydrology** can be described as the study of how water in the environment and the structure and function of vegetation are linked in a reciprocal exchange (Baird and Wilby, 1999). The practice of ecohydrology requires integration across the traditional disciplines of meteorology, plant and animal ecophysiology and hydrology.

2.1.2. Types of flows

Flow management is a complicated science, which is reflected in the excessive terminology surrounding the components. The most important term in this research is **environmental flow**, often referred to as E-flow. During the 2017 Brisbane River Symposium, the definition of environmental flows was updated to it's latest version: *"the quantity, timing, and quality of freshwater flows and levels necessary to sustain aquatic ecosystems which, in turn, support human cultures, economies, sustainable livelihoods, and well-being."* (Arthington et al., 2018). The term was, at this symposium, endorsed by more than 750 delegates from 50 nations. It is therefore currently the most accepted, as well as the most inclusive definition for the science of flow management for the protection of natural ecosystems and water requirements of associated stakeholders (including ecosystems). It is essentially the unallocated flow intentionally left in the river. It should not be confused with **ecological flow** which is supposed to indicate the flow necessary to maintain the character of an ecosystem only. Stakeholders are excluded from the latter definition and hence ecological flow can be seen as a component of environmental flow. **Instream flow requirement** is, as defined by the Instream Flow Council, *"the amount of water flowing through a natural stream course that is needed to sustain, rehabilitate, or restore the ecological functions of a stream in terms of hydrology, geomorphology, biology, water quality, and connectivity at a particular level"* (Council, 2002). Contrary to environmental flow, the wording of this definition suggests that the floodplains are not included, as it only takes the "instream" ecosystem into account. Finally there is **base flow**, which has been defined by the United States Geological Survey as *"That part of the stream discharge that is sustained primarily from groundwater discharge. It is not attributable to direct runoff from precipita-*

tion or melting snow" (Carter et al., 2005). Baseflow should not be confused with minimum flow or low flow conditions. This research deals primarily with environmental flows and ecological flows, as a component of environmental flows.

2.1.3. Biomonitoring and macroinvertebrates

Biomonitoring in rivers involves the use of organisms to assess the impact of a certain stimulus on, for example, a river. Biological indicators, often referred to a bio-indicators, are organisms which, by their own presence or absence in a system, indicate the existence or abundance of a particular critical factor (Martin and Coughtrey, 1982). Thus all organisms have a defined tolerance to a certain environmental natural or unnatural stimulus. They can only exist in a certain location if the conditions stay within their range, named their 'zone of tolerance'. This is illustrated in Figure 2.1. Within this zone of tolerance, exposure to stressors can be tolerated to a certain extent when the bio-indicator shows little to no signs in the 'zone of indifference,' where the vigor remains stable. As the upper limit of the zone of tolerance is met, stress is increased and the bio-indicator will start showing signs of impact. After the zone of tolerance comes the zone of intolerance, where the species can no longer survive (Martin and Coughtrey, 1982). The idea of biomonitoring is that by observing or measuring the effects the environment has on its resident organisms, one can assess the overall river health. Biomonitoring is a popular tool for studying the impact of environmental exposure to stressors due to its simplicity and low cost.

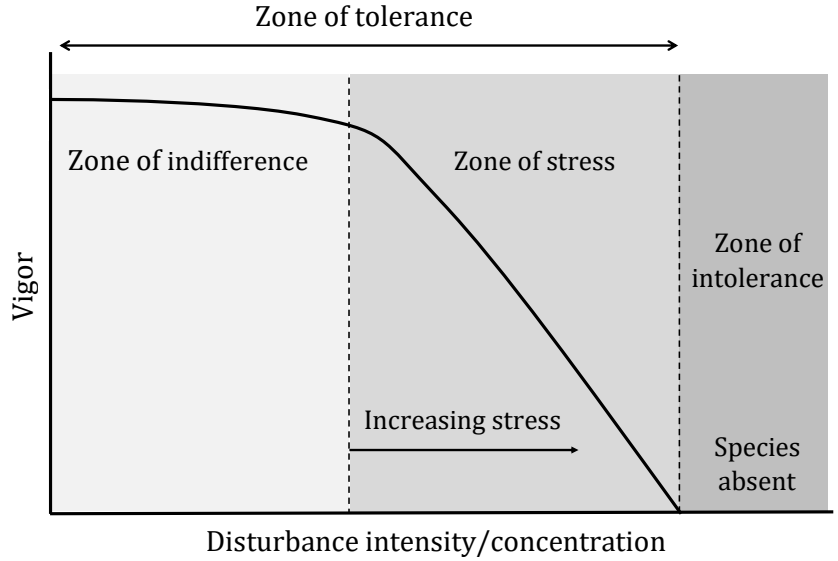

Figure 2.1: Reponse of an organism to environmental stressors in terms of tolerance and vigor, adapted from (Martin and Coughtrey, 1982; Phillips and Rainbow, 2013)

This research will use macroinvertebrates as bio-indicators to assess the hydrodam induced impacts through altered flow regimes. Stream macroinvertebrates are organisms without a backbone that live underwater in rivers and streams, and can be seen by the naked eye (Postlethwait and Hopson, 2009). Many of them live in the water as juveniles (nymphs or larvae), and become flying insects as adults. When underwater, macroinvertebrates must be able to navigate moving water as well as the substrate on the stream bottom. They have developed many life strategies, most in direct response to their living environment. For example, the species that live in slow moving pools often hide in and under the substrate on the stream bottom to prevent being seen by predators. Many macroinvertebrates that are found in riffles stick to rocks using suction devices, and the species found in glides usually are flatter to prevent being swept away by the flow (Postlethwait and Hopson, 2009).

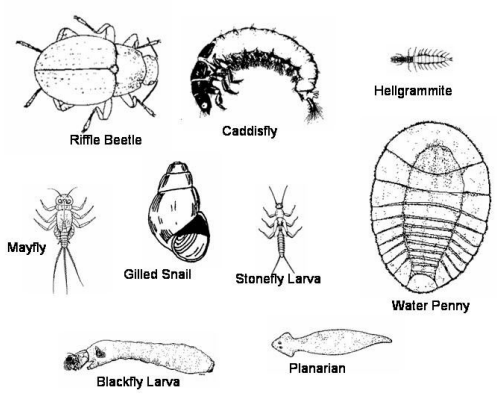

Figure 2.2: Example of sensitive macroinvertebrates (Michigan Tech, 2004)

Macroinvertebrates have been used extensively for biomonitoring of numerous environmental stressors because they are sensitive to many stream-related conditions (Rosenberg and Resh, 1993). They also exhibit enough stability in assemblage structure over time to make them useful as long-term indicators for stream health (Richards and Minshall, 1992). They are furthermore easy to collect and many stay in a small area for most of their lives. In general, macroinvertebrates are sensitive to the introduction of pollution, high levels of sediment, flashy flow regimes, high water temperatures and low levels of dissolved oxygen (Rosenberg and Resh, 1993). The most sensitive species are presented in Figure 2.2. As was mentioned before, water quality parameters fall outside of the scope of this study. The impacts that the components of the flow regime and sediment dynamics have on macroinvertebrates are described in detail in sections 2.3 and B.3, respectively.

2.2. Theory of the Natural Flow Regime

The ecological integrity of river ecosystems depends on their natural dynamic character. Therefore, a flow regime is of great importance in sustaining riverine ecosystems. The natural flow regime paradigm hypothesizes that the structure and function of a riverine ecosystem, and the associated adaptations of the riparian and aquatic species within this ecosystem, are dependent on a pattern of temporal variation in river flows (Lytle and Poff, 2004). There are five critical components of flow regime which influence ecological integrity. These are magnitude, frequency, duration, timing, and rate of change, as shown in Figure 2.3 (Poff et al., 1997).

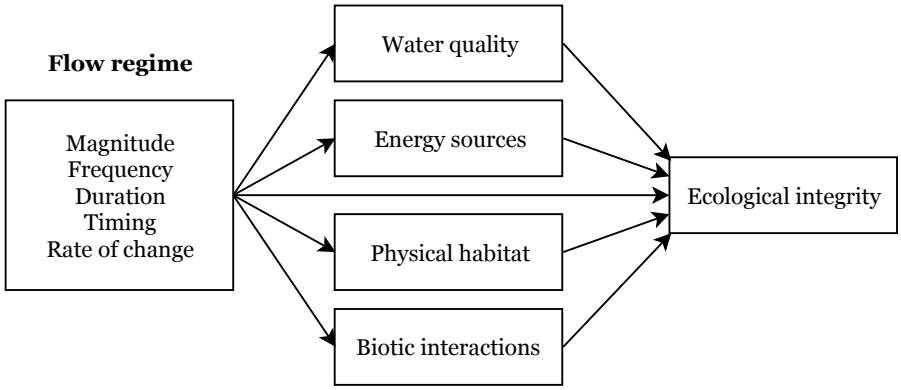

Figure 2.3: The five components of flow regime influencing ecological integrity (Poff et al., 1997)

The magnitude of flow refers to the amount of water moving past a fixed location per unit time. The frequency is associated with how often a flow above a given magnitude recurs over some specified time interval. This is inversely related to magnitude: higher magnitude flows occur less frequently. The duration is the period of time associated with a specific flow condition whereas the timing refers more to the predictability and regularity with which a flow of a certain magnitude occurs. Finally, rate of change: flashiness, how quickly flow changes from one magnitude to another (Poff et al., 1997). These five components together form a flow regime, which impacts ecological integrity directly and indirectly through water quality, energy sources, physical habitat and biotic interactions.

2.2.1. Geomorphic and ecological functions of flow

The flow regime has an important function in maintaining ecosystems, thus the living and non-living environment. This section will consider the geomorphic and ecological functions of flow. Naturally variable flows create and maintain the dynamics of in-channel and floodplain conditions and habitats that are essential to

aquatic and riparian species, as shown in Figure 2.4. The different functions are labelled A through E.

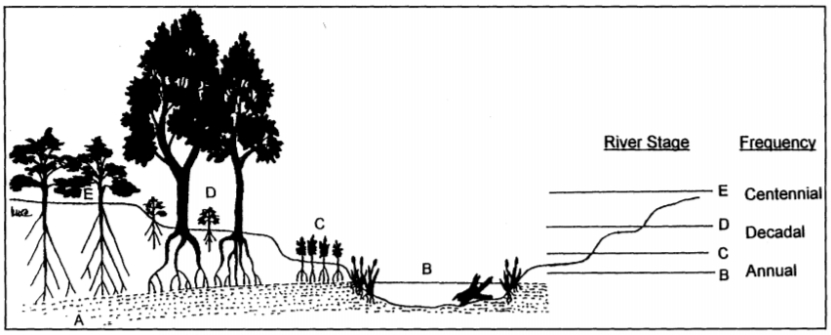

Figure 2.4: Geomorphic and ecological functions of flow (Poff et al., 1997)

Label A represents water tables that support riparian vegetation and that define in-channel baseflow habitat. These are maintained by groundwater inflow and flood recharge. Regarding the components of the natural flow regime, floods of varying magnitude and timing are required to maintain a diversity of riparian plant species and aquatic habitat. Label B shows that small floods which occur frequently transport fine sediments, which maintains high benthic productivity and creates a fish spawning habitat. Looking at the components of the flow regime, these are floods with a low magnitude, but a high frequency. Label C shows that medium-size floods inundate low-lying floodplains and deposit sediment, allowing for the development of pioneer species. These floods also transport accumulated organic material into the channel, assisting in the maintenance of the characteristic form of the active stream channel. Larger floods that recur in the order of decades inundate the alluvial terraces, where later successional species establish, as shown by label D. Finally, label E shows very rare floods with big magnitudes which can uproot mature riparian trees and deposit them in the channel. This forms a suitable habitat for many aquatic species (Poff et al., 1997).

The geomorphic and ecological functions of flow as described by Poff et al. (1997) highlight the importance of the flow regime for the inundation of watershed areas at different times and frequencies. Bunn and Arthington (2002) built on this by suggesting that the natural flow regime of a river influences aquatic biodiversity through multiple interrelated mechanisms as shown in Figure 2.5, which perform over various spatial and temporal scales.

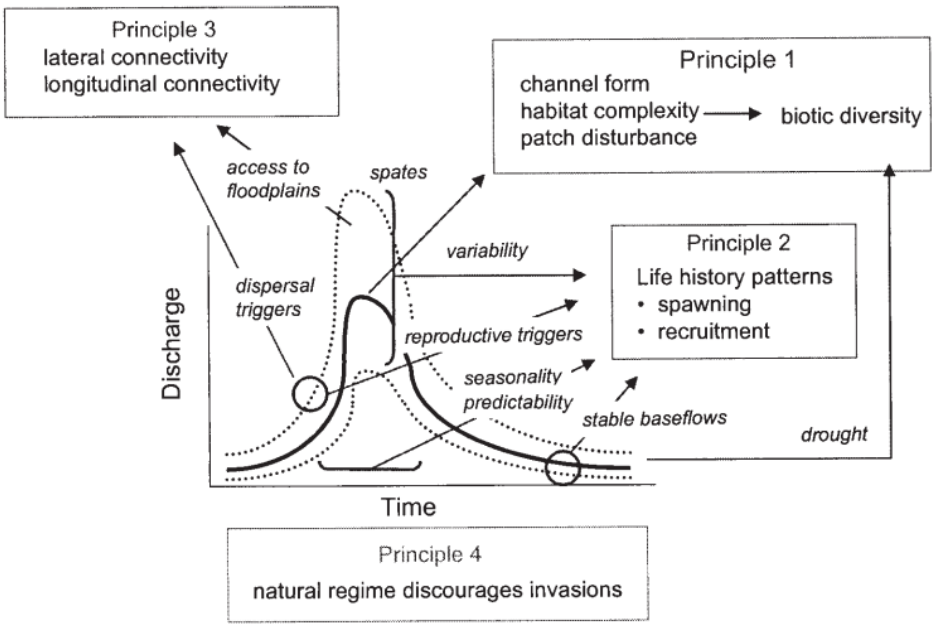

Figure 2.5: Four key principles influencing aquatic biodiversity (Bunn and Arthington, 2002)

The first principle states that flow is a large determinant of physical habitat in streams, which in turn is a determinant of biotic structure. Flow influences stream habitats at the catchment scale, reach scale and patch scale. This habitat then affects the amount and distribution of species, as well as the diversity and composition of species type. Important links can be made between physical habitat and species ranging from algae and aquatic plants to invertebrates and fish (Bunn and Arthington, 2002).

The second principle states that aquatic species have over time evolved life strategies in response to historical natural flow regimes. Therefore alteration of this natural flow regime can lead to failure of recruitment and loss of biodiversity. Flow plays a large role in the lives of species with critical life events, such as reproduction, spawning, larval survival, growth pattern or recruitment, that are linked to the flow regime. These may be synchronized with temperature and day length, for example. When flows are altered, and certain aspects are no longer in harmony with the natural seasonal conditions, aquatic species will be affected negatively. In large flood plain rivers many aquatic species such as benthic microorganisms, phytoplankton, zooplankton, and fish are cued to rising flood levels. They emerge from resting stages or spawning in response to the cue of rising water levels and inundation. Again, altering these conditions will offset cues and hence change life history patterns (Bunn and Arthington, 2002). Specific examples of ways in which species have historically adapted to altering flow regimes are observed delayed spawning in fish due to changed temperature regimes below dams (Zhong and Power, 1996) and reduced seasonality leading to diminished synchronal breeding in gammarid shrimps (Bunn, 1988).

The third principle reads that preservation of longitudinal and lateral connectivity in a natural way are essential to the survival of populations of many aquatic species. These species need to able to move freely through the stream, or between the river and floodplain wetlands. If this connectivity is not properly maintained, populations can be physically detached from parts of their habitat, leading to failed recruitment and possible local extinction (Bunn and Arthington, 2002). For the importance of longitudinal connectivity, an example of dependent species are large migratory macroinvertebrates such as shrimps and crabs. These species are an important part of subtropical ecosystems because of their impact on vital ecosystem processes such as primary production, organic matter processing, and sedimentation. Water abstraction and dam construction impact these migratory macroinvertebrates greatly, however. Larvae might be drawn into the water intake points and juvenile species face severe predation downstream of the dam. Additionally the blockage of migratory pathways may interfere with the completion of the life cycles of certain species such as diadromous fishes. Lateral connectivity is especially of importance to biodiversity. The lateral development of floodplain habitats during flooding creates important spawning, nursery and foraging areas. These are used by many fish species and a variety of other vertebrates. Therefore the flood duration and timing decide how long species will have access to these habitats, and whether fish will remain trapped in isolated floodplain waterbodies or make it back into the river system.

The fourth principle is about the invasion of foreign species, which becomes easier when flow regimes are altered (Bunn and Arthington, 2002). Foreign species are non-native or 'exotic' to an environment. Those species are outside of their natural range (Welcomme, 1992). When a natural flow regime is altered, it may favor non-native species, giving them a competitive edge. The integration and hence long-term success of an invading fish species is a lot more probable in a river ecosystem permanently changed by human influences than in a lightly disturbed system (Moyle and Light, 1996). The most important reason for this is human disturbed systems are usually very alike across broad spatial and temporal scales. These systems furthermore tend to favor species that are also favored by humans (Gido and Brown, 1999). For example, the creation of reservoirs and more constant flow regimes by damming rivers favors introduced species which are naturally abundant in lakes and river backwaters in their native range (Moyle, 1986).

The four principles teach us that different aspects of the natural flow regime are important for the integrity of certain ecological processes. An overview of the different types of flow that support various ecological functions is given in Table 2.1. Any changes to the magnitude, frequency, duration, timing and rate of change of these flows hence makes ecological processes vulnerable.

Table 2.1: Ecological functions supported by different flow levels (Forslund et al., 2009)

Flow	Ecological function
Low (base) flows	*Natural (normal):* • Provide adequate habitat for aquatic organisms • Maintain suitable water temperatures, dissolved oxygen, and water chemistry • Maintain water tables levels in the floodplain and soil moisture for plants • Provide drinking water for terrestrial animals • Keep fish and amphibian eggs suspended • Enable fish to move to feeding and spawning areas • Support hyporheic organisms (those living in saturated sediments)
	Drought: • Enable recruitment of certain floodplain plants • Purge invasive introduced species from aquatic and riparian communities • Concentrate prey into limited areas to benefit predators
High pulse flows	• Shape physical character of river channel, including pools and riffles • Determine size of stream bed substrates (sand, gravel, and cobble) • Prevent riparian vegetation from encroaching into channels • Restore normal water quality conditions after prolonged low flows, flushing away waste products and pollutants • Aerate eggs in spawning gravels and prevent siltation • Maintain suitable salinity conditions in estuaries
Large (peak) floods	• Provide migration and spawning cues for fish • Trigger new phase in life cycle (e.g. in insects) • Enable fish to spawn on floodplains, provide nursery area for juvenile fish • Provide new feeding opportunities for fish and waterfowl • Recharge floodplain water table • Maintain diversity in floodplain forest types through prolonged inundation (different plant species have different tolerance) • Control distribution and abundance of plants on floodplains • Deposit nutrients on floodplains • Deposit gravel and cobbles in spawning areas • Flush organic materials (food) and woody debris (habitat structures) into channels • Purge invasive introduced species from aquatic riparian communities • Disburse seeds and fruits of riparian plants • Drive lateral movement of river channels, forming new habitats (secondary channels and oxbow lakes) • Provide plant seedlings with prolonged access to soil moisture

2.3. Flow impacts on macroinvertebrates

Changes to the natural flow regime affects different species in various ways and on different scales. This section focuses on the expected and observed flow impacts on macroinvertebrates, because the collected empirical data available for this research is a macroinvertebrate biomonitoring dataset. Extence et al. (1999) created the concept of Lotic-invertebrate Index for Flow Evaluation (LIFE). This is a method for linking benthic macroinvertebrate data to prevailing flow regimes. From this study, some conclusions were drawn, for example that summer flow variables are most influential in predicting macroinvertebrate community structures in most chalk and limestone streams. When it comes to impermeable catchments, however, invertebrate communities are much more affected by short-term hydrological events. Moreover, the research showed that biota present in rivers with regulated or altered flows tend to be most strongly affected by non-seasonal, interannual flow variation (Extence et al., 1999).

Schneider and Petrin (2017) researched the impact of water chemistry, habitat and flow characteristics on macroinvertebrates (and benthic algae) by comparing 20 regulated with 20 unregulated rivers. The results suggested that overall flow regime affected the species pool of macroinvertebrates from which recolonization

after extreme events could occur. Looking at individual components of the flow regime, macroinvertebrate taxon richness decreased with lower relative minimum discharges. According to the authors, this can be attributed to the temporary drying of parts of the riverbed. It should also be noted that the research showed that, generally, macroinvertebrate and benthic algal assemblages were more closely related to water quality parameters than to hydrological flow variables.

Monk et al. (2008) carried out a long-term spatio-temporal hydroecological analysis of instream ecological responses to river flow regime variability at 83 sites across England and Wales. Results showed that the effect of two major supra-seasonal droughts on inter-annual variability of the LIFE scores is evident. Both droughts showed a gradual decline before and a recovery of LIFE scores after the low flow period. The instream community response to high magnitude flow regimes was also evident, although less so.

Other responses from empirical studies are as follows. Munn and Brusven (1991) showed a reduction in species richness amongst macroinvertebrates due to erratic (diurnal) patterns of flow. These erratic flow patterns have also caused macroinvertebrates to strand (Kroger, 1973), and the standing crop, the total dried biomass of the living organisms present in a given environment, of benthic macroinvertebrates to decrease (Layzer et al., 1989). An increased stability of baseflow and reduction of flow variability can lead to an increase of nuisance larval blackflies (Davies and Walker, 2013) as well as the reduced diversity of macroinvertebrates (Armitage, 1977; Ward and Short, 1978).

The results of empirical studies of flow regime changes on macroinvertebrates shows a range of responses, and in some cases conflicting results. The different responses of biota after extreme events may be explained by recolonization, to some extent. Furthermore, as mentioned in section 2.2.1, life history patters, behavioral adaptations, or morphological changes may play an important part in the varying responses of the biota (Lytle and Poff, 2004; Bunn and Arthington, 2002). Finally, covariation of flow regime with other, potentially influential variables such as water quality aspects may lead to variation in species response.

2.4. Hydropower

The aim of this research is to link flow regime changes brought on by hydropower plants and their operation. Therefore this section will elaborate on the technology of these plants and the potential impacts of hydropower operation on the hydrograph of the river.

2.4.1. Technology

Most conventional hydropower plants include four major components: a large dam, a turbine, a generator and transmission lines. A schematic overview of a hydropower dam is given in Figure 2.6. The general idea is that energy of falling water is captured in order to generate electricity. An efficient hydrodam requires a large river that has a large drop in elevation. The dam hence stores large amounts of water behind it in a reservoir, at the bottom of which there is a water intake leading into the dam. Gravity causes the water to fall through the penstock inside the dam. At the end of the penstock there is a turbine propeller, which is rotated by the falling water. The shaft from the turbine is connected to the generator, which produces the power. Power transmission lines are connected to the generator that carry electricity. The water continues past the propeller through the tailrace into the river past the dam (USGS, 2016).

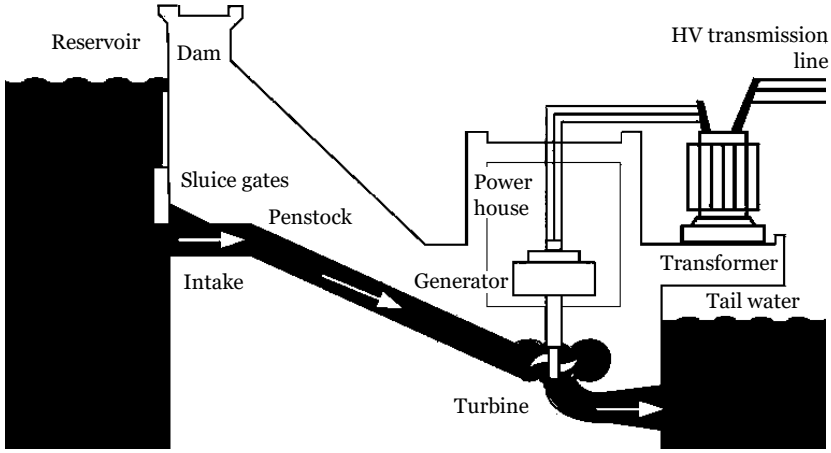

Figure 2.6: Schematic sideview of a hydropower dam, adapted from (Saadat, 1999)

2.4.2. Impacts on the hydrograph: expected effects

A hydropower dam can have different functions besides generating power. It may be used for flood control, water supply or have a combination of functions. It is important to understand that different functions of dams influence the operation and therefore will alter the natural flow regime in different ways. The nature and magnitude of the alterations brought on by dams will then in turn decide the operational strategies necessary to potentially restore environmental flows (Richter and Thomas, 2007). The potential impacts to the natural flow regime are presented in Figure B.4, where 2.7a is a dam operated for hydropower, 2.7b is operated for flood control, and 2.7c is operated for water supply downstream.

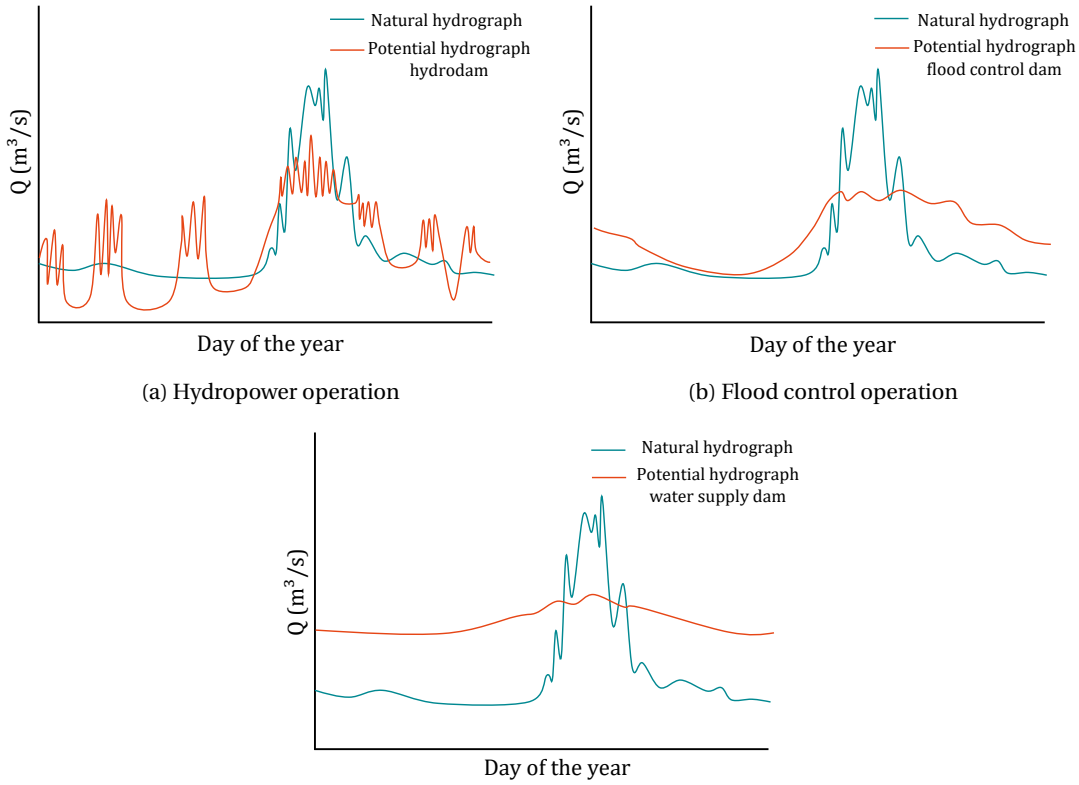

(a) Hydropower operation

(b) Flood control operation

(c) Water supply operation

Figure 2.7: Potential impacts of dam operations on the hydrograph

Dams for hydropower(Figure 2.7a)

Most smaller hydropower dams are said to be operated as 'run-of-the-river' facilities with little water storage capacity compared to the flow volume in the river. Therefore it is often assumed that these hydrodams only alter the flow regime on a minor scale. However, larger hydropower dams usually have large reservoirs that capture high water flows to store them for later use. This allows the dam to generate power according tot energy demand. The hydrograph hence often sees lowered flood peaks, followed by a rapidly fluctuating hydrologic pattern corresponding to power generation blocks. These power generation blocks are often followed by periods of very small to no released to allow the reservoir to fill up again. This cycle may cause a blocky hydrograph. In any case, hydropower operation is associated with fast water level fluctuations (Richter and Thomas, 2007). When generating power, the flow releases from a hydrodam can be much higher than the natural flow regime, after which the reservoir-filling period only allows releases that may be lower than the natural flow regime. It should be noted that the seasonal timing of these fluctuations is of great importance when looking at ecological impacts. The most important hydrograph changes that hydrodram operation causes are the elimination of small floods, the introduction of (more frequent) high flow pulses, and the lowering of water levels below the natural flow regime to the point of extremely low to no flow (Richter and Thomas, 2007). These effects are shown in Figure 2.7a.

(Hydropower) dams for flood control (Figure 2.7b)

A flood control dam aims to capture a part of the inflowing floodwater, and release that water at a lower discharge. Therefore, the general impact that a flood control dam has on the hydrograph is to cutting of the peaks. Following this, in order to release all the flood water, long periods of high water levels, or long high-flow pulses may be introduced. In general, small to medium sized floods may be eliminated from the flow regime, depending on the dam size and reservoir capacity (Richter and Thomas, 2007). The potential impacts are visually presented in Figure 2.7b.

(Hydropower) dams for water supply (Figure 2.7c)

Dams operated for water supply capture a lot of the high flow events and store these for a certain period of time in the upstream reservoir, releasing the flow according to downstream water demand. Regarding the five components of the flow regime, the timing of flows can be completely altered. Seasonality becomes a dam-controlled factor: these dams can theoretically store wet-season flows and not release them until the dry season. This has a dampening effect on the hydrograph: base flows are increased and flood peaks are reduced (Richter and Thomas, 2007). Figure 2.7c shows these impacts graphically.

2.4.3. Other impacts of hydrodams in Myanmar

Besides hydroecological impacts, hydropower plants can have many other effects on (human) livelihoods. These will not be discussed in detail, as they fall outside of the scope of this study. Nevertheless, the most important non-ecological potential impacts of hydrodams in Myanmar specifically, are briefly listed below (Kattelus et al., 2015).

- Major floodings of vast areas due to the construction of reservoirs (Foundation of Ecological Recovery, 2003)
- Erosion of the river banks downstream, especially in the delta (Foundation of Ecological Recovery, 2003)
- Salt intrusion in the downstream reaches near the delta (Foundation of Ecological Recovery, 2003)
- Forced resettlement of residents in the planned dam sites (Magee and Kelley, 2009)
- Reduction in cultural diversity (Magee and Kelley, 2009)
- Endangerment of agriculture-based human development (Affeltranger, 2008)
- Increased public unrest in non-ceasefire minority ethnic areas, where dams are mostly planned (Greacen and Palettu, 2007)

2.5. Links between ecosystems, the flow regime, and human well-being

Water resource management is about maximizing the economic and social welfare of water users. Sustaining ecosystems is an important aspect of this is for many reasons. There are various ways in which people, especially those with lower incomes, depend on ecosystems and the services they provide. Examples of this are basic elements of survival, improved community health and more security. The previous sections in this chapter established that the flow regime is the most important determinant of ecosystem function for river and wetland ecosystems. This section will explain how human well-being is dependent on the flow regime through ecosystem services (Forslund et al., 2009).

There are four types of ecosystem services; provisioning, regulating, cultural, and supporting. Environmental flows mainly support a variety of provisioning services such as clean water, plants, building materials and food. One of the most important products derived from rivers for humans are fish and fishery products, for example. Regarding regulating ecosystem services, erosion, pollution, flood control, and pest control are dependent on the flow regime. The cultural services that properly managed rivers provide are aesthetic, religious, historical, and archaeological values, which in countries like Myanmar are fundamental to a nation's heritage. The supporting ecosystem services, which mainly support the other three categories, are nutrient recycling, maintenance of biodiversity and primary productivity. Human well-being is dependent upon various services from these ecosystems, which are often interrelated. The concept of human well-being consists of essential aspects to improve the quality of the lives of people. This ranges from basic elements necessary for human survival such as food, water and shelter, to higher levels of achievement which usually differ per person (Forslund et al., 2009).

A loss of ecosystem services though for example an altered flow regime by a hydrodam can result in economic costs, in terms of declining profits, damage repair, cost of healthcare, and lost opportunities. The highest cost usually hits the rural poor, who often depend on nature's services directly for their livelihoods. Therefore, recognising the values of riverine ecosystems, and investing in them appropriately through environmental flow may be a key to achieving the development goals as well as poverty alleviation. Calls for maintaining environmental flows are often included in international agreements and even specific demands for maintaining environmental flows are starting to be adopted into national water laws in certain nations. However, looking at a global scale, very few countries have developed and executed environmental flow policies (Forslund et al., 2009).

Summary of Theoretical Background

This chapter aimed to lay the theoretical foundation for this research. **Ecological flow** indicates the flow necessary to maintain the character of an ecosystem. It is part of **environmental flow**, which describes the flow regime necessary to sustain aquatic ecosystems in order to support human cultures, economies, sustainable livelihoods, and well-being. The natural flow regime is defined by flows with different magnitudes, frequencies, duration, timing and rate of changes. This flow regime has a large impact on the structure and function of a riverine ecosystem, and the associated adaptations of the riparian and aquatic species within this ecosystem. The **four principles** of flow that influence aquatic biodiversity are as follows (Bunn and Arthington, 2002):

1. Flow is a large determinant of physical habitat in streams, which in turn is a determinant of biotic structure.
2. Aquatic species have over time evolved life history strategies in response to natural flow regimes.
3. preservation of longitudinal and lateral connectivity in a natural way are essential to the survival of populations of many aquatic species.
4. An altered flow regime allows the successful invasion of exotic species, threatening the native species.

Zooming in on **macroinvertebrates**, the taxa are affected by flow components in direct and indirect ways. Empirical research shows that the response to stressors varies per taxa. These different responses can be attributed to differing recolonization possibilities and rates, varying life history patterns, behavioral adaptations, and the co-variation of sediment and flow with other influential factors.

A **hydropower dam** is a large dam which captures falling water in order to generate electricity. These dams have different impacts on the flow regime, depending on their operation. A dam operated for maximum electricity generation will likely have a high frequency of high flow pulses, whereas a dam operated for flood control will dampen the flood peaks. Dams operated for water supply have the potential to eliminate the natural seasonality of flow by increasing low flow and cutting of the flood peaks. It is important to maintain riverine ecological integrity through an environmental flow regime, for many people are dependent on the associated **ecosystem services** for their well-being.

3

Study locations

This chapter aims to describe the study locations. It begins with a an introduction about Myanmar with a water management, climate, hydropower and ecohydrology section. Subsequently, the chapter will go into detail about the study river basins, the Myitnge and the Myittha, establishing the relevant hydrological and ecological components.

3.1. Myanmar

3.1.1. Myanmar rivers

Myanmar is a lower middle-income country, encompassing almost 700,000km^2. It shares borders with India and Bangladesh to its west, Thailand and Laos to its east, and China to its north and northeast. The nation has a population of over 55.6 million and the income per capita per year is US$6,300 (CIA, 2018). The union of Myanmar is made up of seven states, namely Rakhine, Kayin, Mon, Chin, Shan, Kaya and Kachin states. There are also seven divisions: Ayeyarwady, Tanintharyi, Yangon, Mandalay, Sagaing, Bago and Magwe. The nation has three parallel chains of forest-clad mountain ranges that run north to south from the Himalayan mountain range: the Western Yoma, often referred to as the Rakhine Yoma, the Bago Yoma and the Shan Plateau. These mountain ranges divide up the river into the three river systems: the Ayeyarwady, the Sittaung, and the Thanlwin. There is an abundance of natural resources available to the country, with a forest cover of almost 50% and plenty renewable internal freshwater resources. In fact, Myanmar is one of the water-richest countries in Asia with approximately 1,003km^3 of annual water resources (FAO, 2016). Almost 90% of these surface water resources are available during the wet season from May until October and only 10% in the remaining dry season. Of the annual flow, only about 3% is withdrawn, of which agriculture is largest user by far (FAO, 2016). Therefore water resources in Myanmar are considered very abundant. However, major challenges in the water resources management exist because of the irregular temporal and spatial distribution. In certain areas it has posed such a challenge to provide adequate water supply that the nation has been recognized to have economic water scarcity by the International Water Management Institute (Johnston et al., 2015).

There are about 60 rivers in Myanmar, most of which in a North to South direction towards the Bay of Bengal. Approximately 506 freshwater fish species have been recorded up to date in the largest rivers of Myanmar, 56 of which are endemic, meaning they are native or restricted to a certain place (Kennard et al., 2017; Baran et al., 2018). About 13,000km^2 of permanent water bodies and 70,000km^2 of seasonal floodplains exist across the country (CIA, 2018). Myanmar's Ayeyarwady river is part of the large group of rivers that arise from the eastern Himalayas. These rivers and their tributaries are fed by tropical monsoons, meaning their runoff is highly variable between seasons and from year to year. The Ayeyarwady is one of the world's longest and largest remaining free-flowing rivers. It provides habitat to many important freshwater species and ecosystem services. The freshwater ecology is largely unknown, but is often assumed to be similar to that of the Mekong river, a transboundary river in Southeastern asia which also finds its source in the eastern Himalayas. The Ayeyarwady has a discharge ranging from 2,300 to 32,600m^3/s throughout an average year along the river. It has the potential to cause major flood damage, especially in the lowland floodplains and delta (eWater Ltd, 2018). The Ayeyarwady and Chindwin (which joins the Ayeyarwady in the center of Myanmar) rivers have a valuable role in the development of Myanmar. The key human users dependent upon the flow of these rivers are the farmers who require water for irrigation, the communities dependent on the river for water supply,

the navigation sector (both cargo and passengers), fishermen, and the rapidly expanding hydropower sector (Ra, 2011).

This study focuses on two major tributary rivers: the Myitnge and the Myithha. The Myitnge is a large tributary of the Ayeyarwady located in the central eastern part of Myanmar. It joins the Ayeyarwady just south of Mandalay. The second study river is the Myittha, a western tributary of the Chindwin, which flows into the Ayeyarwady in the center of Myanmar. The study rivers and major rivers of the Ayeyarwady basin are presented in figure 3.1.

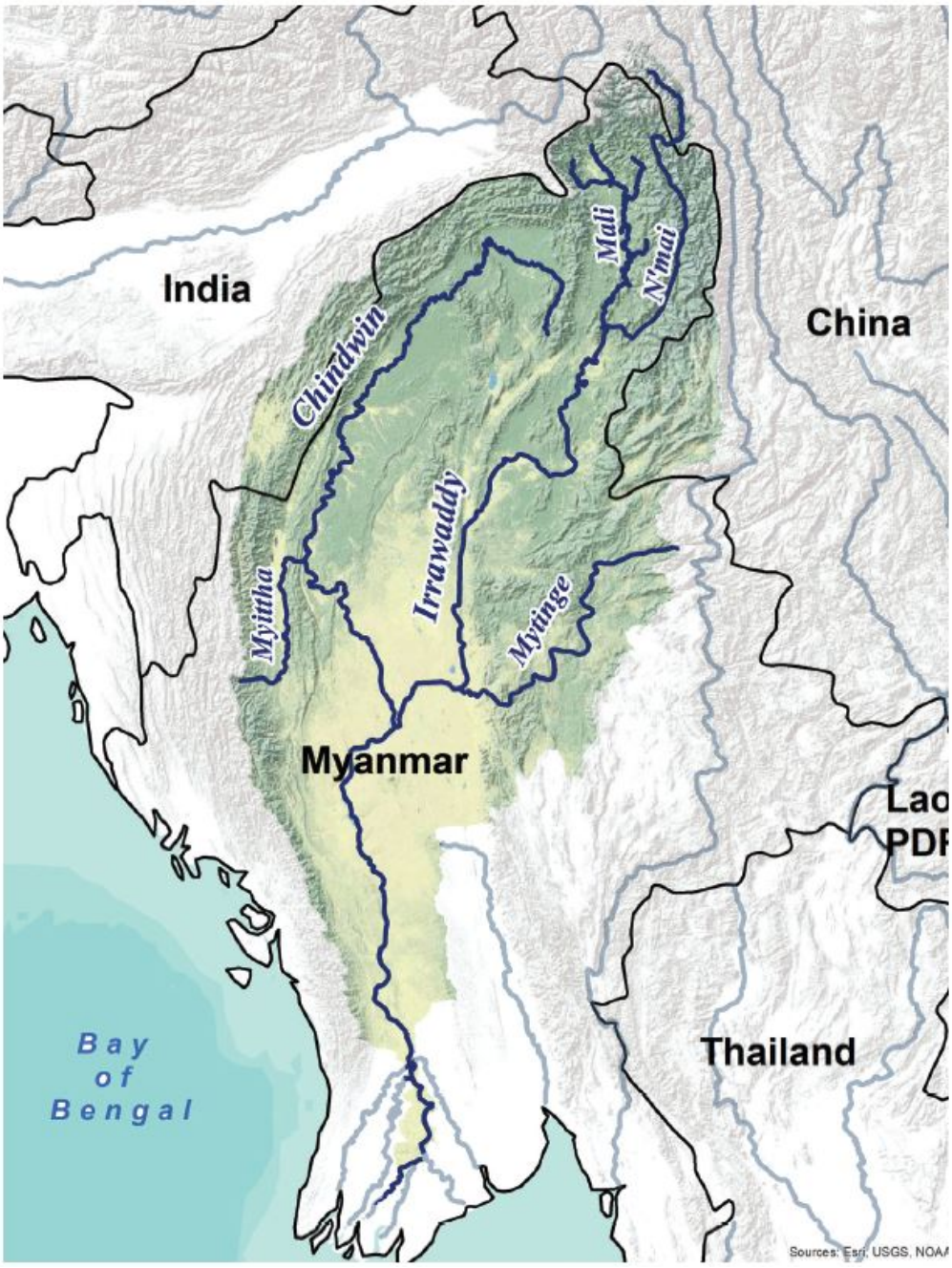

Figure 3.1: Large rivers in the Ayeyarwady catchment (TNC, WWF, and the University of Manchester, 2016)

3.1.2. Climate

The climate of Myanmar varies a lot across the nation and is influenced by many factors. First and foremost, Myanmar's climate pattern is influenced by the monsoon, causing the spatial annual precipitation to

vary considerably across the nation. More than 95% of the annual national mean precipitation is received from the Southwest Monsoon, which takes place from May until October. The reversal of the wind patterns, from November to February (Northeast Monsoon), brings a dryer and cooler climate to Myanmar. The mean maximum temperature is about 37.8°C in Central Myanmar. These high temperatures are usually reached between March and May. The mean minimum temperature is between 4.4°C and 10.0°C, in the Northern part of Myanmar between January and February (Group, 2016). Graph 3.2 shows the mean monthly temperatures and precipitation across the nation between 1901 and 2015. Myanmar has dealt with many meteorological, hydrological and seismic hazards, such as major cyclones in 1968, 1975, 1982, 1994, 2006, and the Cyclone Nargis which took place in May of 2008. Furthermore, historical floods took place in 2004, 2010 and 2015 (Aung et al., 2017).

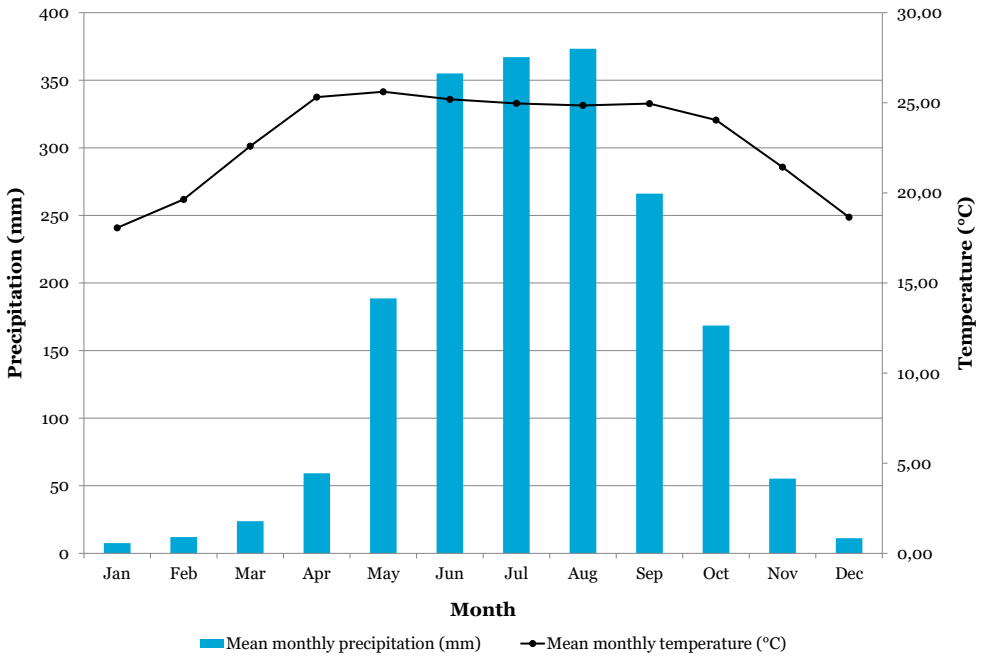

Figure 3.2: Mean monthly precipitation and temperature in Myanmar, 1901-2015 (Group, 2016)

Within the country's borders there are important features of relief which exert a dominant influence on it's meteorology. The country is furthermore significantly made up of lowland plains, which are located in Central Myanmar. The area is known as the Central Dry Region and is formed by the valleys of the Ayeyarwady river. It is least affected by the Southwest Monsoon, due to high mountains surrounding the area which cause a rain shadow effect (Aung et al., 2017).

Seasonality and the Monsoon

In Myanmar, three seasons can be identified. The first is the winter, also known as the Northeast Monsoon season, which takes place from November to February. The start of November often brings with it a sudden halt of the monsoon rains in Myanmar. Mid November the temperature starts dropping. In the winter season low temperatures prevail over the whole country, bringing with it clear skies and low humidity. Mid-December the calm weather in Northern Myanmar is often disturbed by a series of storms which travel Eastwards across Northern Myanmar throughout the subsequent two months. The precipitation amounts associated with these storms are small, but critical for winter crops grown in the Northern Myanmar region (Aung et al., 2017).

The second season, which commences in March and usually lasts until the middle of May, is the hot weather season. During the start of this dry period with rising temperatures, the winds are variable and much less persistent. There are almost no storms, and the coast is calm. By April, the wind speeds start increasing along the coast, but the temperature continues to rise. The temperatures typically reach up to 40°C in the

Central Dry Region during this time. As May approaches, local storms accompanied by violent winds and torrential precipitation mark the end of this hot weather season (Aung et al., 2017).

Between the end of May and October, the Southwest Monsoon takes place, which can be divided into four parts. These four parts are the early monsoon from the end of May until the end of June, the mid or peak monsoon from July until the end of August, the late monsoon from September until the withdrawal date (usually somewhere in October), and finally the post monsoon which is between October and November. The Southwest monsoon usually makes its appearance in Southern Myanmar around the third week of May. It gradually expands and travels northwards, having established itself across the whole country by the beginning of June. The mountain ranges over the West coast along Rakhine and Tanintharyi Regions cause abundant amounts of precipitation along the coastal area with an average annual rainfall of about 5080 mm. The Delta area receives only half of that. Even less precipitation is received in the Central Dry Region, where the rain shadowing effect caused by the Yomas causes an average annual rainfall of only 635 mm. The Southwest monsoon usually starts to retreat from Myanmar around the end of September. In October and the beginning of November, the rainfall decreases considerably across most of the nation. In the Central Dry Region, however, rainfall reaches a peak locally due to the passage of some final monsoon depressions from the Bay of Bengal after crossing the Rakhine and Bangladesh coasts (Aung et al., 2017).

3.1.3. The growing hydropower sector

According to the International Hydropower Association, Myanmar has only developed a little over 3% of it's 100 GW hydropower potential as of 2016. More specifically, hydropower provided Myanmar with about two-thirds of the country's energy in 2015, with 3,151 MW of installed capacity from 25 operational projects. Up until 2016, an additional 46 GW of technically feasible potential was recognized, and a number of these projects are now under construction or at the advanced planning stage. The plans to substantially increase the hydropower capacity of Myanmar in the future are spatially presented in Figure 3.3. The hydropower plants that are currently under construction will, if completed, already increase the capacity by almost 10 GW in the next 15 years. The partial economic liberalization of Myanmar has sparked the government's interest in developing its hydropower potential. The exponential increase in the development of hydropower projects aims to meet both the domestic energy demand and to gain foreign capital from electricity exports (Kattelus et al., 2015). This means that Myanmar's hydropower potential will be exploited not only for the domestic growing energy demand, but also to export power to Thailand, China, India and Bangladesh (Thein and Myint, 2008). Foreign companies from these nations become involved in the hydropower plans through dam funding, dam development as well as equipment supply (Kattelus et al., 2015). As can be seen in Figure 3.3, the majority of the hydropower projects are (planned) on the Salween River, the Upper Irrawaddy River and the Chindwin basin. Most of these projects are large-scale hydropower schemes and export-oriented. The figure also shows that the development is focused on large main streams and remote areas close to the borders. This shows the influence of the neighbouring countries: India and Bangladesh planning hydropower projects in the northwest, China in the north and east and Thailand in the southwest. The ongoing economic reforms in Myannmar support the energy policies seeking increased hydropower exports through new legislation and free trade agreements (Kattelus et al., 2015).

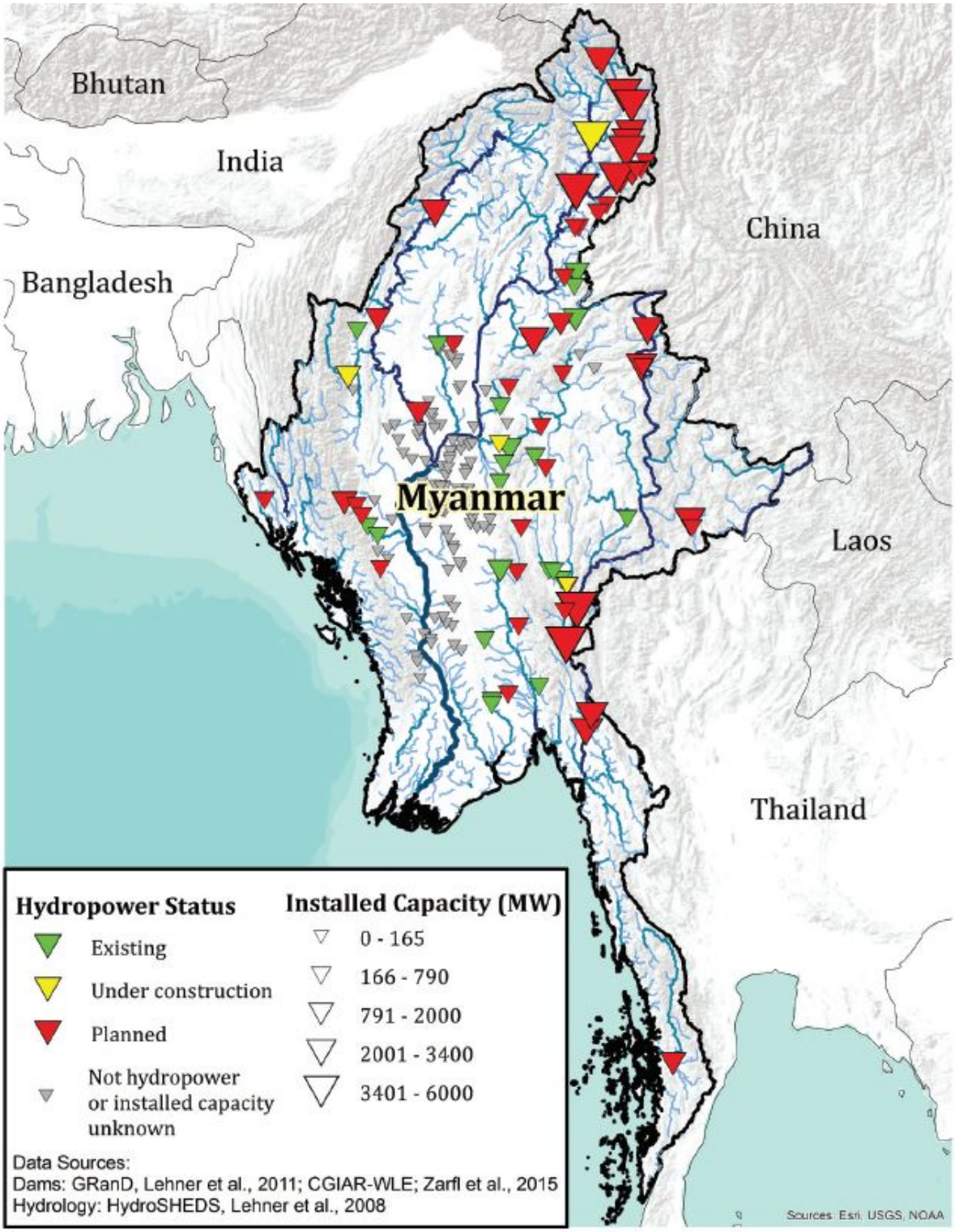

Figure 3.3: Current and future hydropower plants in Myanmar (TNC, WWF, and the University of Manchester, 2016)

3.1.4. Ecohydrology

The ecohydrological status of Myanmar remains largely unknown up until today. However, in 2017, an investigation was carried out and completed for the Ayeyarwady basin to assess its current state. Among other analyses, it identified the most important environmental assets and values that need to be considered for the Ayeyarwady basin. These include essential goods and services, as well as specific conservation and biodiversity objectives. The research team hence consulted and engaged with many local stakeholders to gain an

understanding of the most important environmental assets, and their relationships to flow. They came to the conclusion that, for the Ayeyarwady, the main factors and processes to focus on are as follows (Kennard et al., 2017):
Five groups of biodiversity assets:

1. Migratory species
2. Rare and endemic species
3. Critical habitat - floodplain wetlands
4. Critical habitat - rivers and streams
5. Key Biodiversity Areas (KBAs)

One provisioning ecosystem service:

1. Fisheries production

And three ecological processes that underpin the above assets and values:

1. Floodplain primary productivity
2. Lateral connectivity (floodplain inundation)
3. Longitudinal connectivity

As both the Myitnge and the Myittha rivers are (indirect) tributaries of the Ayeyarwady, and are hence part of the waterbasin, this study assumes the same key environmental components. Each of these components is explained in more detail in the ensuing subsections.

Migratory species

The Ayeyarwady and Salween rivers are two of the largest remaining free-flowing rivers globally. They are estimated to have around 506 fish species, about the same number as all of Europe (Baran et al., 2018), of which 388 can be found in the Ayeyarwady. A vital part of the lifecycle of some important riverine species is migrating through the river network. Many require flow-driven cues to undergo these longitudinal movements. Especially for upstream migrations, many species require very specific and predictable hydrologic conditions to move against the current or to locate appropriate spawning beds. These species are of importance from a fisheries perspective (Hortle, 2009) and/or have a significance from a conservation point of view (Dudgeon, 2011). Furthermore, large migratory macroinvertebrates, such as shrimps and crabs, have a direct impact on ecosystem level processes such as primary production and organic matter processing (Kennard et al., 2017).

Rare and endemic species

Many freshwater species are very vulnerable to localized disturbances because they have specialized habitat requirements, limited distributions, and small populaton sizes. Among the fish species recorded in the Ayeyarwady, there is an estimated amount of 50% endemism, especially in the upper Ayeyarwady sub-basin, where the Myitnge is located, and the Chindwin basin, where the Myittha is located (Kennard et al., 2017; Baran et al., 2018).

Figure 3.4: Aythya baeri (BirdLife International, 2018)

Critical habitat - floodplain wetlands

During the flooding season, a large amount of river fish, crustaceans, and other biota move into seasonally connected floodplain wetlands (Pettit et al., 2017). These areas become crucial nursery habitats and places of high production of food resources (Davies Jr et al., 2008; Ward et al., 2016). Furthermore, wetlands in the Ayeyarwady basin are known to provide feeding and breeding habitats for waterbirds. For example, the critically endangered Baer's pochard, Aythya baeri (illustrated in FIgure 3.4), relies on these wetlands for survival (Kennard et al., 2017).

Critical habitat - rivers and streams

Looking at the dry season, most aquatic species become confined to the river channels. Hence the deeper pools become refuges during this time and sufficient base-flows are required. These base flows are necessary to preserve water depth and water quality. Additionally, stable base flows give aquatic biota access to fringing riparian vegetation and logs along the river banks. These areas provide important habitat and food resources to many species (Kennard et al., 2017). For primary and secondary production, shallow riffle areas are critical, especially in smaller fast-moving rivers. During high flows, these productive areas can be drowned out. Furthermore, if the flows become extremely low, the surface areas of productive riffle areas are significantly decreased. This, in turn, reduces the productive habitat for consumers downstream (Kennard et al., 2017).

Key Biodiversity Areas

Key biodiversity areas (KBAs) are areas that are considered important for biodiversity. They are marked as such by meeting certain international criteria, based on globally threatened and range-restricted species (Zöckler and Kottelat, 2018). Figure C.2 in Appendix C shows 132 identified KBAs, of which several already benefit from the special status of protected area. Preserving these areas from degradation is believed to ensure the viability of habitat and species conservation. As can be seen in the the figure, there are multiple KBAs in and around the study area river basins Zöckler and Kottelat (2018).

Fisheries production

Fisheries are a major source of animal protein and income for many communities that live within the Ayeyarwady basin. In fact, fisheries provide jobs for approximately 3.2 million people in Myanmar (800,000 full-time jobs and 2.4 million part-time jobs) (Baran et al., 2018). Overall there are 388 fish species recorded in the Ayeyarwady basin, of which 311 are present in Myanmar. The others have been recorded across the border in India and China (Zöckler and Kottelat, 2018). In neighboring river basins such as the Mekong, extensive studies have concluded that mainstream hydropower developments will impact fisheries resources greatly. This is partly due to the river fragmentation causing disturbance to fish migrations, and partly because of the loss of nutrients due to trapped sediment behind the dams, resulting in a loss of water productivity (Baran et al., 2015).

Floodplain primary production

River floodplains and wetlands are very effective in hosting primary production, more so than river channels (Davies Jr et al., 2008). The area and duration of inundation of such an area are important components in influencing annual primary production. These factors are determined by variation in annual flood magnitude and the local topography (Kennard et al., 2017).

Lateral connectivity

As mentioned before, floods are crucial to connect the river channels to flood plains. Many species of fish, crustaceans and other biota move onto and off of seasonally inundated floodplains. These movements are vital to maintain genetic integrity and population sizes by allowing these species to complete their life cycles. For example, certain fish can only gain access to their nursery habitats and food, and return safely to the river system if the duration, timing and extent of flooding allow this. Some species may become trapped in isolated floodplain waterbodies (Kennard et al., 2017).

Longitudinal connectivity

Longitudinal connectivity is necessary for species to move throughout the river network and between marine and freshwater ecosystems. This process is also crucial for the life cycle of certain species (Kennard et al., 2017). (Hydropower) dams become obstructions to the longitudinal movement of biota and materials such as sediments and nutrients along river channels. Therefore, following the impoundment of a river, a disappearance or decline of important migratory fish species is often observed (Bunn and Arthington, 2002).

3.2. Myitnge

3.2.1. River basin specifications

The Myitnge river, the lower reach of the Namtu river, has a total length of about 530 km, at the end of which it flows into the Ayeyarwady just south of Mandalay. It has a watershed area of approximately 30,000km^2. Starting at its mountainous origin at about 1400m above sea level, the Myitnge passes through a hilly region, after which it enters alluvial plains. A digital elevation map of the catchment is given in Figure 3.5. From the origin until the Yeywa dam, the river bed consists mostly of rocks, and hence it can be classified as a bedrock channel. This means that the potential rate of removal of sediment exceeds sediment supply, as is usually the case in high mountain areas with steep slopes.

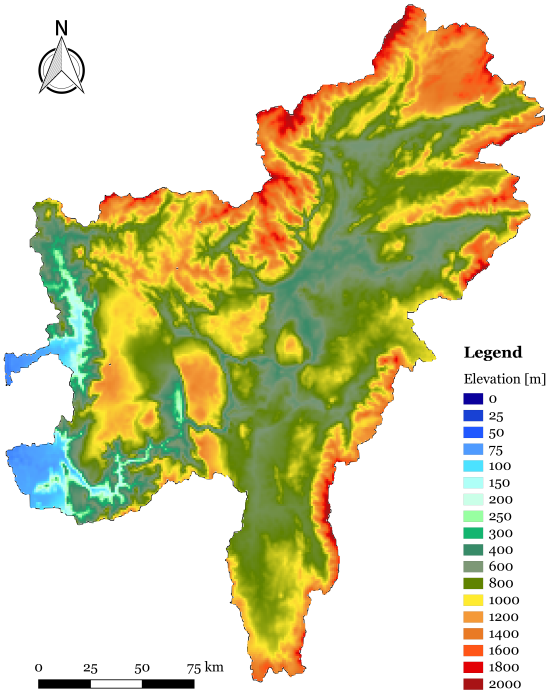

Figure 3.5: Digital elevation map of Myitnge catchment

The channel morphology upstream is primarily controlled by geologic structures, and has a straight step-like long profile. There are some waterfalls and rapids in this part of the river. Having passed the Yeywa dam, the Myitnge gradually becomes an alluvial river in which the bed and banks are made up of mobile sediment and soil. The channels in the lower parts of the Myitnge are shaped by the magnitude and frequency of the floods and the ability of the flood to erode, transport and deposit sediment. The upstream region has a subtropical monsoon climate as described in section 3.1.2, but downstream of Shwesaryan, the climate becomes a more tropical steppe climate, referring to a transitional climate between the tropical wet and tropical dry climates. The controlling factors of such a climate are similar to that of the tropical dry climate, though temperatures are cooler and annual precipitation is higher (Khaing, 1992).

The geological map, soilmap and landcover map of the Myitnge basin can be found in Appendix C. As can be seen in C.4a, the Myitnge consists mostly of orthic acrisols. Acrisols form on old landscapes that have a rolling hills and a tropical humid climate. The age, mineralogy, and considerable draining capacity of these soils has led to low levels of plant nutrients, an abundance of aluminum, and high erodibility. This makes the soil relatively unsuitable for agriculture. Nevertheless, traditional shifting cultivation of acid-tolerant crops has adapted well to the conditions found in acrisols. The natural vegetation on this soiltype is woodland (FAO-Unesco, 1974). The very downstream part of the basin consists of pelic vertisols, which are characterized by strong vertical mixing of the soil particles over many periods of wetting and drying. The soil is relatively saline and usually has well-defined layers of calcium carbonate or gypsum. These soils usually occur on level or mildly sloping topography in climatic zones that have distinct wet and dry seasons, such as the Myitnge. Although vertisols contain sginificant levels of plant nutrients, their high clay content can make cultivation labor-intensive (FAO-Unesco, 1974). A very small part of the very downstream part of the basin consists of chromic luvisols, which have a mixed mineralogy and significant nutrient content, making them very suitable for a wide variety of agriculture (FAO-Unesco, 1974).

Looking at the geological map in Figure C.3, a large part of the Myitnge basin is made up of upper Paleozoic metamorphics and intrusive rocks. There is also a significant fraction consisting of lower Paleozoic rocks. There are some undivided precambrian rocks on the edges of the basin, which are much older than the rest of the watershed area. Finally there are some Neogene sedimentary rocks and Jurassic metamorphics and sedimentary rocks more upstream in the basin, which are the newest geological features of the basin (USGS et al., 1998).

The land cover, featured in Figure C.5a of Appendix C, shows that the largest part of the basin consists of closed to open shrubland that is lower than $5m$. The type of vegetation associated with this land cover can be broadleaved or needleleaved, and evergreen or deciduous. Quite a significant proportion in the northern part of the catchment consists of closed to open (>15%) broadleaved evergreen or semi-deciduous forest that is taller than $5m$. Nearer to the Myitnge river network there are mainly rainfed croplands (more downstream), and mosaic cropland with grassland, shrubland and forest. There is also a bit of broadleaved deciduous forest/woodland that is taller than $5m$, mostly in the center of the catchment (ESA 2010 and UCLouvain, 2010).

The average natural flow regime of the river (based on data between 1981 and 2004) is presented in Figure 3.6. The graph was constructed from data collected by the Department of Meteorology and Hydrology at Shwesaryan village before the dam construction. The hydrograph shows that in a normal year, the flow varies naturally between 200 and $300 m^3/s$ from December until May, after which it rapidly increases to a peak of about $1200 m^3/s$, usually reached between the beginning of August and the end of September.

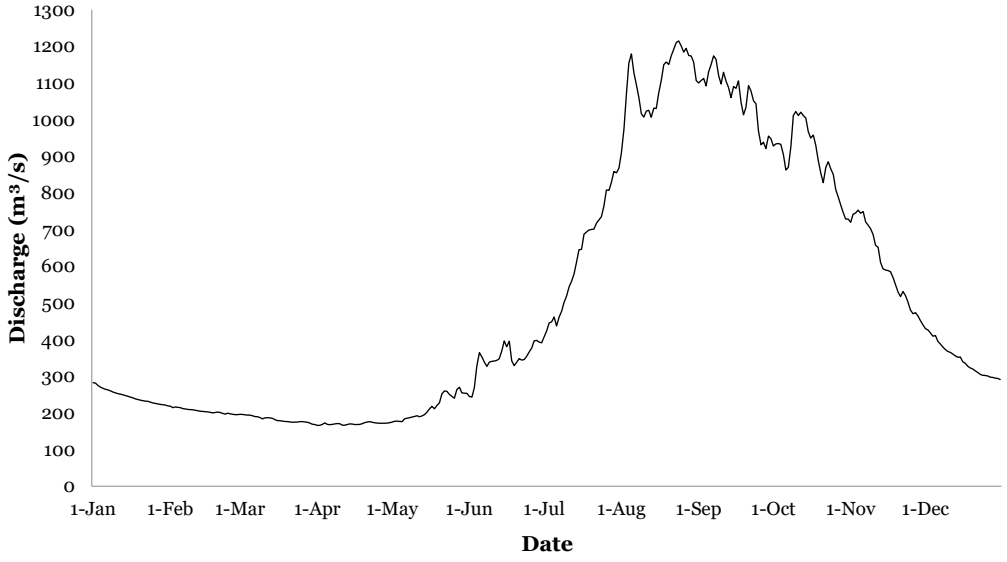

Figure 3.6: Average annual hydrograph of Myitnge river before dam construction (1981-2004), based on data provided by the Department of Meteorology and Hydrology in Myanmar

3.2.2. Hydropower

The construction of the 790 MW Yeywa hydropower project on the Myitnge river began in 2004. The stakeholders involved are the Irrigation department of Myanmar, Chinese companies such as China National Electric Equipment Corporation, China International Trust and Investment Corporation, Technology Co. Ltd., Sinohydro Corporation Ltd., the China Gezhouba Water and Power Group Co. Ltd. and China National Heavy Machinery Corporation (IFC, 2017). These companies provided all major structures and equipment. Furthermore, the project was financially supported by China's Export-Import Bank (Kattelus et al., 2015). The Yeywa hydropower dam, as presented in Figure 3.7, is the largest existing hydropower dam in Myanmar, and was completed in 2011. The project comprises a 134-metre-high roller compacted concrete dam with a 790 MW power station located on the left bank at the foot of the dam. There is also an ungated spillway located in the central section of the dam for flood water discharge. The powerhouse is located at the foot of the dam (Kyaw et al., 2006; IFC, 2017).

Figure 3.7: Yeywa dam and reservoir (photo by Nattapon Sritrairat)

The dam has been operational since 2011, and the current operation is presented in Figure 3.8. The figure shows that 2011 was mostly used for filling up the reservoir, after which the dam seemed to be operated under a run-of-the-river regime.

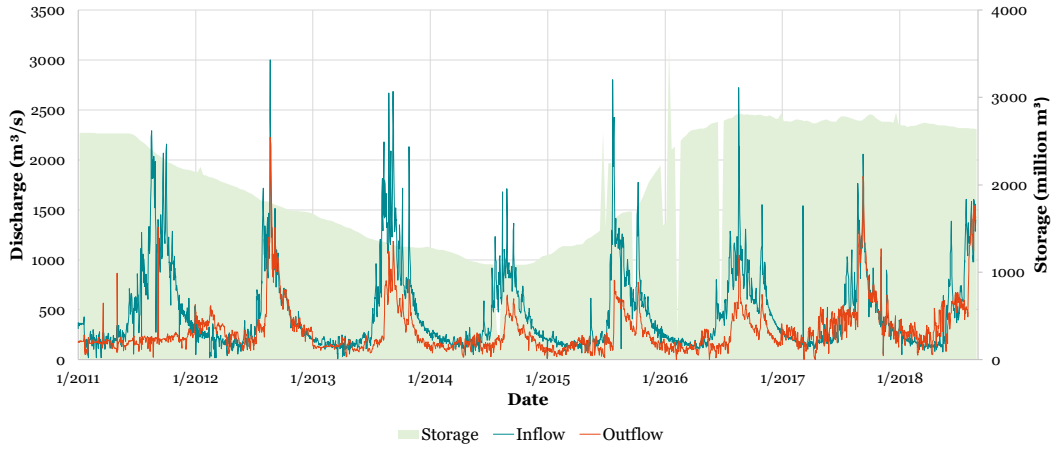

(a) Yeywa dam operation 2011-2018

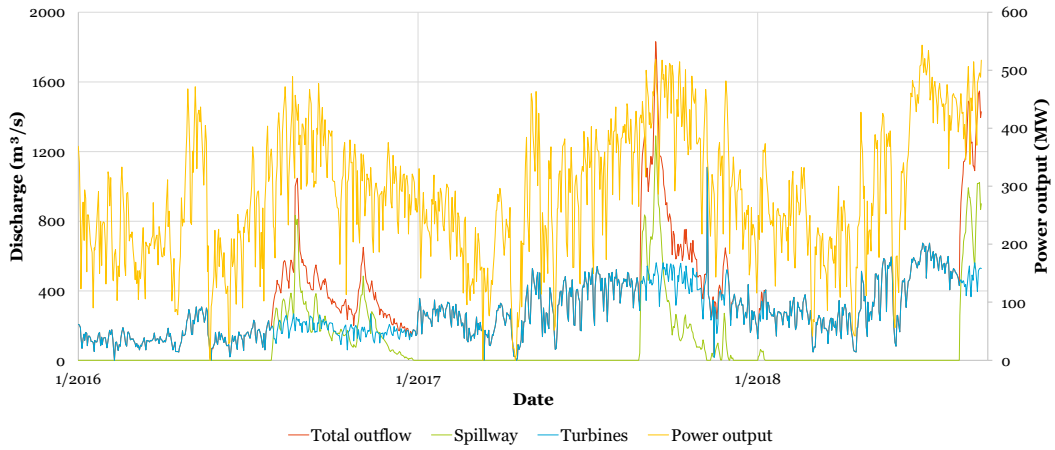

(b) Yeywa dam power generation and outflow (consisting of turbine flow and spillway flow)

Figure 3.8: Yeywa dam operation, based on data provided by Yeywa dam operators in November of 2018

Upstream of the dam is a 75 km long and narrow reservoir along the Myitnge's main branch with a total surface area of about 59 km^2 and a storage capacity of about $2.6km^3$. The power plant is connected by double-circuit 230 kV transmission lines to Belin at a distance of 38 km and Meiktila at 118 km (Kyaw et al., 2006; IFC, 2017). Figure 3.9 shows the reservoir upstream of the Yeywa dam. The dark blue line represents the natural (old) Myitnge, the dark green the reservoir area in the dry season, and light green the reservoir in the wet season.

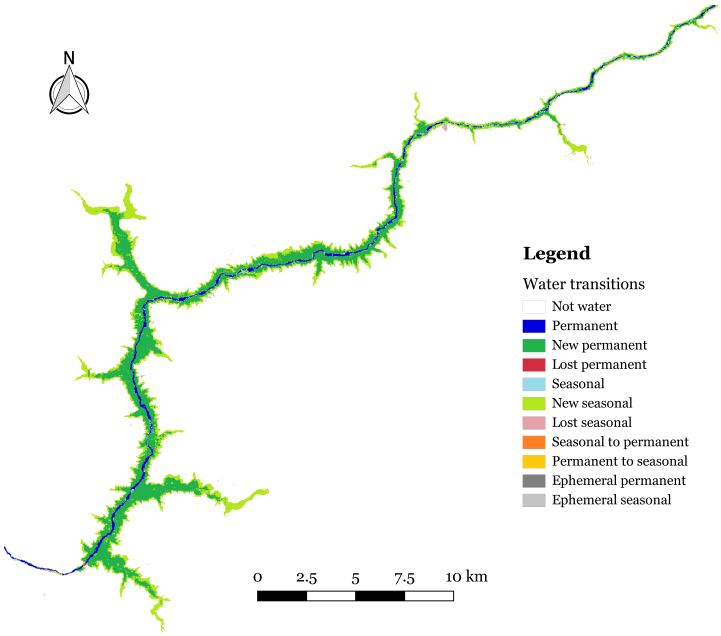

Figure 3.9: Water transitions in the Myitnge reservoir, data from EC JRC/Google (Pekel et al., 2016)

Future plans

Besides the existing Yeywa hydropower plant, there are at least four more hydropower projects confirmed in the next ten years for the Myitnge basin. These are the Hsipaw dam, the Kyaukmne dam (more commonly known as the Upper Yeywa dam), and the Middle Yeywa dam upstream of the existing Yeywa, and the Deedoke downstream of the existing Yeywa (TNC, WWF, and the University of Manchester, 2016). An overview of the existing, planned and under construction dams is given in figure 3.10. The idea is to create a cascaded run-of-the-river system that will provide all of Mandalay with electricity (TNC, WWF, and the University of Manchester, 2016).

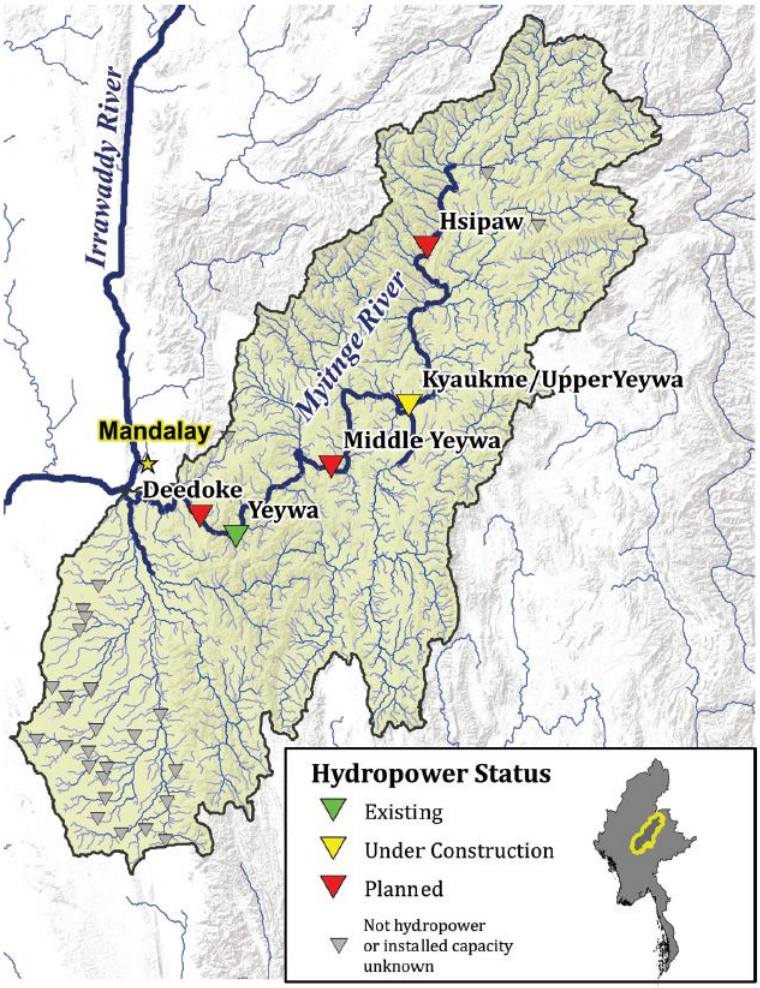

Figure 3.10: Hydropower overview in the Myitnge river basin (TNC, WWF, and the University of Manchester, 2016)

3.2.3. Key ecological processes and values

According to a state of the basin assessment carried out for the entire ecohydrology of the Ayeyarwady, the crucial biodiversity assets, ecological processes and associated ecosystem services in the Myitnge basin are as presented in Table 3.1. The table shows the estimated relative importance (or occurrence, depending on the category) of these factors for the entire river basin. Each aspect is scored as a 3, 2, or 1 for high, medium, or low, respectively. The results show that when looking at biodiversity assets, migratory species are plentiful and are of vital ecological importance in this river basin. There are many flowing rivers and streams, but few KBAs. Floodplain wetlands and rare or endemic species have both received a medium score, because of their occurrence. Looking at the ecological processes, floodplain primary productivity, lateral and longitudinal connectivity all have received a medium score for estimated importance. The fisheries production as a ecosystem value within the Myitnge basin has also been estimated of medium importance in relation to the remaining Ayeyarwady river.

Table 3.1: Ecosystem components of the Myitnge and their relative importance (Kennard et al., 2017)

Component	Type	Myitnge basin score
Biodiversity assets	*Migratory species*	3
	Rare/endemic species	2
	Floodplain wetlands	2
	Flowing rivers and streams	3
	Key Biodiversity Areas	1
Ecological processes	*Floodplain primary productivity*	2
	Lateral connectivity	2
	Longitudinal connectivity	2
Ecosystem values	*Fisheries production*	2

Figure C.2 in Appendix C shows the identified KBAs. In the Myitnge basin lie six KBAs, ranging from 37 to 881km^2. Table 3.2 shows the numbers (corresponding to map C.2), area names, priority and surface area.

Table 3.2: Key Biodiversity Areas in the Myitnge basin (Wildlife Conservation Society, 2013)

KBA number	KBA name	Priority	Area (km^2)
39	Mehon	More information needed	881
43	Myaleik Taung	High	37
60	Peleik Inn	Medium	37
68	Taung Kan at Sedawgyi	More information needed	37
72	Yemyet Inn	Medium	42
93	Maletto Inn	Medium	386

An ecological example from Myitnge: Batagur trivittata

The Burmese roofed turtle shown in Figure 3.11, Batagur trivittata, was a critically endangered endemic species historically known to be present only in the Ayeyarwady, Chindwin, Sitaung, and lower Salween rivers of Myanmar. Excessive egg collection, the cultivation of seasonal agricultural fields at the expense of nesting beaches, and long-term over-harvesting of adult species led to major population declines. By the 1970s, the Burmese roofed turtle was assumed to be extinct (Lee and Zöckler, 2018). During a Wildlife Conservation Society expedition in 2001, however, the species was “rediscovered” in the Myitnge (Platt et al., 2005). Unfortunately the Myitnge population is now thought to be extinct once more after the construction of the Yeywa dam which flooded many nesting areas when filling up the reservoir, and allowed many fishermen to reach the upstream areas of the Myitnge (Lee and Zöckler, 2018).

Figure 3.11: Batagur trivittata (Asian Turtle Trade Working Group, 2000)

3.3. Myittha

3.3.1. River basin specifications

The second study area is the basin of the Myittha river. The Myittha meanders actively from it's origin in the Chin hills north towards Kalewa, where it enters the Chindwin. The digital elevation map presented in figure 3.12 clearly shows the high Chin mountain range on the west side. The lower (blue) area on the east shows the floodplain areas, where most of the villages and agriculture are located.

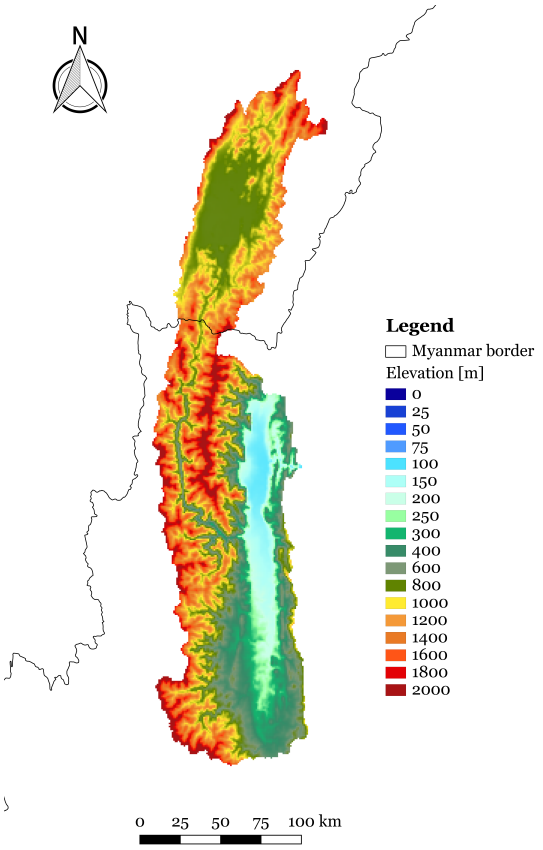

Figure 3.12: Digital elevation map of Myittha catchment

The geological map, soil map, and landcover map are again presented in Appendix C. The basin consists of mostly humic cambisols in the mountaineous regions within the Myanmar borders, as shown in Figure C.4b. Cambisols are characterized by the absence of a layer of accumulated clay, humus, soluble salts, or iron and aluminum oxides. Because of their aggregate structure and significant content of weatherable minerals, they are very suitable for agricultural purposes (FAO-Unesco, 1974). In the lower floodplain area, the soil consists of ferralic cambisols (again, favorable for agriculture) and humic gleysols. Gleysols are usually characterized by both chemical and visual evidence of iron reduction. These soils are formed under waterlogged conditions due to rising groundwater. In Myanmar the land consisting of this soil is cultivated for rice or, when drained, field crops and trees. Across the Indian border in the Myittha basin, a significant amount of orthic acrisols comprise the area, the characteristics of which have been explained in section 3.2.1 (FAO-Unesco, 1974).

Looking at the geology, the basin consists almost entirely of Paleogene sedimentary rocks. Other than that, the area with a lower elevation consist of Quaternary sediments, which are relatively new compared to the surrounding geology. There is also a very small fraction of Cretaceous sedimentary rocks in the south of the basin, which are the oldest in the basin (USGS et al., 1998).

Like the Myitnge, the land cover of the Myittha is mostly closed to open shrubland that is shorter than $5m$, as shown in Figure C.5b. There are also significant amounts of rainfed croplands, mosaic cropland, and mosaic vegetation across the whole watershed area. In the south of the basin there are significant amounts of open broadleaved deciduous forest/woodland taller than $5m$. Near the downstream Myittha there are areas of post-flooding or irrigated croplands. Finally there are some areas of closed to open broadleaved evergreen or semi-deciduous forest spread across the more mountainous waterbasin regions (ESA 2010 and UCLouvain, 2010).

Figure 3.13 shows the average monthly low and high water levels in the Myittha, as well as two extremes (in 2012 and 2015). This graph is based on data provided by the Department of Meteorology and Hydrology in Myanmar. The extreme monthly water levels were measured at the station near Kalaymyo between 2008 and 2017. The graph shows that in July and August of 2015, the water level was about twice as high as the average water level during that time of the year. Furthermore, in 2012, the water level was at it's lowest for the observation period, but this still does not appear to be far off the mean. This suggests quite a stable baseflow throughout the year.

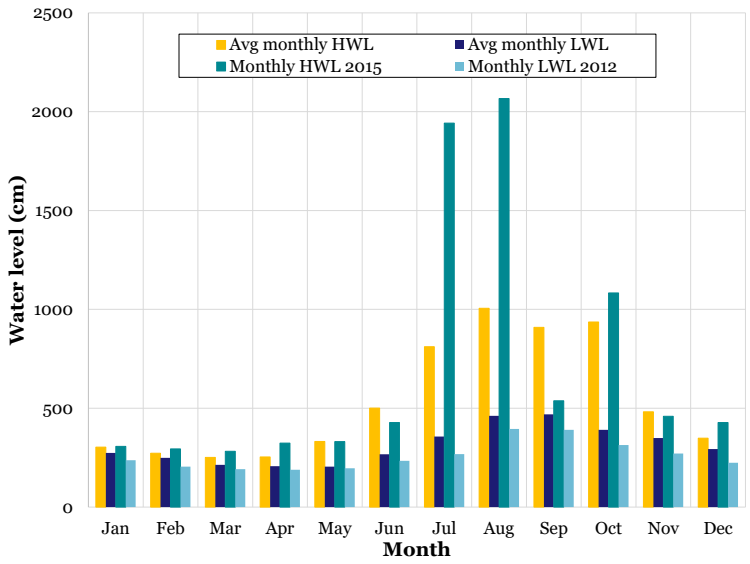

Figure 3.13: Average and extreme monthly water levels of Myittha river (2008-2017), based on data provided by the Department of Meteorology and Hydrology in Myanmar

3.3.2. Hydropower

There are two existing dams in the Myittha basin area, namely the Myittha dam and the Yazagyo dam. The 40 MW Myittha multipurpose dam in Gangaw District, Magway Region, is currently the only dam actually on the Myittha River. The dam was completed by the Myanmar Ministry of Agriculture, Livestock and Irrigation. It comprises a 63m high earth dam and a reservoir with storage capacity of 0.325 km^3, inundating 12 km^2. The power plant of the Myittha dam is connected to Gangaw by a 40 km long 66 kV transmission line (IFC, 2017). The Yazagyo dam, located near the village with the same name, was constructed to reduce floods, irrigate crops and generate hydropower for local electricity consumption. The project started in 2003 on Nerinzara Creek with three saddle dikes with a total length of more than 2,700m. The 4 MW earth dam, completed in 2015, has a reservoir with a storage capacity of 0.064km^3. It is mainly used to irrigate over 32km^2 of agricultural fields (Global New Light of Myanmar, 2015).

Future plans

There are plans for a 380 MW dam on the Manipur, a mountainous tributary to the Myittha, originating in Manipur State, India. The Manipur project was designed as a 168m high dam with a reservoir storing 1.554 km^3. The power plant will be connected to Gangaw-Kalay by a 32 km long 230 kV transmission line. Although this was the original plan, it is unlikely that the project will be completed by 2021 (IFC, 2017).

Figure 3.14: Ardea insignis (HBV Alive, 2019)

3.3.3. Key ecological processes and values

According to the same state of the basin assessment carried out for the entire ecohydrology of the Ayeyarwady, the key biodiversity assets, ecological processes and associated ecosystem services in the Myittha basin are as presented in Table 3.3 (Kennard et al., 2017). As explained before, the assessment scores the estimated relative importance and/or occurrence of each factor for the river basin as a 3, 2, or 1 for high, medium, or low, respectively. The results show that in the Myittha, rare and/or endemic species have a score of 3, meaning they are plentiful and are of great importance. They are therefore also at a great risk. For example, the White-bellied Heron, Ardea insignis, is listed as a critically endangered and near-endemic to a few areas in Myanmar (WCS, 2015). One of these areas is in Chin state, where the Myittha basin is located. A Wildlife Conservation Society survey from 2009-2011

indicated that human disturbance and loss of habitat are significant threats
to this species, presented in Figure 3.14, in Myanmar (WCS, 2015).

Flowing rivers and streams also score high, highlighting the dense river network and its ecological significance. When looking at other biodiversity assets, migratory species and floodplain wetlands score a 2, meaning they are of medium importance. Regarding the ecological processes, floodplain primary productivity, lateral and longitudinal connectivity all have received a medium score for estimated importance. The fisheries production as a ecosystem value within the Myittha basin has been given little importance, most likely due to the small population density in the area.

Table 3.3: Ecosystem components of the Myittha and their relative importance (Kennard et al., 2017)

Component	**Type**	**Myittha basin score**
Biodiversity assets	*Migratory species*	2
	Rare/endemic species	3
	Floodplain wetlands	2
	Flowing rivers and streams	3
	Key Biodiversity Areas	1
Ecological processes	*Floodplain primary productivity*	2
	Lateral connectivity	2
	Longitudinal connectivity	2
Ecosystem values	*Fisheries production*	1

Table 3.3 presents a low score for the occurrence of KBAs in the Myittha basin. Figure C.2 in Appendix C shows the identified KBAs in Myanmar. In the Myittha basin lie three KBAs, and one that partly falls inside the study basin area. Table 3.4 gives an overview of the numbers (corresponding to map C.2), area names, priority and surface areas within the Myittha basin.

Table 3.4: Key Biodiversity Areas in the Myittha basin (Wildlife Conservation Society, 2013)

KBA number	**KBA name**	**Priority**	**Area (km^2)**
9	Bwe Pa	More information needed	152
28	Kennedy Peak	More information needed	108
50 (partly)	Natmataung N.P	High	1100
73	Zeihmu Range	More information needed	81

Summary of Study Locations chapter

Myanmar, encompassing almost 700,000km^2 is one of the water-richest countries in Asia, but still major challenges in the water resources management exist because of the irregular temporal and spatial distribution. The nation has three parallel chains of forest-clad mountain ranges that run north to south from the Himalayan mountain range, dividing up the river into the three river systems, of which the Ayeyarwady is one. The Ayeyarwady, one of the world's longest and largest remaining free-flowing rivers, is fed by tropical monsoons. Thee basin provides habitat to many important freshwater species and ecosystem services, as well as playing a key role in the development of Myanmar through agriculture and fisheries.

The country is positioned along the path of the Asian monsoon circulation and separated from neighboring countries by high mountain walls. More than 95% of the annual national mean precipitation is received from the Southwest Monsoon, which takes place from May until October. The reversal of the wind patterns, from November to February (Northeast Monsoon), brings a dryer and cooler climate to Myanmar. The mean maximum temperature is about 37.8°C in Central Myanmar and the mean minimum temperature is between 4.4°C and 10.0°C, in the Northern part of Myanmar.

Myanmar has only developed a little over 3% of it's 100 GW hydropower potential as of 2016. Therefore there are plans to substantially increase the hydropower capacity of Myanmar in the future to meet both the domestic energy demand and to gain foreign capital from electricity exports.

This study focuses on two major tributary rivers: the Myitnge and the Myithha. The 530km long Myitnge is a large tributary of the Ayeyarwady located in the central eastern part of Myanmar. It has a watershed area of approximately 30,000km^2, originating in the mountains at about 1400m above sea level. In an average hydrologic year, the flow in the Myitnge river varies naturally between 200 and 300m^3/s from December until May, after which it rapidly increases to a peak of about 1200m^3/s, usually reached between the beginning of August and the end of September. The river hosts the 790 MW Yeywa hydropower dam, which was completed in 2011. It is the largest existing hydropower dam in Myanmar, with a 75 km long and narrow reservoir along the Myitnge's main branch with a total storage capacity of about 2.6km^3. There are plans for atleast four more confirmed hydropower projects in the next ten years for the Myitnge basin, with the aim of creating a cascaded run-of-the-river system that will provide all of Mandalay with electricity.

The second study river basin, the Myittha, meanders actively from it's origin in the Chin hills north through a large agricultural floodplain area towards Kalewa, where it enters the Chindwin. The average water level at Kalaymyo station ranges from 2,5m in the dry season to about 10m in the wet season. The 40 MW Myittha dam and the 4 MW Yazagyo dam exist in the basin. The former has a reservoir with storage capacity of 0.325 km^3, inundating 12 km^2, whereas the latter has a reservoir with a storage capacity of 0.064km^3. There are plans for a 380 MW dam on the Manipur, a mountainous tributary to the Myittha, originating in Manipur State, India.

According to Kennard et al. (2017), the most important environmental assets and values that need to be considered for the Ayeyarwady basin (and hence in the study areas) are five groups of biodiversity assets, three ecological processes that underpin the above assets and values, and one provisioning ecosystem service. The biodiversity assets are migratory species, rare and endemic species, floodplain wetlands, rivers and streams, and Key Biodiversity Areas (KBAs). The ecological processes are floodplain primary productivity, lateral connectivity and longitudinal connectivity. The ecosystem service of greatest importance is fisheries production. The most important ecological aspects of the Myitnge are migratory species and flowing rivers and streams. In the Myittha rare or endemic species as well as flowing rivers and streams are most important.

4

Methodology

This chapter aims to explain the methods and materials used in this research. A schematisation of the steps involved in the method is presented in Figure 4.1, and descriptions are provided in the ensuing sections. A summary of the entire research methodology is given in the summary box at the end of the chapter.

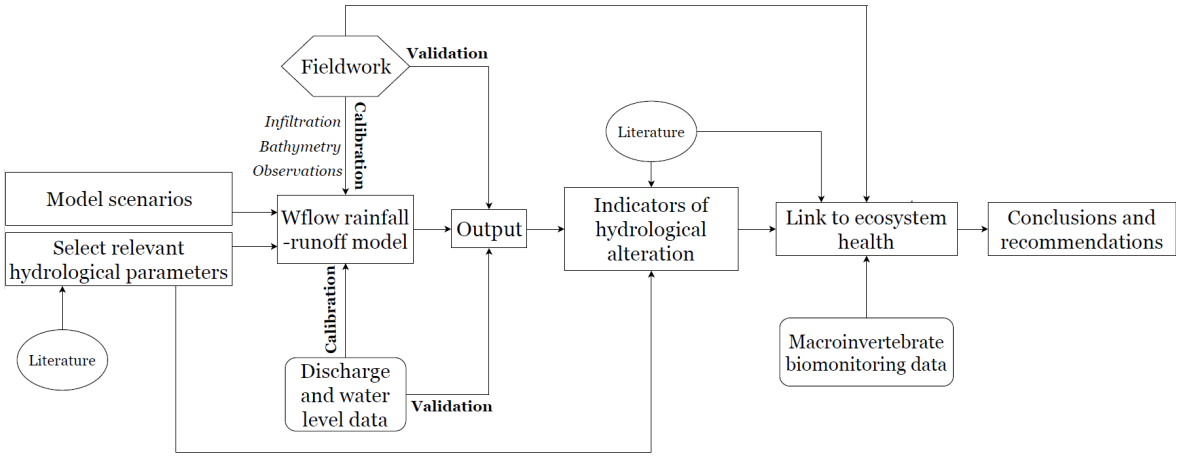

Figure 4.1: General methodology of study

The aim of the research is to quantify the hydrological alterations to the natural flow regime by Yeywa hydrodam operations and to assess the impact of these alterations on the ecohydrology of the Mytinge basin. Furthermore the aim is to evaluate the suitability of the *WFlow_sbm* rainfall-runoff model as a tool for environmental flow management. Important hydrological parameters have been discussed in detail in Chapter 2. The *WFlow_sbm* model and the model scenarios will be explained in section 4.1 of this chapter. The model will partially be calibrated on data collected directly from the field. The methods and materials for the fieldwork are described in section 4.2. The field data are partially used as input for the model, and partially for the environmental flow assessments. The methods used for the latter are described in section 4.3. The data required for all these analyses that jointly form the methodology, and the means of obtaining and validating these data, is elaborated on in the final, section 4.4.

4.1. The WFlow_sbm hydrological model

In this research, the *WFlow_sbm* hydrological model is used, which is part of the Deltares OpenStreams project (Schellekens, 2018). The *WFlow_sbm* model is a distributed hydrological model that maximizes the use of globally available spatial data while minimizing the required calibration. It consists of a set of python programs that can be run on the command line and perform hydrological simulations. The model uses PCRaster, which in turn makes use of a dynamic modelling language within a GIS framework. PCRaster is

an environmental modelling language to build dynamic spatial environmental models. Section 4.1 will start with a general model overview, after which the data requirements will briefly be listed. The model processes are visually presented in subsection 4.1.2 and described in more detail in Appendix D. The model outputs and created input scenarios are discussed in subsections 4.1.3 and 4.1.4, respectively. The chapter concludes with information on methods for calibrating, validating and evaluating the model.

4.1.1. Model overview

This section will briefly discuss the use of *WFlow_sbm* for the purpose of this research. Subsequent sections will feature more detail on the underlying processes of the model.

The first step of the *WFlow_sbm* model is to delineate the river network and watershed based on digital e data. Subsequently, land use maps and soil maps (as presented in Appendix C) are added to the model and used to estimate some physical parameters of the soil and land characteristics. The model requires potential evaporation as input and converts that into actual evaporation using land cover types and soil water content. The rainfall interception is calculated using Gash (1979; 1995). In order to determine the average precipitation and evaporation from the wet canopy, the model computes the total precipitation and evaporation under saturated-canopy conditions for each storm event separately first. Different parameters such as the rooting depth, the Leaf Area Index (LAI), the ratio of evaporation from the wet canopy to average rainfall ($\overline{E}_w/\overline{R}$), the fraction of the incident radiation that is reflected from the land's surface (albedo), the Canopy Gap Fraction, and the maximum canopy storage, are assigned to each land cover type. These parameters are used by the *WFlow_sbm* model through look-up tables, from which input parameter maps are created.

The soil is modelled using a simple bucket model that assumes the exponential decay of the saturated hydraulic conductivity K_{sat} with depth. Using the Darcy equation, lateral subsurface flow is modelled, whereas soil depth is assumed a function of different land uses, and hence scaled using the Topographic Wetness Index.

The surface runoff is modelled using a kinematic wave routine. When rain falls onto a surface of the soil that is partially saturated, the model assumes that that rainfall directly becomes runoff. To quantify the effects of urban areas, the model makes use of a sub-cell parameterization. More specifically, a fraction of a cell represents a compacted soil surface with reduced infiltration capacity.

As *WFlow_sbm* is a fully distributed model, the calculations are done for each grid cell of the basin in question. Each gridcell presents a 500m x 500m bucket with a total depth divided into saturated and unsaturated areas. The model output is hence streamflow per gridcell. The results from the modelling are used for further hydrological analysis of alterations in flow regimes using the analyses discussed in Section 4.3.

The data requirements of the *WFlow_sbm* model depend somewhat on the application it is used for. The fundamental static data requirements are a Digital Elevation Model (DEM), a land cover map and a physical soil parameters map, which have all been discussed in Chapter 3 and presented in Appendix C. The required dynamic data (in the form of spatial time series or map-stacks are precipitation, potential evaporation and transpiration and temperature. Using these data, the model is able to produce results. There are a lot more input variables that determine the output, however. More information on the necessary data for the model and how it is collected can be found in section 4.4. This includes both primary and secondary collected data.

4.1.2. Model processes

An overview of the different processes and fluxes in the *WFlow_sbm* model are given in Figure 4.2. An elobration on the calculations for reference evaporation, as well as the rainfall interception model and soil model is given in in Appendix D.

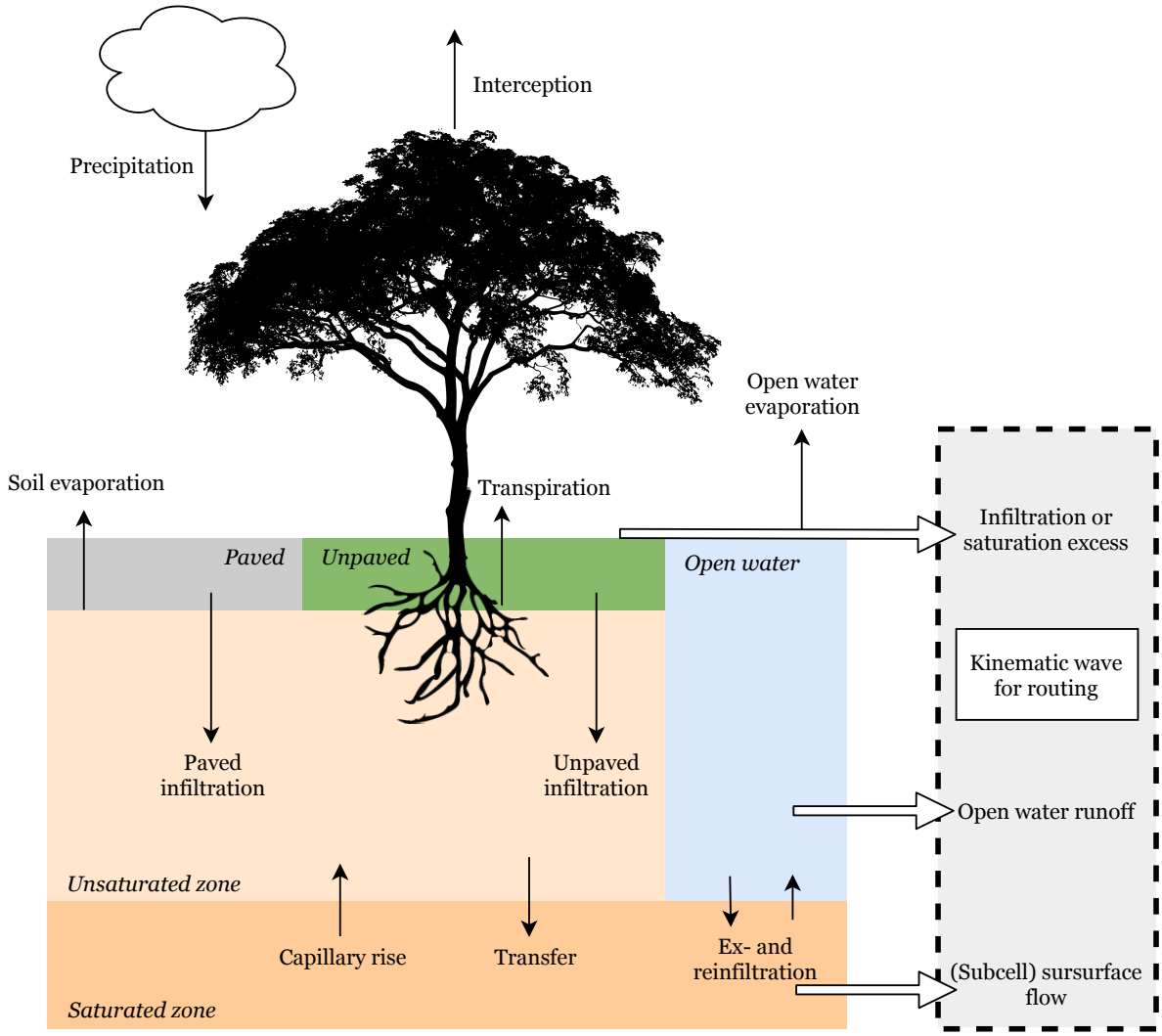

Figure 4.2: Overview of the different processes and fluxes in the *WFlow_sbm*, adapted from (Schellekens, 2018)

The kinematic wave

For the routing, *WFlow_sbm* uses a kinematic wave, which describes flow over planes. The wave assumes that that the lateral flow is equal to the difference between the rates of rainfall and infiltration, and the channel flow to be flow per unit width of plane (Chow et al., 1988). Regarding the Saint Venant governing equations, the kinematic wave neglects local acceleration, convective acceleration, and the pressure terms in the momentum equation, and uses the full continuity equation. This is illustrated by the modified equations 4.1 and 4.2 (Chow et al., 1988).

$$g(S_o - S_f) = 0 \quad [Momentum] \tag{4.1}$$

$$\frac{\partial Q}{\partial x} + \frac{\partial A}{\partial t} = 0 \quad [Continuity] \tag{4.2}$$

In these equations, g is the gravitational acceleration in m^2/s, S_O is the channel bottom slope, and S_f is the friction slope. The terms $\frac{\partial Q}{\partial x}$ and $\frac{\partial A}{\partial t}$ are the rate of change of channel flow with distance and the rate oc change of cross-sectional area with time, respectively. As equation 4.1 shows, the kinematic wave assumes that friction and gravity balance each other out so that $S_o = S_f$.

The celerity of the wave created by a change in the flow (through a change in flow rate or the water level) is defined as the velocity with which this change moves along the river. For a kinematic wave the wave motion

is described by the continuity equation only: kinematics (through mass and force) control the wave motion. The kinematic wave celerity, c_k is given by

$$c_k = \frac{dQ}{dA} = \frac{dx}{dt} \tag{4.3}$$

This means that an observer moving with the flow at a velocity of c_k would see the flow rate increasing at a rate of $dQ/dx = q$.

4.1.3. Model outputs

There are several variable outputs that the *WFlow_sbm* can deliver, and in different formats. One of these is output timeseries in csv format. For each section, a sample map is created which determines how the timeseries is averaged/sampled. Each variable is stored as a timeseries in the specified directory with its given filename. The model can save the actual value, but also other types of summary maps, as listed:

- summary: saves the actual value of the variable
- summary_avg: saves the average value over all timesteps of the variable
- summary_sum: saves the sum over all timesteps of the variable
- summary_min: saves the minimum value over all timesteps of the variable
- summary_max: saves the maximum value over all timesteps of the variable

Output can also be saved as mapstacks which are time series data (grids), or as export grid data in netcdf-format. An example of a streamflow gridded map output is given in figure 4.3. Amongst the many output types, the most important output for this research is streamflow and water level data timeseries. These are extracted from the model both as daily gridded mapdata and as a summary csv file at the gauge stations. For validation and calibration purposes, the gauge stations are chosen based on where the fieldwork was carried out as well as where the existing secondary data sets were measured.

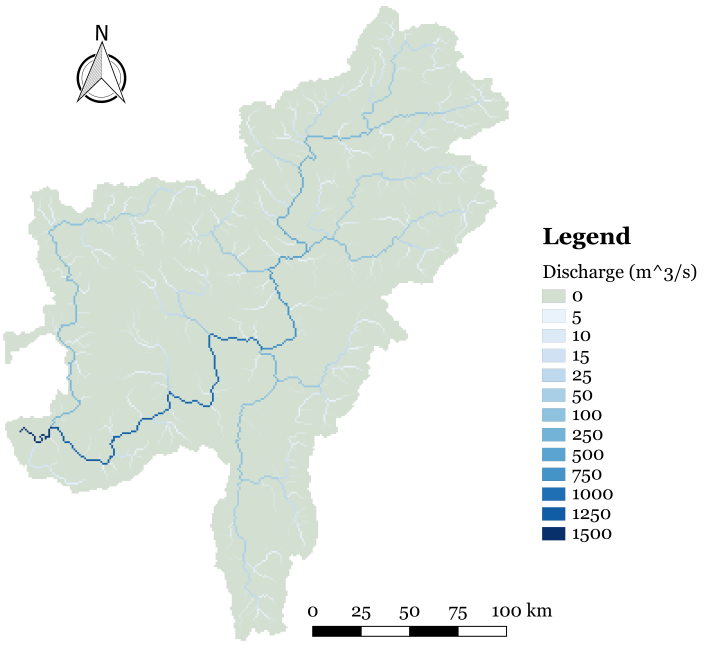

Figure 4.3: Example of gridded map output for modelled streamflow in Myitnge catchment

Another model output used in this research is river width, which is an important parameter for calibrating on fieldwork data, as well as for ecological purposes. The variable is estimated from the DEM, the upstream area and the yearly average discharge (Finnegan et al., 2005). The yearly average discharge, which is an input parameter in the model, is scaled for each point in the drainage network with the upstream area. This is based on the work of Finnegan et al. (2005), who proposed an expression for scaling the steady state width

of river channels as a function of discharge, channel slope, roughness (through the Manning coefficient), and the width-to-depth ratio. The width-to-depth ratio is presented in the model as the parameter α, given by $\alpha = W/D$ where W and D are bank-full river width and depth, respectively. This is discussed further in section 4.1.5.

For further validation and calibration purposes, the output mapstack grids extracted are: sum, maximum, and average precipitation, average canopy storage, and average temperature. The output CSV files, and their associated sample maps are:

Table 4.1: Variable csv outputs used in this research with their codes and sample maps

Sample map	Code	Variable output
Gauges map	self.SurfaceRunoff	Streamflow at the locations specified by the gauges map [m^3/s]
	self.WaterLevel	Water level above the bottom at the specified gauge locations [m]
	self.Bw	Width of the river at the gauge locations [m]
Subcatchment map	self.Precipitation	Gross precipitation per timestep over the whole catchment area [mm]
	self.PotenEvap	Potential evapotranspiration per timestep over the whole catchment area [mm]
	self.ActEvap	Actual evapotranspiration per timestep over the whole catchment area [mm]
	self.ActEvapOpenWater	Actual open water evaporation per timestep over the whole catchment area [mm]
	self.Interception	Actual rainfall interception per timestep over the whole catchment area [mm]
Landcover map	self.PotenEvap	Potential evapotranspiration per timestep per landcover type [mm]
	self.ActEvap	Actual evapotranspiration per timestep per landcover type [mm]
	self.CanopyStorage	Amount of water on the canopy per timestep per landcover type [mm]

When modelling reservoir operation scenarios, the model outputs are the runoff and water level upstream and downstream of the reservoir, as well as the reservoir storage volume, at every timestep.

4.1.4. Input scenarios

To explore the current and future impacts of dam operations, scenarios are created. These scenarios are conceptually presented in figure 4.4. For each of these scenarios, an expected flow regime is simulated. This flow regime is subsequently analyzed through environmental flow assessment methods, described in section 4.3.

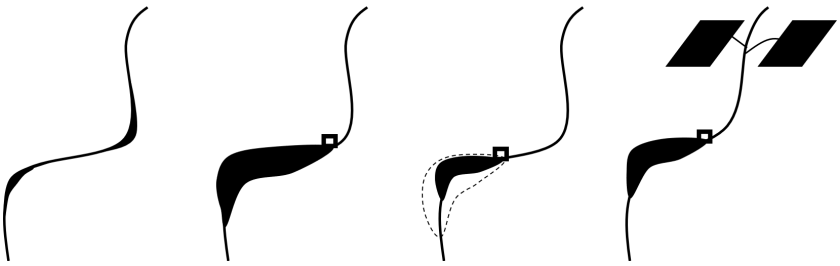

Figure 4.4: Model scenarios: Myitnge river schematically presented from above with (potential) reservoir upstream (bottom left)

Scenario 0: Natural flow regime

Scenario 0 aims to describe the unaltered river: the natural flow regime. For the Myitnge, the *WFlow_sbm* model is calibrated to represent the natural flow regime on streamflow measurement data from before the start of the dam construction (1982-2004). For the Myittha, it is calibrated based on water level data from before the dam, for no streamflow data is available.

Scenario 1: (Maximum) power operation

Scenario 1 aims to explore what happens when a hydrodam starts controlling the flow regime with the goal of generating electricity. For the Myitnge this scenario is, first of all, based on the current operation of the Yeywa dam. The power generation magnitude and efficiency are subsequently increased, and the impact of this on the flow regime simulated and evaluated.

The reservoir is based on a simple water balance function, and is modelled as follows. The model is provided with a map that includes the location of the Yeywa reservoir. The model is furthermore provided with a set of lookup tables that link the reservoir on the map with reservoir characteristics:

- **ResTargetFullFrac.tbl**: the target full fraction (of max storage) for the reservoir, which is between 0 and 1.
- **ResTargetMinFrac.tbl**: the target minimum full fraction (of max storage), which is also between 0 and 1 but should always be more than the ResTargetFullFrac (above)
- **ResMaxVolume.tbl**: The maximum reservoir storage (above which water is spilled) [m^3]
- **ResDemand.tbl**: The water demand of the reservoir (all combined) [m^3/s]
- **ResMaxRelease.tbl**: The maximum discharge that can be released if the reservoir water level is below the spillway [m^3/s]

Precipitation and upstream runoff go into the reservoir, and evaporation and outflow go out. The minimum flow is scaled using a simple sigmoid curve, which takes into account the target minimum full fraction. The actual outflow also considers the target full fraction.

Scenario 2: Flood mitigation

The dam can also be operated for flood mitigation. By managing the reservoir volume accordingly, the reservoir will have some spare storage space to dampen incoming floods. This scenario assumes that the reservoir will not always be filled for power generating purposes. Dam releases are based on historical floodings (i.e. with certain return periods). The impact of this type of operation on the flow regime is estimated and assessed.

Scenario 3: Water for irrigation

Down and upstream of the Yeywa dam is an expanding agricultural area. Because of the rainfall and hydrological patterns, the need for irrigation is highest in the central dry zone, in which the downstream end of the Myitnge is located (FAO, 2016). Therefore, in scenario 3 an increased agricultural water demand is simulated by incorporating an expanded irrigation area map. The map is based on FAO data, showing the global areas equipped for irrigation (in 2005) (Siebert et al., 2013). This scenario assumes that all areas equipped for irrigation are actually cultivated and irrigated by water from the Myitnge. The irrigation water demand is estimated by the model by an algorithm which works as follows. The irrigation water demand is the fraction of the crop water requirement that is not satisfied by rainfall, soil water storage and groundwater. Therefore, for each defined irrigation area, the difference between potential transpiration and actual transpiration is determined (further explained in Appendix D), which is assumed as the irrigation demand. Subsequently, this difference is converted to a flux demand [m^3/s] at the corresponding intake point at the river (Schellekens, 2018). The irrigation intake is taken as a single point, at the location of an existing irrigation pump (see Figure 4.5). Taking into account the available water in the river, the irrigation demand is converted to a supply in mm over the entire defined irrigation area. In the next time-step of the model, the supply is assumed as extra water available for infiltration in the irrigation area. The altered flow regime is simulated and evaluated.

Figure 4.5: Existing irrigation intake on the Myitnge

4.1.5. Calibrating and validating the model

The *WFlow_sbm* model, like most hydrological models, aims to represent the behaviour of the study catchment areas as well as possible. The model uses forcing inputs and model parameters, where the latter are inherent properties of the hydrological system and are mostly assumed constant in time for the modelled period. Model parameters need to be specified, which can be done through direct measurements, derivation from analysis of measured variables, derivation from literature, or/and calibration (Savenije, 2009). This section will elaborate on how the model is calibrated and validated.

Calibration of *WFlow_sbm*

The most important calibration of the *WFlow_sbm* model is done through the altering of input variables which impact the hydrograph, which is a graph plotting discharge as a function of time at a particular point in the river. The variables are listed below (Schellekens, 2018).

- N: This is the Manning coeffient, given an indication of the roughness of the various land cover types and streams. This coefficient controls the shape of the hydrograph, especially the peaks. The values from literature are presented in table E.4 in Appendix E.
- M: This soil parameter represents the decay of the saturated hydraulic conductivity with depth. It is graphically presented in Figure 4.6. Once the depth of the soil has been set for the different land-use types, this parameter is the most important variable in calibrating the model. This variable controls the baseflow resession of the hydrograph and part of the stormflow curve.
- K_{sat}: This is the saturated hydraulic conductivity, which depends on the landcover types. Increasing these values will lower the hydrograph (baseflow) and flatten the peaks, depending on the catchment shape. Beginning values for K_{sat} are estimated from infiltration tests carried out during fieldwork, as explained further in section 4.2.3.
- $S_{cap,soil}$: This is a measure for the storage capacity of the soil. Increasing the value of this will decrease the outflow.

The model also provides the possibility to match streamflow data at the outlet, if this (observed) data is provided. In this research this option is not used, however. This is for two reasons. The first is that the provided discharge data from the Myitnge may not be of the desired quality, and hence is not necessarily the streamflow that the model should strive to match. This is further discussed in Chapter 5. The second reason is that one of the aims of the research is to see what kind of environmental flow recommendations can be derived from *WFlow_sbm* only. The objective is to see if the natural flow regime can be simulated in areas with scarce data availability, without streamflow measurements.

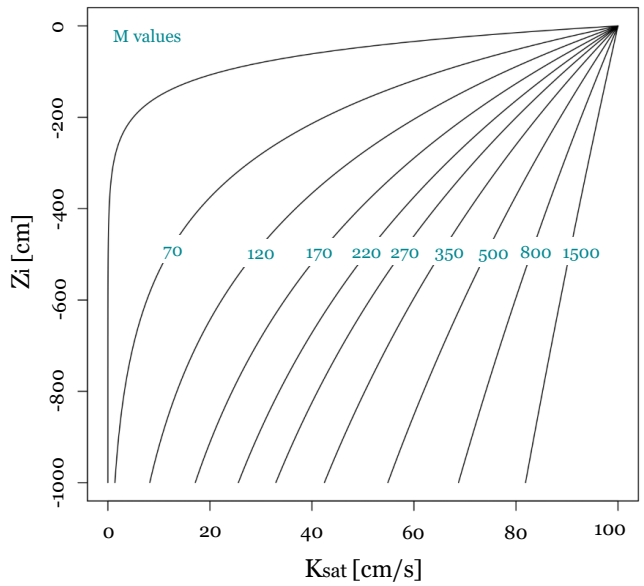

Figure 4.6: Decay of saturated hydraulic conductivity with depth: the M parameter, assuming that K_0=100

Validation of results and model evaluation

The results of the model are validated against secondary data, namely data collected from sources in Myanmar. In the Myitnge discharge data exists from 1982 until 2016 at the Shwesaryan Pagoda station location, based on water levels measurements and a rating curve. Furthermore there exists in- and outflow data from

the Yeywa dam between 2011 and mid 2018, which is retrieved from the dam operators directly. Gauges are specified within the model at these locations so that model runoff can be compared to the existing data for validation. For the Myittha river, only maximum and minimum monthly water levels for the 2008-2017 period exist, measured at the Kalaymyo hydrological station. Therefore, a gauge is built into the model at this station in the Myittha bank, so that model produced minimum and maximum water levels can be compared to the measured ones.

The evaluation of the hydrologic model behavior when simulating the natural flow regime of the Myitnge is done through visual aids, mathematical criterion and E-flow assessment results. Visual aids allow researchers to evaluate models by using graphical means to compare observed and simulated values. This evaluation method is often considered qualitative and biased because the model fit is evaluated by eye. The visual aids used in this research include three plots:

1. Hydrograph over the simulation period: observed versus simulated flows over time
2. Q-Q plots of the observed data against the simulated data
3. Flow duration curves: observed versus simulated flows

A drawback of this type of evaluation is the dependence on the viewer's own experience and references, which makes it relatively subjective (Houghton-Carr, 1999).

The mathematical criteria essentially (relatively) quantify the distance between observed and simulated flows. The ones used in his research are as follows.

1. **Coefficient of determination** R^2, given by:

$$R^2 = \left(\frac{\sum_{i=1}^{n}(Q_{obs,i} - \bar{Q}_{obs})(Q_{sim,i} - \bar{Q}_{sim})}{\sqrt{\sum_{i=1}^{n}(Q_{obs,i} - \bar{Q}_{obs})^2}\sqrt{\sum_{i=1}^{n}(Q_{sim,i} - \bar{Q}_{sim})^2}} \right)^2 \tag{4.4}$$

   This coefficient is sensitive to peak flows due to the squared term. This is at the expense of better performance during low flow conditions, however. It should also be noted that this coefficient is based on correlation only (Krause et al., 2005).

2. **Nash-Sutcliffe Efficiency** NSE, given by:

$$NSE = 1 - \frac{\sum_{i=1}^{n}(Q_{obs,i} - \bar{Q}_{sim,i})^2}{\sum_{i=1}^{n}(Q_{obs,i} - \bar{Q}_{obs})^2} \tag{4.5}$$

   This criterion is also sensitive to higher flows at the expense of improvements on the low flow predictions Krause et al. (2005).

3. **Logartihmic Nash-Sutcliffe efficiency** $NSLE$, presented below:

$$NSLE = 1 - \frac{\sum_{i=1}^{n}(\log Q_{obs,i} - \log \bar{Q}_{sim,i})^2}{\sum_{i=1}^{n}(\log Q_{obs,i} - \log \bar{Q}_{obs})^2} \tag{4.6}$$

   The logarithmic Nash-Sutcliffe Efficiency parameters reacts less on peak flows and stronger on low flows than the regular Nash-Sutcliffe Efficiency.

4. **Relative efficiency criteria** E_{rel}**, as presented:**

$$E_{rel} = 1 - \frac{\sum_{i=1}^{n}(\frac{Q_{obs,i} - Q_{sim,i}}{Q_{obs,i}})^2}{\sum_{i=1}^{n}(\frac{Q_{obs,i} - \bar{Q}_{obs}}{\bar{Q}_{obs}})^2} \tag{4.7}$$

   This coefficient is sensitive to low flows only and not reactive to peak flows at all.

5. **Root mean square error** $RSME$**:**

$$RMSE = \sqrt{\frac{\sum_{i=1}^{n}(Q_{sim} - Q_{obs})^2}{n}} \tag{4.8}$$

   The root mean square error calculates individual differences (residuals) and aggregates them. This forms a measure for the predictive power of the model.

For all criteria except RSME, a value as close as possible to 1 is desired when calibrating. These mathematical criteria should be applied with caution because they do not evaluate the same types nor ranges of values.

The validation of the model also focuses on the aspects of the output that are most relevant for ecology: the prediction of magnitude, frequency, duration, timing and rate of change of the flow regime. This will be done by means of some of the processed data, namely the environmental flow assessments. If the Range of Variability of the indicators of hydrologic alteration (see section 4.3) give the same or similar results for the modelled output and the measured data, then the model retains enough physical realism to be useful for the desired practical application of this research, and is deemed successful. The Range of Variability approach (explained in section 4.3) of the indicators of hydrologic alteration can also be used to compare the observed and simulated flow data directly.

4.2. Field data collection

4.2.1. Visual hydrology

A lot of the model parameters can be calibrated based on what is simply observed with the eye in the field. Natural landscapes are defined on the basis of climate, topography, vegetation and geology, of which a lot can be observed without instruments. For example, a landcover map extracted from satellite data can be partially validated just by visiting different locations and observing landcover types. This is of crucial importance because interception and transpiration, both of which are primarily determined by vegetation cover which is a function of landcover, are the two largest parts of total evapotranspiration. This means that getting an indication of the types and extent of vegetation can be a determining factor in the model outcome. Observing processes in the field will also help make sense of possible discrepancies between measured and simulated data.

In both the Myitnge and the Myittha catchments, the visual hydrology consists of driving around the catchment area, and sailing along the river with a boat, to take photographs as well as notes of the observed processes. A visit to the Yeywa dam and an interview with some dam operators is executed. In the Myittha, a fieldtrip with a geologist and geographist from Kalay Technological University also allows for some insights.

4.2.2. Bathymetry

Bathymetry refers to the study of the underwater topography of, in this case, the river bed. For the river width, the Nikon rangefinder Forestry Pro is used, as displayed in Figure 4.8d. This device is a hypsometer: a combination of a clinometer and laser rangefinder. It measures heights and distances up to 500m. Amongst other applications it can measure the width of wider rivers, when using other methods becomes unpractical. The device digitally indicates the measured distance in meters and angles in degrees. There are several modes, which are used to get values for river bank height and river width. The modes used in this research are the horizontal distance mode for bank width and the three-point measurement mode for river bank heights. The former calculates the horizontal distance to the target by measuring the linear distance and angle. The latter uses the horizontal distance data to the target (1st point) and angle data of two points (2nd and 3rd) to calculate the vertical separation.

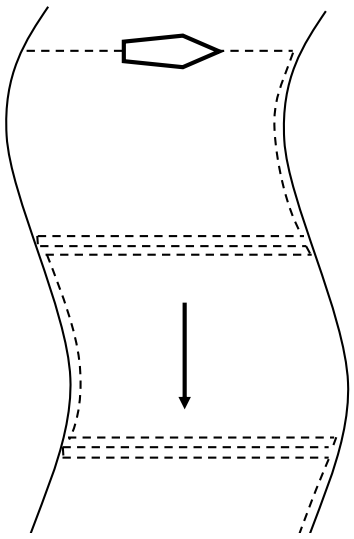

Figure 4.7: Boat route for cross-sections

For measuring the river depth and bottom profile, the Garmin Striker 4 (fishfinder) is used. This device, presented in Figure 4.8b, sends a continuous sweep of frequencies to the river bottom using sound waves, ranging from low to high. The device interprets the frequencies individually upon their return. It measures depths up until 570m, and has a built in GPS so that a location tag is saved with the depth data (GARMIN, 2018). The Garmin GPS receiver is accurate to within 10 meters (Garmin, 2017). The device has a dual-beam transducer with Garmin CHIRP sonar for images and target separation in both shallow and deeper water. Bottom contours are visible, also at higher boat speeds, and signal noise can be suppressed at greater depths for an accurate interpretation of the river bottom (GARMIN, 2018). The transducer is attached to a bamboo stick,

as shown in Figure 4.8a. The bamboo stick is graduated using a tape measure. Once in the boat, the bamboo stick is held perpendicular to the water, and dipped under the water surface until a certain level where it is completely submerged. This level is noted down as the offset for the depth measurement. The boat goes across the river slowly and as straight as possible, following a route that takes each cross-section multiple times, as presented, in Figure 4.7. The depth measurements are marked as waypoints which are stored in the device with an associated set of coordinates and water temperature.

(a) Attaching the transducer to a graded bamboo stick

(b) Display of Garmin during measurements

(c) Logging the cross-section profile

(d) Using the rangefinder to obtain river width

(e) Logging depth longitudinally

Figure 4.8: Measuring river bathymetry during fieldwork

4.2.3. Infiltration and hydraulic conductivity

Hydraulic conductivity is a property of soils and rocks that describes the ease with which water can move through the medium. It gives an estimation of the infiltration capacity for different landcover types. To estimate this parameter, the inverse auger hole test is carried out. The principle of the inverse auger-hole method is as follows. If one infiltrates water continuously into unsaturated soil, the soil around and below the area becomes almost saturated and the wetting front becomes a rather sharp boundary between wet and dry soil after a while. The theory of calculating the saturated hydraulic conductivity using the inverse auger hole test is as follows (Oosterbaan and Nijland, 1994). Let us define a point just above the wetting front at a distance z below the soil surface in the area where the water infiltrates. The matric head of the soil at this point is defined by h_m. At the soil surface, the head is $z + h + |h_m|$, and the average hydraulic gradient between two points can be defined by:

$$S = (z + h + |h_m|)/z \tag{4.9}$$

When z becomes large enough, s approaches unity. This means that the mean flow velocity in the wetted soil below approaches the hydraulic conductivity, as according to Darcy's law. This assumes that the soil is partially saturated. The inversed auger hole method is based on these principles. If a hole is bored into the soil and filled with water until the soil below and around the hole is practically saturated, the infiltration rate will become constant (approximately). The total infiltration will then become equal to the infiltration rate multiplied by the surface area of infiltration. Assuming the hole is deep enough and the soil is partially saturated, infiltration will become equal to the saturated hydraulic conductivity multiplied by the infiltration area. Because of the nature of the experiment, infiltration occurs both through the bottom and the sidewalls of the hole, as shown in Figure 4.9b (Oosterbaan and Nijland, 1994). Therefore the total equation becomes

$$Q = 2\pi K r(h + r/2) \tag{4.10}$$

Where Q is the infiltration, K is the saturated hydraulic conductivity, r is the radius of the hole and h is the height of water level in the hole. The value of Q can be found from the rate at which the water level in the hole decreases. Incorporating this into equation 4.10, eliminating Q, and upon integration and rearrangement, equation 4.11 is obtained (Oosterbaan and Nijland, 1994).

$$K = 1.15r \frac{\log(h_0 + r/2) - \log(h_t + r/2)}{t - t_0} \tag{4.11}$$

The parameter t represents the time since the start of measuring, h_t is the height of the water column in the hole at time t, and h_0 is the height of the water column in the hole at $t = 0$.

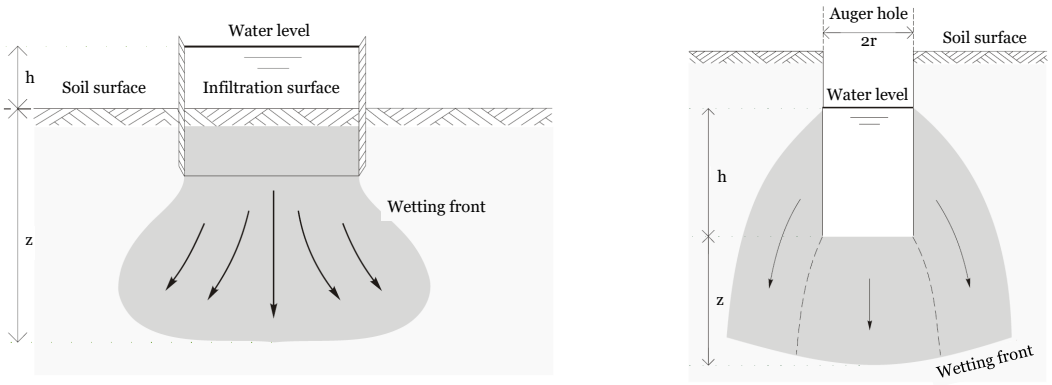

(a) Theory: infiltration process beneath a cylinder infiltrometer (Oosterbaan and Nijland, 1994)

(b) Auger hole test: infiltration from a water-filled auger-hole into the soil (Oosterbaan and Nijland, 1994)

Figure 4.9: Auger hole test: theory and practice

The values for h_t are obtained by subtracting the depth of the water level in the hole below reference level from the depth of the hole below reference level. This depth is measured at appropriate intervals so that the saturated hydraulic conductivity can be calculated. By plotting $h_t + r/2$ on the log axis of semi-log paper, and t on the linear axis, a straight line should appear, which has the slope (Oosterbaan and Nijland, 1994):

$$\tan\alpha = \frac{\log(h_0 + r/2) - \log(h_t + r/2)}{t - t_0} \tag{4.12}$$

The saturated hydraulic conductivity can subsequently be estimated from (Oosterbaan and Nijland, 1994):

$$K = 1.15r \tan\alpha \tag{4.13}$$

Having discussed the theory, the procedure will now be specified for the study areas. The test is carried out at various locations (preferably with different land covers and associated soil types) in both the Myitnge and Myittha catchments. A hole is dug at at least 30cm deep using an auger bore. The diameter of the hole is measured and noted down. Subsequently, a static reference object is placed next to the whole from which distances are measured throughout the experiment. Before pouring in water, the depth of the hole is measured from the reference point until the bottom of the hole using a tape measure. The hole is then filled with water, which is left to drain away freely. The hole is refilled with water several times until the soil around the

hole is saturated over a considerable distance and the infiltration rate has become (relatively) constant. Next, water is poured into the hole, and the distance from the reference point until the surface of the water is noted for time t_0. The timer is simultaneously started, and the distance between the reference object and the water surface is measured, at first every few seconds, and after a while at longer intervals. The results of $h + r/2$ and t are then plotted on semi-log paper, and an average K_{sat} per landcover type estimated, as explained (Oosterbaan and Nijland, 1994).

4.3. Environmental flow assessments

Most environmental flow assessments can be grouped into four distinct categories. These categories are hydrological, hydraulic rating, habitat simulation (or rating), and holistic methodologies (Tharme, 2003). This research focuses on hydrological methods. The main reason for this is that there is a global trend towards a hierarchical application of environmental flow assessments using at least two stages (Tharme, 2003). The first is almost always an exploration phase, which primarily uses hydrological methodologies. Therefore these types of analyses provide a useful basis for environmental flow assessments. The second tends to be a more comprehensive assessment, which demands extensive multidisciplinary expertise and input (Tharme, 2003; Arthington et al., 1998). Considering this and the lack of resources (in the form of data, time, finances, and multidisciplinary technical capacity) available for this study, this seconds step of analysis is excluded. Another analysis that is carried out for this study, however, is a habitat inundation analysis on the basis of historical flood frequencies in combination with measured cross-sectional profile. This method is detailed in section 4.3.2. This is a combination of a hydrological and hydraulic rating method.

4.3.1. Hydrological methods

Hydrological methods are based on analysis of historic discharge data, either measured or simulated. These analyses aim to provide overall flow guidelines to conserve ecological integrity and do not operate at a specific species or process level. In general, hydrological methods assume that there is a certain threshold of water below which biota are at risk, resulting in some recommendations for preliminary environmental flow targets. Hydrological methods are still the most widely used approaches internationally for environmental flow assessments (Tharme, 2003). This is most likely due to their ease of use in combination with low costs, also making them suitable for data scarce regions such as the study areas of this research.

Hydrological indices can be grouped into five categories , as first proposed by Richter et al. (1996), and later expanded by Poff et al. (1997), and Olden and Poff (2003). These categories have been elaborated on extensively in Chapter 2, but are listed again:

1. Magnitude of flow events
2. Duration of flow events
3. Timing of flow events
4. Frequency of flow events
5. Rate of change of flow conditions

The hydrological methods used for environmental flow recommendations are at both a preliminary level and a management level, as shown in Figure 4.10. The former relates mostly to the magnitude of flow events, whereas the latter takes into account more flow regime components. On a preliminary level, the Tennant method and flow duration curve analysis is used. For management, indicators of hydrological alteration analyses are applied.

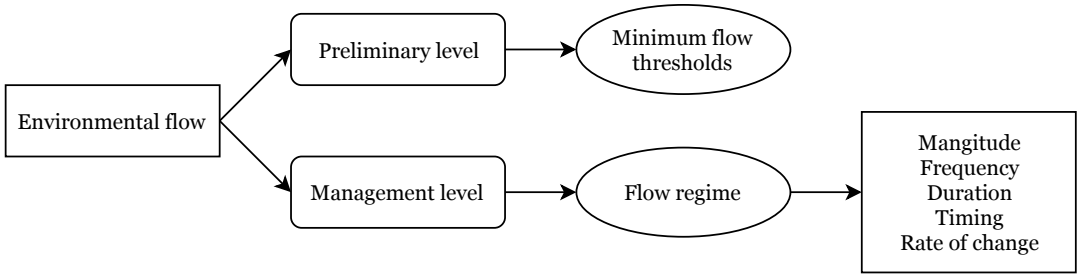

Figure 4.10: Environmental flow analysis

The objective is to investigate ecological instream flow regimes considering hydrological alterations using multiple hydrological indicators on a preliminary and management level.

The Tennant Method

The method developed by Donald Leroy Tennant (Tennant, 1976), also often referred to as the "Montana method", was based on original field data collected from 11 rivers in Montana, Nebraska and Wyoming. It was further supported by data from hundreds of gauged flow regimes in over 20 states in the United States. It assumes that some proportion of the Mean Annual Flow (MAF) is required to sustain the biological integrity of a river ecosystem. The result was recommended percentage values of MAF to sustain predefined ecosystem attributes. As can be seen in Table 4.2, 10% of the MAF was considered to be the lowest instantaneous flow to sustain short-term survival of aquatic life while a flow of more than 30% MAF was considered to provide flows where the biological integrity of the river ecosystem as a whole was sustained. A flow of 200% is the maximum flush, and the optimal range is between 60% and 100%. The Tennant method differs from many other hydrological methods in that an extensive amount of field habitat, hydraulic and biological data was carried out for its development.

Table 4.2: MAF (Tennant, 1976)

Description of flow	**Recommended flow regime (% MAF)**	
	Dry season	*Wet season*
Flushing or maximum	200%	200%
Optimum range	60-100%	60-100%
Outstanding	40%	60%
Excellent	30%	50%
Good	20%	40%
Fair or degrading	10%	30%
Poor or minimum	10%	20%
Severe degradation	<10%	<10%

FDC, ecosurplus and ecodeficit

Vogel et al. (2007) proposed ecosurplus and ecodeficit to evaluate the ecological instream flow regimes of a river basin. Computation of ecosurplus and ecodeficit was based on the Flow Duration Curve (FDC). This curve can be constructed relatively easily using daily streamflow. It shows the percentage of time for daily streamflow exceeding or equaling the pre-defined streamflow threshold. The curve was obtained by sorting the daily streamflow, Qi, in descending order and computing the exceedance probability, P, based on the following equation:

$$P = \frac{m}{n+1} \tag{4.14}$$

In equation 4.14, m is the rank of the inflow value, where the largest discharge value corresponds to $m = 1$, and n is the total number of discharge data points. The curve then plots the discharge against exceedance probability. An example of such as curve is given in Figure 4.11. The FDC only applies for the period for which it was derived. If this is a long period, i.e. more than 10 to 20 years, the FDC becomes a cumulative density function, which may be used to estimate the percentage of time that a specified discharge will be equalled or exceeded in the future.

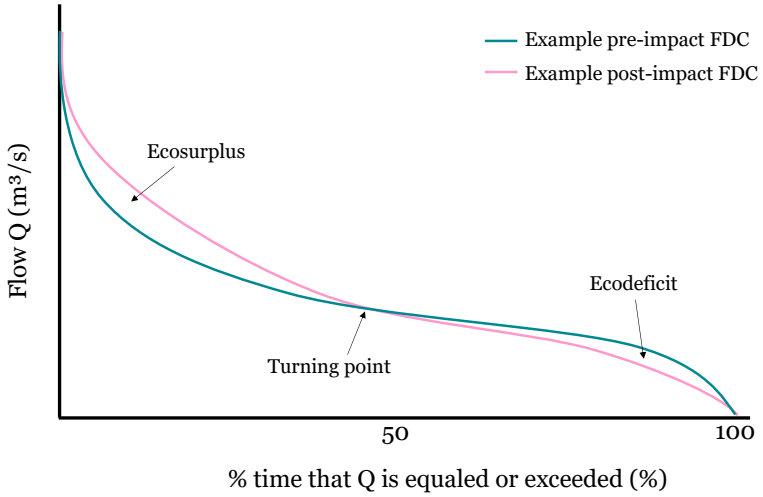

Figure 4.11: Example of a Flow Duration Curve pre- and post a flow changing impact (e.g. a dam)

The area circled by the pre-impact FDC and the post-impacy FDC exceeding 75% percentile is defined as ecosurplus. Conversely, the area circled by the pre- and post-impact FDCs below 25% percentile is defined as the ecodeficit. The range between the 25th and 75th percentiles is considerate the adaptive range for the river ecosystem (Eslamian, 2014).

Indicators of Hydrological Alteration (IHA)

Indicators of Hydrological Alteration were developed by Richter et al. (1996) to challenge the more traditional statistical approach of selecting relevant hydrological indicators for ecological change. The aim of the method is to, first of all, statistically characterize temporal variability in hydrologic regimes using biologically relevant statistical attributes. The second objective is to quantify hydrologic changes associated with the presumed perturbations by comparing the hydrologic regimes from pre- and post-impact time frames.

There are four steps involved in defining IHA (Richter et al., 1996):

1. First of all, a data series for the pre- and post impact periods is defined. For the Myitnge rivers, this periods is before the start and after the end of the construction of the Yeywa dam. For the Myitnge the pre-impact period is between 1982-2004 and the post-impact period is between 2011-2017. For the Myittha, the pre- and post impact periods are both modelled, as there is no existing flow data, and no perturbation directly on the river yet.

2. Next, for each year in each data series (pre- and post impact), the hydrologic attributes are calculated. The computed attributes are the 32 ecologically relevant hydrologic parameters, as presented in Table 4.3.

3. Subsequently, the inter-annual statistics are computed: measures of central tendency and dispersion for the 32 parameters from Table 4.3 in each data series, based on the values calculated in step 2. This produces 64 inter-annual statistics for each data series (32 of central tendency and 32 of dipersion).

4. Finally, the values of the IHA are calculated. The 64 inter-annual statistics between the pre- and post dam data series are compared by calculating the percentage deviation of the post-impact condition relative to the pre-impact condition. The method is hence used to compare the state of one system to itself over time, or in the case of the Myithha, to compare the current conditions to simulated results based on a model of future system modifications.

Table 4.3: Summary of IHA and their characteristics (Richter et al., 1996)

IHA statistics group	Regime characteristics	Hydrologic parameters
Group 1: Magnitude of monthly water conditions	Magnitude Timing	Mean value for each calender month
Group 2: Magnitude and duration of annual extreme water conditions	Magnitude Duration	Annual minima 1-day means Annual maxima 1-day means Annual minima 3-day means Annual maxima 3-day means Annual minima 7-day means Annual maxima 7-day means Annual minima 30-day means Annual maxima 30-day means Annual minima 90-day means Annual maxima 90-day means
Group 3: Timing of annual extreme water conditions	Timing	Julian date of each annual 1 day maximum Julian date of each annual 1 day minimum
Group 4: Frequency and duration of high and low pulses	Magnitude Frequency Duration	No. of high pulses each year No. of low pulses each year Mean duration of high pulses within each year Mean duration of low pulses within each year
Group 5: Rate and frequency of water condition changes	Frequency Rate of change	Means of all positive differences between consecutive daily means Means of all negative differences between consecutive daily means No. of rises No. of falls

The hydrologic parameters presented in Table 4.3 are both bioloically relevant and sensitivent to human influence. The table shows that they have been divided up into five groups. The first in the magnitude of monthy water conditions. This group incudes 12 parameters, each of which measures the central tendency of the daily water conditions. These parameters describe the "normal" daily conditions, and hence provide a general measure of habitat availability or suitability. The similarity of monthly means within a year gives an indication of the hydrologic constancy, whereas inter-annual variation in the mean water condition for a given month gives an indication of environmental contingency (Richter et al., 1996).

The second group, that of the magnitude and duration of annual extreme conditions, contains 10 parameters. These extreme conditions have varying durations. The listed indicators provide some insights to the environmental stress and disturbance during a year. It is also possible, however, that some of these extremes are necessary as triggers for certain crucial processes. The inter-annual variation in the magnitude of these extremes gives an indication of the contingency (Richter et al., 1996).

The third group, describing parameters related to the timing of annual extreme water conditions, also relate to environmental disturbances by describing the seasonal nature of these disturbances. The timing of the extremes that trigger life-cycle phases is crucial to the survival of certain species. The timing of extreme events also demonstrates environmental contingency (Richter et al., 1996).

The fourth group includes parameters connected to the frequency and duration of high and low pulses. The indicators together aim to illustrate the pulsing behavior of environmental variation within a year, and assess the shape of these pulses. Within this assessment, pulses are defined as periods within a year in which "the daily mean water condition either rises above the 75th percentile (high pulse) or drops below the 25th percentile (low pulse) of all daily values for the pre-impact time period" (Richter et al., 1996).

The fifth and final category describes the rate and frequency of change in conditions. The parameters

in this group measure the abruptness and number of intra-annual cycles of environmental variation, which provides insights to the rate and frequency of environmental change (Richter et al., 1996).

It should be noted that this method allows for an estimation of the extent to which a perturbation has impacted the hydrology of a river system, but does not allow for strong conclusions about the cause (Richter et al., 1996). However, a control site is not available for the study sites, so this method becomes a useful tool with a low data demand for planning environmental flow management activities, especially in combination with other ecosystem metrics.

The IHA parameters are calculated for each study site by making use of the IHA software developed by The Nature Conservancy (The Nature Conservancy, 2009a,b). To analyse the change between two time periods or two flow regimes, the the Range of Variability Approach (RVA) is applied, a method by Richter et al. (1997). Using the RVA, a range of variation in each of the thirty-two parameters described above are selected as initial flow management targets. The RVA targets are intended to guide the design of river management strategies. The RVA allows for interim management targets that are readily available before definite long-term conclusions can be drawn about ecosystem impacts.

The RVA uses the pre-impact natural variation of IHA parameter values as a reference for defining the extent to which natural flow regimes have been changed. This natural variation can also be used to define initial environmental flow goals. Richter et al. (1997) propose that dam management should aim to keep the distribution of annual values of the IHA parameters as close as possible to the pre-impact distributions. The analysis calculates a series of Hydrologic Alteration factors, which quantify how much the parameters have been changed. The procedure is as follows. The full range of pre-impact data for each parameter is divided into three different categories. The boundaries between categories are based on either percentile values (for non-parametric analysis) or a number of standard deviations away from the mean (for parametric analysis). The expected frequency that the post-impact values of the IHA parameters should fall within each category are subsequently calculated. This expected frequency is calculated by taking the number of values in the category during the pre-impact period multiplied by the ratio of post-impact years to pre-impact years. After this, the program computes the frequency with which the post-impact annual values of IHA parameters actually fall within each of the three categories. The final step is to calculate a Hydrologic Alteration for each of the three categories as:

$$\frac{\text{(Observed frequency –Expected frequency)}}{\text{Expected frequency}} \tag{4.15}$$

If the value of this alteration factor, as calculated by equation 4.15 is positive, the frequency of values in the category has increased from the pre-impact to the post-impact period. A negative value suggests that the opposite is true, and the frequency of values has decreased.

4.3.2. Habitat inundation analysis

Section 2.2.1 in Chapter 2 illustrated that naturally variable flows create and maintain the dynamics of in-channel and floodplain conditions and habitats that are essential for ecology. The section highlighted the significance of the flow regime for the inundation of watershed areas at different times and frequencies. Therefore, the impact of different dam scenarios on the inundation frequency and extent of the downstream basin is a very relevant assessment for the ecological integrity of the basin. To do this, the impact of the dam operation scenarios on the flow regime is combined with Gumbel's frequency analysis. The aim of the assessment is to compare how often floods of a certain magnitude are supposed to occur in the natural regime to how often they actually occur according to the simulated scenario regime. Flood frequency analysis involves the fitting of a probability model to the sample of annual flood peaks in a certain basin over an observation period. The established model parameters can subsequently be used to predict more extreme events. The Gumbel method is one of the probability distribution methods often used to model stream flows, hence probabilities of the observed flood peaks in the natural regime of the Myitnge are calculated using Gumbel's ditribution. The curve of probabilities versus flood peaks is subsequently plotted on log-probability paper and a smooth curve is fitted over the data. By extrapolating the curve for higher return periods, extreme values can be obtained (Savenije, 2007). Looking at Figure 2.4 (Poff et al., 1997) in Chapter 2, floods with annual, decadal and centennial return periods are important for the geomorphology and ecology of the basin. Therefore, the habitat inundation analysis will compare how often a flood with T=1, T=2, T=5, T=10 and T=100 occurs for each of the dam scenarios over a simulation period of 25 years.

4.4. Data sources and quality control

The methodology presented in the previous sections of this chapter require a considerable amount of data, some of which is collected first-hand (primary) and some is collected from secondary sources. This section gives an overview of the required data, how that data is collected, and how the quality of the data is evaluated.

4.4.1. Primary data collection

The primary data is collected during field visits to the study sites, the methods of which are described in detail in section 4.2. The fieldwork was carried out during October and November of 2018. A map showing which experiments were carried out at which locations is presented in Figures 4.12 and 4.13. The locations for the field experiments and observations were dependent on a couple of factors. First of all, the accessibility of the basin was limited for different reasons. These reasons include safety restrictions, as some roads were blocked due to political unrest. Furthermore, the river was not always accessible by road, nor by foot. Because of the season, flow speeds were relatively high and it was not possible to take a boat all the way upstream. Therefore, the locations of the bathymetry measurements were somewhat dependent on the locations of fishermen's boats.

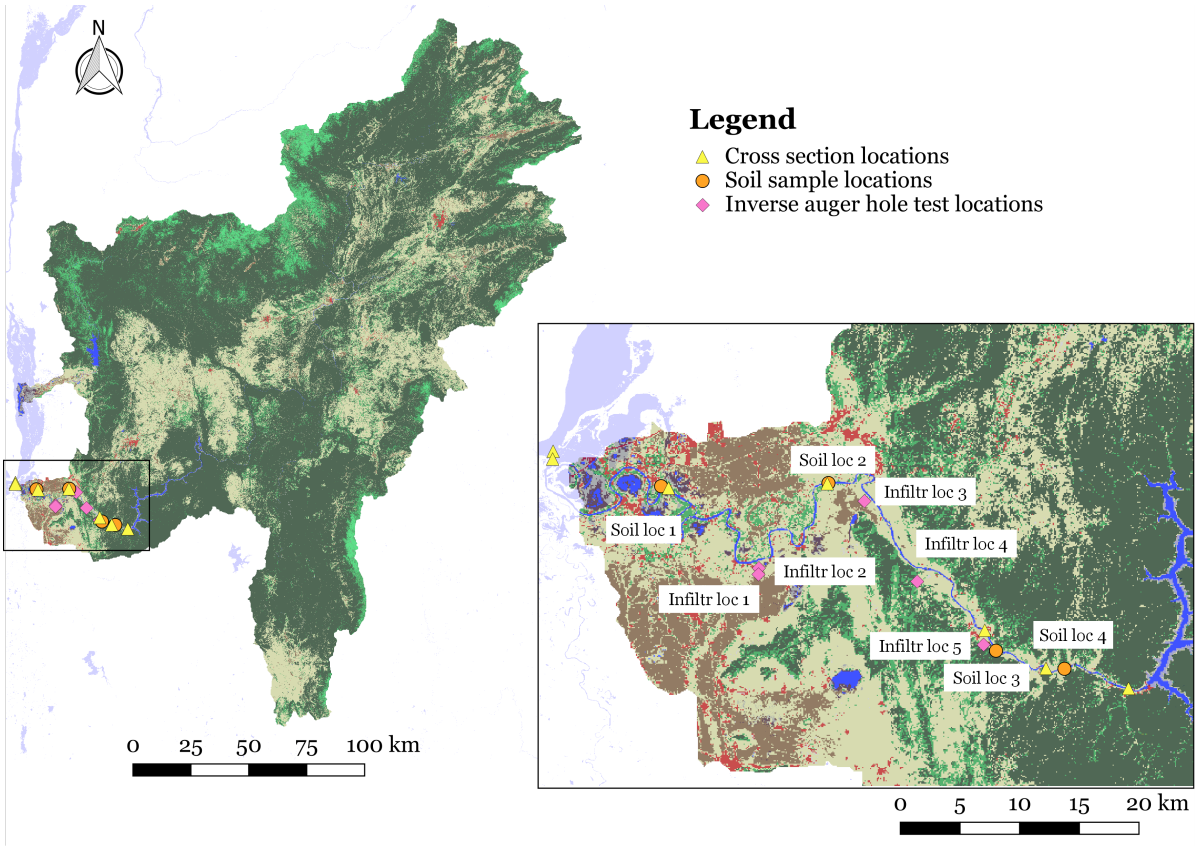

Figure 4.12: Fieldwork overview Myitnge: cross sections, soil samples and inverse auger hole tests

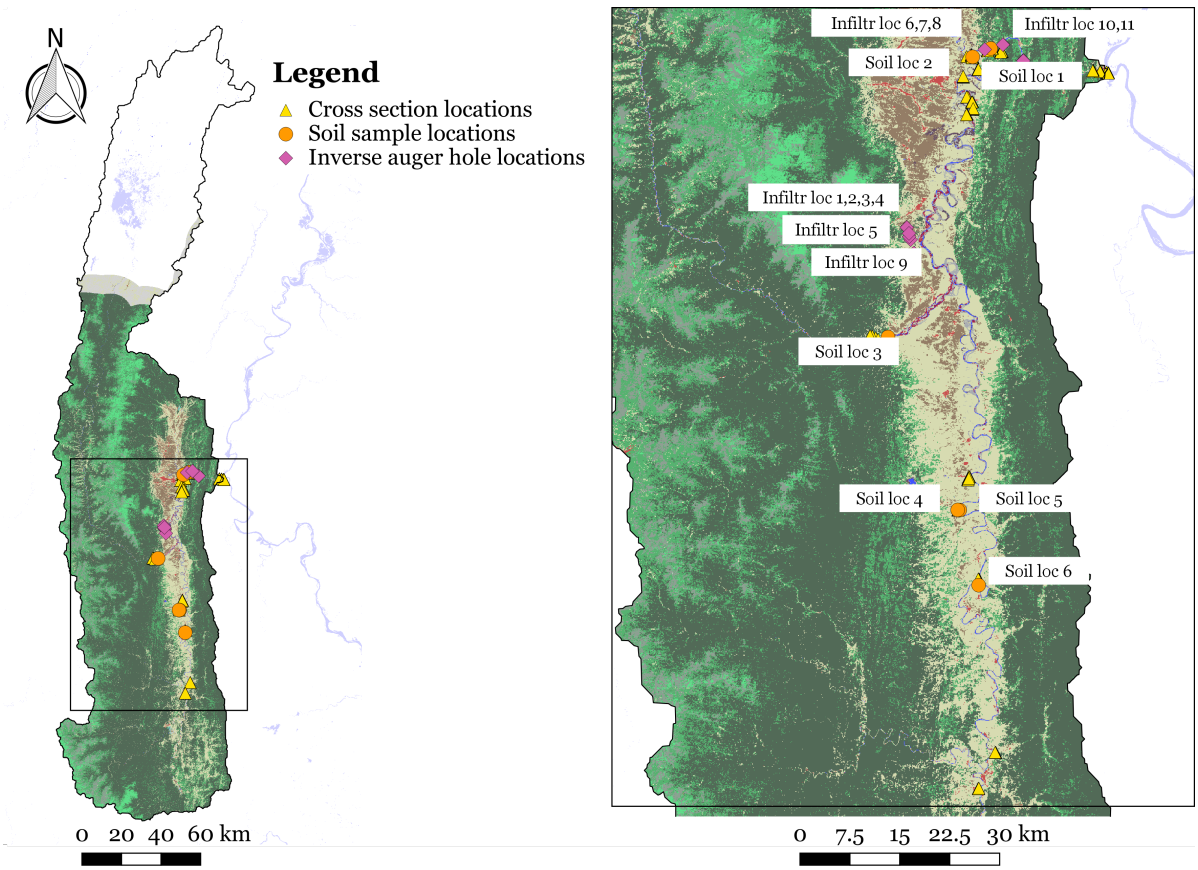

Figure 4.13: Fieldwork overview Myittha: cross sections, soil samples and inverse auger hole tests

4.4.2. Secondary data collection

Discharge and waterlevel data

The discharge and waterlevel data was provided by the Department of Meteorology and Hydrology in Myanmar. Discharge data was provided from 1982-2016 at Shwesaryan station, and from 2011 through halfway 2018 by the Yeywa dam operators. The latter is both dam outflow data and inflow into the reservoir (deduced from the water balance of the reservoir). The provided water level data is monthly minima and maxima for the period ranging from 2008-2015. The data source locations are presented in Figure 4.14.

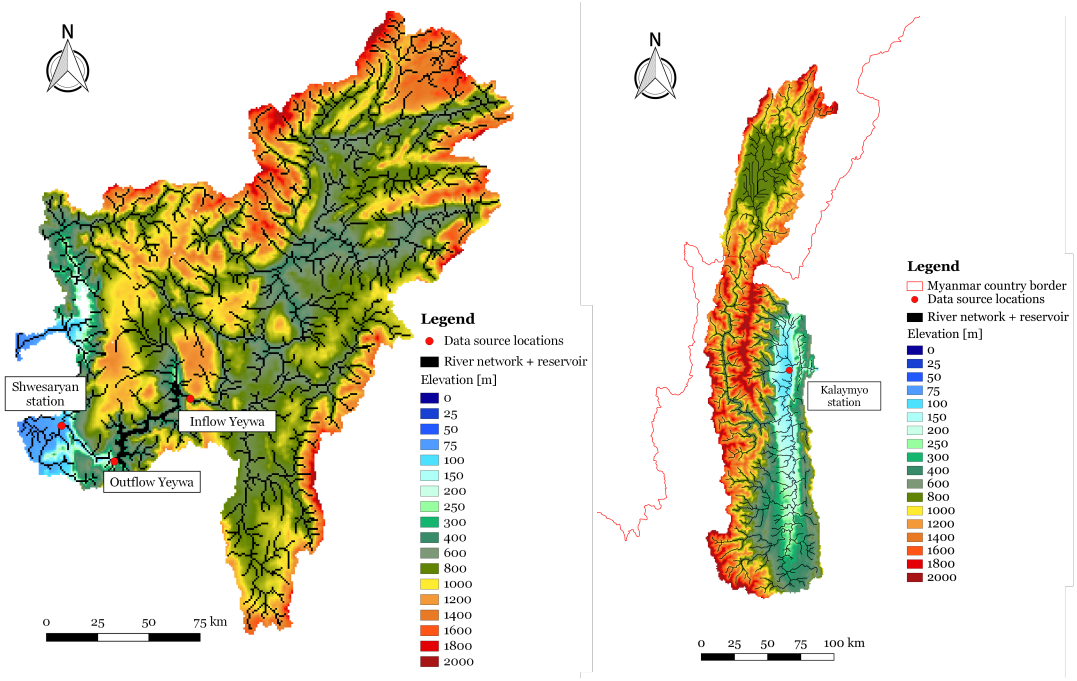

(a) Myitnge data source locations

(b) Myittha data source locations

Figure 4.14: Locations of the measurements from secondary data sources in the the study basins

LAI

LAI (Leaf Area Index) maps for the *WFlow_sbm* model are monthly average LAI. The results are based on combined AVHRR and MODIS data, derived from Liu et al. (2012). The averages are taken over the time period from 1981 until 2012 (Schellekens, 2018).

Precipiation, evapotranspiration and temperature

The research used the Water Resources Reanalysis: a forcing based on the ERA-Interim meteorological data bilinearly interpolated to 0.25° ($\approx 27km$). It includes a topographic correction for temperature using a spatially and temporally varying environmental lapse rate (ELR) and a developed precipitation dataset referred to as the Multi-Source Weighted-Ensemble Precipitation (MSWEP). MSWEP is a relatively new fully global historic precipitation product of 1979–2015 with a 3-hourly temporal resolution and a 0.25°spatial resolution. MSWEP exhausts the complementary advantages of gauge-, satellite-, and reanalysis-based data to provide reliable precipitation estimates. Because the dataset has a consistent precipitation record from 1979, trend assessments are also possible. Daily gauge corrections have been incorporated, using observations from more than 70,000 stations across the world (Beck et al., 2018). It should be noted that Myanmar has only contributed to the MSWEP efforts by providing ground observations from two stations, unfortunately. When applying the daily gauge corrections, MSWEP also accounts for differences in gauge reporting times. There is furthermore a correction made for the systematic terrestrial precipitation biases such as orographic effects, which uses river discharge observations from more than 13,000 stations globally (Beck et al., 2018). Global analyses suggest that MSWEP produces more realistic patterns in mean, magnitude, and frequency of precipitation. In two comprehensive large-scale evaluations, MSWEP performed best overall (Beck et al., 2017b,a). MSWEP is available via http://www.gloh2o.org.

Macroinvertebrates samples

As discussed in section 2, stream assemblages are integrally linked to physical and chemical characteristics of the river. Therefore macroivertebrate samples were collected upstream and downstream of de Yeywa dam from November of 2016 until april of 2017.

4.4.3. Downscaling the global data

For the downscaling of the forcing data, the EartH2Observe downscaling tools are used in combination with a high-resolution DEM of the study regions (Schellekens and Weilan, 2017). These tools contain a number of Python based meteorological scripts that work on the forcing of the eartH2Observe project. The scripts retrieves the data from the WRR2 dataset on the server. The meteorological variables temperature and air pressure are downscaled using a DEM based elevation correction. Furthermore, the potential evaporation is computed from the retrieved datasets using the Hargreaves equation, while making elevation corrections for temperature, air pressure and radiation, and shading corrections for radiation. Hargreaves is a simplified form of the Penman-Monteith equation using temperature and an annual radiation cycle as input (Hargreaves and Allen, 2003). The different steps for downscaling the data are presented in figure 4.15 and are described in the following (Schellekens and Weilan, 2017):

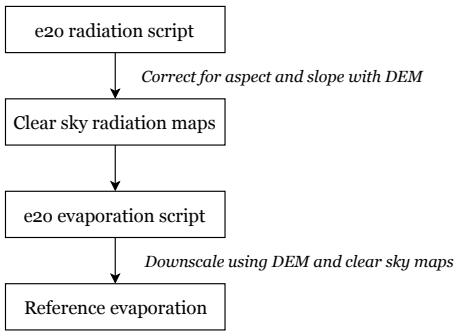

Figure 4.15: Earth to observe (E2O) downscaling process

- e2o_radiation.py makes clear sky radiation maps and inclination correction masks for optional use by the e2o_calculateEvaporation.py script
- e2o_getvar.py downloads and and resamples variables from the meteorological forcing dataset (WRR2 in this study). This script resamples and extracts the data and can optionally downscale precipitation and temperature.
- e2o_calculateEvaporation.py calculates reference evaporation from the meteorological forcing dataset using Hargreaves. It makes use of elevation based downscaling combined with radiation downscaling (using the e2o_radiation output).

4.4.4. Validating the data

Water balance

It is important to check that the model is not logging or gaining water. The mass balance must be valid, so the model is checked through a water balance. The water balance is a version of the general control volume equation, representing the basis of the continuity, momentum, and energy equations for many hydrological processes. By substituting the conservation of mass into the Reynolds transport theorem, the integral equation of continuity for an unsteady flow with variable density is obtained. If the flow has constant density, ρ can be divided out of both terms, and rewriting lead to.

$$I(t) - O(t) = \frac{\Delta S}{\Delta t} \tag{4.16}$$

In Equation 4.16, I is the inflow, O is the outflow, and $\frac{\Delta S}{\Delta t}$ is the rate of change of storage over a specific finite time step. All three terms are in L^3/T

In this research, the water balance is applied to the study river basins. For a catchment water balance, the input equals the precipitation P while the output comprises the actual evapotranspiration E and the river discharge Q at the outlet of the catchment. Hence, with A as the surface area of the catchment and S as storage, the water balance may be written as:

$$(P - E) \cdot A - Q = \frac{\Delta S}{\Delta t} \tag{4.17}$$

Furthermore, if the account period for which the water balance is created is sufficiently long, the rate of change in the amount of water stored can be assumed to become negligible. The balance is established for 23 years of data for both the Myitnge and the Myittha, corresponding to 1982 up to and including 2004. It is important that the balance is taken over hydrological years, so that the amount of water in store is expected not to vary much for each year. Looking at the seasonality of the study areas, a hydrological year equal to the calendar year seems reasonable.

This water balance is checked manually through the extraction time series of precipitation, actual evapotranspiration, and lateral subsurface flow over the whole catchment, and runoff at the downstream end of the catchment over 23 years. There are also some built in water balance checking functions in *WFlow_sbm*, namely self.SoilWatbal, self.InterceptionWatBal, self.SurfaceWatbal, and self.watbal. These are the water balance of the soil, the water balance of the vegetation, the water balance of the surface water and the total water balance, respectively. Each of these are for the whole catchment area and can be taken on a scale ranging from daily until over the entire model period.

Budyko curve

The Budyko curve plots the ratio of actual evapotranspiration over precipitation against potential evaporation over precipitation. The former is known as the evaporative index, and the latter represents the aridity/dryness index. Budyko (1974) postulated that every catchment across the globe roughly follows the Budyko curve, given by:

$$\frac{E}{P} = \left[\phi \tanh(\frac{1}{\phi})(1 - e^{-\phi})\right]^{1/2} \tag{4.18}$$

In equation 4.18, E is the actual evapotranspiration, P is precipitation, and ϕ represents the aridity index, which is equal to the potential evapotranspiration over the precipitation (Arora, 2002). The equation is graphically presented in Figure 4.16

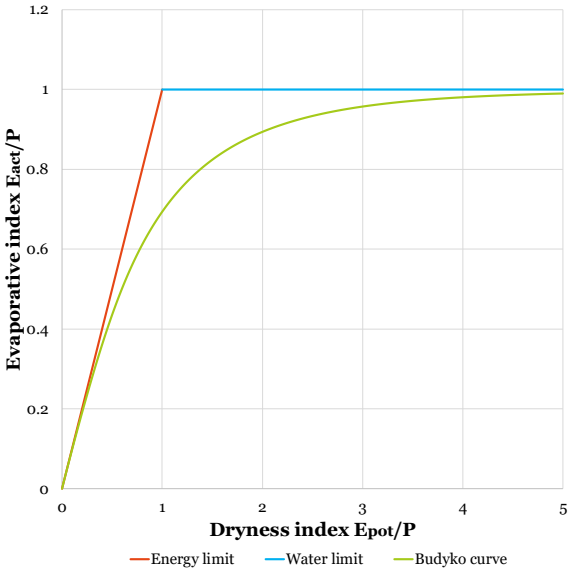

Figure 4.16: Theoretical Budyko curve, adapted from citebudyko1974climate and Arora (2002)

As the figure shows, the predicted evaporation ratio asymptotically approaches unity for higher values of aridity ratios. Plotting the study rivers on this curve will give some idea about how the areas compare to the reference condition for the water balance. Assuming that the curve indeed depicts the expected partitioning of precipitation into runoff, vertical deviations from the curve would suggest a change in partitioning between actual evaporation and runoff, and horizontal deviations suggest changes in the climatic conditions (Arora, 2002).

Summary of the Methodology chapter

The study aims, first of all, to accurately model the natural flow of the Myitnge and Myittha rivers. This is done by using the distributed hydrological rainfall-runoff *WFlow_sbm* model. The model requires static and dynamic data which is mostly globally available from different satellites, and derivatives of this. The model is calibrated and validated on data collected in the field, as well as some secondary data sources. Primary data was collected during October and November of 2018 at several locations along and in the Myitnge and Myittha rivers in Myanmar. The field data collection focused on river bathymetry and the infiltration capacity of the soil through the saturated hydraulic conductivity. Furthermore, different operational dam scenarios are developed that respectively favored maximum power generation, flood protection, and irrigation demand. These scenarios are incorporated into *WFlow_sbm* to estimate the impact on discharge. This leads to the second part of the research, which focuses on the impact of these scenarios on the natural flow regime. Using modelled discharge results, multiple environmental flow assessments are carried out, comparing pre- and post impact situations. Finally, these analyses are combined and linked to existing macroinvertebrate biomonitoring samples as well as ecological relations from literature to answer the question of how the dams have impacted a vital part of the ecohydrology of the Myitnge and Myittha rivers. Dam-management recommendations are designed for environmental flows in the study areas based on the environmental flow assessments. These recommendations aim to provide water managers with guidelines on the quantity and timing of flows necessary to help sustain ecosystems and the associated services they provide.

5

Results and discussion

The results and discussion chapter is structured as follows. The chapter begins with observed river processes and fieldwork results and discussion. Subsequently, all the model simulation results are presented and discussed. The environmental flow assessments of the simulated flow regimes are presented in a separate section following these model results. The impact on ecohydrology is presented and discussed in section 5.4. The chapter concludes with a discussion of the overall validity of the results.

5.1. Observed river processes and fieldwork

5.1.1. River morphology and processes

This section will describe some of the morphological processes in the catchment that were observed during the field visits. The section will start with the Myitnge river, after which the Myittha will be illustrated.

Myitnge

It is evident that the Myitnge basin has abundant and thick vegetation across a large part of the area. Therefore the interception rate is assumed to be very high in the model. The rate of infiltration of the water also appears to be dependent on the land cover. In some of the dryer agricultural zones for example, water infiltrates extremely slowly, whereas the uneven mixed forest areas have fast infiltration rates. Downstream of the Yeywa dam quite some preferential overland flow paths can be observed, mainly due to human land use and alterations. This gives precipitation an easy route directly into the river in certain areas, which limits infiltration to some extent. Some tributaries can also be observed which stream directly into the Myitnge, but these seemed relatively small compared to the main river.

(a) Myitnge upstream near Yeywa dam

(b) Myitnge downstream near mouth

Figure 5.1: Myitnge river: upstream versus downstream

A large part of the catchment area upstream of the Yeywa consists of mountains. These mountains have steep slopes and are heavily forested, suggesting high overland flow and interception rates, and little infiltration. Just downstream of the dam there are tall riverbanks which seem to have eroded a lot and even partially

collapsed with past high water levels and/or floods. On top of these high river banks there are quite some alluvial terraces that are cultivated for agricultural purposes. Further downstream the banks start to lower, the river meanders and there are a lot of cultivated agricultural floodplains. Upstream of the Yeywa dam there are only a few villages left, as some were displaced for the creation of the reservoir.

Furthermore, there is quite some mining and even some caves can be observed in the area downstream of the Yeywa. Some backswamps exist behind the natural levees of the river. According to locals, when the river floods, water and sediments will go over these natural levees and enter the backswamps. This makes the soil very fertile and useful for agricultural purposes.

(a) Collapsed riverbanks (b) Mining near river (c) Alluvial terraces

Figure 5.2: Observation in the Myitnge river basin

Myittha

While studying the area it became clear that the Myittha basin has a lot of of oxbow lakes, as also shown in Figure 5.3. The map shows the water transitions in part of the Myittha basin between 1984 and 2015. It is evident from the map that this is a very dynamic river with a wide meander.

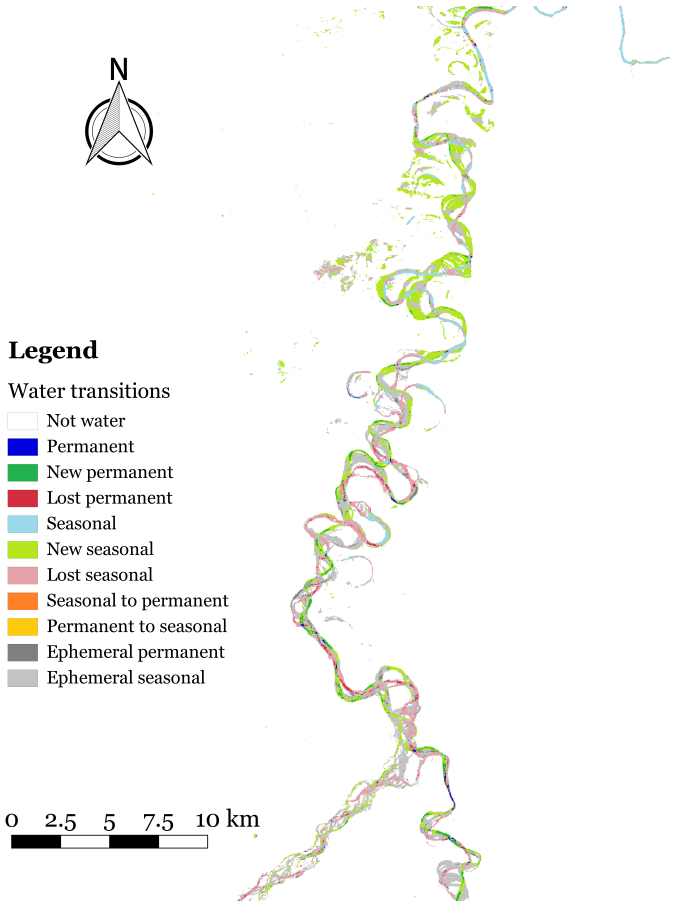

Figure 5.3: Water transitions in part of Myittha basin, data from EC JRC/Google (Pekel et al., 2016)

The dynamic character of the river and the occurrence of oxbow lakes suggest that the river has a large erosive capacity. This hypothesis is also supported by the turbidity data: very high turbidity was observed throughout the river, even in the Manipur (mountainous tributary of the Myittha), and the upstream Myittha. The river is located in low lying plains with a very wide meander. There is a lot of observable deposition in the convex banks, and lateral erosion and undercutting in the concave banks, as shown in Figure 5.4a. The Myittha river overall had a low water level during the fieldwork period (November), even though the rainy season had only just ended. There are many sand and gravel bars, which are elevated regions of sediment deposited by the streamflow, as presented in Figure 5.4b. Considering these observations, it is likely that the Myittha has a very slow recession curve and a lot of groundwater storage, which are important observations for the water balance and the model.

(a) Deposition (left) and erosion (right) in the bends (b) Sand/gravel bars (deposition)

Figure 5.4: Deposition and erosion in the Myittha river

Overall the western bank of the Myittha was observed to consist of a compost of silt, sand, pebbles, larger rocks and only some clay. The eastern bank, however, consists mostly of silt and clay, almost no pebbles or rocks and only some sand. On the Western side of the catchment lie the Chin hills, which are from the Cretaceous period. The Pontaung-Ponnya mountain range on the eastern bank is much younger, from the Eocene period. The latter consists of smaller mountains, whereas the Chin hills are much higher. The observed difference in the river banks is demonstrated in Figure 5.5, where 5.5a shows the western bank, and 5.5b shows the eastern bank.

(a) Western riverbank (b) Eastern riverbank

Figure 5.5: Myittha river: western versus eastern banks

During interviews, most local people mentioned the Myittha flood of 2015, which was the worst they had experienced in their lifetimes. According to people living near the river, as well as some geological and hydrological researchers from Kalay Technical University, this flood rejuvenated the Myittha river's geomorphology and erosion pattern completely. Some of the damage done by the flood, which supposedly had a return period of 100 years, is still visible three years later as is illustrated by Figure 5.6. Figure 5.6a shows floodplains where people used to live right near the riverbank. All the homes were washed away during the flood, and the area has become uninhabitable according to the villagers. Figure 5.6b shows a part of the river where the bank has collapsed into the river due to the flood.

(a) Entire floodplain has become uninhabitable for people (b) Major collapse of parts of the riverbank

Figure 5.6: Damage done by 2015 Myittha flood

5.1.2. Field experiments

The results for the cross-sections and river bank height measurements were used for the habitat inundation analysis. The infiltration tests carried out gave values for the saturated conductivity of different land uses. These results, presented in Appendix F, should be handled with care, however, because the spatial and temporal heterogeneity.

5.2. Model results

The results of the *WFlow_sbm* model are presented in the ensuing subsections. The first subsection contains a discussion of the accuracy of the provided observed data for the Myitnge basin. The subsequent subsections present and examine the simulated natural flow regime and flow scenario results.

5.2.1. Data discussion

The flow data used for calibration was provided by the Department of Meteorology and Hydrology in Myanmar. Figure 5.7a shows the total annual runoff plotted against the total annual precipitation for the observed and simulated data. The linear trend shows the best fit for the observed data; the runoff only increases slightly whereas precipitation increases significantly. The best fit of the linear trend for the simulated data projects this as a much steeper relation. Furthermore, in the original discharge data, there are some clear outliers, such as the two points where the total annual precipitation is lowest (less than 1300 mm) and yet the total runoff is second and fourth highest of all the years. The simulated data seems to give a more realistic response, as the total runoff increases with annual precipitation. Furthermore, plotting the forcing data of the Myitnge in the Budyko curve shows that the extracted theoretical runoff coefficient from this curve gives a value of 0.7 for the Myitnge. This suggests that 70% of the precipitation leaves the catchment as runoff. Given the amount of vegetation in the catchment, this value seems to be an overestimation. The points of discussion given in this section give enough reason to distrust the observed data. Therefore, the calibration of the simulated regime will not strive to meet the observed data exactly. This is further discussed in section 5.2.2.

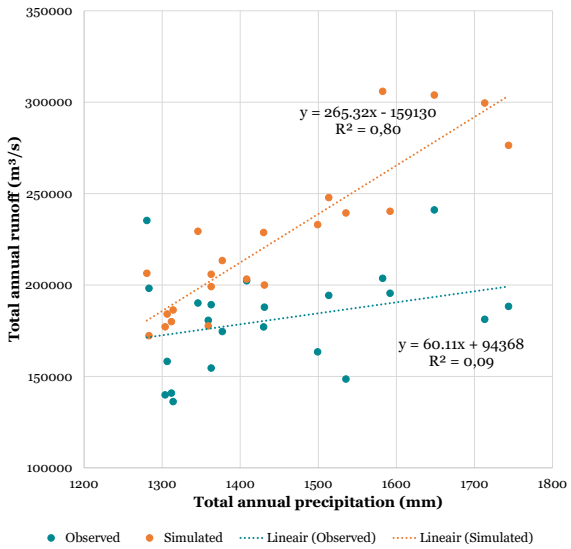

(a) Yearly total precipitation versus yearly total runoff: observed and simulated results in the Myitnge basin

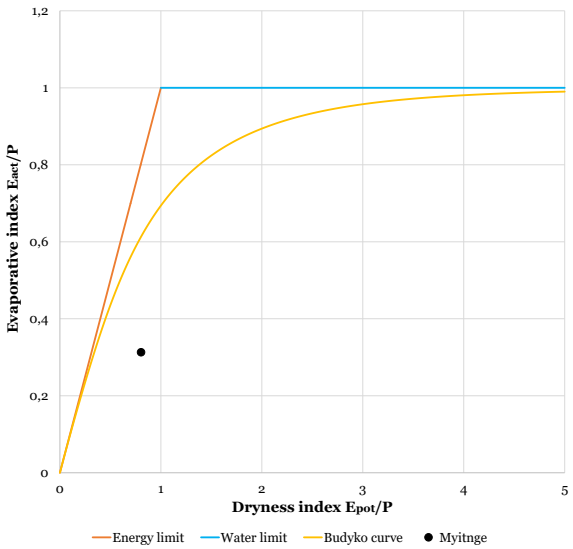

(b) Theoretical budyko curve and the plotted Myitnge catchment areas

Figure 5.7: Data dicussion plots

5.2.2. Natural flow regime

Myitnge

This section presents the results for the simulated natural flow regime for the Myitnge and the Myittha. Some of the results for the calibration phase are presented in Appendix G. The final simulated natural flow hydrograph for the Myitnge is plotted against the observed Shwesaryan data in graph 5.8.

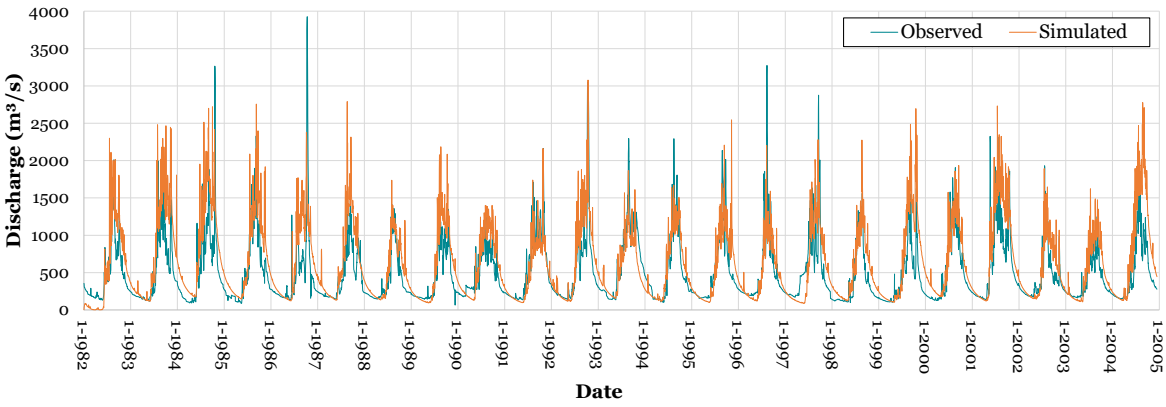

Figure 5.8: Natural flow regime: observed (Shwesaryan) versus simulated

Figure 5.9 shows the Q-Q scatter plot and the flow duration curves for the observed and simulated data. These graphs show that the simulated low (base) flows seem to match the observed low flows relatively well. The recession is a lot slower for most of the years, however, as demonstrated by the simulated discharge remaining higher than the observed discharge at the end of the wet season. The slope of the falling limb of the simulated hydrograph is less steep than the falling limb slope of the observed hydrograph for most of the simulated years. This seems to be a process-based structural error in the model. The higher (peak) flows are not always simulated very well. This is shown by the dispersion on the right hand side for higher flows in the QQ plot in figure 5.9, and the discrepancy between the observed and simulated flow duration curves for higher flows.

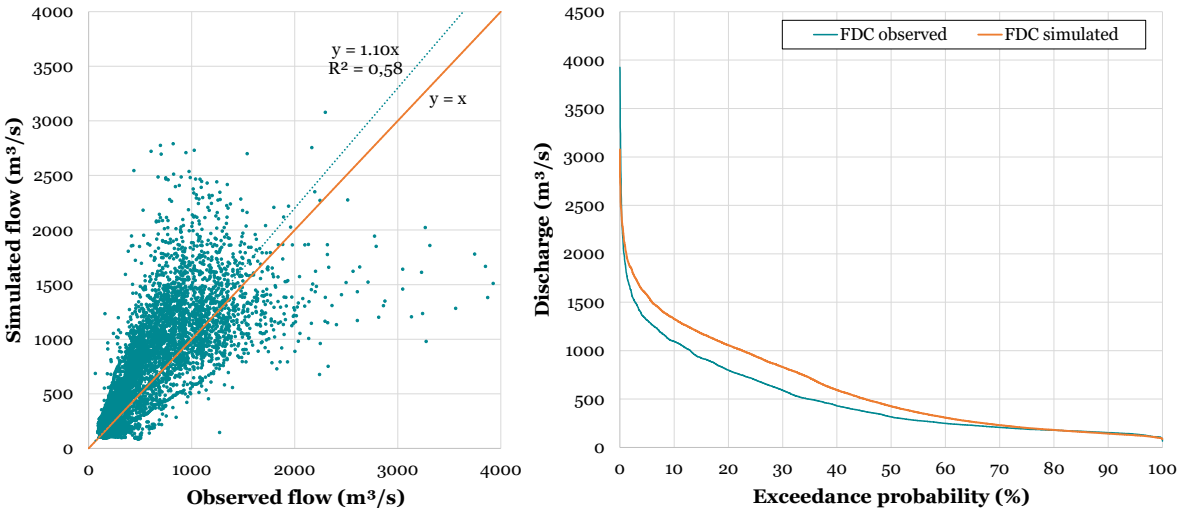

Figure 5.9: Q-Q plot and FDC for the observed (Shwesaryan) and simulated natural flow regime

The results of the mathematical criteria are presented in Table 5.1.

Table 5.1: Results mathematical criteria for model evaluation

R^2	NSE	$NSLE$	E_{rel}	$RMSE$
0.62	0.49	0.64	0.47	328

The results show that the model performs relatively well. The R^2 value, which is especially sensitive to peak flows, shows a relatively good correlation between the simulated and observed data. The NSE, also sensitive to higher flows, scores slightly lower, but still has an acceptable value (Krause et al., 2005). The $NSLE$ parameter, which reacts stronger to low flows, is relatively high, again showing the model predicts low flows quite well. E_{rel}, which is sensitive to low flows only, has an acceptable value of just below 0.5. Finally, the $RMSE$ has a value of $328 m^3/s$, which is quite high compared to an average observed flow of about $500 m^3/s$. Further insight is gained when plotting the observed discharge against the log mean square error, as illusrtated in Figure 5.10. From the figure it appears as though higher flows tend to give higher mean square errors. Therefore the $RMSE$ value may be biased as it is influenced by large discrepancies between observed and simulated values during higher flows and peaks.

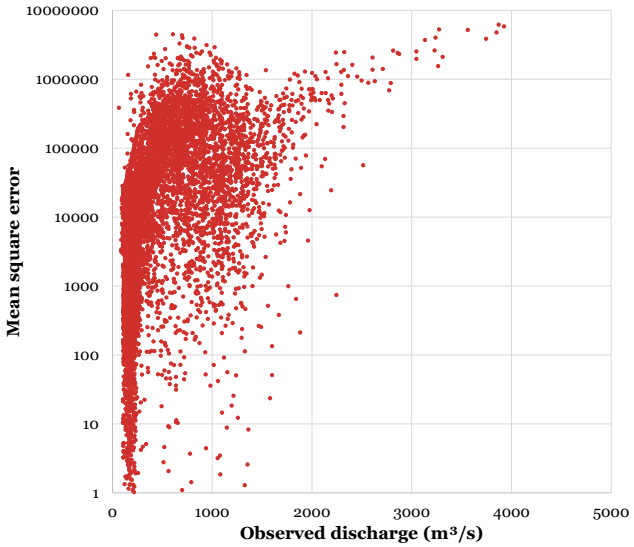

Figure 5.10: Mean square error (plotted on a log scale) for different observed flows

Figure 5.11 shows the simulated natural flow upstream of the Yeywa against the inflow data provided by the Yeywa dam operators. It should be noted that the Yeywa inflow data is based on the water balance of the reservoir and the operational outflow of the Yeywa dam. The observed inflow data fluctuates substantially, because of the operational dam releases which are subtracted from the water balance. The simulated data fluctuates less, but matches the magnitude relatively well. Again, the recession of the simulated hydrograph at the end of the rainfall season is delayed compared to the observed inflow, suggesting a slower model recession. This is shown by the simulated flow remaining significantly higher than the observed data between October and February, most likely caused by a structural error in the model.

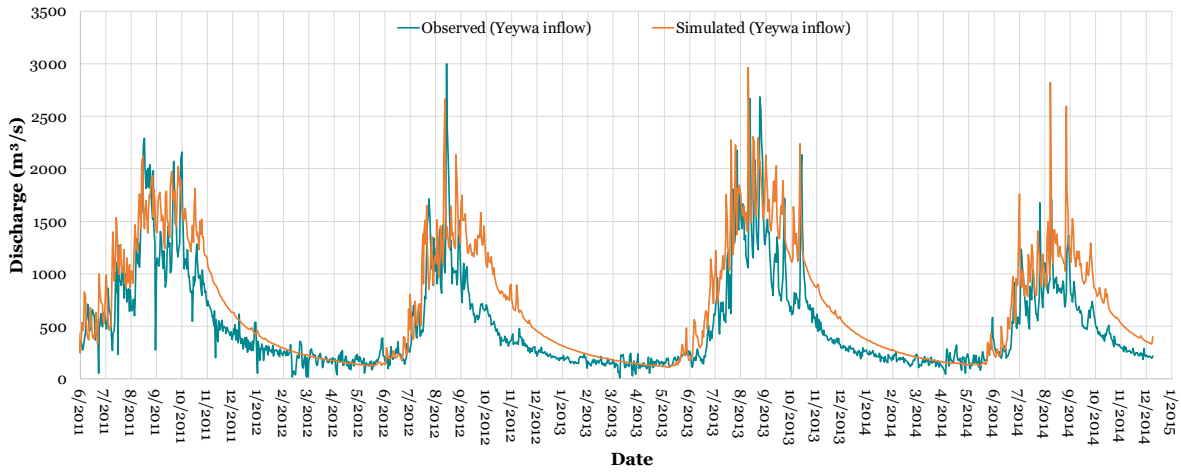

Figure 5.11: Natural flow regime: observed (Yeywa inflow) versus simulated flow at the upstream point

Myittha

Figures G.3 and G.4 in Appendix G show the results for one of the calibration steps. It shows the observed and simulated extreme monthly water levels between 2008 and 2014 when the ration of the bank-full river width to depth is 120. The results show that generally the simulated water levels consistently underestimate the observed water levels. From June until the December, the simulated monthly low water levels are relatively close to the observed data. The simulated natural flow regime after calibration based on water levels is presented in Figure 5.12:

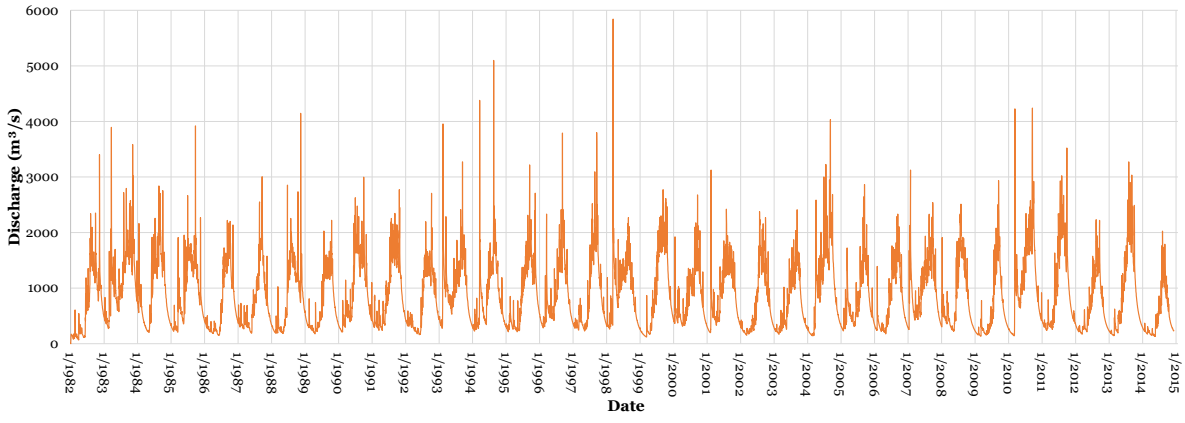

Figure 5.12: Simulated natural flow regime of the Myittha

The flow duration curve of the simulated discharge of the Myittha is presented in Figure 5.13

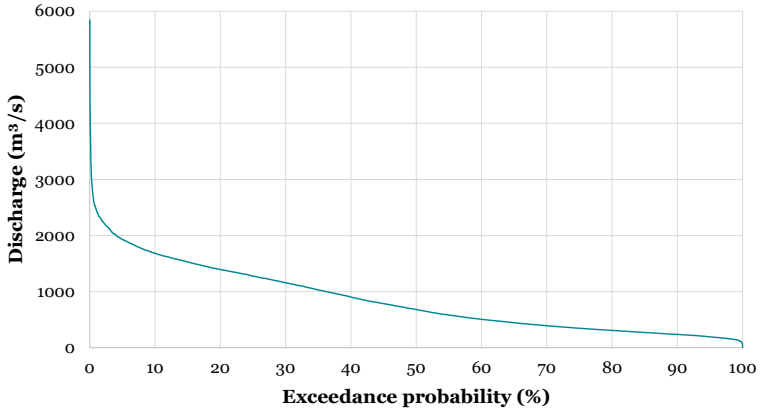

Figure 5.13: Simulated Flow Duration Curve of the Myittha

The obtained natural flow regime can not be validated against any observed streamflow data, which makes the level of uncertainty very high. Based on observations made in the field, it seems like the simulated discharge may be too high during the month of observation (November). An estimation of flow can be made by using the Manning equation:

$$Q = \frac{1}{n} A R^{2/3} \sqrt{S} \tag{5.1}$$

In Equation 5.1, Q $[m^3/s]$ is the flow rate, n $[-]$ is Manning's Roughness Coefficient, R $[m]$ is the hydraulic radius which is equal to the cross sectional area of flow over the wetted perimeter, and S $[m/m]$ is channel slope. The Manning Roughness Coefficient is estimated at 0.040 for clean, winding streams (Chow, 1959). The hydraulic radius is estimated from the cross-sectional measurement, and the channel slope estimated from the measured longitudinal profile. The cross-section and longitudinal profile were measured in the field using the Garmin fishfinder at the location. The result given in equation 5.2

$$Q = \frac{1}{0.040} 144 \cdot 1.89^{2/3} \sqrt{0.01} \approx 550 m^3/s \tag{5.2}$$

The resultant flow of the Manning calculation is in the same order of magnitude as the model result, which gives a value around 700 m^3/s in mid-November for most of the simulated years. Hence, the simulated flow regime can be assumed to not be completely misguided. As expected, the model overestimates the flow slightly at the end of the wet season. This may again be due to the structural error in the model that makes the hydrograph recession too slow. Nevertheless, *WFlow_sbm* gives some idea on the natural hydrograph and seasonality in the Myittha basin.

5.2.3. Flow scenarios

Scenario 1: (Maximum) power operation

The first scenario that was simulated is that of different operational dam capacities. The results are presented in Figure 5.14.

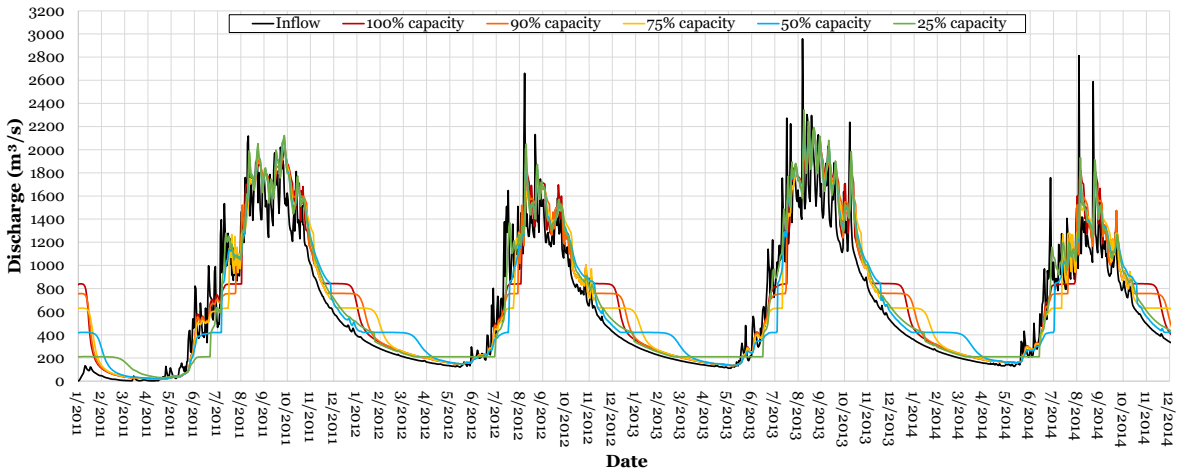

Figure 5.14: Simulated hydrographs for Yeywa dam running at different capacities between 2011 and 2014

Graph 5.14 shows that the higher capacities are not feasible over the entire season. All simulations assume that the dam starts to spill when the reservoir is at 100% storage capacity, and cannot operate under 65% of reservoir storage capacity. These values are based on the technical specifications provided by the dam operators during the visit. Running the Yeywa dam at 100% capacity (i.e. all four turbines working at maximum capacity), is achievable between mid July and the end of December. After this, less than 25% of capacity is possible due to water shortage in the dry season. A capacity of 90% only prolongs this period by about 10 days. At a capacity of 75%, the generation is possible between the start of July and somewhere around the end of January, giving about 7 operational months on average. Running the dam at 50% capacity allows generation between mid june until somewhere between the middle of February and the beginning of March, again after which only the upstream inflow can be used for generation. Running the operation at 25% capacity is (generally) possible all year long, giving 12 fully operational months. The maximum possible generation that is attainable all year long (in an average season) is 29%.

If the historical precipitation, temperature and evaporation data is used to simulate the 80% capacity scenario for 22 years, the following hydrograph is obtained at the location of the Shwesaryan station:

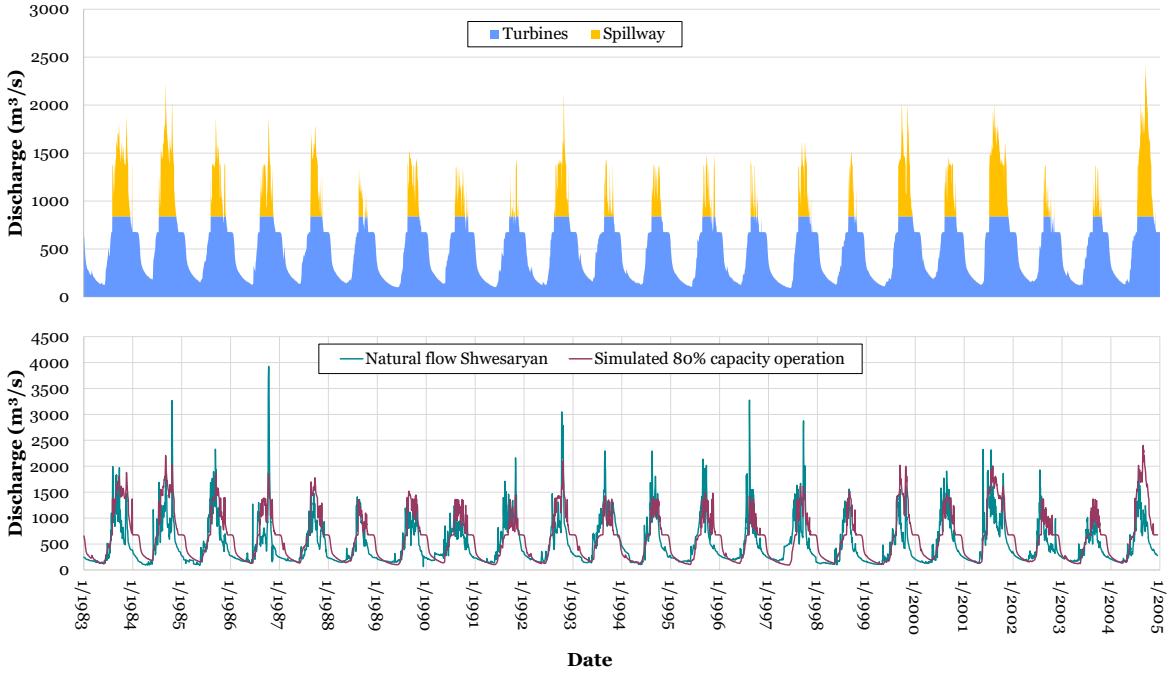

Figure 5.15: Simulated hydrograph for Yeywa dam running at a minimum of 80% capacity (when possible) for 22 years

Figure 5.15 shows that at 80% capacity, the peaks of the natural flow regime are cut off. Furthermore there appears to be a delay in the start of the dry season because the dam keeps discharge unnaturally high to operate at such a capacity. The first flow peaks of the wet season also appear to be slightly delayed due to the operation.

A similar hydrograph is created for 29% capacity, as presented in Figure 5.16:

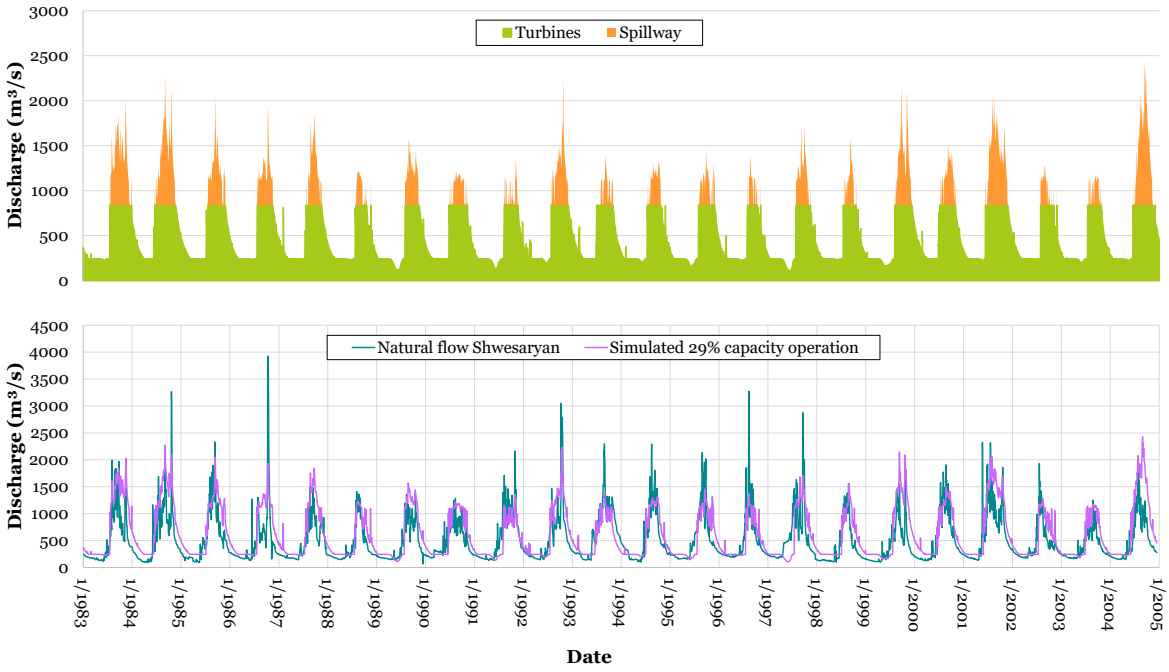

Figure 5.16: Simulated hydrograph for Yeywa dam running at atleast 29% capacity (when possible) for 22 years

The results appear to be much closer to a run-of-river regime, as the natural inflow is directly let through the turbines. The graph shows that outflow is kept slightly higher than natural during the dry season, and the flood peaks are cut-off during the wet season.

Environmental flow assessments are carried out for these simulated flow regimes in section 5.3.

Scenario 2: Flood mitigation

For a scenario where the Yeywa dam serves as an instrument for flood mitigation, floods were defined based on their return period (see section 5.3.4). If the Yeywa has to protect the downstream area from floods with a return period of 2 years, a maximum discharge of 2000m^3/s should be allowed through the dam. In the natural flow regime this threshold is exceeded on 129 days in 11 seperate years over a 22 year period. When operating the Yeywa dam at 29% capacity over the same time period, this discharge magnitude is met or exceeded on a total of 40 days only. Increasing the dam operative capacity decreases this number of flood days further. This suggests that the moderation of floods is a consequence and side-effect of operating the Yeywa hydrodam at a higher capacity. Figure 5.17 therefore shows the 100% capacity flow regime that would most effectively mitigate floods given the Yeywa technical specifications. This scenario only allows a flood with a return period of two years twice over 22 years. This is shown by the red line in the figure, which was exceeded only in 1984 for three days and in 2004 for 18 days in the simulated regime.

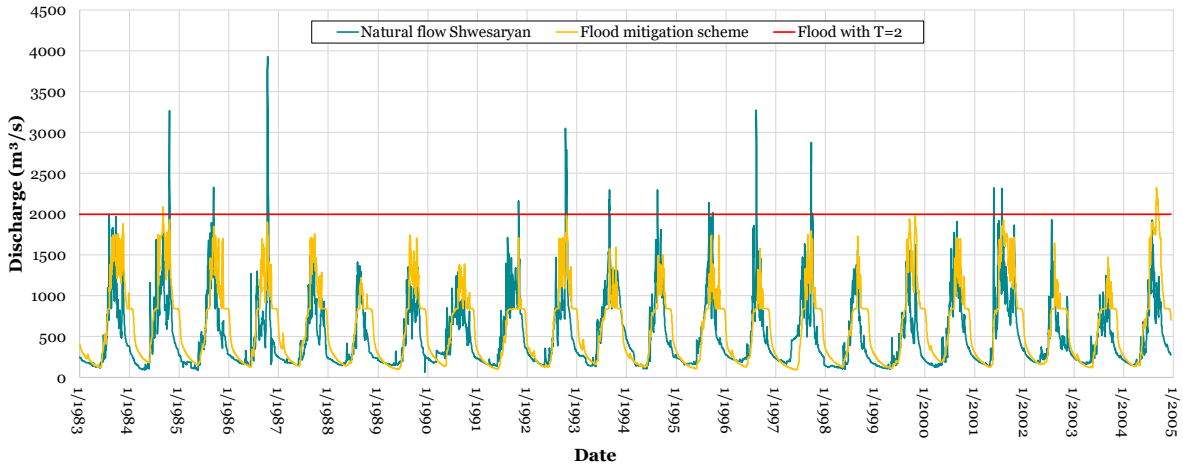

Figure 5.17: Results of flood mitigation flow regime when Yeywa is operating at 100% capacity

There is a limit to the extent to which floods can be diminished, however. The Yeywa dam cannot operate under 65% of reservoir storage capacity, and the turbines have a combined maximum capacity of $840 m^3/s$. Furthermore, the reservoir only starts to spill when the reservoir is full (i.e. at 100% of reservoir storage capacity). Therefore the floods can only be partially reduced by allowing the turbines to work at full capacity. More specifically, due to the extreme seasonality in the catchment and the small amount of active storage in the reservoir, the dam cannot optimally mitigate floods. There is not enough of a storage buffer to store the excessive amount of runoff in the wet season, so a lot of it becomes runoff over the spillway. Nevertheless, the flow regime presented in Figure 5.17 is evaluated in section 5.3

Scenario 3: Water for irrigation

For the third scenario, an increased agricultural water demand was simulated by incorporating an expanded irrigation area map. A global digital map of irrigated areas was used. This map has a spatial resolution of 0.1 degrees, and was created on the basis of cartographic information and FAO statistics (Siebert et al., 2013). The resulting hydrograph is presented in Figure 5.18.

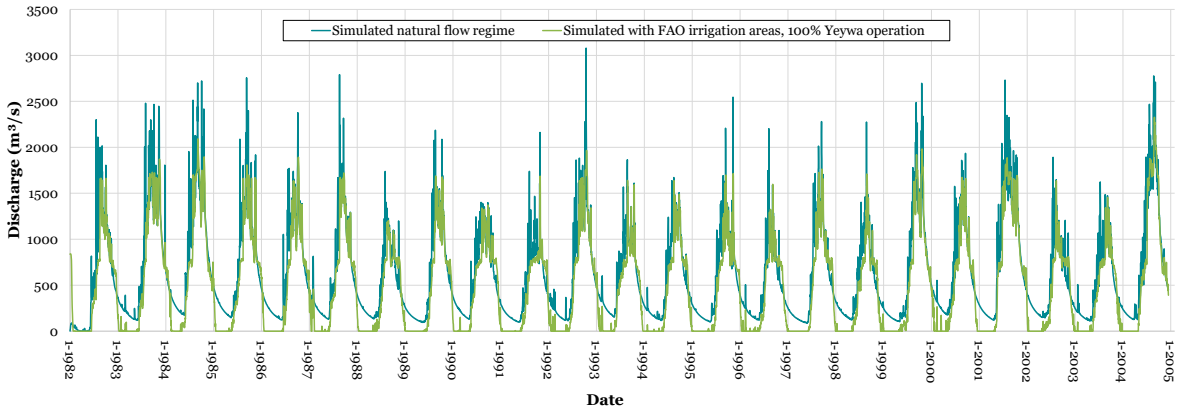

Figure 5.18: Results of increased irrigation (all FAO areas utilized) flow regime at the Shwesaryan station location. Scenario assumes Yeywa is operating at 100% capacity

The analysis assumes that all areas equipped for irrigation are actually irrigated, and that all water is taken from a single inlet at the main branch of the Myitnge. Furthermore the scenario assumes that the difference between potential transpiration and actual transpiration is the crop demand. This causes the flow to drop to zero for most of the dry season, when all the water in the river is taken out for agricultural purposes.In reality the crop demand will most likely be lower than the simulated 'transpiration deficit'. Crop water demand (i.e. actual transpiration of a crop) depends on atmospheric conditions, on the biology and biological properties

of the plant species, on the phase of growth, on the physical properties of the soil and on the water content of the plant. Therefore, the estimation for the irrigation demand is fairly simplistic. Despite this and the other relatively unrealistic assumptions, the figure gives an indication of the possible impact on the hydrology in the most extreme case. The graph shows that a significant drop in the baseflow conditions can be expected during the dry season, when the crops water demand surpasses the rainfall. The peaks are also lowered, but this partially due to the Yeywa operation at 100%.

5.3. E-flow assessments

5.3.1. Tennant method

The results of the Tennant method for the Myitnge are presented in Table 5.2. The values are based on the observed data at the Shwesaryan station.

Table 5.2: Tennant analysis results Myitnge river

Description of flow	**Recommended flow regime** (m^3/s)	
	Dry season	Wet season
Flushing or maximum	989	989
Optimum range	297-494	297-494
Outstanding	198	297
Excellent	148	247
Good	99	198
Fair or degrading	49	148
Poor or minimum	49	99
Severe degradation	49	49

Figure 5.19 presents the observed Yeywa operation between 2011 and 2018, as according to the dam operators. The figure also shows some of the bands and thresholds for the Tennant boundaries. According to Tennant, as long as at least 30% MAF is released the biological integrity of the river ecosystem as a whole is sustained (Tennant, 1976). This threshold is marked by the dark green line in the figure. The current operation drops below this quite a bit, especially between 2014 and 2017.

Tennant (1976) also concluded that 10% of the MAF is the minimum instantaneous flow needed to sustain short-term survival. At this flow, several components of the ecosystem are at risk. He found that depths and velocities were significantly reduced, substrate was highly exposed, gravel bars were dried up, streambank cover was significantly reduced, fish were crowded into the deeper pools, and the water level inside riffles became so low that larger fish could no longer pass (Tennant, 1976). This is marked by the red band on the bottom of Figure 5.19. As illustrated by the graph, the current operations dips below this threshold a few times per year, even after the reservoir had been filled.

The Tennant method is based on empirical relationships between the specified percentage of MAF and the prescribed ecological condition of rivers in the USA. Hence the assumed spatial transferibility to Myanmar remains a source of uncertainty. Furthermore, Mann (2006) examined the validity of the original Tennant predictions in multiple states of the USA, concluding that Tennant's original dataset and recommendations are most applicable in low gradient streams (<1%), but not representative of high gradient streams. Large parts of the Myitnge basin have high gradients and hence these environmental flow recommendations should not be interpreted too strictly. Furthermore, the analysis is based on percentages of an annual average, which is not necessarily representative when a basin has such a high degree of seasonality as the Myitnge does. Using percentage recommendations of seasonal or even monthly flow would alleviate this issue.

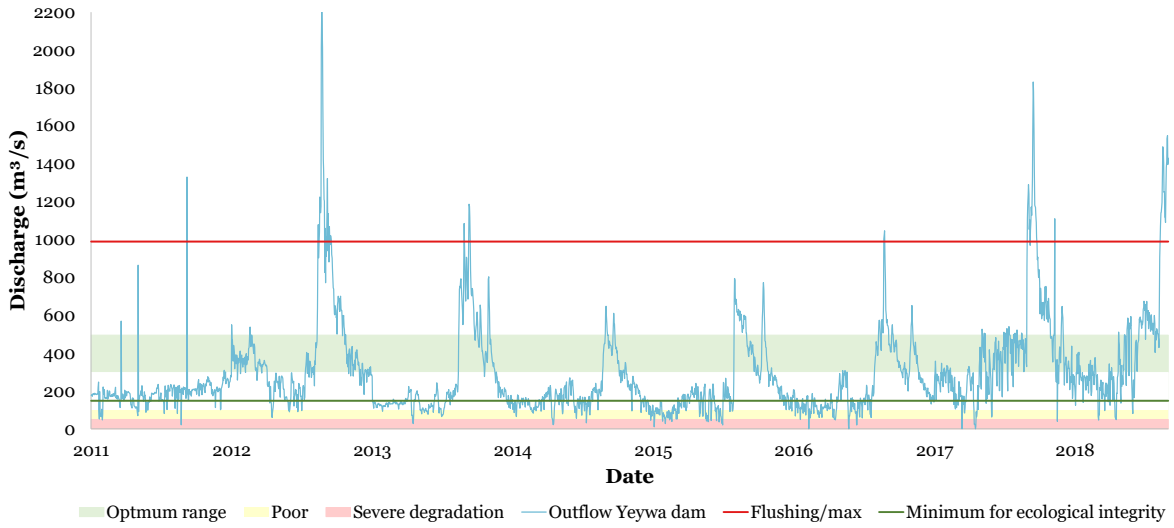

Figure 5.19: Results of Tennant ranges in the Myitnge: Yeywa operational outflow between 2011-2018

The graph in Figure 5.20 shows the results of simulated flow regimes between 2011 and 2015 for different Tennant minimum flow requirements. The figure illustrates that under optimum operation, the outflow is kept unnaturally high (i.e. higher than the inflow) during the dry season.

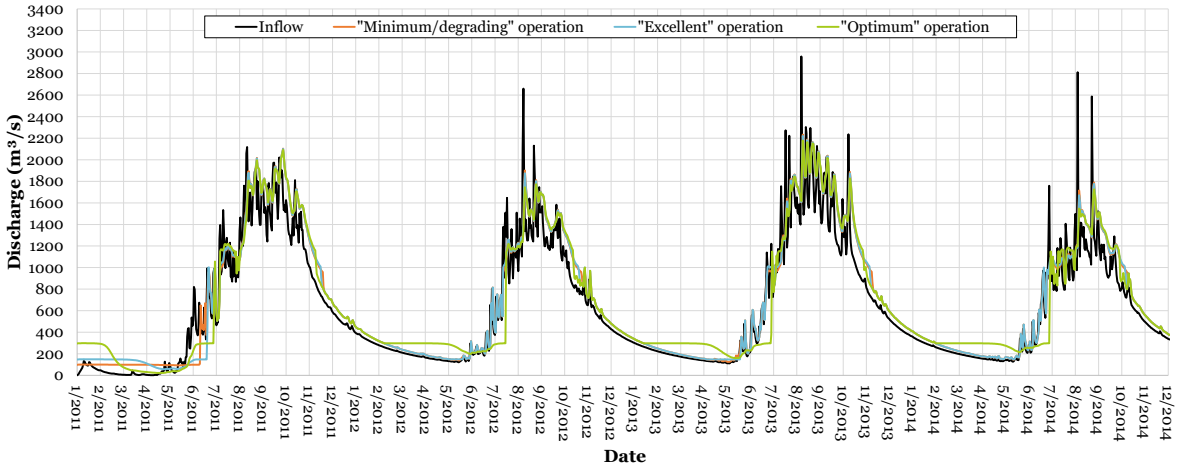

Figure 5.20: Simulated flow regimes for operation scenarios based on Tennant criteria

Figure 5.21 shows the Tennant thresholds for the simulated Myittha natural flow regime. Again, the analysis uses percentages of an annual average, which is not necessarily representative when a basin has such a high degree of seasonality.

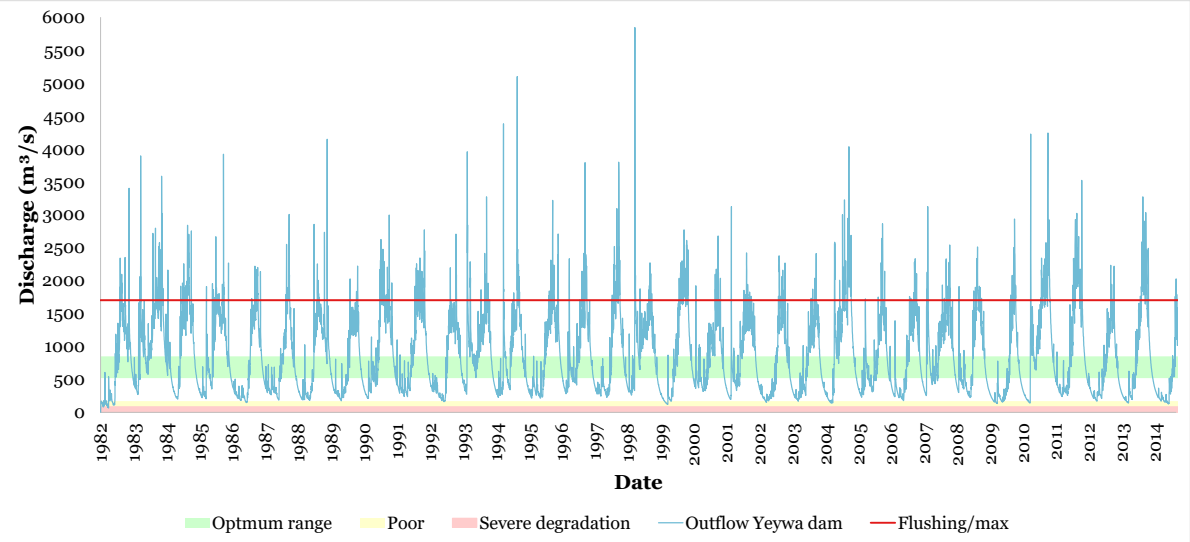

Figure 5.21: Results of Tennant ranges in the Myittha: simulated natural flow

The Tennant method can be useful, because it enables water managers to obtain a preliminary estimate of the quantity of flow necessary for instream habitats. The limitations of the method dictate that its use should be restricted to the initial planning phase, however, and that it should be followed by more intensive field analysis.

5.3.2. Flow Duration Curve, ecosurplus and ecodeficit

The results for the flow duration curves in the different simulated scenarios are presented in Figure 5.22. As the figures show, there is barely an ecosurplus for all four scenarios, although it is highest for the 29% capacity simulation. The ecosurplus is an amount of water affluence to the river ecosystem requirement. For both the 80% and the flood mitigation scenarios, there is almost no ecodeficit, the amount of water deficiency to the river ecosystem requirement. The 29% scenario actually provides more water than the river ecosystem requirement in the dry season. The irrigation scenario causes a significant ecodeficit, however, as the FDC drops to zero between an exceedance probability of 65% and 100%.

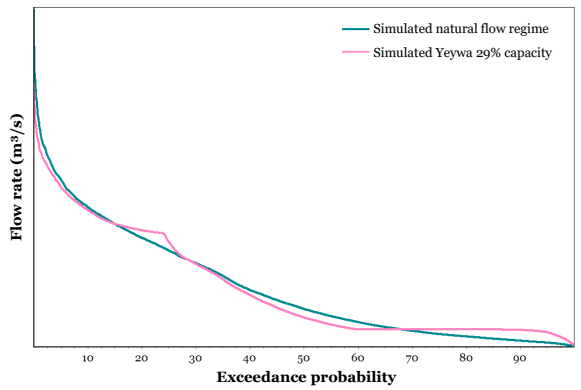

(a) FDC when Yeywa is operated at 29% capacity

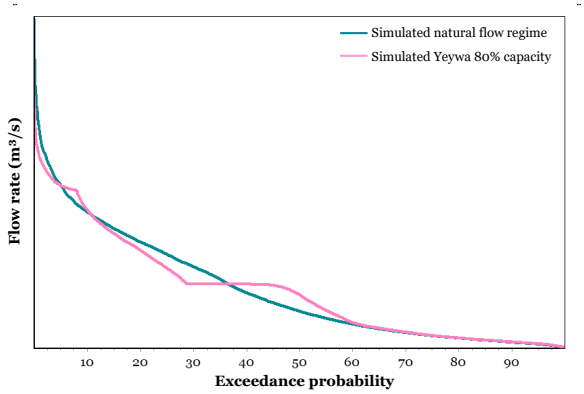

(b) FDC when Yeywa is operated at 80% capacity

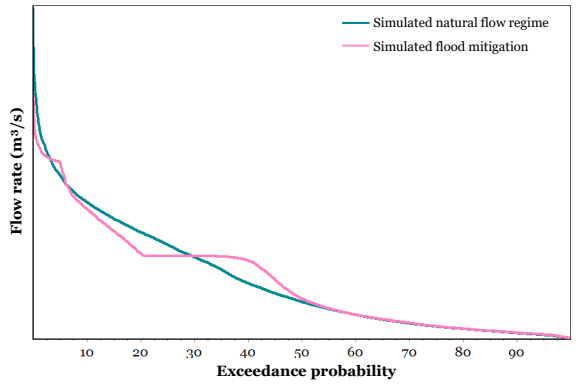

(c) FDC when Yeywa is operated for flood mitigation

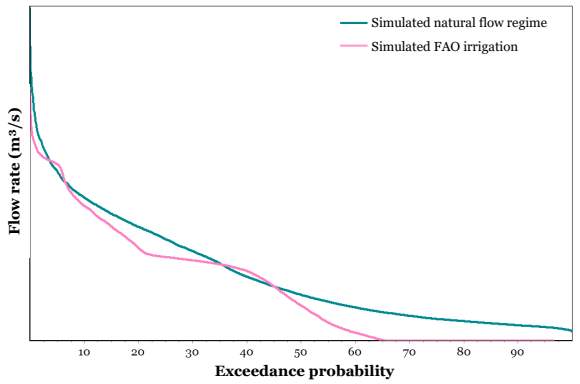

(d) FDC when Yeywa is operated for irrigation

Figure 5.22: FDC curves for the different scenarios

The ecodeficit and ecosurplus analysis provides some insight to how damaging certain regimes are for ecology, and how much water there is for river ecosystems. It is a relatively generalized method, however, and does not allow any in depth-analysis of certain ecosystem components. It also does not give insights to timing, rate of change and frequency components of the flow regime. Therefore, the next section will present results for the IHA analyses.

5.3.3. IHA analyses

Observed versus simulated data

Figure 5.23 shows the overall results for the hydrological alteration of the Myitnge based on the observed data at the Shwesaryan station. The pre-impact period was defined as 1982-2004 (when construction began), and the post-impact period starts in 2011 (when the Yeywa became operational) until 2016, which is the end of the data record.

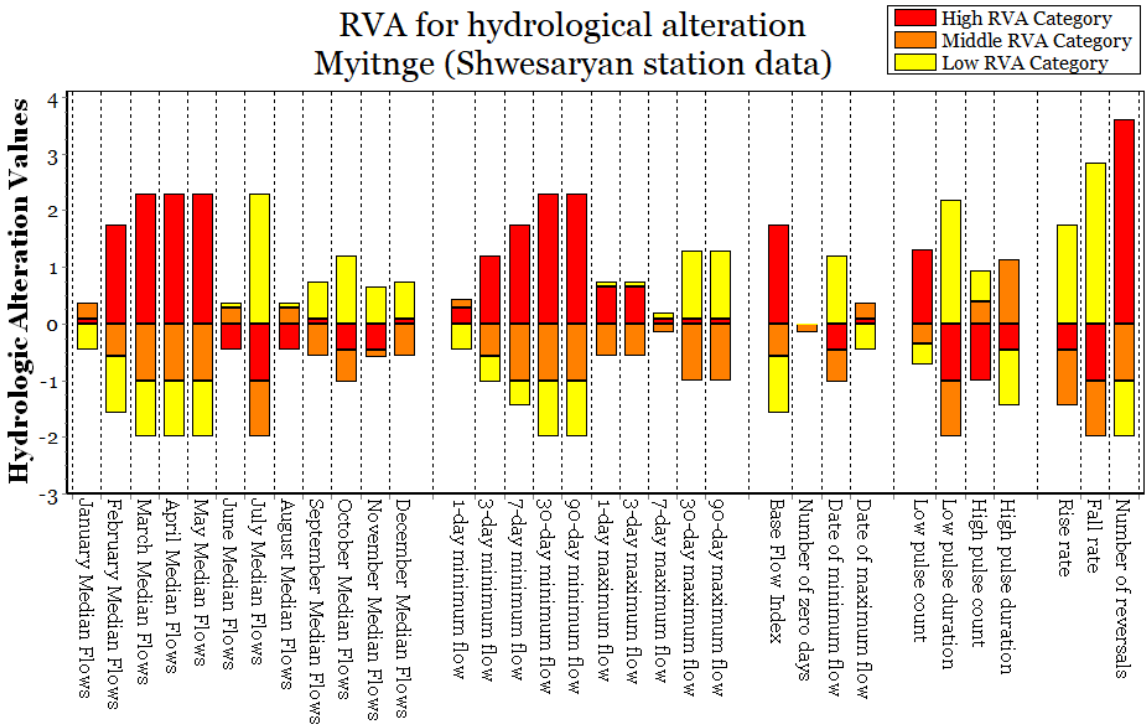

Figure 5.23: Results of the range of variability approach for indicators of hydrological alteration using the pre- and post-impact observed data at Shwesaryan station

As explained in the methodology, the Range of Variability (RVA) approach uses the natural variation of IHA parameters in the pre-dam period as a reference for defining the extent to which natural flow regimes have been changed in the post-dam period. The full range of pre-impact data for each parameter is divided into three different categories, corresponding to the the yellow, orange, and red bars in the graph. The boundaries between categories are based on percentile values for a non-parametric analysis. The category boundaries are placed at 17 percentiles from the median, yielding an automatic delineation of three categories of equal size. The analysis assumes that the frequency with which the "post-impact" values of the IHA parameters should fall within each category is 33% for each of the three categories. Subsequently the frequency with which the "post-impact" annual values of IHA parameters actually fall within each of the three categories is calculated. This expected frequency is equal to the number of values in the category during the pre-impact period multiplied by the ratio of post-impact years to pre-impact years. The Hydrologic Alteration value, represented on the y-axis of Figure 5.23 is calculated for each of the three categories as the difference between the observed frequency and the expected frequency scaled to the expected frequency. A positive Hydrologic Alteration value means that the frequency of values in the category has increased from the pre-impact to the post-impact period, while a negative value means that the frequency of values has decreased.

The most notable results regarding the indicators of hydrological alteration when looking at the observed data are the following:

- The magnitudes of monthly median flow have gone up between January and May, and down for the remaining months (June - December). The most extreme alterations are during the end of the dry season in april and may, where the magnitudes have gone up by 84% and 73% from the natural flow regime, respectively.
- The annual 1-day, 3-day, 7-day, 30-day and 90-day minima have all gone up post-impact. Especially the 30- and 90-day minima have significantly increased, by a factor of 0.45 and 0.41 respectively.
- The annual 1-,3- and 7-day maxima have also increased, all by a factor around 0.1 only. The 30- and 90-day maxima have been reduced in the post-impact period by 14% and 22%, respectively.

- The julian dates of the annual 1-day maxima and minima are both earlier in the post-impact period. This suggests a shift in the timing of extreme water conditions.
- The number of high pulses has decreased and the duration of these high pulses has gone down. The number of low pulses has increased but the duration of these has actually gone done significantly.
- The rise rate of the flow regime has gone down, whereas the fall rate has increased by more than 230%.
- The number of reversals has gone up quite significantly. This makes sense when regarding the operation of the reservoir, which has to fill up before it can be emptied when there is insufficient precipitation.

The environmental flow components of the hydrograph are highlighted in Figure 5.24 for the pre- and post-impact period. The figure shows that there are fewer extreme low flows, and no large floods. The post-impact period is only six years, however, so not too many conclusions should be drawn from this figure.

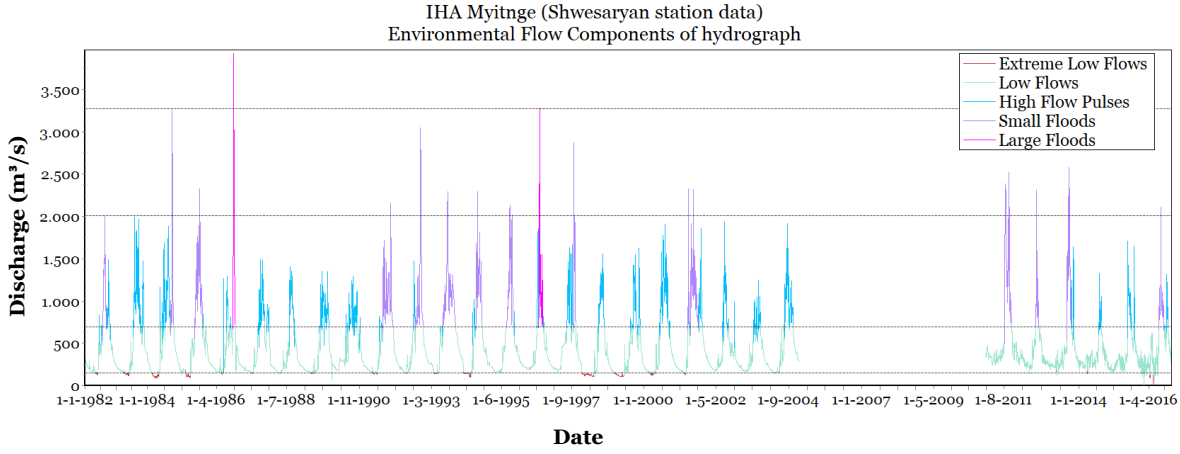

Figure 5.24: Environmental flow components of the hydrograph in the pre-impact and post-impact period, based on observed data (Shwesaryan station)

The same analysis was carried out for the simulated natural flow regime. The results for the range of variability approach for indicators of hydrological alteration is presented in Figure 5.25. It uses the simulated data for the natural flow in the pre-impact period, and the observed data for the post-impact period.

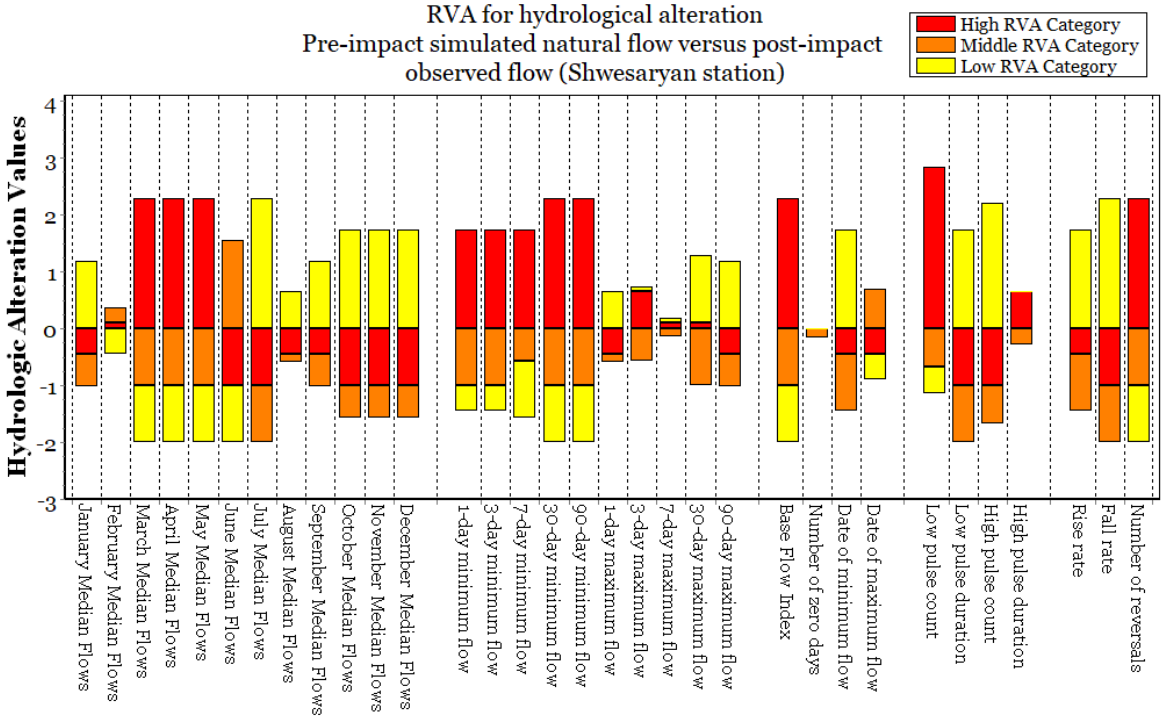

Figure 5.25: Results of the range of variability approach for indicators of hydrological alteration using the pre-impact simulated data and post-impact observed data (Shwesaryan station)

As part of the evaluation of the model, an equivalent analysis was carried out to compare the observed and simulated data. The observed flow data between 1983 and 2004 was compared to the simulated data of the natural flow regime in the same period. The result is presented in Figure 5.26. The figure shows the magnitudes of monthly flow conditions have relatively high hydrologic alteration values. The greatest hydrological alterations on the high RVA category are median flows for January, October, November and December (magnitude indicators) and the number of reversals (rate of change indicator). In the low RVA category the greatest hydrological alterations are the May median flows (magnitude indicator) and the base flow index (frequency indicator). The annual maxima are simulated very well according to the figure, as are the duration and timing indicators. Although the fall- and rise rate are acceptably different, the number of reversals has the highest hydrologic alteration value, suggesting that the model is not able to predict the reversal behaviour very well.

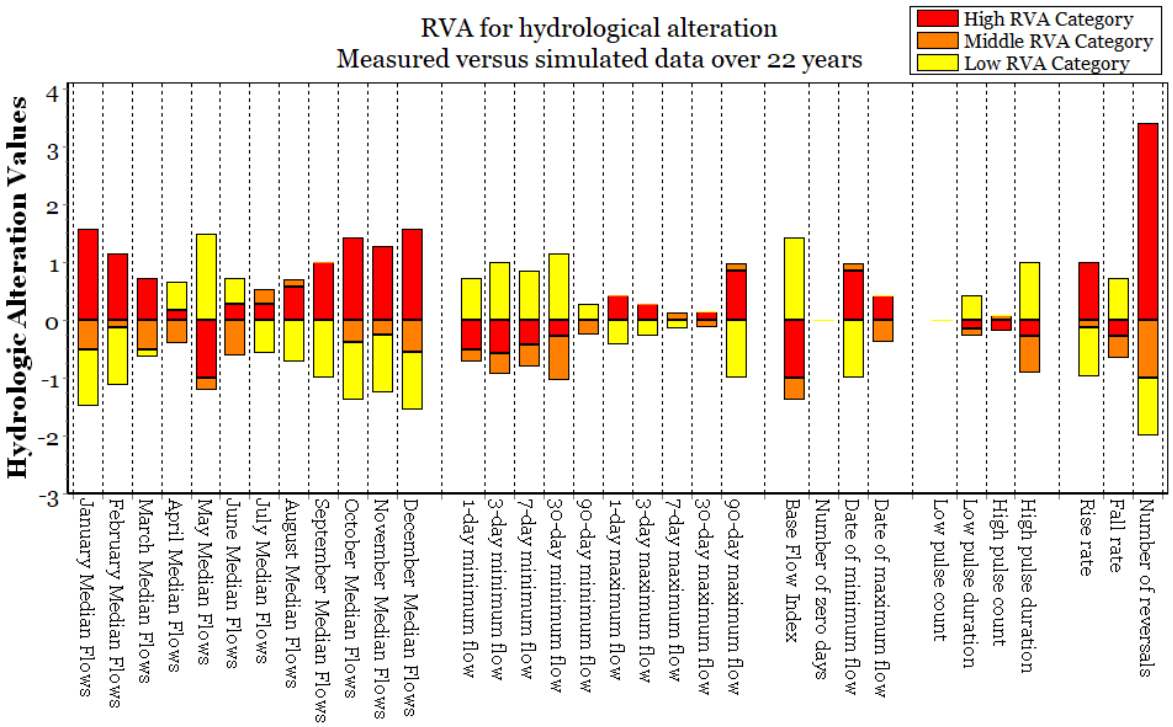

Figure 5.26: Results of the range of variability approach for indicators of hydrological alteration between observed and simulated data

Model scenarios

The scenarios created are as follows; operating the Yeywa for (maximum) power, flood mitigation, and water for irrigation. The obtained flow regimes were compared with the simulated natural flow regime. The results for hydrological alteration are presented for two power scenarios: Yeywa operated at 29% and Yeywa operated at 80%. Interestingly, the 80% scenario seems to alter the flow regime less in terms of magnitude (with the exception of the low flow months January and December), duration of extreme flow conditions and the timing of flow conditions. The 29% scenario only scores better on the frequency of flow conditions indicators. The reason for this is most probably that the 29% capacity scenario keeps the flow slightly higher throughout the entire dry season, and the 80% capacity scenario can only operate at such a level for a certain period of time, depending on the reservoir storage. After this, the turbines only let through the inflow and hence the hydrograph becomes almost equal to the natural flow regime. This is also illustrated in the hydrographs that were presented in Figures 5.15 and 5.16. The better score in the magnitude of flow in the months December and January for the 29% capacity scenario also makes sense, as the 80% scenario keeps the flow unnaturally high during these months. The RVA also shows that the rate of change indicators are both hydrologically altered significantly, and the magnitudes of these alterations do not differ considerably between the capacities. Figure 5.27a looks very similar to the RVA for the observed data, as presented in Figure 5.23. Assuming the model performs well, this suggests that the dam is currently operated at a capacity that is close to 29%.

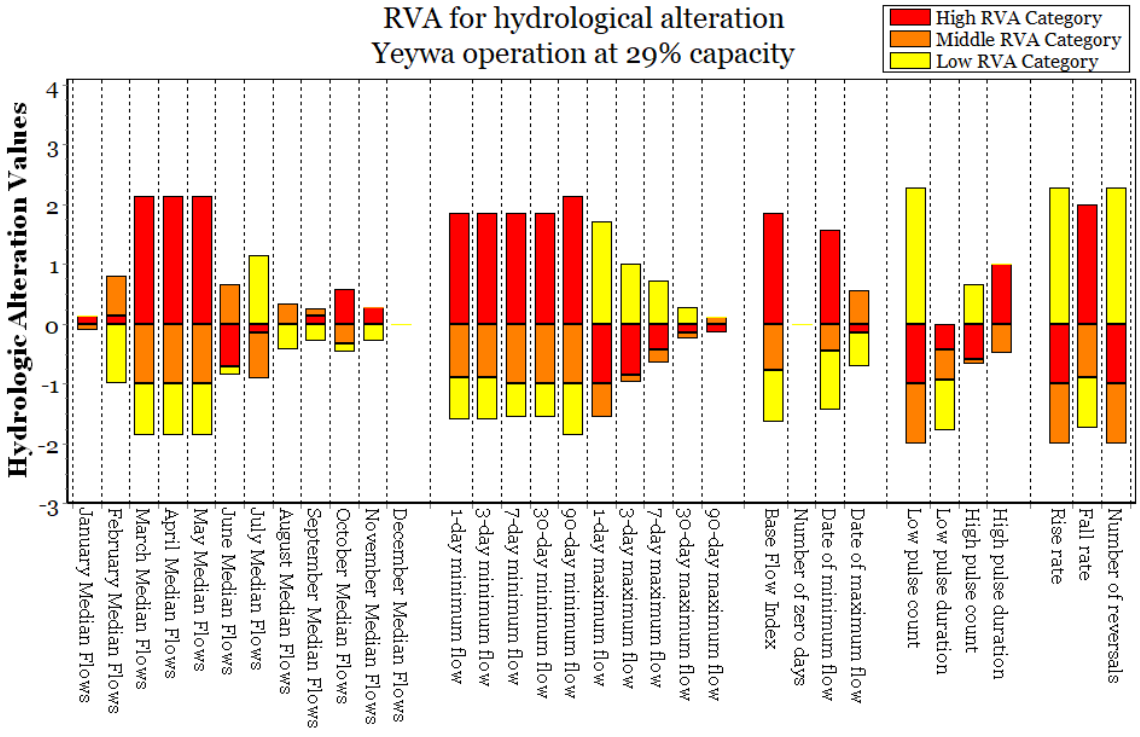

(a) Yeywa operated at 29%

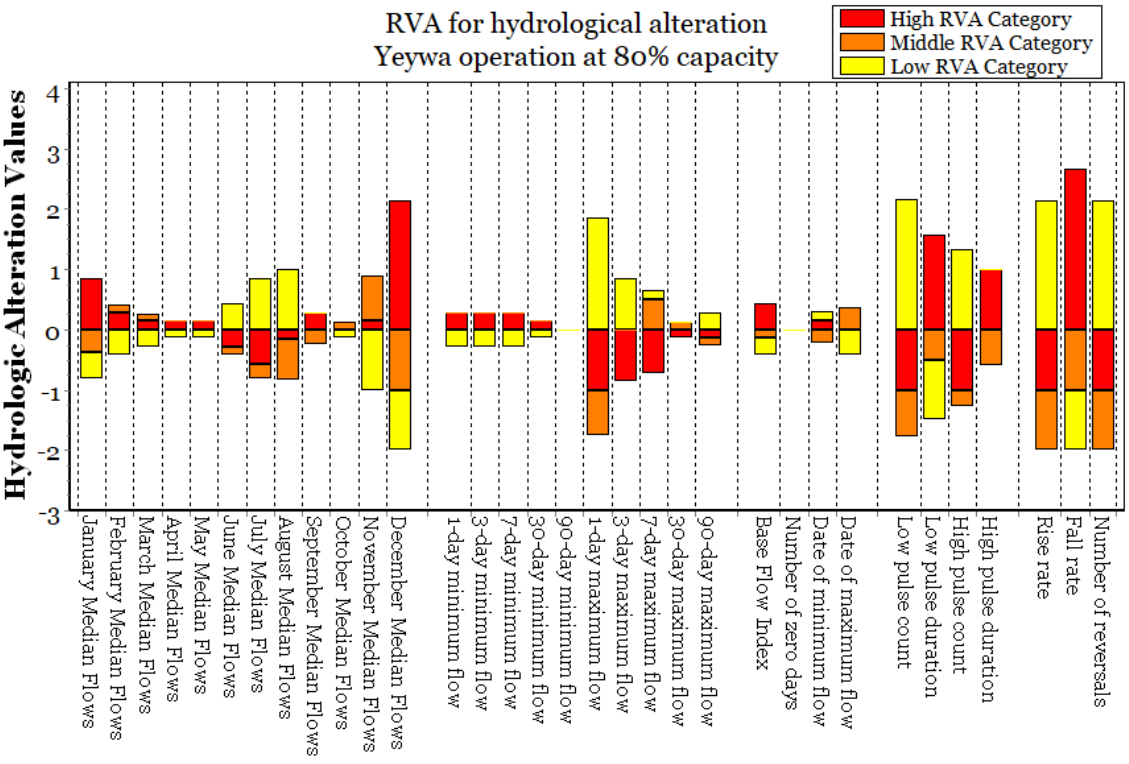

(b) Yeywa operated at 80%

Figure 5.27: Results of the range of variability approach for indicators of hydrological alteration using the simulated natural flow as pre-impact data and the simulated flow when the Yeywa dam is operated at at different capacities as the post-impact data

Regarding the environmental flow components, a summary of the most important changes is given in

Table 5.3 at the end of the section.

Figure 5.28 illustrates the RVA of hydrological alteration for the flood mitigation scenario. The results are very similar to the 80% scenario, although it scores lower on median December and January flows, and higher on indicators of timing of extreme flow conditions.

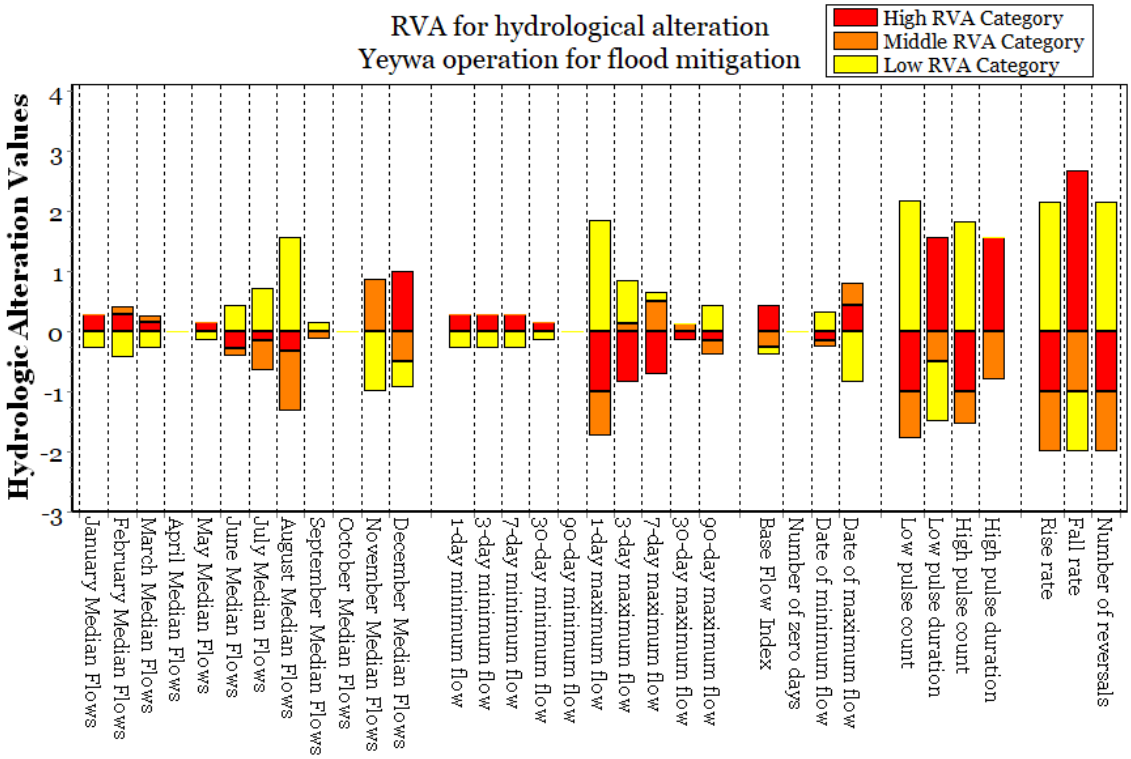

Figure 5.28: Results of the range of variability approach for indicators of hydrological alteration using the simulated natural flow as pre-impact data and the simulated flow when the Yeywa dam is operated for flood mitigation as the post-impact data

Figure 5.29 shows the RVA for hydrological alteration for the final scenario: the irrigation analysis. The results are striking, as almost all indicators seem to have very high alteration values, except for September and October median flows and the maxima with longer durations. The middle and high categories mostly have negative hydrological alteration values, meaning the value has decreased. The low RVA category has mostly positive alteration values for the indicators, suggesting an increase.

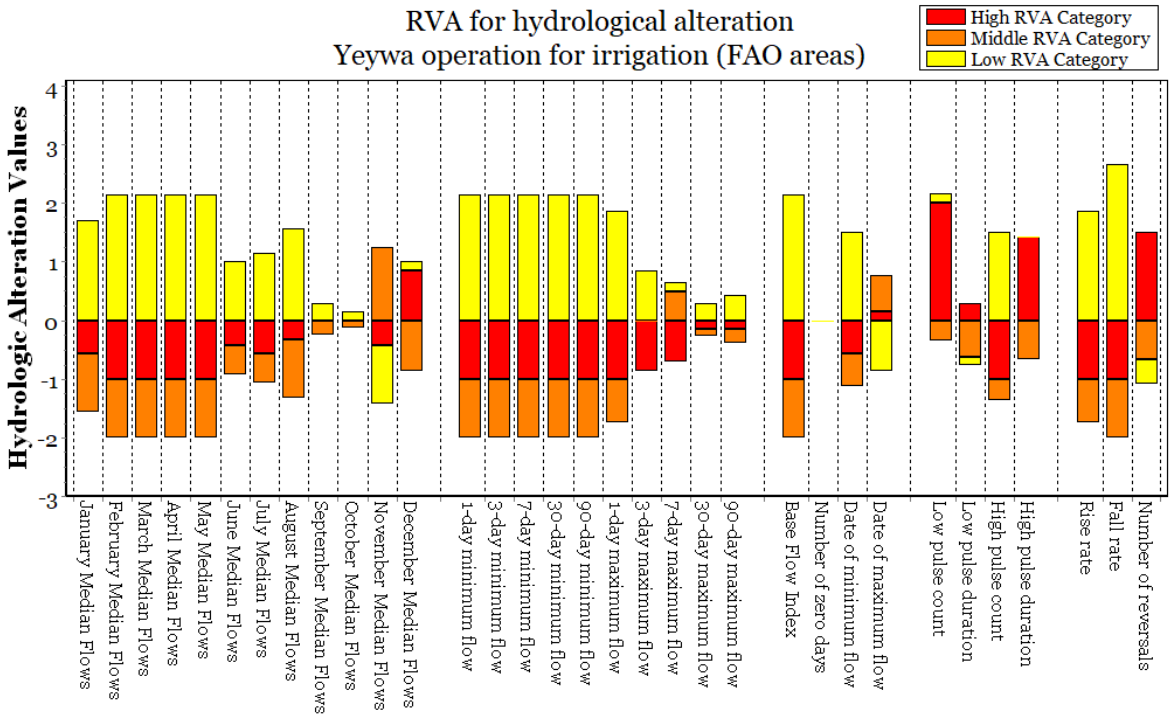

Figure 5.29: Results of the range of variability approach for indicators of hydrological alteration using the simulated natural flow versus the simulated flow when the Yeywa dam is operated irrigation (based on FAO irrigation areas)

In addition to the RVA of hydrological alteration, the environmental flow components were analyzed. A summary of the most important results for each scenario is given in Table 5.3.

Table 5.3: Summary of the changes in environmental flow components for the simulated scenarios

EFC component		**Scenario**			
		29% capacity	*80% capacity*	*Flood mitigation*	*Irrigation*
Extreme low flows	*Peaks*	Slightly lowered	Remains the same	Remains the same	Lowered
	Duration	Slightly longer	Longer	Longer	Significantly longer
	Timing	Later	Remains the same	Remains the same	Slightly earlier
	Frequency	Lowered	Lowered	Lowered	Remains the same
High flow pulses	*Peaks*	Slighly lowered	Slightly increased	Slightly increased	Increased
	Duration	Slightly longer	Longer	Longer	Longer
	Timing	Remains the same	Later	Later	Later
	Frequency	Slighly lowered	Lowered	Lowered	Lowered
Small floods		Only 1 small flood of average duration in the post impact period	Only 1 small flood of slightly longer duration in the post impact period	Only 1 small flood of slightly shorter duration in the post impact period	Only 1 small flood of slightly shorter duration in the post impact period
Large floods		No large floods	No large floods	No large floods	No large floods

The results show that the irrigation scenario induces the largest changes to the environmental flow components of the hydrograph. The extreme drop in flow during the dry season to facilitate crop demand is most likely the main reason for this. The 29% capacity scenario presents the least alterations in the environmental flow components, which is plausible as this scenario stays close to the natural flow regime for most of the year. The impact of the hydrological alterations presented and discussed in this section are evaluated for their impact on ecology in section 5.4.

5.3.4. Habitat inundation analysis

For the habitat analysis, the impact of the dam operation scenarios on the flow regime was combined with Gumbel's distribution method. The method was used to model the annual maximum discharge of the Myitnge for the measurement period of 28 years (1981 to 2008). The year 2009 is taken as a threshold because that is when the diversion of the river began, and hence the extremes after are no longer representative for the natural flow regime. From the regression analysis equation, R^2 gives a value of 0.9765 which shows that Gumbel's distribution is suitable for predicting the expected flow in the river. Using the graphs, the peak flood values for different return periods were obtained. The obtained Gumbel and Log-Gumbel plot for the pre-dam observed period is presented in Figure 5.30.

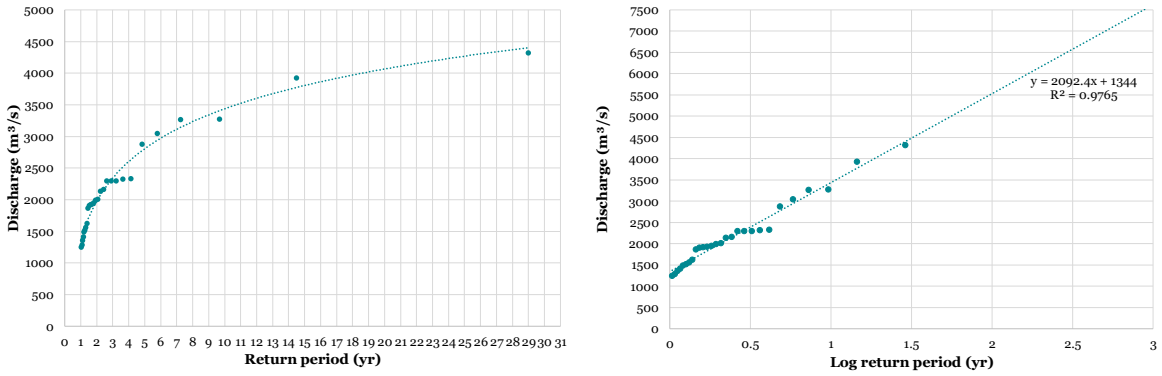

(a) Gumbell plot

(b) Logaritmic plot with extrapolation

Figure 5.30: Gumbell analysis Myitnge based observed data from Shwesaryan during the pre-dam period

Referring back to figure 2.4 in Chapter 2, research has shown that floods with certain return periods have different geomorphic and ecological functions. Floods of varying magnitude and frequency are required to maintain a diversity of riparian plant species and aquatic habitat. In the natural flow regime, medium sized floods with a return period of 1 year have a magnitude of about $1240 m^3/s$ and a 2 year return period gives a $2000 m^3/s$ flood. Floods with a 5 year and a 10 year return period have an estimated magnitude of $2750 m^3/s$ and $3430 m^3/s$, respectively. Using the extrapolation of the Gumbell-plot, a flood with a centennial return period should have a magnitude of at least $5500 m^3/s$.

Looking at the simulated hydrograph for the different operation scenarios, the frequency of occurrence of these floods is counted before and after the dam for both the observed and the simulated data. The results are presented in Table 5.4.

Table 5.4: Results habitat inundation analysis: the amount of days over a 22 year simulation that the scenarios experience floodings with defined return periods

	Natural (obs)	Natural (sim)	29% cap	80% cap	Flood mitigation	Irrigation
T=1	884	1079	1013	1018	895	864
T=2	129	98	40	21	22	19
T=5	25	4	0	0	0	0
T=10	11	0	0	0	0	0
T=100	0	0	0	0	0	0

The small floods which should occur multiple times per year transport fine sediments, which maintains high benthic productivity and creates a fish spawning habitat. These seem to remain plentiful in each scenario. When looking at floods with a return period of two years, however, the amount of days reduce significantly, ranging from from 129 days in the observed flow regime to only 19 in the irrigation scenario. The same is true for floods with a return period equal to five years. These medium-size floods are supposed to inundate low-lying floodplains and deposit sediment, allowing for the development of pioneer species. These floods also transport accumulated organic material into the river, assisting in the maintenance of the form of the channel (Poff et al., 1997). The results suggest that even just by operating the dam at 29%, crucial ecological and geomorphic functions of the river can be greatly impacted.

Larger floods with a 10-year return period do no longer occur in all of the scenarios (except in the observed natural flow regime). These inundate the alluvial terraces, where later successional species establish. This ecological process is hence also at great risk. It should also be noted that the simulated natural flow overestimates the amount of days that floods with a yearly return period occur. Regarding floods with higher return periods, the simulated regime consistently underestimates the amount of days. This indicates that the magnitude of flow may not be properly simulated for the natural flow regime, as has also been discussed in previous sections of this chapter.

Finally, the very rare floods with big magnitudes (T=100) which can uproot mature riparian trees and deposit them in the river, do not occur over the simulation periods. This may partially be due to the short simulation time period, however. Unfortunately the forcing data availability does not allow for a longer simulation, however.

5.4. Impact on ecohydrology

5.4.1. Affected ecological processes

Sections 5.2 and 5.3 presented in detail how the Myitnge river can be altered hydrologically by the Yeywa dam. This section will consider the ecological implications of these alterations. The most important ecological impacts are listed, divided up per scenario:

Current operation (observed)

- Due to the different magnitudes of flow the habitat availability for aquatic organisms is at risk. The reliability and availability of water for terrestrial animals are also at risk. Furthermore, the access by predators for nesting sites becomes easier.
- The annual longer day (30-day, 90-day) minima have gone up significantly, and the longer day maxima have actually reduced. This suggests that the distribution of plant communities in floodplains and ponds may be altered because of differences in plant colonization site creation. This change in the regime also can have a great impact on the stressful conditions such as soil moisture stress and anaerobic stress in plants.
- The changes in timing of annual extreme water conditions due to the Yeywa show earlier Julian dates for both minima and maxima. This means that the compatibility of the river regime with life cycles of organisms is changed. Because of this, behavioural mechanisms such as spawning cues for migratory fish are altered. These migratory fish are very important in the Myitnge, as illustrated in Section 3.2.3 of Chapter 3. The dates have not been altered significantly, however, so the impact is assumed to be small in the current operation.
- The frequency of flow did show big changes in both the pulse counts and duration. This mostly influences the bedload transport and channel sediment textures. It also controls the availability of floodplain habitats for aquatic organisms, however.
- The large hydrological alteration values for rate of change indicators suggest that there may be entrapment of organisms on floodplains, and drought stress on plants. These fast rise and fall rates are detrimental for macroinvertebrates.

29% capacity scenario

- The magnitude and duration of annual extreme water conditions is altered most suggesting possible changes in the nutrient exchanges between rivers and floodplains. This also impacts the distribution of plant communities and structuring of the river morphology and physical habitat conditions.
- The rate of change parameters also see significant changes in this regime, again suggesting entrapment and drought stress on low-mobility organisms on the streamedge.

80% capacity scenario

- The frequency of flow conditions indicators are altered most in this scenario, together with the rate of change indicators. The former suggests an impact on bedload transport and substrate disturbances, as well as altered nutrient exchanges and habitat availability.
- The rate of change indicators, which have have changed post-impact, influence the ecolhydrology as listed above for the 29% scenario.

Flood mitigation scenario

- This scenario gives similar, but more extreme results than the 80% scenario. The same ecological influences are expected.

Irrigation scenario

- The magnitudes of flow have been altered completely for all months except the peak of the wet season. Habitat availability, as well as water availability and reliability for animals and plants are affected by this. For this particular scenario, the extreme droughts due to the agricultural water can cause soil moisture stress in areas not irrigated, as well as water quality issues by changing water temperature and oxygen levels.
- The duration of extreme flow events has changed significantly, which can lead to implications as listed for the 29% scenario.
- As for all the scenarios, the rate of change indicators have been altered, so entrapment of species, and desiccation stress is expected on both plants and organisms.

In all scenarios, large floods have significantly reduced or completely disappeared from the flow regime. These floods are meant to maintain the balance of species in river communities however, as well as to create sites for recruitment of colonizing plants. As the habitat inundation analysis also demonstrated, they have the function of shaping the physical habitat of the floodplain. More specifically, with fewer floods, the lateral movement of the river does not allow the forming of new habitats (such as secondary channels and oxbow lakes). Finally, without large floods, fewer organic materials and woody debris are transported, providing the ecosystem with less food and habitat structure. For example, woody debris serves as an important site for invertebrate attachment and production.

5.4.2. Impact on macroinvertebrates

As mentioned in Chapter 2, aquatic insects have great ecological significance to healthy aquatic ecosystem functioning and are suitable indicators of ecosystem health. Although the Yeywa became operational only in 2011, macroinvertebrates can show a rapid response to perturbations and environmental stress. This is mainly because most species have annual life cycles, and some even have multiple generations per year or two or three year life cycles. The results for the biomonitoring of the Myitnge are presented in Figure 5.31, based on the raw data in Figure H.1 of Appendix H.

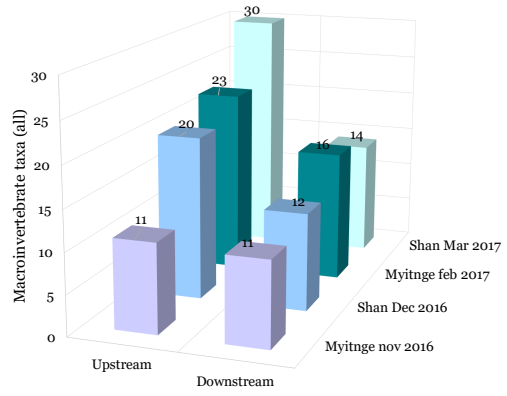

(a) Differences in average macroinvertebrate taxa up- and downstream of hydrodam

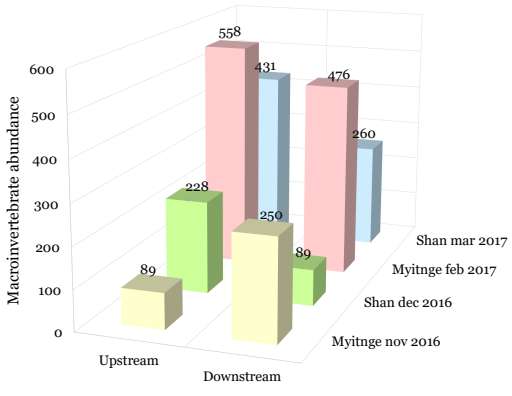

(b) Differences in average macroinvertebrate abundance up- and downstream of hydrodam

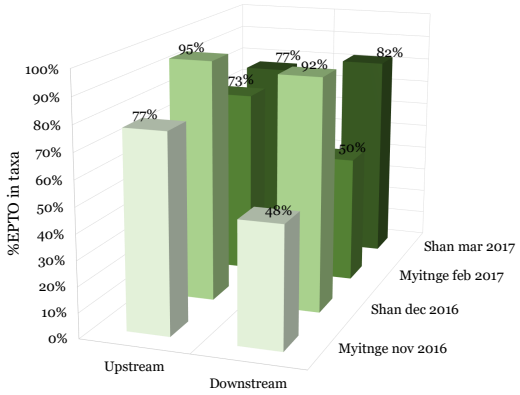

(c) Differences in % EPTO in macroinvertebrate taxa up- and downstream of hydrodam

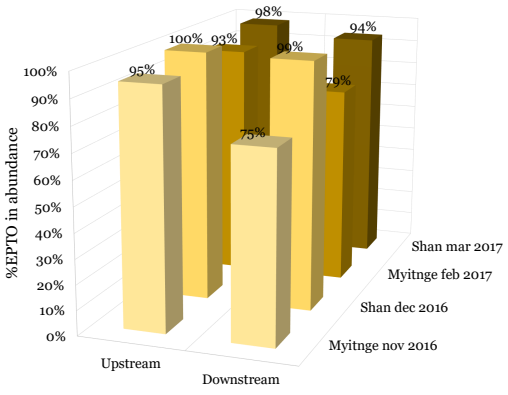

(d) Differences in % EPTO in macroinvertebrate abundance up- and downstream of hydrodam

Figure 5.31: Results of macroinvertebrate biomonitoring samples

Any conclusions drawn from the biomonitoring samples are based on the assumption that the situation upstream of the dam is representative of the pre-impact conditions. The abundances and taxa are furthermore assumed to be 'relative' because kick samples represent a semi-quantitative approach. The results show a general decreasing trend in taxa and abundance (with the exception of the abundance in the Myitnge in November of 2016). The Ephemeroptera, Plecoptera, Trichoptera, and Odonata (EPTO) species are particularly important for ecological and biomonitoring studies because they are only found in abundance in clean waters and are very sensitive to disturbances. As Figures 5.31c and 5.31d show, the percentage of EPTO in the taxa and abundance also decreases from the upstream to the downstream (with the exception of the EPTO in abundance in the Shan during March of 2017). The scale of this biomonitoting experiment can be argued to be too small to draw conclusions, however. Only a few sites were sampled, at a relatively low temporal frequency. Furthermore, literature has shown that macroinvertebrates are mostly sensitive to water quality, sediment and temperature changes, and much less to hydrological alterations (Rosenberg and Resh, 1993). Worrall et al. (2014) showed that hydrological variables only account for a relatively small proportion of the total ecological variability, and that a range of other factors were more critical for macroinvertebrate community response. Water quality, sediment, and temperature changes are often caused by hyrdological modifications, however, so indirectly (and directly, to some extent) the flow regime does impact the macroinvertebrates. Biomonitoring in the Myitnge basin in the context of this research is not optimal, because the sediment dynamics, water quality and temperature components were not considered. Although association between all the listed indicators and macroinvertebrates is clear, establishing causality for the reduced taxa and abundance in the Myitnge is much more difficult. Nevertheless, the biomonitoring samples are insightful and indicate that the Yeywa dam has impacted the ecology as the loss of certain taxa sensitive to change is already evident. On the other hand, for rivers such as the Myitnge in Myanmar, biomonitoring of macroinvertebrates may be the best ecological impact indicator available, and the only practical choice that allows for

some empirical insights. More frequent spatial and temporal sampling is advised for robust results, however.

5.5. Discussion of the overall validity of results

The data and methods adopted in this research have caused the propagation of a significant amount of uncertainty in the results. A summary of this is illustrated in Figure 5.32, where the red, orange and yellow labels present sources of uncertainty, respectively in order of importance.

As detailed in section 5.2.1, the observed discharge time series adopted for the calibration of the the simulated discharge were derived from gauge height and rating curves. There were quite some inconsistencies within the data and strange relations between the data, however. The rating curve for the Myitnge, which has not been publicized and hence remains unknown to the author, is assumed to possess limitations because it has not been updated since 1982. Especially the higher flows can carry quite some uncertainty due to the unreliable rating curve. Therefore the calibration of the model focused on getting the baseflows correct. Constraints in data availability were a major factor determining the selection of a hydrological modelling approach in the context of the study aims. Reference (observed) discharge estimates were limited to one station in the entire Myitnge basin, and the data from the Yeywa operators. In the Myittha there were no discharge observations whatsoever. It should hence be noted that adopting a model with a large number of parameters when the amount of observations is limited will introduce the possibility of equifinality and complexity. Additionally, difficulties in access to ground observations of climatic forcing data led to the choice of global gridded products for the estimation of these variables. The quality of these products remains unknown, however, because Myanmar has only recently began to contribute to providing ground observations for validation. Despite the acceptable performance of the model in terms of the adopted metrics, the capacity of the model was too limited to reproduce the observed discharge peaks and mimic the number of reversals of the natural flow regime (see Figure 5.26).

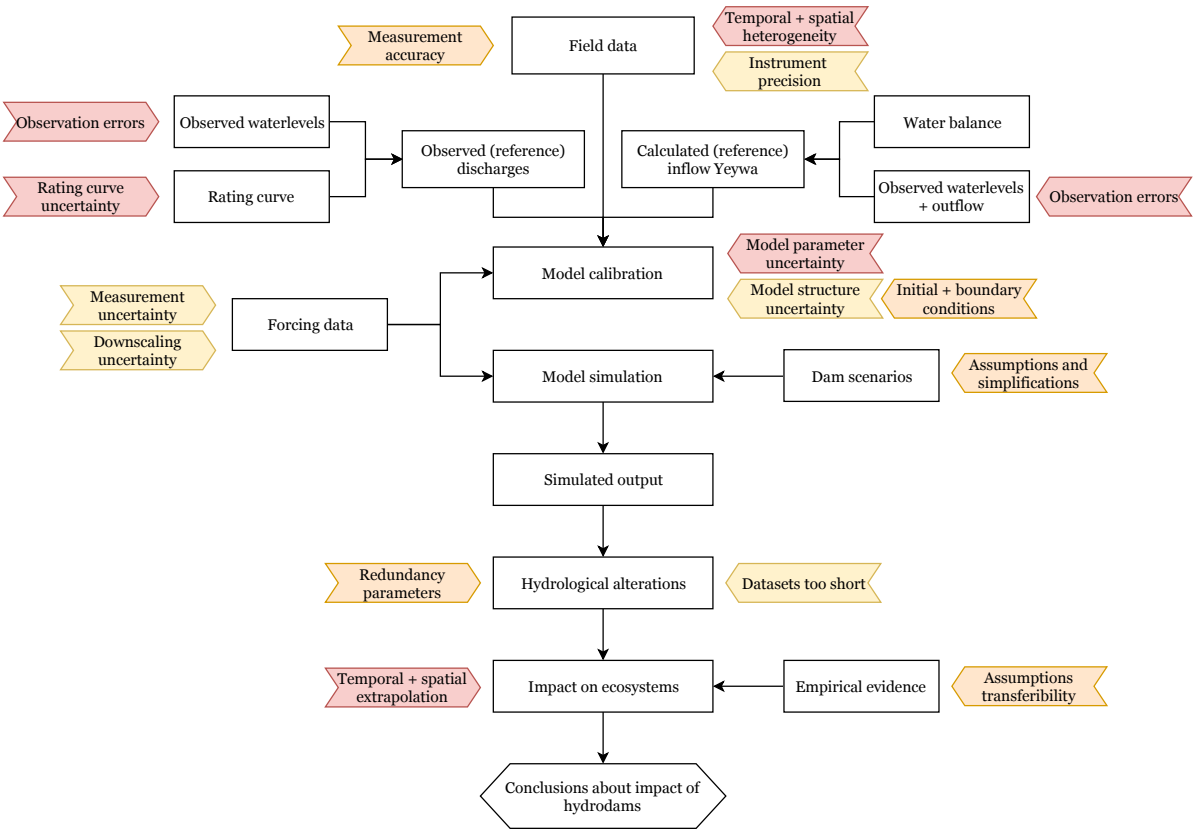

Figure 5.32: Non-exhaustive representation of the sources of uncertainty in data and methodology of the research

Additional sources of error include possible biases in the adopted forcing data, and the downscaling of this data to the relevant spatial resolution. Furthermore the *WFlow_sbm* model, as all hydrological models do, only has a limited ability to properly reproduce all relevant mechanisms involved in the rainfall-runoff

process. The *WFlow_sbm* model was developed for steep catchments and relatively thin soils. Therefore, within the context of this study, the lateral movement of groundwater may be very wrong in terrain that is not steep. Significant parts of the study basins are flat and flood plain areas, suggesting uncertainty in model results. The model was applied on a daily basis, although it is suggested that a storm-based approach will yield better results in situations with more than one storm per day (Schellekens, 2018). In the rainy season of Myanmar there are often multiple large storms per day, and hence a storm-based approach would have benefited the validity of the results. The temporal resolution of the forcing and calibration data, however, did not allow for such an analysis.

As the figure shows, uncertainty always remains due to errors in models structure and parameters. This uncertainty should be properly assessed for a more informed model application. For example, zooming in on the soil bucket model, elaborated on in Appendix D, there are several simplifications that contest the validity of the results. The numerical solution of the soil water flow is a simple explicit scheme and the lateral groundwater flow follows topography rather than true hydraulic head. Additionally, due to the simple representation of the unsaturated zone, results for deep soils (i.e. soils deeper than $2m$) may be unrealistic (Schellekens, 2018). Furthermore, as discussed in detail, there seems to be a structural process error in the model that causes the recession of the simulated discharge to be too slow. This is apparent from the results of the model in the months following the end of the rainy season (see Figures 5.8 and 5.11).

Regarding the hydrological alterations and environmental impact assessments, a few sources of uncertainty and their impact on the results should be mentioned. Hydrological methods for environmental flow assessments such as the ones used in this study are simple, fast and inexpensive desktop approaches with a low data need, making them suitable for water resource planning purposes. However, they are also very simplistic, inflexible, and have a low resolution output. Despite the recent advances made to improve ecological relevance of flow indices and to set flow targets, there are still a limited amount of direct ecological links between the hydrological indices and ecosystem components. The analyses do not properly address the dynamic nature of the flow regime and are hence argued to be suitable only for low controversy situations. The Yeywa dam, as the largest dam currently installed in Myanmar, in combination with the additional plans on the Myitnge river (see Chapter 3), have the potential for a big impact and hence requires a more in depth analysis of the hydrological and ecological implications.

Furthermore, the indicators of hydrological alteration are known to possess some redundancy due to their multicollinearity. The research of Gao et al. (2009) showed that IHA statistics are highly inter-correlated and the use of a single or just a few indices of hydrologic alteration can minimize statistical redundancy. This in turn can lead to considerable reductions in the complexity associated with the formulation and development of reservoir operation policies and river regulation schemes that optimize elements of environmental flow. The correlation coefficients among the IHA statistics for both a simulated and empirical datasets are presented in Figure 5.33. It was furthermore found that the ecodeficit, the indicator presented in section 5.3.2 for this study, appeared to be the best generalized index among all the indices in the simulated data set (Gao et al., 2009).

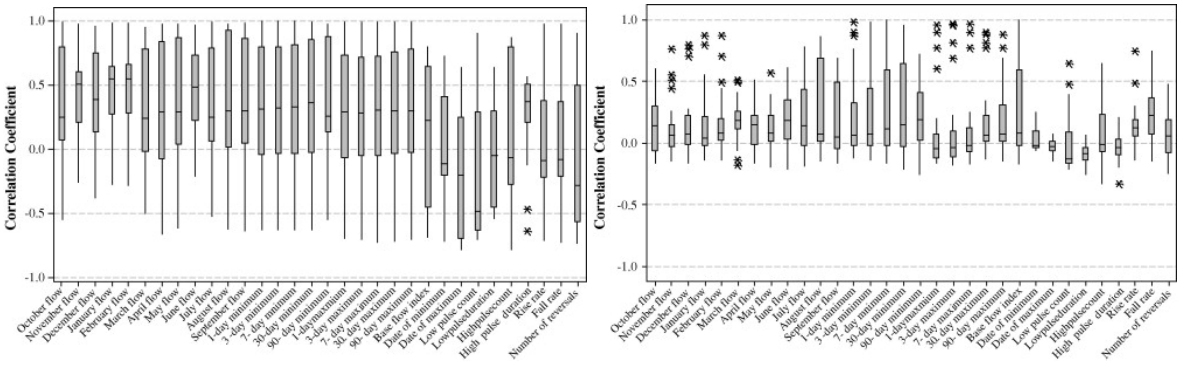

(a) Correlation coefficients among the IHA statistics for the simulated data set (Gao et al., 2009)

(b) Correlation coefficients among the IHA statistics for the empirical data set (Gao et al., 2009)

Figure 5.33: Correlation coefficients among the IHA statistics (Gao et al., 2009)

Moreover, the IHA statistics are only meaningful when calculated for a long enough hydrologic record. It is suggested that the length of record necessary to obtain reliable analysis is at least 20 years of daily records for

the pre-impact period and 20 years for the post-impact period (Richter et al., 1997; The Nature Conservancy, 2009b). The Yeywa was completed in 2011, meaning that the hydrological alteration analysis is based on a few years only. The simulations provided data for more than 20 years, but these carry a large amount of uncertainty with them, as illustrated in detail in the sections and paragraphs above.

The estimated impacts on the ecosystem presented in the results are mostly based on relations between hydrology and ecology from literature. These relations have often been established from empirical studies in areas where data is plentiful. The spatial transferability of the ecohydrological relations to Myanmar ecosystems hence remains a source of uncertainty that ought to be addressed. The results of the biomonotoring do not have this problem, although the scale of the experiments does not allow for strong conclusions to be made. Ecosystems and their components are inherently complex, and causality is difficult to prove when it comes to environmental flow studies such as this research. For example, the basin is changed by more than just the dam, as areas are being urbanized or cultivated for agriculture. The methodology's ecological predictive capability hence remains unsure.

6

Conclusions and Recommendations

This study had three objectives. First of all, the study intended to examine the extent and manner by which the natural flow regime of the Myitnge has been hydrologically altered by the Yeywa dam. As a second goal, the study aimed to assess the ecological processes that have been or could potentially be most affected by these hydrological modifications in the Myitnge. Finally, the study had the purpose to evaluate the suitability of the *WFlow_sbm* model as a tool for environmental flow management in Myanmar. The conclusions are structured according to these objectives. Recommendations are given in section 6.4.

6.1. Impact of Yeywa dam on hydrology

The results of this study demonstrated that different elements of the flow regime can be altered (to some extent) depending on the Yeywa operational scenario. For a 29% scenario, the magnitudes and duration of flow are altered completely compared to the natural regime. In a scenario where this capacity is raised to 80%, the frequencies and rates of change within the flow regime are altered, whereas the magnitudes and duration remain relatively close to the natural flow regime. This is mainly because this scenario only remains feasible for a certain amount of time during the year, depending on the seasonal water supply. The same is true for the flood mitigation scenario. For the irrigation scenario, the high water uptake to meet the crop demand alters the magnitudes and duration to an even larger extent.

It is remarked that the operational scenarios implemented in this study have a limited capacity to simulate reservoir operations under real conditions, and hence the impact on the flow regime remains an estimation. However, the results obtained in this study provide substantial evidence for the need to adopt a reservoir policy that is flexible and adaptive depending on expected seasonal inflows if ecological integrity is to be maintained. There is potential for the optimisation of the operation of the Yeywa reservoir with this goal in sight, but this potential remains limited to the availability of inflows, which in turn is dependent on the natural seasonality and the size of the reservoir.

Nevertheless, the Yeywa dam fragments the Myitnge river and can alter the river regime. The extent to which it can control the Myitnge flow, however, is not significantly high. According to the results, raising the capacity at which the dam is operated can only be done for a limited amount of time, as the (seasonal) inflow upstream of the dam allows. Therefore, the ability of the Yeywa dam to alter the hydrological regime will remain limited: the flow let through the turbines and spilled over the spillway (and thus the flow components associated with this) will not deviate much from the natural regime. This makes sense, as the Yeywa dam was designed as for a run-of-the-river scheme. The results also show, however, that a combination of Yeywa operation and increased irrigation uptakes reduces the water supply significantly, which poses a much larger risk and threat to ecohydrology.

6.2. Impact on ecological processes

The impacted ecological processes have been illustrated in detail in section 5.4.1 of Chapter 5. Habitat availability for different species of plants and animals, as well as the river's ability to structure the channel morphology are the elements most at risk due to the Yeywa dam. This is evidenced by the reduced macroinvertebrate taxa and abundance downstream of the dam in the biomonitoring results (see section 5.4.2 in Chapter 5), as well as the assumed extinction of the Burmese roofed turtle, Batagur trivittata. The latter is most likely

due to the flooding of many nesting areas when filling up the Yeywa reservoir, and the increased access of fishermen to the upstream areas of the river due to the Yeywa dam infrastructure and a more controlled river due to the dampening by the reservoir (Lee and Zöckler, 2018). Furthermore, Myitnge's vital (as recognized by the Ayeyarwady SOBA (Kennard et al., 2017)) migratory fish are potentially at a great risk due to the obstruction the dam poses to their route, and the potential changes in spawning cues due to changes in timing of hydrological extremes.

Out of the modelled schemes, the largest ecological impacts are associated with the irrigation scenario. The discharge drops considerably due to the increased irrigation uptake, which can have detrimental impacts on ecological integrity. Interestingly, the ecological impacts are not significantly different between the different Yeywa operational capacity scenarios. The primary reason for this is the extreme seasonality associated with the monsoon. These conclusions remain somewhat questionable, however, due to the uncertainty propagation elaborated on in Section 5.5 of the previous chapter. Nevertheless, the results show that the dam alone does not alter most of the components of the natural flow regime (and hence presumably the associated ecological factors) significantly, because the attainable operational capacity is limited by seasonal inflow. Ecological impacts of hydrological alterations and their significance should ideally be assessed with biological indicators based on monitoring data that are specifically sensitive to hydrological alterations. Therefore, a more comprehensive assessment, using for example habitat simulation or holistic methodologies, is recommended.

6.3. Applicability of the model for E-flow assessments

Most severe hydrological alterations can in many cases already be detected with simple tools that analyze the extent of the pressures or the alteration of habitats. Therefore, a tool with a low data demand such as the *WFlow_sbm* model can be valuable in countries like Myanmar, where hydrological and ecological data is scarce. The results demonstrated that the model can produce the natural flow regime relatively well in terms of duration of annual extreme conditions, timing, and frequency. When it comes to the magnitudes of flow during certain months and the rates of change of the regime, however, the model does not perform as well as would be desirable for realistic environmental flow assessments. The former is most likely because the model appears to contain a structural process error that causes the recession at the end of the monsoon to be too slow. Therefore, the simulated flow remains above the observed flow for most of the months succeeding the cessation of the wet season. Although the observed flow regime reaches the baseflow level a couple of months earlier, a very similar magnitude baseflow is reached by the simulated regime eventually. The rising limb is simulated very well, regarding both the aspects of timing and magnitude of flow. The results of the Myittha natural flow regime demonstrated the model's ability to simulate a river without streamflow data, although it was still validated and calibrated based on water level data as well as observed and estimated processes.

The simulated flow regime of the Myitnge was validated based on observed streamflow data. The availability of these data allows the hydrological environmental flow analyses without the use of a model. However, *WFlow_sbm* allows for the creation of future scenarios, such as increasing the dam capacity and irrigation uptake, as was demonstrated by this study. The uncertainties and assumptions in the variables such as those illustrated in Chapter 5 suggest that the results obtained in this study should be interpreted mostly on a relative basis. The obtained flow regimes allow for a comparative analysis between scenarios and the associated ecological impacts. The absolute values of the simulated flows for each scenario should not necessarily be taken as correct representations of expected behaviour, however. As with any (hydrological) analysis, a greater availability of data with higher resolution and accuracy may allow the generation of more accurate simulations. These results in turn lend themselves to more refined hydrological and ecological analyses. If efforts in data collection for Myanmar are continued, future research on environmental flows will benefit from the availability of greater quantity and quality of data, and thereby a reduction in the uncertainty propagation.

6.4. Recommendations

6.4.1. Recommendations for Yeywa dam management

The results of this study showed that operating the dam at a high capacity cannot be sustained throughout the year. Because of the extreme seasonality, the water let through the turbines will eventually become equal to the natural upstream inflow, suggesting no hydrological alteration whatsoever on the daily basis for part of the water year. Hydropeaking during the day fell outside of the scope of this study. More specifically, the results showed that running the dam at 29% capacity is the highest attainable operation that can last throughout the entire dry season, keeping the discharges slightly higher than they would be naturally. Therefore, one

of the main recommendations is to avoid keeping the outflow below the natural inflow in the dry season, and to run the turbines at maximum capacity during the monsoon period. The former is a minimum that should be mandated to protect the downstream channel area from dewatering causing water stress and habitat issues, especially in combination with irrigation water intake. The latter is beneficial from an ecological and economic point of view as it maximizes the electricity generation while the natural flow regime is maintained.

6.4.2. Recommendations for further research

This section will briefly give an illustration of suggested further research. It should be noted that the recommendations given here are non-exhaustive. First and foremost, it is recommended to look at hydrodam impacts in Myanmar on a smaller temporal scale. This would allow an analysis of the occurrence and impact of hydropeaking, which can have detrimental effects on many species including macroinvertebrates (Leitner et al., 2017). Different environmental flow analyses such as hydraulic, holistic and habitat simulation methodologies may also offer new insights on the ecological impacts and hence should be explored.

Furthermore, the impact of the Yeywa dam on sediment dynamics (trapping, transport, depositing etc.) is very relevant with regards to ecology, erosion, bank stability and river morphology in general. Therefore it is recommended that future studies explore influences in this regard.

This study focused on the flow regime change by reservoir operation. However, other factors are also altered by reservoir water impoundment. Although these factors are not addressed in this research, water temperature and water quality parameters play critical roles in metabolic rates, physiology, and life history traits of freshwater species. These are therefore interesting impacts to explore and analyze in more depth.

Moreover, additional dams (and reservoirs) in the upper streams of the Myitnge and the Myittha have been under construction and are planned in order to meet the increasing energy required by development. This has been discussed in Chapter 3. A comprehensive evaluation (and modelling) of the impact of the cascaded dam system on the ecohydrology of the basin would hence be a plausible and beneficial next research step.

In-stream conditions can easily be altered by a variety of other factors operating at the basin scale, such as land use practices and riparian conditions. More specifically, forestry, agriculture, and urbanization modify land cover characteristics that in turn influence runoff patterns, hence affecting the timing and quantity of river discharge. Forestry and agriculture also influence the supply of sediment to streams, altering habitat characteristics, and significantly impacting fish and macroinvertebrate populations. Therefore, future research into these mechanisms is recommended.

Bibliography

ABC News (2010). Burma: a brief political history. Retrieved December 3, 2018, from https://www.abc.net.au/news/2009-08-12/burma-a-brief-political-history/1388478.

Affeltranger, B. (2008). Inter-basin water transfers as a technico-political option: Thai-burmese projects on the salween river. *International water security, domestic threats and opportunities*, pages 161–179.

Armitage, P. D. (1977). Invertebrate drift in the regulated river tees, and an unregulated tributary maize beck, below cow green dam. *Freshwater biology*, 7(2):167–183.

Arora, V. K. (2002). The use of the aridity index to assess climate change effect on annual runoff. *Journal of hydrology*, 265(1-4):164–177.

Arthington, A. H., Bhaduri, A., Bunn, S. E., Jackson, S. E., Tharme, R. E., Tickner, D., Young, B., Acreman, M., Baker, N., Capon, S., et al. (2018). The brisbane declaration and global action agenda on environmental flows (2018). *Frontiers in Environmental Science*, 6:45.

Arthington, A. H., Brizga, S. O., and Kennard, M. J. (1998). *Comparative evaluation of environmental flow assessment techniques: review of methods*. Land and Water Resources Research and Development Corporation, Canberra.

Asian Development Bank (2018). Myanmar: Economy. Retrieved September 7, 2018, from https://www.adb.org/countries/myanmar/economy.

Asian Turtle Trade Working Group (2000). Batagur trivittata. The IUCN Red List of Threatened Species 2000. Retrieved February 15, 2019, from https://www.iucnredlist.org/species/10952/97345781.

Aung, L. L., Zin, E. E., Theingi, P., Elvera, N., Aung, P. P., Han, T. T., Oo, Y., and Skaland, R. G. (2017). Myanmar climate report. Technical report, DMH, Norwegian Meteorological Institute.

Baird, A. J. and Wilby, R. L. (1999). *Eco-hydrology: plants and water in terrestrial and aquatic environments*. Psychology Press.

Baran, E., Guerin, E., and Nasielski, J. (2015). Fish, sediment and dams in the mekong. Penang, Malaysia: WorldFish, and CGIAR Research Program on Water, Land and Ecosystems (WLE). 108 pp.

Baran, E., Win, K. K., Zi, Z. W., Khin, M. N., Ghataure, G., and Khin Maung, S. (2018). Soba 4.1: Fisheries in the Ayeyarwady basin. Technical report, NWRC. Retrieved October 9, 2018, from https://www.airbm.org/the-ayeyarwady-state-of-the-basin-assessment-soba/.

Beck, H. E., van Dijk, A. I., de Roo, A., Dutra, E., Fink, G., Orth, R., and Schellekens, J. (2017a). Global evaluation of runoff from ten state-of-the-art hydrological models. *Hydrology and Earth System Sciences*, 21(6):2881–2903.

Beck, H. E., Vergopolan, N., Pan, M., Levizzani, V., van Dijk, A. I., Weedon, G. P., Brocca, L., Pappenberger, F., Huffman, G. J., and Wood, E. F. (2017b). Global-scale evaluation of 22 precipitation datasets using gauge observations and hydrological modeling. *Hydrology and Earth System Sciences*, 21(12):6201–6217.

Beck, H. E., Wood, E. F., Pan, M., Fisher, C. K., Miralles, D. G., van Dijk, A. I., McVicar, T. R., and Adler, R. F. (2018). Mswep v2 global 3-hourly 0.1° precipitation: methodology and quantitative assessment. *Bulletin of the American Meteorological Society*.

BirdLife International (2018). Baer's pochard. The IUCN Red List of Threatened Species 2018. Retrieved February 15, 2019, from https://www.iucnredlist.org/species/22680384/129599398.

Budyko, M. (1974). Climate and life. academy of sciences, main observatory of leningrad.

Bunn, S. E. (1988). Life histories of some benthic invetebrates form streams of the northern jarrah forest, western australia. *Marine and Freshwater Research*, 39(6):785–804.

Bunn, S. E. and Arthington, A. H. (2002). Basic principles and ecological consequences of altered flow regimes for aquatic biodiversity. *Environmental management*, 30(4):492–507.

Carter, J., Driscoll, D. D., and Williamson, J. (2005). Atlas of water resources in the Black Hills Area, South Dakota. Technical report, USGS. Retrieved September 15, 2018, from `https://pubs.usgs.gov/ha/ha747/`.

Chen, J. M. and Cihlar, J. (1996). Retrieving leaf area index of boreal conifer forests using landsat tm images. *Remote sensing of Environment*, 55(2):153–162.

Chow, V. T. (1959). *Open-channel hydraulics*, volume 1. McGraw-Hill New York.

Chow, V. T., Maidment, D. R., and Mays, L. W. (1988). *Applied Hydrology*. McGraw-Hill.

CIA (2018). World factbook: Burma. Retrieved August 25, 2018, from `https://www.cia.gov/library/publications/the-world-factbook/geos/bm.html`.

Council, I. F. (2002). Instream flows for riverine resource stewardship. *Instream Flow Council, USA*.

Cullenward, D. and Victor, D. G. (2006). The dam debate and its discontents. *Climatic Change*, 75(1-2):81–86.

Culp, J. M., Wrona, F. J., and Davies, R. W. (1986). Response of stream benthos and drift to fine sediment deposition versus transport. *Canadian Journal of Zoology*, 64(6):1345–1351.

Davies, B. R. and Walker, K. F. (2013). *The ecology of river systems*, volume 60. Springer Science & Business Media.

Davies Jr, P. M., Bunn Jr, S. E., and Hamilton Jr, S. K. (2008). Primary production in tropical streams and rivers. In *Tropical stream ecology*, pages 23–42. Elsevier.

Donohue, I. and Garcia Molinos, J. (2009). Impacts of increased sediment loads on the ecology of lakes. *Biological Reviews*, 84(4):517–531.

Draut, A. E., Logan, J. B., and Mastin, M. C. (2011). Channel evolution on the dammed elwha river, washington, usa. *Geomorphology*, 127(1-2):71–87.

Dudgeon, D. (2011). Asian river fishes in the anthropocene: threats and conservation challenges in an era of rapid environmental change. *Journal of Fish Biology*, 79(6):1487–1524.

Efford, I. E. (1975). Assessment of the impact of hydro-dams. *Journal of the Fishery Research Board of Canada*, 32(1).

ESA 2010 and UCLouvain (2010). Globcover land cover maps. Downloadable GIS Data from the ESA GlobCover 2009 Project. Retrieved August 25, 2018, from `http://due.esrin.esa.int/page_globcover.php`.

Eslamian, S. (2014). *Handbook of engineering hydrology: fundamentals and applications*. CRC Press.

eWater Ltd (2018). Soba 1.2: Surface water resources. Technical report, NWRC. Retrieved October 9, 2018, from `https://www.airbm.org/the-ayeyarwady-state-of-the-basin-assessment-soba/`.

Extence, C., Balbi, D., and Chadd, R. (1999). River flow indexing using british benthic macroinvertebrates: a framework for setting hydroecological objectives. *Regulated Rivers: Research & Management*, 15(6):545–574.

FAO (2016). Aquastat website. Retrieved February 8, 2019, from `http://www.fao.org/nr/water/aquastat/main/index.stm`.

FAO-Unesco (1974). Soil map of the world. Technical report, Food and Agriculture Organization of the United Nations. Retrieved February 9, 2019, from `http://www.fao.org/3/as360e/as360e.pdf`.

Finnegan, N. J., Roe, G., Montgomery, D. R., and Hallet, B. (2005). Controls on the channel width of rivers: Implications for modeling fluvial incision of bedrock. *Geology*, 33(3):229–232.

Forslund, A., Renöfält, B.M., B. S., Cross, K., Davidson, S., Farrell, T., Korsgaard, L., Krchnak, L., McClain, M., Meijer, K., and Smith, M. (2009). Securing water for ecosystems and human well-being: The importance of environmental flows. *Swedish Water House report*, 24.

Foundation of Ecological Recovery (2003). Briefing paper: Salween hydropower project (thai-burma border). Retrieved January 6, 2018, from `www.terraper.org/articles/BriefingSalweenThai-BurmaJune03.pdf`.

Gao, Y., Vogel, R. M., Kroll, C. N., Poff, N. L., and Olden, J. D. (2009). Development of representative indicators of hydrologic alteration. *Journal of Hydrology*, 374(1-2):136–147.

Garmin (2017). About gps. Retrieved February 22, 2019, from `https://www8.garmin.com/aboutGPS/`.

GARMIN (2018). Striker™ plus 4. Retrieved September 29, 2018, from `https://buy.garmin.com/en-US/US/p/pn/010-01870-00`.

Gash, J. (1979). An analytical model of rainfall interception by forests. *Quarterly Journal of the Royal Meteorological Society*, 105(443):43–55.

Gash, J., Wright, I., and Lloyd, C. R. (1980). Comparative estimates of interception loss from three coniferous forests in great britain. *Journal of Hydrology*, 48(1-2):89–105.

Gash, J. H., Lloyd, C., and Lachaud, G. (1995). Estimating sparse forest rainfall interception with an analytical model. *Journal of Hydrology*, 170(1-4):79–86.

Gido, K. B. and Brown, J. H. (1999). Invasion of north american drainages by alien fish species. *Freshwater Biology*, 42(2):387–399.

Global New Light of Myanmar (2015). Yazagyo dam to drive development of kalay township. Retrieved January 7, 2019, from `http://www.globalnewlightofmyanmar.com/yazagyo-dam-to-drive-development-of-kalay-township/`.

Greacen, C. and Palettu, A. (2007). Electricity sector planning and hydropower in the mekong region. *Democratizing water governance in the Mekong region*, pages 93–125.

Grill, G., Lehner, B., Lumsdon, A. E., MacDonald, G. K., Zarfl, C., and Liermann, C. R. (2015). An index-based framework for assessing patterns and trends in river fragmentation and flow regulation by global dams at multiple scales. *Environmental Research Letters*, 10(1):015001.

Group, T. W. B. (2016). Climate change knowledge portal. Retrieved November 13, 2018, from `http://sdwebx.worldbank.org/climateportal/index.cfm?page=country_historical_climate&ThisCCode=MMR`.

Hargreaves, G. H. and Allen, R. G. (2003). History and evaluation of hargreaves evapotranspiration equation. *Journal of Irrigation and Drainage Engineering*, 129(1):53–63.

HBV Alive (2019). White-bellied heron (ardea insignis). Retrieved February 20, 2019, from `https://www.hbw.com/species/white-bellied-heron-ardea-insignis`.

HDRO (2018). Human development indices and indicators: 2018 statistical update. Retrieved January 3, 2018, from `http://report.hdr.undp.org/`.

Hjulström, F. (1955). *Transportation of detritus by moving water*. Special Publications of SEPM. Retrieved January 5, 2018, from `http://archives.datapages.com/data/sepm_sp/SP4/Transportation_of_Detritus.htm`.

Holtz, R. D. and Kovacs, W. D. (1981). *An introduction to geotechnical engineering*. Prentice-Hall, New Jersey.

Hortle, K. G. (2009). Fisheries of the mekong river basin. In *The Mekong*, pages 197–249. Elsevier.

Houghton-Carr, H. (1999). Assessment criteria for simple conceptual daily rainfall-runoff models. *Hydrological Sciences Journal*, 44(2):237–261.

IFC (2017). Baseline assessment report hydropower: Strategic environmental assessment of the hydropower sector in myanmar. Technical report, International Finance Corporation.

IHA (2015). Country profile: Myanmar. Retrieved August 28, 2018, from `https://www.hydropower.org/country-profiles/myanmar`.

Jalón, D. G. D., Bussettini, M., Rinaldi, M., Grant, G., Friberg, N., Cowx, I. G., Magdaleno, F., and Buijse, T. (2017). Linking environmental flows to sediment dynamics. *Water Policy*, 19(2):358–375.

Johnston, R., Rajah, A., Balasubramanya, S., Sellamuttu, S. S., McCartney, M., Pavelic, P., Douangsavanh, S., Lacombe, G., Sotoukee, T., Suhardiman, D., Cho, K. L., Myint, A., Thein, K., Zan, A. K., Joffre, O., and Htut, Y. T. (2015). Improving water management in Myanmar's dry zone for food security, livelihoods and health. Technical report, IWMI. Retrieved November 10, 2018, from `http://www.iwmi.cgiar.org/Publications/Other/Reports/PDF/improving-water-management-in-myanmars-dry-zone-for-food-security-livelihoods-and-health.pdf`.

Jones, J., Murphy, J., Collins, A., Sear, D., Naden, P., and Armitage, P. (2012). The impact of fine sediment on macro-invertebrates. *River Research and Applications*, 28(8):1055–1071.

Kattelus, M., Rahaman, M. M., and Varis, O. (2015). Hydropower development in myanmar and its implications on regional energy cooperation. *International Journal of Sustainable Society*, 7(1):42–66.

Kennard, M. J., Marsh, N., and Bunn, S. E. (2017). Soba 1.4: Ecohydrology assessment. Technical report, NWRC. Retrieved October 9, 2018, from `https://www.airbm.org/the-ayeyarwady-state-of-the-basin-assessment-soba/`.

Khaing, M. T. (1992). The river morphology of the lower reach of the myitnge river. *University of Mandalay*.

Kondolf, G. M. (2000). Assessing salmonid spawning gravel quality. *Transactions of the American fisheries Society*, 129(1):262–281.

Krause, P., Boyle, D., and Bäse, F. (2005). Comparison of different efficiency criteria for hydrological model assessment. *Advances in geosciences*, 5:89–97.

Kroger, R. L. (1973). Biological effects of fluctuating water levels in the snake river, grand teton national park, wyoming. *American Midland Naturalist*, pages 478–481.

Kyaw, U. W., Zaw, U. M., Dredge, Alan Fischer, P., and Steiger, K. (2006). Yeywa hydropower project, an overview. Technical report, Department of Hydropower, Ministry of Electric Power, Myanmar. Retrieved September 15, 2018, from `http://burmalibrary.org/docs4/Yeywa%20profile.pdf`.

Layzer, J. B., Nehus, T. J., Pennington, W., Gore, J. A., and Nestler, J. M. (1989). Seasonal variation in the composition of the drift below a peaking hydroelectric project. *Regulated Rivers: Research & Management*, 3(1):29–34.

Lee, D. and Zöckler, C. (2018). Soba 4.6: Aquatic habitats in the Ayeyarwady basin and their biodiversity. Technical report, NWRC. Retrieved October 9, 2018, from `https://www.airbm.org/the-ayeyarwady-state-of-the-basin-assessment-soba/`.

Leitner, P., Hauer, C., and Graf, W. (2017). Habitat use and tolerance levels of macroinvertebrates concerning hydraulic stress in hydropeaking rivers–a case study at the ziller river in austria. *Science of The Total Environment*, 575:112–118.

Liang, S., Li, X., and Wang, J. (2012). *Advanced remote sensing: terrestrial information extraction and applications*. Academic Press.

Liu, Y., Liu, R., and Chen, J. M. (2012). Retrospective retrieval of long-term consistent global leaf area index (1981–2011) from combined avhrr and modis data. *Journal of Geophysical Research: Biogeosciences*, 117(G4).

Lytle, D. A. and Poff, N. L. (2004). Adaptation to natural flow regimes. *Trends in ecology & evolution*, 19(2):94–100.

Ma, Y., Huang, H. Q., Nanson, G. C., Li, Y., and Yao, W. (2012). Channel adjustments in response to the operation of large dams: The upper reach of the lower yellow river. *Geomorphology*, 147:35–48.

Magee, D. and Kelley, S. (2009). Damming the salween river. *Contested waterscapes in the Mekong Region: Hydropower, livelihoods and governance*, pages 115–142.

Mann, J. L. (2006). Instream flow methodologies: an evaluation of the tennant method for higher gradient streams in the national forest system lands in the western us. *Colorado State University Fort Collins, Colorado*, page Master of Science thesis.

Martin, M. H. and Coughtrey, P. J. (1982). *Biological Monitoring of Heavy Metal Pollution*. Applied Science Publishing.

McCully, P. et al. (1996). *Silenced rivers: The ecology and politics of large dams*. Zed Books.

Michigan Tech (2004). Pollution sensitive macroinvertebrates. Retrieved January 3, 2018, from `http://techalive.mtu.edu/meec/module05/PollutionSenisitiveMacroinvertebrates.htm`.

Milliman, J. D. and Syvitski, J. P. (1992). Geomorphic/tectonic control of sediment discharge to the ocean: the importance of small mountainous rivers. *The Journal of Geology*, 100(5):525–544.

Monk, W. A., Wood, P. J., Hannah, D. M., and Wilson, D. A. (2008). Macroinvertebrate community response to inter-annual and regional river flow regime dynamics. *River Research and Applications*, 24(7):988–1001.

Moyle, P. B. (1986). Fish introductions into north america: patterns and ecological impact. In *Ecology of biological invasions of North America and Hawaii*, pages 27–43. Springer.

Moyle, P. B. and Light, T. (1996). Biological invasions of fresh water: empirical rules and assembly theory. *Biological conservation*, 78(1):149–161.

Munn, M. D. and Brusven, M. A. (1991). Benthic macroinvertebrate communities in nonregulated and regulated waters of the clearwater river, idaho, usa. *Regulated Rivers: Research & Management*, 6(1):1–11.

Murphy, J. F., Jones, J. I., Pretty, J. L., Duerdoth, C. P., Hawczak, A., Arnold, A., Blackburn, J. H., Naden, P. S., Old, G., Sear, D. A., et al. (2015). Development of a biotic index using stream macroinvertebrates to assess stress from deposited fine sediment. *Freshwater biology*, 60(10):2019–2036.

Myanmar Climate Change Alliance (2012). Impact of climate change and the case of myanmar. Retrieved February 9, 2019, from `https://myanmarccalliance.org/en/climate-change-basics/impact-of-climate-change-and-the-case-of-myanmar/`.

Nyunt, M. (2008). Development of environmental management mechanism in myanmar. *Asia Europe Journal*, 6(2):293–306.

Olden, J. D. and Poff, N. (2003). Redundancy and the choice of hydrologic indices for characterizing streamflow regimes. *River Research and Applications*, 19(2):101–121.

Oosterbaan, R. J. and Nijland, H. J. (1994). Determining the saturated hydraulic conducivity. In Ritzema, H., editor, *Drainage Principles and Applications*, chapter 12, pages 461–465. ILRI, Wageningen.

Pardo, I. and Armitage, P. D. (1997). Species assemblages as descriptors of mesohabitats. *Hydrobiologia*, 344(1-3):111–128.

Pearce, A. J., Rowe, L. K., and Stewart, J. (1980). Nighttime, wet canopy evaporation rates and the water balance of an evergreen mixed forest. *Water Resources Research*, 16(5):955–959.

Pekel, J.-F., Cottam, A., Gorelick, N., and Belward, A. S. (2016). High-resolution mapping of global surface water and its long-term changes. *Nature*, 540(1):418–422.

Pettit, N. E., Naiman, R. J., Warfe, D. M., Jardine, T. D., Douglas, M. M., Bunn, S. E., and Davies, P. M. (2017). Productivity and connectivity in tropical riverscapes of northern australia: Ecological insights for management. *Ecosystems*, 20(3):492–514.

Phillips, D. J. H. and Rainbow, P. S. (2013). *Biomonitoring of trace aquatic contaminants*, volume 37. Springer Science & Business Media.

Pitman, J. and Pitman, R. (1986). Transpiration and evaporation from bracken (pteridium aquilinum (l.) kuhn) in open habitats. *Bracken: Ecology, Land Use, and Control Technology. Parthenon Publishing, Carnforth, England*, pages 259–272.

Platt, S., Ko, W. K., Khaing, L. L., Myo, K. M., Lwin, T., Swe, T., Kalyar, and Rainwater, T. (2005). Noteworthy records and exploitation of chelonians from the ayeyarwady, chindwin, and dokhtawady rivers, myanmar. *Chelonian Conservation and Biology*, 4(4):942–948.

Poff, N. L., Allan, J. D., Bain, M. B., Karr, J. R., Prestegaard, K. L., Richter, B. D., Sparks, R. E., and Stromberg, J. C. (1997). The natural flow regime. *BioScience*, 47(11):769–784.

Postlethwait, J. H. and Hopson, J. L. (2009). *Modern biology*. Holt, Rinehart and Winston, Orlando.

Ra, K. (2011). Water quality management at river basin in myanmar. Retrieved October 8, 2018, from `http://www.wepa-db.net/pdf/1203forum/10.pdf`.

Richards, C. and Minshall, G. W. (1992). Spatial and temporal trends in stream macroinvertebrate communities: the influence of catchment disturbance. *Hydrobiologia*, 241(3):173–194.

Richter, B., Baumgartner, J., Wigington, R., and Braun, D. (1997). How much water does a river need? *Freshwater biology*, 37(1):231–249.

Richter, B. D., Baumgartner, J. V., Powell, J., and Braun, D. P. (1996). A method for assessing hydrologic alteration within ecosystems. *Conservation biology*, 10(4):1163–1174.

Richter, B. D. and Thomas, G. A. (2007). Restoring environmental flows by modifying dam operations. *Ecology and society*, 12(1).

Rosenberg, D. M. and Resh, V. H. (1993). *Freshwater biomonitoring and benthic macroinvertebrates*. Chapman & Hall, New York.

Rutter, A., Kershaw, K., Robins, P., and Morton, A. (1971). A predictive model of rainfall interception in forests, 1. derivation of the model from observations in a plantation of corsican pine. *Agricultural Meteorology*, 9:367–384.

Rutter, A., Morton, A., and Robins, P. (1975). A predictive model of rainfall interception in forests. ii. generalization of the model and comparison with observations in some coniferous and hardwood stands. *Journal of Applied Ecology*, pages 367–380.

Saadat, H. (1999). *Power system analysis*. McGraw-Hill.

Salmivaara, A., Kummu, M., Keskinen, M., and Varis, O. (2013). Using global datasets to create environmental profiles for data-poor regions: A case from the irrawaddy and salween river basins. *Environmental management*, 51(4):897–911.

Savenije, H. H. G. (2007). *Hydrology of Catchments, Rivers and Deltas*. Lecture notes, Delft University of Technology.

Savenije, H. H. G. (2009). *Hydrological Modelling*. Lecture notes, Delft University of Technology.

Schellekens, J. (2018). Wflow documentation. Retrieved August 3, 2018, from `https://wflow.readthedocs.io/en/2017.01/"`.

Schellekens, J. and Weilan, F. S. (2017). earth2observe/downscaling-tools: unstable-master. Retrieved November 2, 2018, from `https://github.com/earth2observe/downscaling-tools`.

Schmidt, J. C. and Wilcock, P. R. (2008). Metrics for assessing the downstream effects of dams. *Water Resources Research*, 44(4).

Schneider, S. C. and Petrin, Z. (2017). Effects of flow regime on benthic algae and macroinvertebrates-a comparison between regulated and unregulated rivers. *Science of the Total Environment*, 579:1059–1072.

Siebert, S., Henrich, V., Frenken, K., and Burke, J. (2013). Global map of irrigation areas version 5. Rheinische Friedrich-Wilhelms-University and Food and Agriculture Organization of the United Nations. Retrieved February 10, 2019, from http://www.fao.org/nr/water/aquastat/irrigationmap/index10.stm.

Smith, J. (2011). Two rivers: The chance to export power divides southeast asia. *National Geographic News*, 25.

Spolum, M. (2017). Rethinking hydropower in myanmar. *Myanmar Times*. Retrieved September 20, 2018, from https://www.mmtimes.com/news/rethinking-hydropower-myanmar.html/.

Taft, L. and Evers, M. (2016). A review of current and possible future human–water dynamics in myanmar's river basins. *Hydrology and Earth System Sciences*, 20(12):4913–4928.

Tennant, D. L. (1976). Instream flow regimens for fish, wildlife, recreation and related environmental resources. *Fisheries*, 1(4):6–10.

Thakkar, H. (2008). India's dam building abroad: Lessons from the experience at home? *New Financiers and the Environment: Ten Perspectives on How Financial Institutions Can Protect the Environment. International Rivers, Berkeley, CA*, pages 9–11.

Tharme, R. E. (2003). A global perspective on environmental flow assessment: emerging trends in the development and application of environmental flow methodologies for rivers. *River research and applications*, 19(5-6):397–441.

Thaung Win, P. P. (2015). *An Overview of Higher Education Reform In Myanmar*. Dissertation report, Chiang Mai University Thailand. Retrieved December 27, 2018, from http://www.burmalibrary.org/docs21/Education/Popo-Thaung-Win-2015-An_Overview_of_Higher_Education_Reform_in_Myanmar-en.pdf.

The Nature Conservancy (2009a). Indicators of hydrologic alteration version 7.1. Software retrieved December 6, 2018, from https://www.conservationgateway.org/ConservationPractices/Freshwater/EnvironmentalFlows/MethodsandTools/IndicatorsofHydrologicAlteration/Pages/IHA-Software-Download.aspx.

The Nature Conservancy (2009b). Indicators of hydrologic alteration version 7.1. User's manual.

TheGeoRoom (2015). The hjulstrom curve of river erosion, transportation and deposition. Retrieved January 5, 2018, from https://www.thegeoroom.co.zw/hydrology/hjulstrom-curve.php.

Tin, H. (2000). Myanmar education: Status, issues and challenges. *Journal of Southeast Asian Education*, 1(1):134–62.

TNC, WWF, and the University of Manchester (2016). Improving hydropower outcomes through system-scale planning: an example from myanmar. Retrieved September 18, 2018, from https://global.nature.org/content/improving-hydropower-outcomes-through-system-scale-planning-an-example-from-myanmar.

Townsend, C. R., Uhlmann, S. S., and Matthaei, C. D. (2008). Individual and combined responses of stream ecosystems to multiple stressors. *Journal of Applied Ecology*, 45(6):1810–1819.

UNESCO (2018). Government expenditure on education, total (% of gdp). Retrieved January 3, 2018, from https://data.worldbank.org/indicator/SE.XPD.TOTL.GD.ZS?locations=MM/.

USGS (2016). Hydroelectric power: How it works. Retrieved September 4, 2018, from https://water.usgs.gov/edu/hyhowworks.html.

USGS, Wandrey, C. J., and Law, B. E. (1998). Geologic map of south asia (geo8ag). Downloadable GIS Data. Retrieved November 3, 2018, from https://pubs.usgs.gov/of/1997/ofr-97-470/OF97-470C/index.html.

Vertessy, R. A. and Elsenbeer, H. (1999). Distributed modeling of storm flow generation in an amazonian rain forest catchment: Effects of model parameterization. *Water Resources Research*, 35(7):2173–2187.

Vogel, R. M., Sieber, J., Archfield, S. A., Smith, M. P., Apse, C. D., and Huber-Lee, A. (2007). Relations among storage, yield, and instream flow. *Water Resources Research*, 43(5).

Von Bertrab, M. G., Krein, A., Stendera, S., Thielen, F., and Hering, D. (2013). Is fine sediment deposition a main driver for the composition of benthic macroinvertebrate assemblages? *Ecological indicators*, 24:589–598.

Ward, D., Pettit, N., Adame, M., Douglas, M., Setterfield, S., and Bunn, S. (2016). Seasonal spatial dynamics of floodplain macrophyte and periphyton abundance in the alligator rivers region (kakadu) of northern australia. *Ecohydrology*, 9(8):1675–1686.

Ward, J. V. and Short, R. A. (1978). Macroinvertebrate community structure of four special lotic habitats in colorado, usa. *Internationale Vereinigung für theoretische und angewandte Limnologie: Verhandlungen*, 20(2):1382–1387.

WCS (2015). Wcs myanmar: Birds. Retrieved February 20, 2019, from https://myanmar.wcs.org/Wildlife/Birds.aspx.

Welcomme, R. L. (1992). River conservation—future prospects. *River conservation and management. John Wiley & Sons, Chichester, UK*, pages 454–462.

Wildlife Conservation Society (2013). Myanmar biodiversity conservation investment vision. Technical report, WCS. Yangon, Myanmar.

Worrall, T. P., Dunbar, M. J., Extence, C. A., Laize, C. L., Monk, W. A., and Wood, P. J. (2014). The identification of hydrological indices for the characterization of macroinvertebrate community response to flow regime variability. *Hydrological Sciences Journal*, 59(3-4):645–658.

Yang, C. T. (1996). *Sediment transport: theory and practice*. McGraw-hill New York.

Young, R., Smart, G., and Harding, J. (2004). Impacts of hydro-dams, irrigation schemes and river control works. *Freshwaters of New Zealand*, pages 37–31.

Yu, X. (2003). Regional cooperation and energy development in the greater mekong sub-region. *Energy Policy*, 31(12):1221–1234.

Zhong, Y. and Power, G. (1996). Environmental impacts of hydroelectric projects on fish resources in china. *Regulated Rivers: Research & Management*, 12(1):81–98.

Zöckler, C. and Kottelat, M. (2018). Soba 4.5: Biodiverisity of the Ayeyarwady basin. Technical report, NWRC. Retrieved October 9, 2018, from https://www.airbm.org/the-ayeyarwady-state-of-the-basin-assessment-soba/.

A

Research challenges in Myanmar

This appendix aims to elaborate on some of the challenges a researcher might face in Myanmar. Some of these issues are based on first hand encounters or conversations with other researchers, and are hence without a source.

A.1. Education and research

Up until the beginning of the twentieth century, Myanmar was internationally admired for it's widespread literacy rate and high-quality education standards. During the British colonization, Myanmar further developed their traditional monastic educational standards, as the British established an education centre in Southern Myanmar and the system slowly shifted towards classroom education. In the late 1940s and early 1950s, Myanmar was expected to become one of the fastest developing nations in South-East Asia. Myanmar missed many advances during 50 years of being ruled by an isolationist military government, however, cutting them off from the rest of the world (Tin, 2000). The nation has been struggling to catch up ever since the transition to democracy. As of 2018, Myanmar still ranks as number 148 out of a total of 189 countries in the Human Development Index (HDI) ranking by the United Nations Development Program (HDRO, 2018). Furthermore, according to the World Bank, only 2.1657% of GDP public spending was on education in 2017 (UNESCO, 2018).

During the periods of political unrest, students were one of the groups that actively and persistently opposed the military regime. They organized peaceful demonstrations and protests to express their dissatisfaction with the military government (ABC News, 2010). In response to these protests, the military government closed down all the universities in 1988. They did not reopen until 1990 with a new, government-controlled curriculum. In 1996 they were closed once more for three years (Tin, 2000). As of 2015, there are 163 higher educational institutions in Myanmar but the curriculum remains strictly controlled by the government (Thaung Win, 2015). Partly because of this, there are large education gaps, language barriers and high illiteracy rates across Myanmar (HDRO, 2018).

Currently, at most technological universities in Myanmar, hydrological fieldwork is not part of the curriculum due to financial and logistical restraints. Hence researchers are dependent on the data measured and provided by the government, which has to be bought. The measurement techniques and the quality remains largely unknown when data is collected second-hand via the government. There are some sources of high quality data, but they remain hard to obtain. For example, the Department of Meteorology and Hydrology (DMH) is well valued within the government for the quality and quantity of their data. However, the usage of their data by universities, other government departments and researchers is still limited due to the relatively high cost of data.

Due to the political unrest that exists especially in the Northern Kachin and South-Western Rakhine states, researchers can no longer gain access to certain regions. The restricted areas have been expanding over the past years, limiting the fieldwork areas that can be visited.

A.2. Data collection and availability

There are several issues related to the collection and sharing of hydrological data in Myanmar. First of all, due to the poor (albeit improving) internet infrastructure and language barrier there are few databases that are convenient and accessible. Secondly, although the ministries do collect some data, that data is not often freely shared with other ministries, nor with researchers. In addition to data information gaps, this leads to the same data being collected by different departments or ministries. For example, precipitation data is collected by three different departments of two different ministries within Myanmar: DMH, which is part of the Ministry of Transport, the Agricultural Department (AD) and the Irrigation Department (ID), both part of the Ministry of Agriculture and Irrigation. This has resulted in a clustered spatial distribution of rain gauges, mainly in the central and southern parts of Myanmar. The data is also collected using different measuring techniques, stored differently and often not cross-referenced, compared nor validated. The departments sell the data to other departments and ministries, hence sharing the data freely will reduce a department's income.

With a lack of available ground data, one usually turns to remote sensing products. This raises another concern, however, about the quality of remote sensing and derived (reanalysis) products. This depends on the number of ground observations made available by the country itself for validation. Myanmar, however, has only recently started to contribute to these validation systems.

B

Sediment dynamics

B.1. Introducion to sediments in rivers

Water flowing down a slope in channels with erodible beds may scour the loose particles resting on the bed or banks and move them downstream. This process is referred to as *sediment transport* (Yang, 1996). River inputs are the main source of continental materials exported to the ocean. Additionally, river sediment fluxes constitute one of the main components of the coastal sedimentary budget. Therefore, any change in these fluxes has the potential to significantly change the physical environment of both the riverine and coastal environments (Yang, 1996).

A stable river requires both water and certain metabolites such as sediments, woody debris, particulate organic matter and dissolved solids and gases. A river habitat is formed by interacting geomorphological forces: water (flow), sediments and riparian vegetation. River discharge has the energy to erode, transport and deposit sediments. Riparian vegetation growth consolidates deposited sediments, and existing vegetation has the ability to reduce the erosion capacity of the flow (Milliman and Syvitski, 1992; Yang, 1996).

A disturbance such as a large dam on a river affects not only the natural water flow regime, but often to a greater extent, the natural fluxes of these metabolites(Jalón et al., 2017). Therefore, when we look at the altered flow regime and the extent to which E-flows can become an instrument to improve the ecological status of rivers, we should also consider the fluxes of the metabolites that allow the existence of biological communities. The impacts of hydrodams on sediment dynamics are further discussed in section B.4.

Sediment flows vary greatly on both an annual and a seasonal scale. Therefore, calculating an annual average requires a long-term data set. The amount of sediment carried by a river is highest during floods, for example. During and after a particularly violent storm a river may carry as much sediment as it would in several average years. Mudslides caused by earthquakes can also have a dramatic and unpredictable effect on the amount of sediment in the river. Global warming, which is predicted to cause more intense storms, will likely increase both the unpredictability and rate of river sedimentation (McCully et al., 1996).

B.2. The Hjulström curve

Hjulström (1955) proposed that the transport of debris by moving water is affected by many factors, the most important of which being the flow velocity. He said particles are transported individually or collectively. The former can be in four different states: sliding, rolling, saltation (jumping) along the bottom, and suspension in the water. He furthermore stated that with increasing velocity the mode of transport usually passes successively through these four transport states. When particles move in masses, they form geomorphological features such as ripples, bars, and banks. The physical laws governing sediment transportation are complicated, according to Hjulström. For particles larger than sand ($0.5mm$) the size of particles that can be put in motion increases as the velocity of the water increases. For for smaller particles, however, the minimum velocity that is necessary to bring the particles into suspension does not decrease as the particles become smaller; instead it increases. This means that it is easier to move sand off the bottom than silt, for example. Once a particle is in motion it continues to be transported until the velocity of the water decreases to a certain minimum velocity. The research of Hjulström is presented graphically in Figure B.1 below. It represents the approximate curves for erosion and deposition of uniform materials.

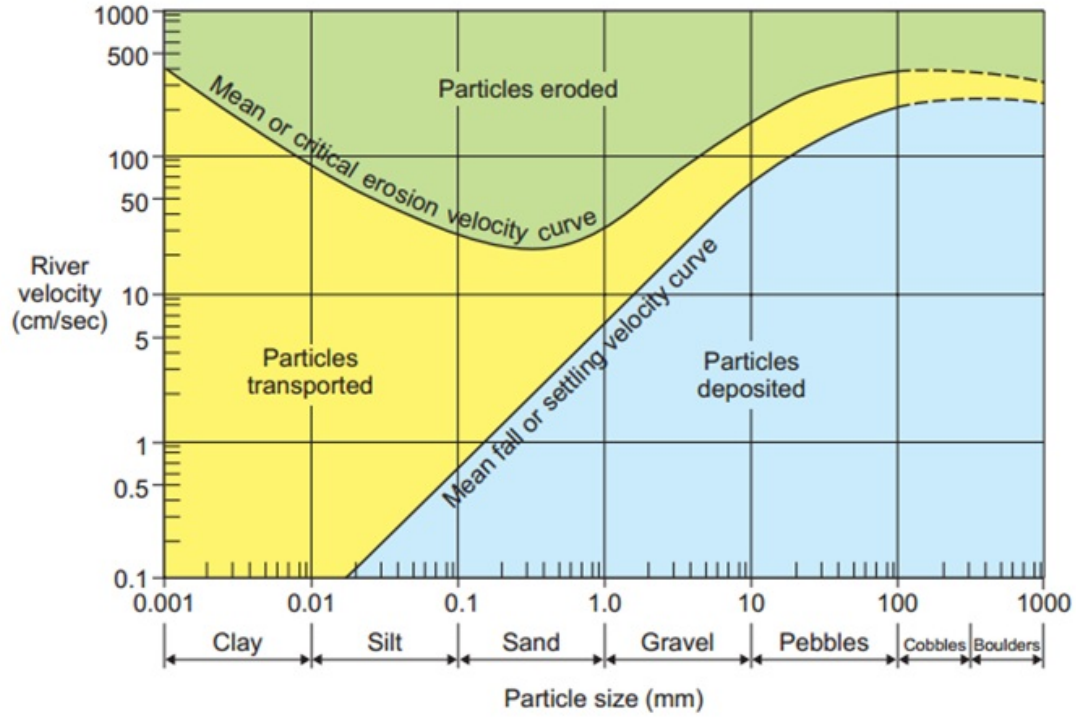

Figure B.1: The Hjulström curve: transport, erosion and deposition of uniform materials. Curve originally created by Hjulström (1955), updated picture of curve from TheGeoRoom (2015)

The graph shows the linkage between sediment grain size on the x-axis, and the velocity needed to erode, transport or deposit on the y-axis. The curved line at the top shows the critical erosion velocity needed to initiate sediment erosion. The bottom line shows the fall or settling velocity. In between these two lines the transportation of sediments takes place. A big gap implies that sediments will be transported further,the opposite happens for a small gap where a relative drop in velocity (critical fall velocity) causes sediments to be deposited. The minimum transporting velocity for particles with the grain size of sand or larger is around 30% less than the velocity needed to remove the particles from the bottom, according to Hjulström. For progressively smaller particles, however, the minimum transporting velocity becomes increasingly less relative to the velocity necessary to make the particles go into suspension.

B.3. Sediment impacts on macroinvertebrates

This section considers the impacts of sediment dynamics on macroinvertebrates. Figure B.2 provides a summary diagram highlighting the direct and indirect mechanisms by which fine sediments affect macroinvertebrates. As the diagram shows, impacts are caused by both suspended and deposited sediment particles. The arrows in the diagram show interacting effects and impacts on macro-invertebrates at the individual, species and community levels. It is important to note that the strength and direction of effects are not given as they are dependent upon the taxa affected; some taxa and communities respond positively to a certain change, whereas others respond negatively to that same change (Jones et al., 2012).

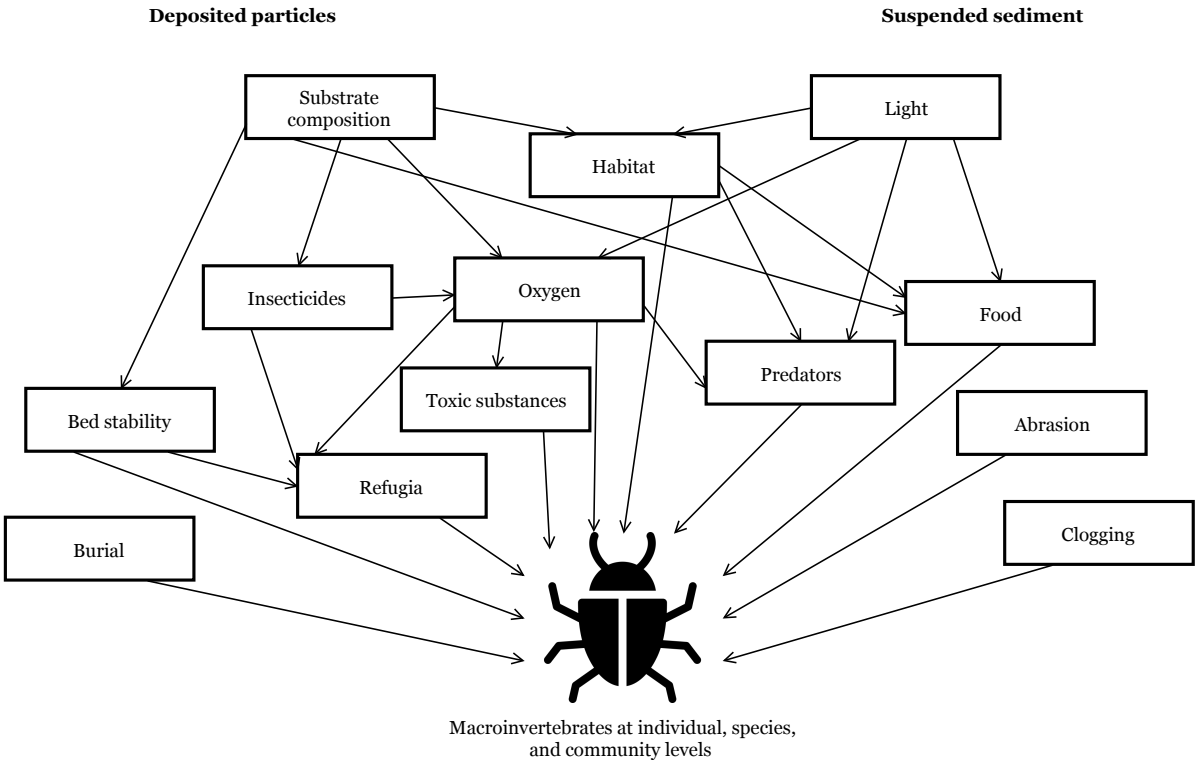

Figure B.2: Direct and indirect mechanisms by which fine sediments impact macro-invertebrates, adapted from (Jones et al., 2012)

The figure shows that the elements of sediment transport can induce different responses by the various components of the macroinvertebrate assemblages. Looking at empirical research, this also seems to be the case. For example, certain taxa are likely to be vulnerable to the chemical changes related to the amount of organic matter deposited on the river bed (Von Bertrab et al., 2013). Other taxa, however, may be more affected by the physical impacts of mineral fine-grained sediment (Townsend et al., 2008). Yet another macroinvertebrate taxa can be susceptible to abrasion from mineral particles either saltating or suspended in the river. This can subsequently lead to dislodgement or damage to the body parts of the taxa (Culp et al., 1986). Furthermore, macroinvertebrate community composition has been observed to respond to changes in habitat availability. These changes are caused both directly or indirectly (i.e. through predation, see Figure B.2) by increased or decreased (fine-grained) sediment inputs (Pardo and Armitage, 1997).

Murphy et al. (2015) collected biological and sediment data from 179 rivers and streams across England and Wales. The collected data was representative of a range of river types over a gradient of fine sediment loading. Using statistical approaches, the authors aimed to determine relationships between the macroinvertebrate assemblages and fine-grained sediment inputs to river channels. They came to the conclusion that the variables that account best for the residual variation in the macroinvertebrate assemblage are as follows:

- The mass of organic sediment in erosional areas of the stream bed
- The mass of fine sediment in the surface drape of depositional areas
- The percentage of organic content in erosional areas

B.4. Hydropower impacts on sediment: expected effects

Hydrodams interrupt the continuity of sediment transport through river systems, causing several adverse effects. First of all, sediment will accumulate within the reservoir itself, upstream of the dam. This impairs the reservoir operation and decreases its storage capacity. When a river is trapped behind a dam, the sediments it contains sink to the bottom of the reservoir. The proportion of a river's total sediment load captured by a dam, which is referred to as the "trap efficiency", approaches 100% for many hydropower projects (McCully et al., 1996). This is especially the case for hydrodams with large reservoirs. In fact, sedimentation has been the most serious technical problem faced by the dam industry in the past six decades (McCully et al., 1996).

This excessive sediment buildup in turn leads to the abrasion of turbines and other dam components. The efficiency of a turbine inside a hydropower plant is dependent upon the hydraulic properties of its blades. Sediments leading to the erosion and cracking of turbine blade tips reduce their generating efficiency significantly, often requiring expensive repairs (McCully et al., 1996).

Looking at ecological aspects, allowing enough sediment to reach the downstream channel is essential to maintain channel form (Ma et al., 2012; Draut et al., 2011) and to support riparian ecosystems (Donohue and Garcia Molinos, 2009; Kondolf, 2000). There is furthermore increasing evidence of channel erosion and geomorphological changes resulting from sediment starvation downstream of dams, often termed *hungry water*. Some of these channel changes adversely impact urbanized areas, agriculture, valued landscapes, and native species in the associated ecosystems (Schmidt and Wilcock, 2008).

B.5. Field experiments: soil gradation of river sediment

Soil gradation is a classification method for soils that ranks them based on the (distribution of) different particle sizes. This analysis allows some insights on the particles transported by the river.

The procedure that was carried out in the field is as follows. River sediment samples of maximum 200 grams are taken from the river bottom, and the islands in the middle of the river. The soil samples are dried on aluminum foil in the sun and are subsequently weighed and their masses recorded. The sieve analysis that follows the initial weighing consists of shaking the soil sample through a set of sieves that have progressively smaller openings, as presented in Figure B.3. The sieves allow shaking by hand, after which the mass of the soil retained on each sieve is determined using a small set of scales.

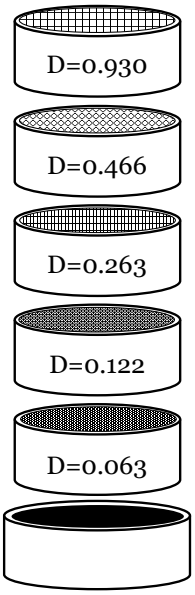

Figure B.3: Soil gradation set-up: hand-held sieve system with different diameters

Once the mass of sediment is retrieved from each sieve with an associated diameter, the cumulative percentages that "pass through" the sieve can be calculated. These cumulative percentages that exceed a certain diameter are plotted arithmetically against log grain size on semi-logarithmic paper. A smooth S-shaped curve drawn through these points is called a grading curve, also known as a particle-size distribution curve. The position and shape of the grading curve determines the soil class. Furthermore, geometrical grading characteristics can be determined from this grading curve. The characteristics calculated in this research are:

$$C_c = \frac{D_{60}}{D_{10}} \quad \text{(Gradation coefficient)} \tag{B.1}$$

$$C_u = \frac{D_{30}^2}{D_{10} D_{60}} \quad \text{(Uniformity coefficient)} \tag{B.2}$$

Where D_x is the diameter corresponding to x% finer in the particle-size distribution. Both these coefficients are shape parameters. Once the uniformity coefficient and the coefficient of gradation have been calculated, they can be compared to gradation criteria from literature. The following criteria are in accordance with the Unified Soil Classification System (Holtz and Kovacs, 1981):

- A well-graded gravel is defined by the criteria: $C_u > 4$ and $1 < C_c < 3$. If both of these criteria are not met, the gravel is classified as poorly graded. If both of these criteria are met, however, the gravel is classified as well graded.
- A well-graded sand means that the following criteria are met: $C_u \geq 6$ and $1 < C_c < 3$. If neither of these criteria are met, the sand is classified as poorly graded. If both of these criteria are true, the sand is classified as well-graded.

In general, a poorly graded soil will have better drainage than a well graded soil because there are more void spaces (Holtz and Kovacs, 1981).

(a) Gradation experiment set-up

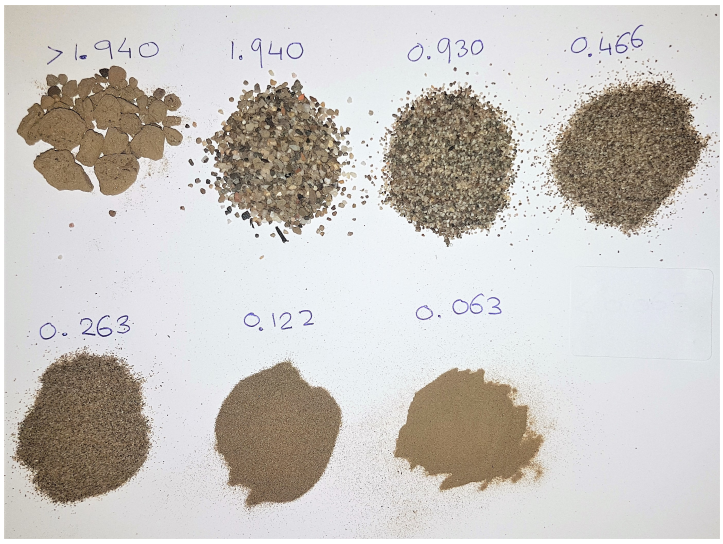

(b) Sieved sand sample: different grain sizes

Figure B.4: River sediment experiment

The results of this experiment are presented in section F.2 of Appendix F.

C

Maps of Myanmar

C.1. Study area basins

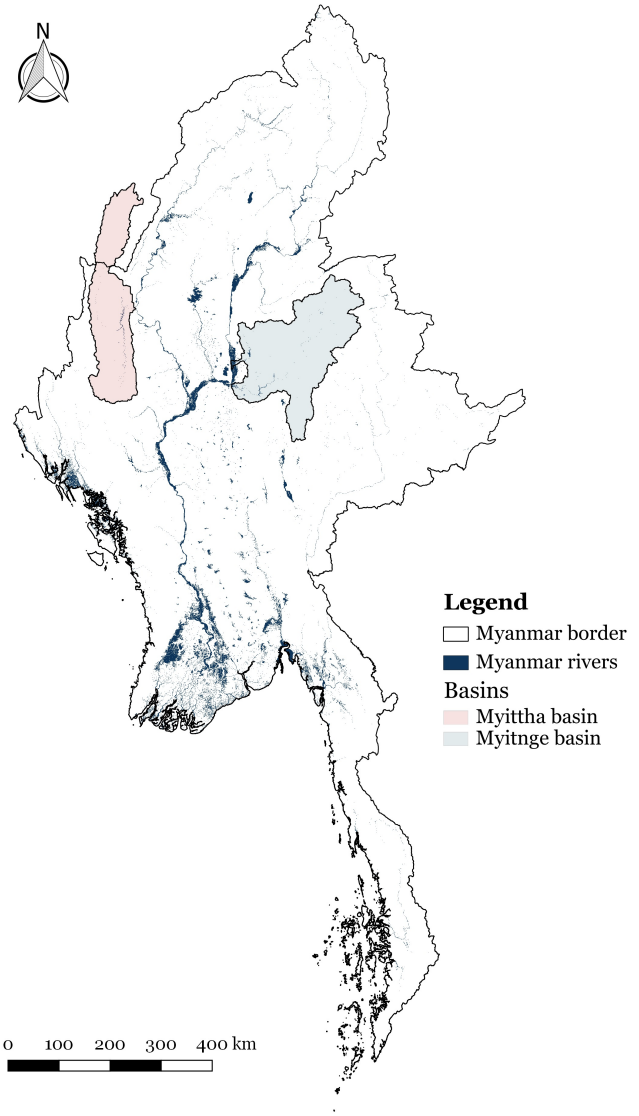

Figure C.1: Study river basins: Myitnge and Myittha

C.2. Key Biodiversity Areas

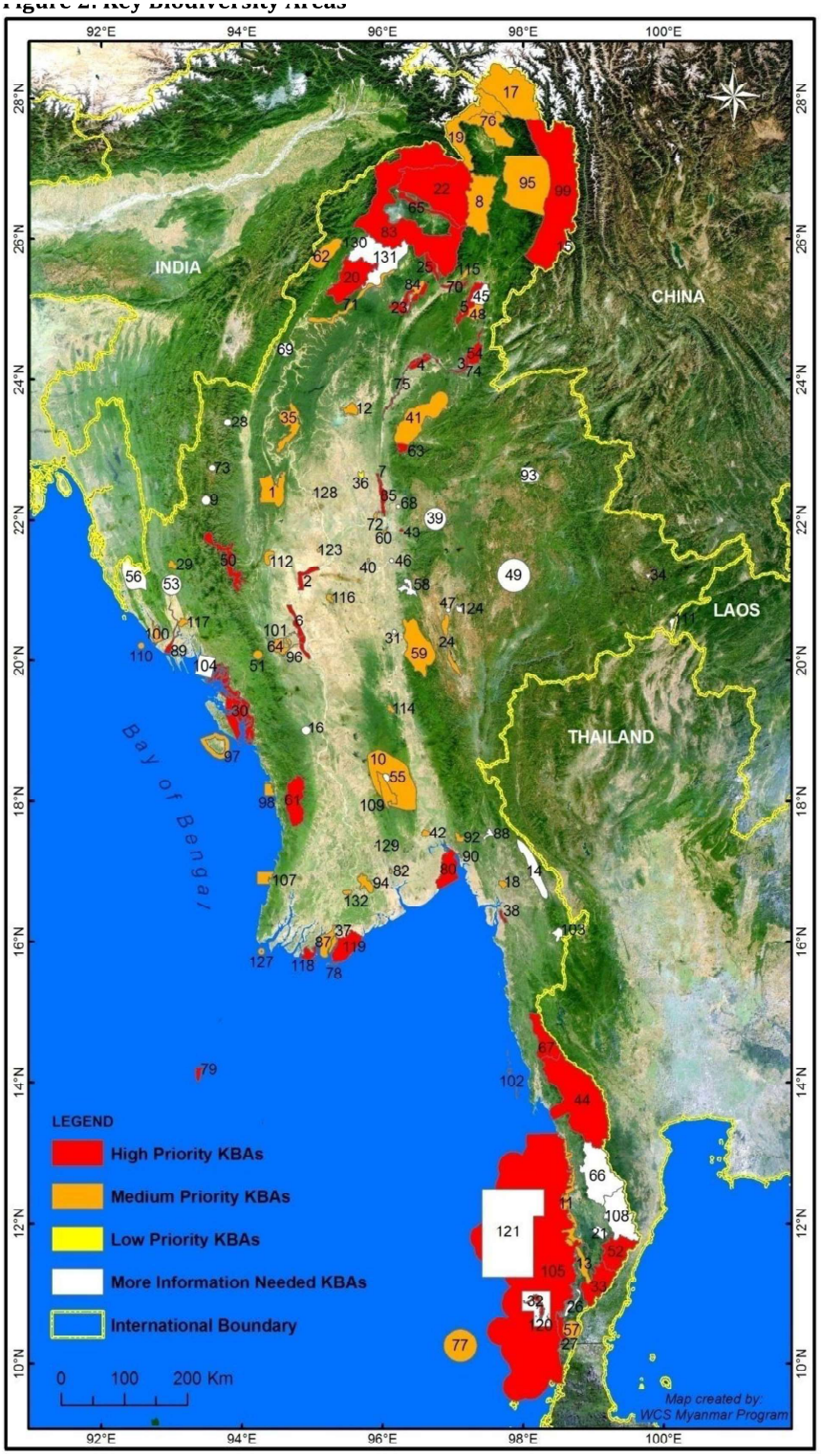

Figure C.2: Key Biodiversity Areas (Wildlife Conservation Society, 2013)

C.3. Geology

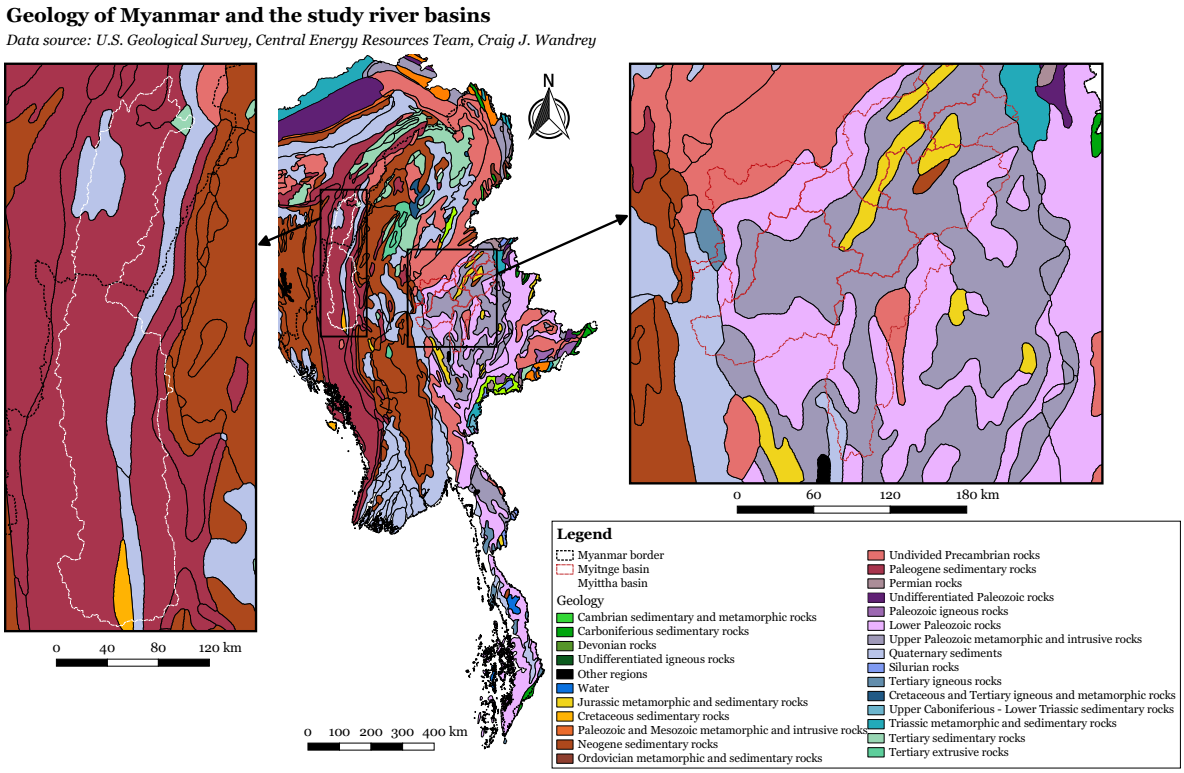

Figure C.3: Geological map of Myanmar, data from (USGS et al., 1998)

C.4. Soil types

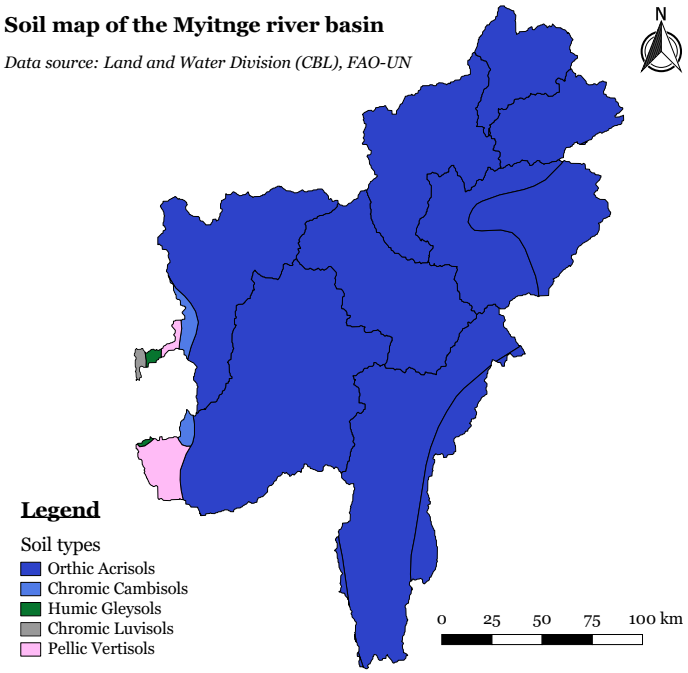

(a) Soil map of Myitnge river basin

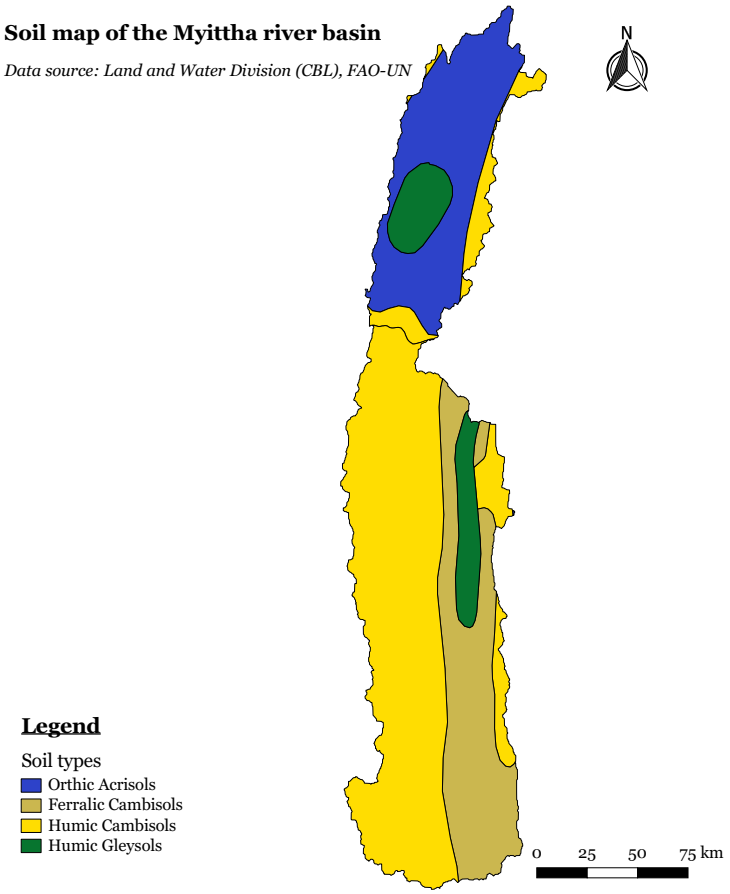

(b) Soil map of Myittha river basin

Figure C.4: Soil maps of the study areas, data from (FAO-Unesco, 1974)

C.5. Land cover

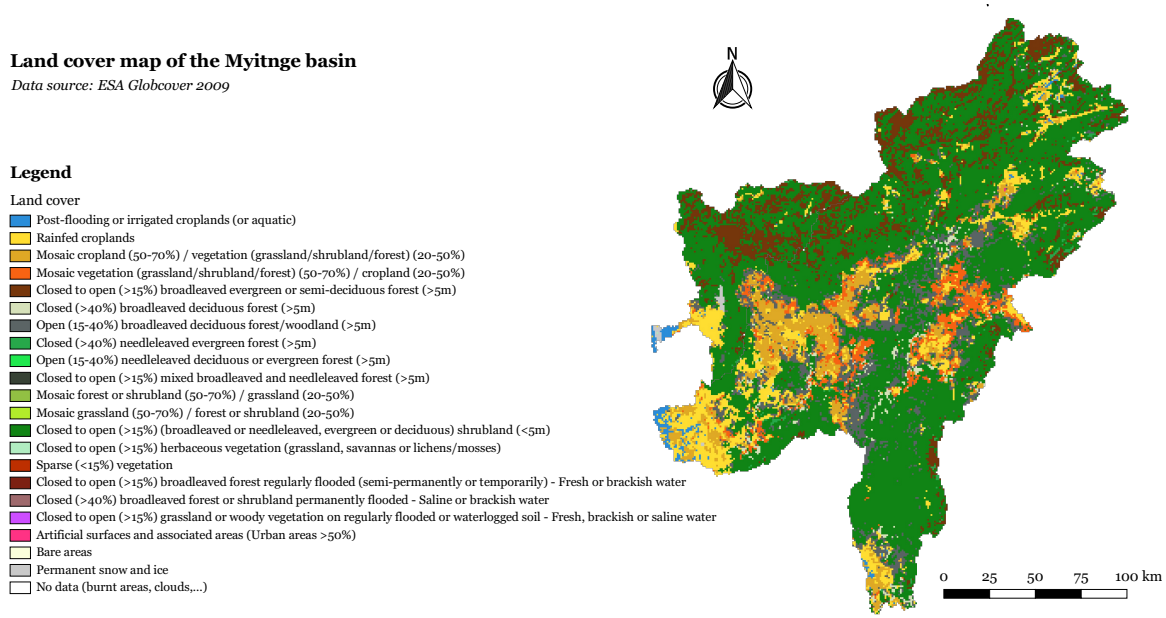

(a) Land cover map of Myitnge river basin

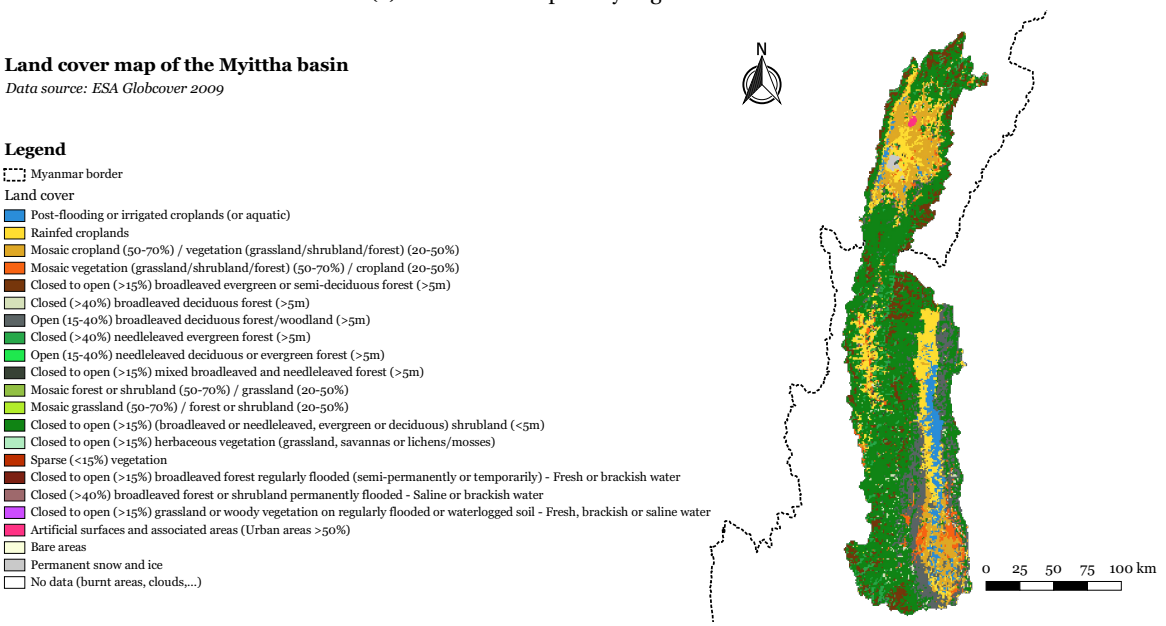

(b) Land cover map of Myittha river basin

Figure C.5: Land cover maps of the study areas, data from (ESA 2010 and UCLouvain, 2010)

D

Model processes

D.1. Potential and reference evaporation

One of the most important model processes to close the water balance is evaporation. The input for evaporation is assumed by the model to be potential evaporation, taken from the Water Resources Reanalysis prodyct which is a forcing based on the ERA-Interim meteorological data. The actual evaporation is then calculated based on landcover through a multiplication factor.

D.2. The rainfall interception model

The capacity of vegetation to intercept and store water is of great importance when modelling runoff as a function of rainfall. The rainfall interception model within *WFlow_sbm* is conceptually based on Rutter's numerical model (Rutter et al., 1971, 1975). The model developed by Rutter aims to calculate a running water balance for the wetted canopy and trunks, requiring hourly rainfall and above-canopy climatic data. It also requires different parameters to describe the structure of the vegetation, and uses an empirical expression for the drainage from the canopy (Rutter et al., 1971). This high data demand makes the model less practical than the simpler analytical model of rainfall interception, as proposed by Gash (1979). The Gash model preserves a lot of the fundamental physics demonstrated in the Rutter model, while simultaneously incorporating the simplicity of a more empirical approach. This model has proved to work well in temperate coniferous and broadleaf forests (Gash et al., 1980; Pearce et al., 1980), but overestimates interception loss significantly in more open forests (Gash et al., 1995). Therefore, a 'sparse canopy' variant of the model was created by Gash 1995 that assumed evaporation from the wet canopy to be linearly dependent on the canopy cover fraction.

The Gash rainfall interception model as used by *WFlow_sbm* requires an analytical integration of the total evaporation loss of intercepted rainfall. This is done by taking average rates for all storms instead of taking actual rainfall and evaporation rates for each storm separately. The evaporation from saturated canopy during rainfall is estimated from the well-known Penman-Monteith equation. The following terms are added separately (Gash, 1979):

- The effect of wetting up the canopy
- The effect of smaller rain events that are unable to saturate the canopy completely
- The evaporation once the rainfall has ended
- The evaporation from tree trunks

It should be noted that a storm-based approach gives the best results in this model, but *WFlow_sbm* makes use of some simplifications, allowing for an analysis that makes use of a daily time step.

The required water amount to completely saturate the canopy is defined by equation D.1 below (Gash, 1979):

$$P_G^{'} = \frac{-\overline{R}S}{\overline{E}_w} ln\left[1 - \frac{\overline{E}_w}{R}(1-p-p_t)^{-1}\right] \tag{D.1}$$

In this equation $\overline{E}_w$ is the mean evaporation rate from the wet canopy (mm/d) and $\overline{R}$ is the average precipitation intensity on the canopy (mm/d). Furthermore, S (mm) is the canopy capacity, defined as the amount of water on the canopy when rainfall and throughfall have stopped and the canopy is saturated. Parameters p

and p_t are the free throughfall coefficient and the proportion of rainfall which is diverted to the tree trunks as stemflow, respectively. Both of these parameters are dimensionless. The loss due to interception is calculated for different phases of a storm using using a series of expressions. Subsequently average values of $\overline{E}_w$ and $\overline{R}$ can be determined for each storm using an analytical integration of the total evaporation and rainfall under saturated canopy conditions. The sum of the components listed in the formulas of Table D.1 gives the total interception loss: these formulas formulate the components of interception loss according to Gash (1979). It should be noted that interceptions losses from the stems are calculated for days where $P \geq \frac{S_t}{p_t}$ only, where S_t is the trunk water capacity (mm). Furthermore, it is assumed that saturated conditions occur when the hourly rainfall exceeds a certain, predefined threshold (Gash, 1979).

Table D.1: Components of interception loss, as according to Gash (Gash, 1979)

For m small storms $(P_G < P_G^{'})$	$(1-p-p_t)\sum_{j=1}^{m} P_{G,j}$
Wetting up the canopy in n large storms $(P_G \geq P_G^{'})$	$n(1-p-p_t)P_G^{'} - nS$
Evaporation from saturated canopy during rainfall	$\bar{E_w}/\bar{R}\sum_{n}^{j=1}(P_{G,j} - P_G^{'})$
Evaporation after rainfall ceases for n large storms	nS
Evaporation from tree trunks in q storms that fill the tree trunk storage	qS_t
Evaporation from trunks in $m+n-q$ storms that do not fill the trunk storage	$p_t\sum_{j=1}^{m+n-q} P_{G,j}$

The variables are as defined above or in the table, and P_G is the gross rainfall incident on the canopy. Making use of these components, $\overline{R}$ can be calculated for all hours where rainfall exceeds the threshold for saturated conditions, which is often taken to be $0.5mm/h$. From this we can derive an estimate of the mean annual rainfall rate onto the saturated canopy.

Gash (1979) showed in his regression analysis of interception loss on incident rainfall that the regression coefficient should become equal to $\overline{E}_w/\overline{R}$. This means that when regressing interception loss on rainfall, an implicit assumption is made that $\overline{E}_w/\overline{R}$ is constant and that the actual deviations from a certain line of individual measurements represent only random deviations from that constant value. This assumption seems to hold, for when we look at many such regressions, interception loss and rainfall appear to be highly correlated. So therefore if we assume that neither $\overline{E}_w$ nor $\overline{R}$ vary a lot over time, $\overline{E}_w$ can be estimated from $\overline{R}$ when there are no climatic observations available. It should be noted that values for evaporation derived in this manner are mostly higher than those calculated using Penman-Monteith (Gash, 1979; Schellekens, 2018).

The *WFlow_sbm* model determines the Gash parameters from Leaf-Area Index (LAI) maps. The LAI was developed to characterize plant canopies in the form of a dimensionless quantity: it indicates the area of ground occupied by plants and is an important structural property of vegetation (Liang et al., 2012). It is defined as the one-sided green leaf area per unit of ground surface area in broadleaf canopies, as presented in Equation D.2 below. For coniferous canopies, as shown in Equation D.3, it is defined as the one-half total needle surface area per unit of ground surface area (Chen and Cihlar, 1996).

$$LAI_{\text{broadleaf canopies}} = \frac{Leaf\ area}{Ground\ area} \quad [-] \tag{D.2}$$

$$LAI_{\text{coniferous canopies}} = \frac{1}{2}\frac{Total\ needle\ surface\ area}{Ground\ area} \quad [-] \tag{D.3}$$

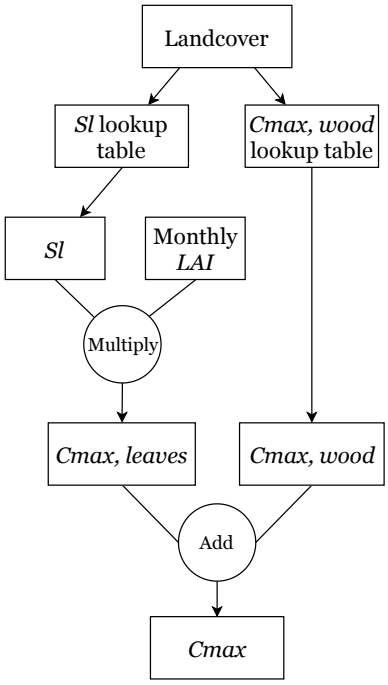

Figure D.1: Conceptual overview of how to obtain C_{max}, adapted from (Schellekens, 2018)

LAI can range from 0, representing bare ground, to over 10, representing dense conifer forests (Chen and Cihlar, 1996). The *WFlow_sbm* model assumes that Gash' canopy storage capacity for the leaves, $C_{max(leaves)}$, relates linearly to the LAI, via the Specific leaf storage, Sl. This is shown in Equation D.4 (Schellekens, 2018).

$$C_{max(leaves)} = Sl * LAI \tag{D.4}$$

Sl is determined in the model via a simple lookup table based on type of landcover type. The values, based on the works of Pitman and Pitman (1986) and Liu et al. (2012) can be found in Table E.1 in Appendix E.

To get to the total canopy storage, C_{max}, $C_{max(wood)}$ is also added, representing the canopy storage for the woody part of the vegetation. These values are categorized based on landcover, and are also presented in a table in Appendix E, Table E.2.

The canopy gap fraction is determined using the extinction coefficient, k, as shown in Equation D.5.

$$Canopy\ Gap\ Fraction = exp(-k * LAI) \tag{D.5}$$

The extinction coefficient k is also related to landcover through a lookup table in the *WFlow_sbm* model. This table, labelled Table E.3, can be found in Appendix E. The process described above is schematically presented in Figure D.1.

D.3. The soil model

The soil model, as presented in Figure D.2, is based on a simple bucket model, based on the Topog_SBM model of Vertessy and Elsenbeer (1999). It is assumed that rainfall that falls onto soil that is (partly) saturated becomes runoff. Hence this water is added directly to the surface runoff model component. The rain that falls onto soil that is not saturated may infiltrate. For this water, a distinction is made between the water that infiltrates in compacted areas and non-compacted areas (Schellekens, 2018).

The rainfall that infiltrates in non-compacted areas is calculated by taking the minimum of the remaining storage capacity, the maximum soil infiltration rate, and the water on non-compacted areas. After adding the infiltrated water to the unsaturated store the same is done for the compacted areas after updating the remaining storage capacity (Schellekens, 2018).

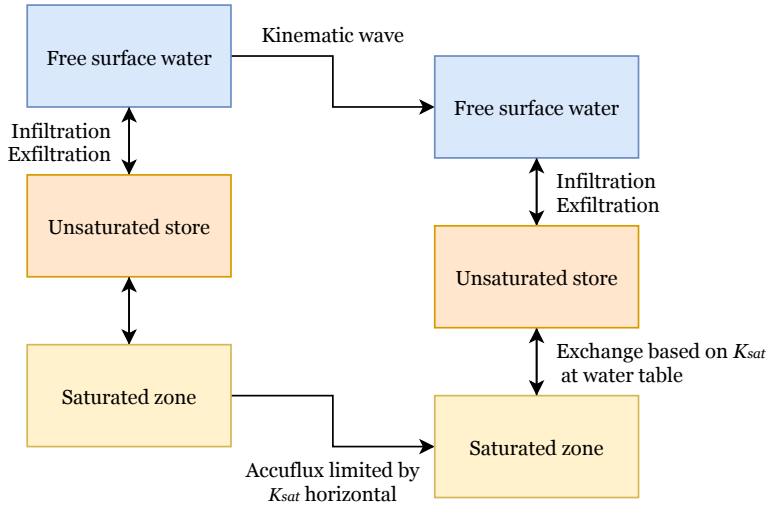

Figure D.2: Schematisation of the soil within the *WFlow_sbm* model, adapted from (Schellekens, 2018)

The model considers the soil as a bucket with a certain depth, z_t, divided into a saturated store (S) and an unsaturated store (U). The magnitudes of these stores are expressed in units of depth. The top of the S store forms a pseudo-water table at depth z_i, hence S at any given time can be presented by:

$$S = (z_t - z_i)(\theta_s - \theta_r) \tag{D.6}$$

In Equation D.6, the saturated water content is represented by θ_s, and θ_r is the residual soil water content. The unsaturated store (U) is split up into storage, U_s, and deficit, U_d, both of which are expressed in units of depth. Equations D.7 and D.8 below give the values for the unsaturated storage and deficit.

$$U_s = U - U_d \tag{D.7}$$

$$U_d = (\theta_s - \theta_r) z_i - U \tag{D.8}$$

The saturation deficit S_d for the entire soil profile is defined by:

$$S_d = (\theta_s - \theta_r) z_t - S \tag{D.9}$$

It is assumed that all the infiltrating precipitation enters the unsaturated U store first, after which it is transferred to the saturated S store. This rate of transfer process, presented by st, is controlled by the saturated hydraulic conductivity at depth z_i and the ratio between U and S_d, as presented in equation D.10.

$$st = K_{sat} \frac{U_s}{S_d} \tag{D.10}$$

Equation D.10 shows that as the saturation deficit S_d decreases, the rate of transfer between the unsaturated and saturated store increases. The saturated conductivity K_{sat} decreases with soil depth z_i in the model, according to the following equation:

$$K_{sat} = K_0 e^{(-f z)} \tag{D.11}$$

In equation D.11, K_0 represented the saturated conductivity at the soil surface and f is a scaling parameter defined by θ_s and θ_r as defined before, and a model parameter M [−]:

$$f = \frac{\theta_s - \theta_r}{M} \quad [m^{-1}] \tag{D.12}$$

The S store is drained laterally via subsurface flow, presented as S_{sf} $[m^2 d^{-1}]$ and described by:

$$S_{sf} = K_0 \tan(\beta) e^{-S_d / M} \tag{D.13}$$

Where β [°] is the element slope angle, and S_d, M, and K_0 as defined before. Figure D.3 shows a schematic drawing of the processes, where the variables are defined as follows:

rf	Rainfall
in	Infiltration
st	Transfer between unsaturated and saturated zone
ie	Infiltration excess
se	Saturation excess
ex	Exfiltration
of	Overland flow
sf	Subsurface flow

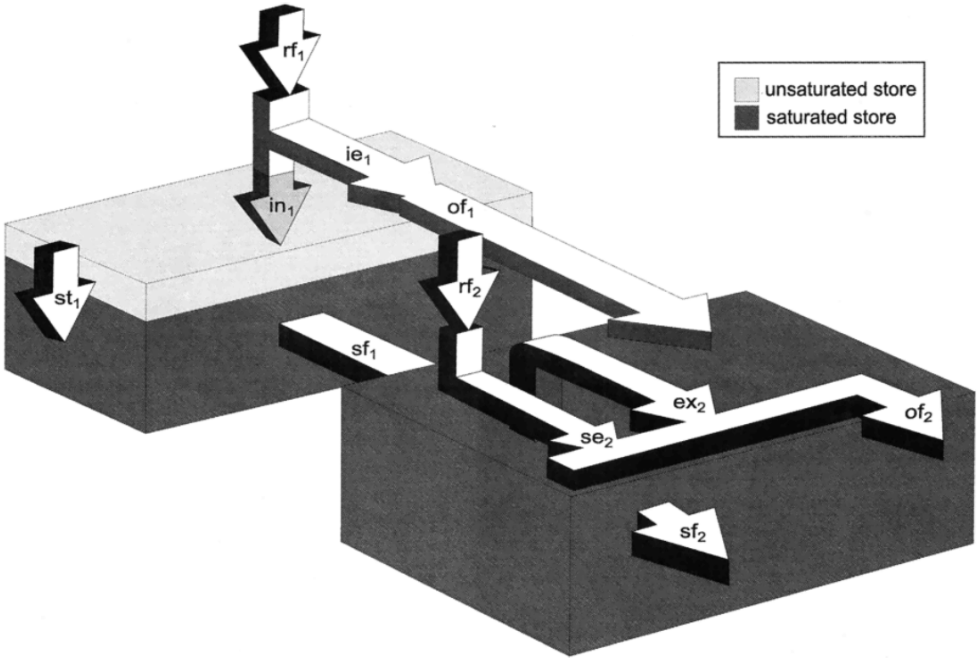

Figure D.3: Schematic representation of the hydrologic processes from the original SBM model (Vertessy and Elsenbeer, 1999)

The potential evaporation that is left after interception has taken place is split up into potential soil evaporation and potential transpiration. Actual soil evaporation is scaled by multiplying the potential soil evaporation by the saturation deficit over the soil water capacity. This means that the evaporation decreases linearly with increasing soil moisture. When the soil is fully wetted, actual soil evaporation will become equal to potential evaporation. The orginal SBM model by Vertessy and Elsenbeer (1999) does not take capillary rise into account, thereby excluding transpiration. *WFlow_sbm*, however, transpiration is assumed to start by taking water from the saturated store if the roots reach the water table (at z_i). Once the saturated store has been exploited, the model resorts to the unsaturated store. For the model to take water from the saturated store, first of all the number of wet roots is determined by equation D.14 below

$$Wet\ roots = 1.0/(1.0 + e^{P(h_{wt} - d_{roots})}) \tag{D.14}$$

In equation D.14, P $[-]$ is the sharpness parameter which determines whether the output is step-wise or more gradual. The parameter h_{wt} $[mm]$ is the water table level in the gridcell below the surface, and d_{roots} $[mm]$ gives the rooting depth, which is the maximum depth of the roots below the surface. For all values of $h_w t$ below the rooting depth, the equation returns a value of 1. When the opposite is true, a 0 is returned by the formula, and when they are equal the result is 0.5 (Schellekens, 2018). To get a value for transpiration from the saturated soil, the returned $Wet\ Root$ function is multiplied by the potential evaporation.

The remaining potential evaporation is used to extract water from the unsaturated store. This is presented in the code below.

```
wetroots = sCurve(WTable, a=RootingDepth, c=smoothpar)
ActEvapSat = min(PotTrans * wetroots, SatWaterDepth)
SatWaterDepth = SatWaterDepth - ActEvapSat
RestPotEvap = PotTrans - ActEvapSat

# now try unsat store
AvailCap = max(0.0,ifthenelse(WTable < RootingDepth,  cover(1.0),  RootingDepth/(WTable + 1.0)))
MaxExtr = AvailCap * UStoreDepth
ActEvapUStore = min(MaxExtr, RestPotEvap, UStoreDepth)
UStoreDepth = UStoreDepth - ActEvapUStore

ActEvap = ActEvapSat + ActEvapUStore
```

Figure D.4: Python code in *WFlow_sbm* model for evaporation from the saturated and unsaturated store (Schellekens, 2018)

Essentially the remaining evaporation demand is split between evaporation of open water and the soil. The former is subtracted from the water that enters the kinematic wave.

The capillary rise is calculated using several steps.

1. K_{sat} at water table z_i is determined
2. Potential capillary rise is determined from: the minimum of K_{sat}, the actual transpiration taken from the unsaturated store, the available water in the saturated store, and the deficit in the unsaturated store
3. The potential rise is scaled using the distance between the roots and the water table using:

$$CS = CSF/(CSF + z_i - RT) \tag{D.15}$$

where CS is a scaling factor for the potential rise, CSF is a model parameter and RT represents the rooting depth.

When the roots reach the water table, CS is set to zero, thereby assuming there is no capillary rise. Water in the saturated store is transferred laterally along the DEM. SUrplus water is added to the kinematic wave, elaborated on in the next section.

E

Look-up tables Wflow

E.1. The rainfall-interception process

E.1.1. Landcovers and their associated Sl values

Table E.1: Different landcover types and their associated Sl values (Pitman and Pitman, 1986; Liu et al., 2012)

Landtype	Specific Leaf Storage, Sl
Water	0
Evergreen needle leaf forest	0.045
Evergreen broadleaf forest	0.036
Deciduous needle leaf forest	0.045
Deciduous broadleaf forest	0.036
Mixed forests	0.03926
Closed shrublands	0.07
Open shrublands	0.07
Woody Savannas	0.07
Savannas	0.09
Grasslands	0.1272
Permanent wetland	0.1272
Croplands	0.1272
Urban/ Built-up	0.04
Cropland/ Natural vegetation mosaic	0.1272
Barren/ Sparsely vegetated	0.04
Snow/Ice	0

E.1.2. Landcovers and their associated $C_{max(wood)}$ values

Table E.2: Different land cover types and their associated $C_{max(wood)}$ values

Landtype	$C_{max(wood)}$
Water	0
Evergreen needle leaf forest	0.5
Evergreen broadleaf forest	0.5
Deciduous needle leaf forest	0.5
Deciduous broadleaf forest	0.5
Mixed forests	0.5
Closed shrublands	0.2
Open shrublands	0.1
Woody Savannas	0.2
Savannas	0.01
Grasslands	0
Permanent wetland	0.01
Croplands	0
Urban/ Built-up	0.01
Cropland/ Natural vegetation mosaic	0.01
Barren/ Sparsely vegetated	0.04
Snow/Ice	0

E.1.3. Landcovers and their associated k values

Table E.3: Different land cover types and their associated k values

Landtype	k
Water	0.7
Evergreen needle leaf forest	0.8
Evergreen broadleaf forest	0.8
Deciduous needle leaf forest	0.8
Deciduous broadleaf forest	0.8
Mixed forests	0.8
Closed shrublands	0.6
Open shrublands	0.6
Woody Savannas	0.6
Savannas	0.6
Grasslands	0.6
Permanent wetland	0.6
Croplands	0.6
Urban/ Built-up	0.6
Cropland/ Natural vegetation mosaic	0.6
Barren/ Sparsely vegetated	0.6
Snow/Ice	0.6

E.1.4. Manning coefficients from literature

Table E.4: Manning's roughness coefficients for main channels and floodplains (Chow, 1959)

Type of channel and description		Manning coefficient		
		Minimum	Normal	Maximum
1. Main channels				
A. Clean, straight, full stage, no rifts or deep pools		0.025	0.030	0.033
B. Same as above, but with more stones and weeds		0.030	0.035	0.040
C. Clean, winding, some pools and shoals		0.033	0.040	0.045
D. Same as above, but with some stones and weeds		0.035	0.045	0.050
E. Same as above, but with lower stages, more ineffective slopes and sections		0.040	0.048	0.055
F. Same as D, but with more stones		0.045	0.050	0.060
G. Sluggish reaches, weedy, with deep pools		0.050	0.070	0.080
H. Very weedy reaches, deep pools, floodways with heavy stand of timber and underbrush		0.075	0.100	0.150
2. Mountain streams, no vegetation in channel, banks usually steep, trees and brush along banks submerged at high stages				
A. Bottom: gravels, cobbles, and few boulders		0.030	0.040	0.050
B. Bottom: cobbles with large boulders		0.040	0.050	0.070
3.Floodplains				
A. Pasture, no brush	(i) Short grass	0.025	0.030	0.035
	(ii) High grass	0.030	0.035	0.050
B. Cultivated areas	(i) No crop	0.020	0.030	0.040
	(ii) Mature row crops	0.025	0.035	0.045
	(iii) Mature field crops	0.030	0.040	0.050
C. Brush	(i) Scattered brush, heavy weeds	0.035	0.050	0.070
	(ii) Light brush and trees in winter	0.035	0.050	0.060
	(iii) Light brush and trees in summer	0.040	0.060	0.080
	(iv) Medium to dense brush in winter	0.045	0.070	0.110
	(v) Medium to dense brush in summer	0.070	0.100	0.160
D. Trees	(i) Dense straight willows in summer	0.110	0.150	0.200
	(ii) Cleared land with tree stumps, no sprouts	0.030	0.040	0.050
	(iii) Same as above, but with heavy growth of sprouts	0.050	0.060	0.080
	(iv) Heavy stand of timber, few trees, little undergrowth, flood stage below branches	0.080	0.100	0.120
	(v) Same as above, with flood stage reaching branches	0.100	0.120	0.160

F

Fieldwork results

F.1. Infiltation

F.1.1. Myitnge

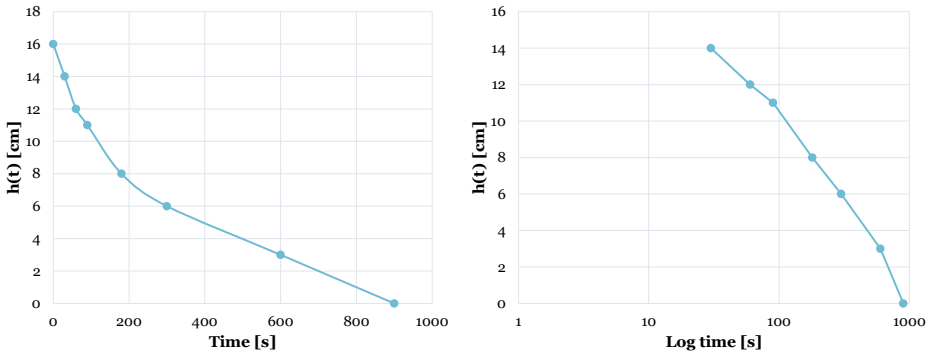

(a) Infiltration croplands in floodplains (location 1) Myitnge basin

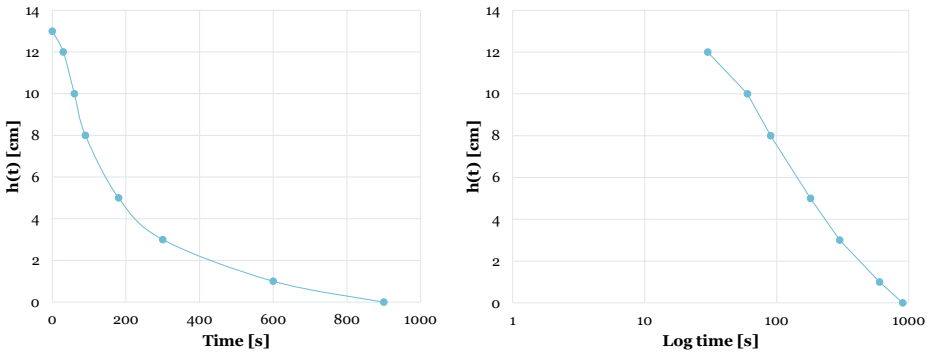

(b) Infiltration croplands in floodplains (location 2) Myitnge basin

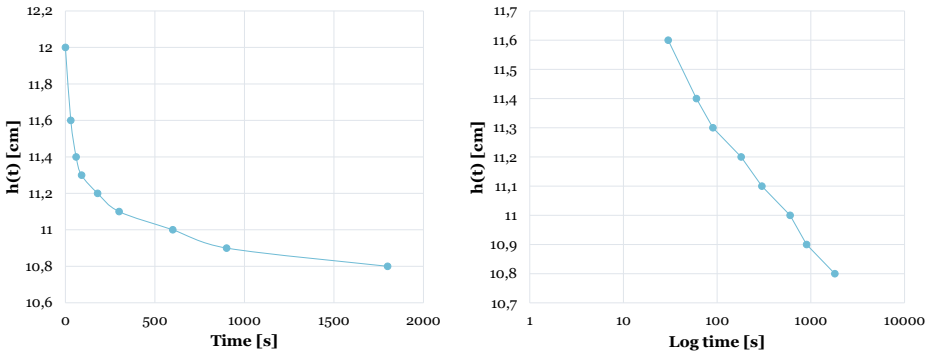

(c) Infiltration croplands on alluvial terrace (location 3) Myitnge basin

Figure F.1: Infiltration experiments croplands Myitnge

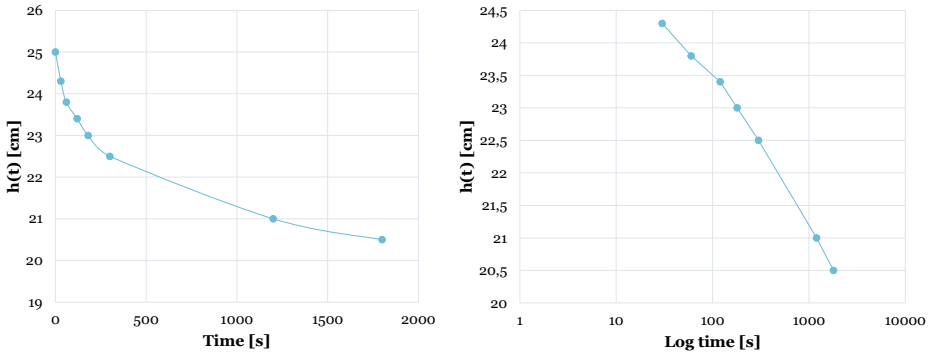

(a) Infiltration mixed forest (location 4) Myitnge basin

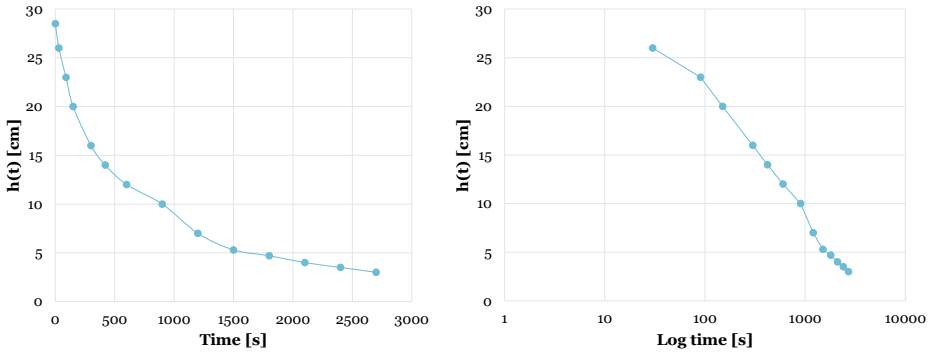

(b) Infiltration deciduous forest (location 5) Myitnge basin

Figure F.2: Infiltration experiments deciduous and mixed forest Myitnge

Table F.1: Saturated hydraulic conductivity K_s per field location in the Myitnge basin

Location	**Landcover**	K_s **[cm/s]**
1	Cropland (floodplain)	0,004774
2	Cropland (floodplain)	0,005695
3	Cropland (terrace)	0,000062
4	Mixed forest	0,000179
5	Deciduous forest	0,001390

These results are used to calibrate the model through the infiltration capacity. While the model used one value for the infiltration capacity by default, for this research a table is created that estimated the infiltration based on landcover.

F.1.2. Myittha

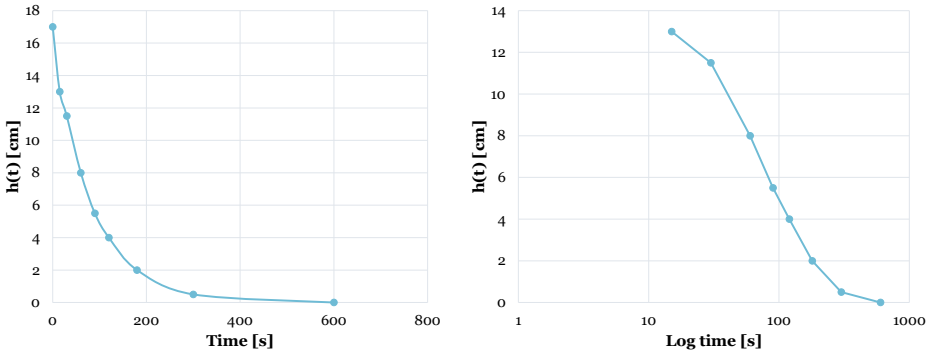

(a) Infiltration deciduous forest (location 1) Myittha basin

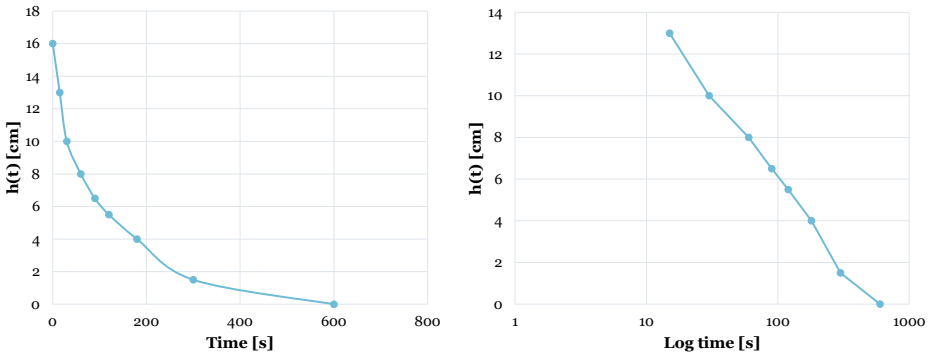

(b) Infiltration deciduous forest (location 2) Myittha basin

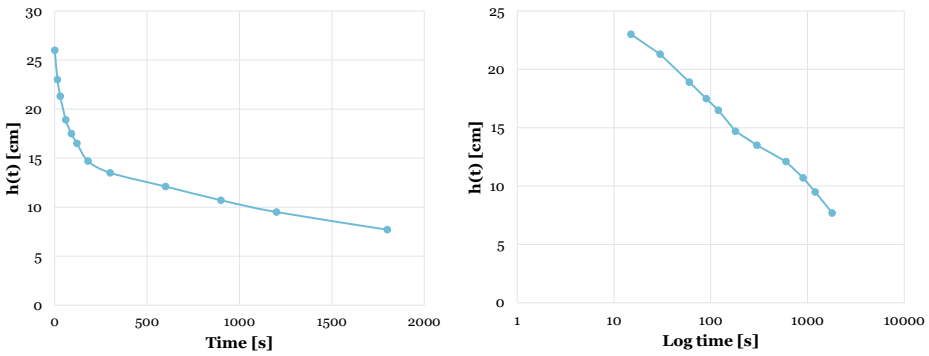

(c) Infiltration deciduous forest (location 3) Myittha basin

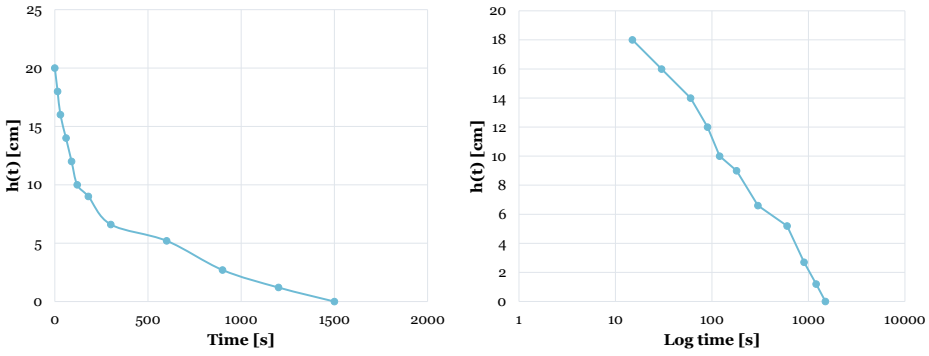

(d) Infiltration deciduous forest (location 4) Myittha basin

Figure F.3: Infiltration experiments deciduous forests Myittha

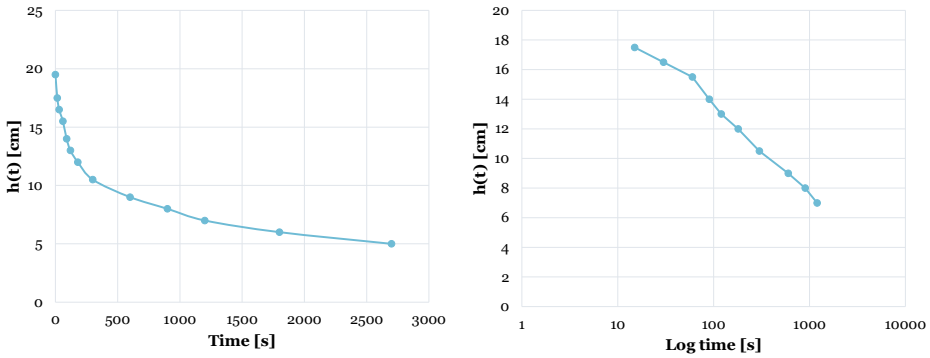

(a) Infiltration mixed forest (location 5) Myittha basin

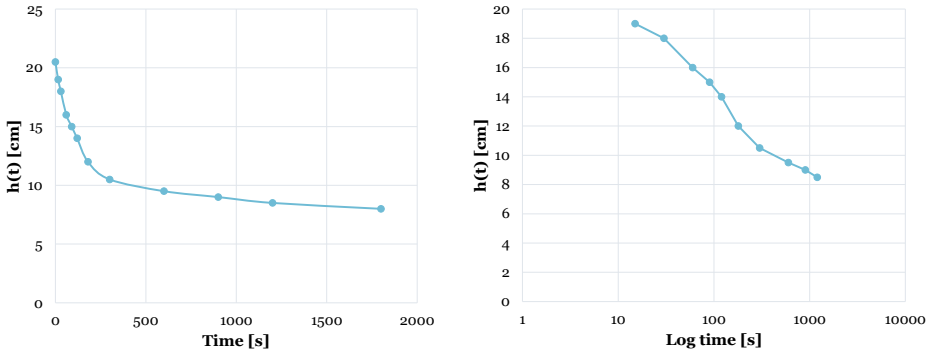

(b) Infiltration mixed forest (location 6) Myittha basin

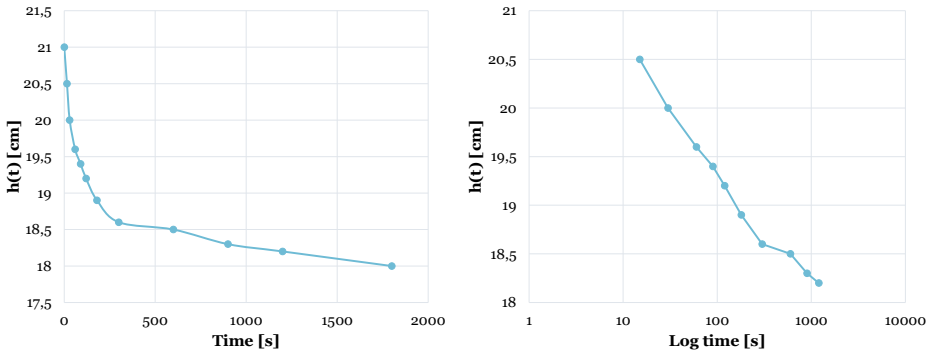

(c) Infiltration mixed forest (location 7) Myittha basin

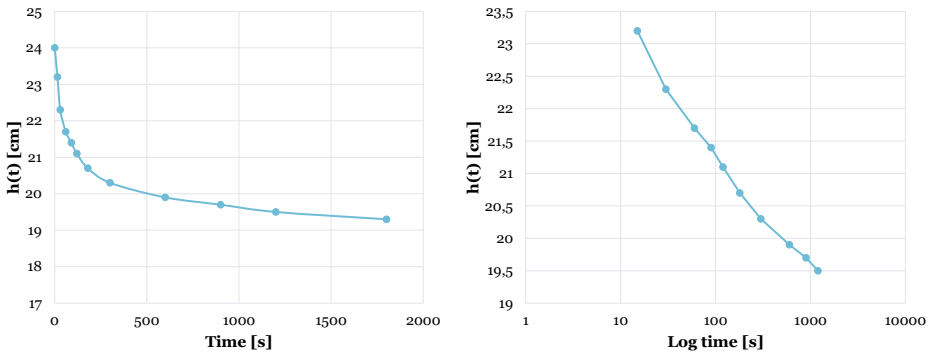

(d) Infiltration mixed forest (location 8) Myittha basin

Figure F.4: Infiltration experiments mixed forest Myittha

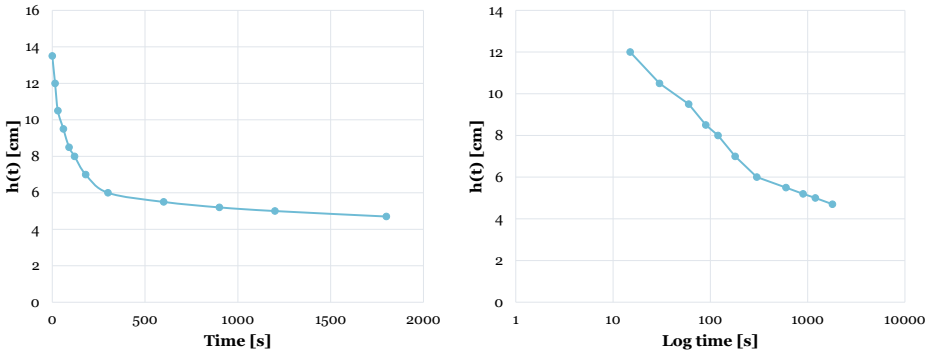

(a) Infiltration cropland (location 9) Myittha basin

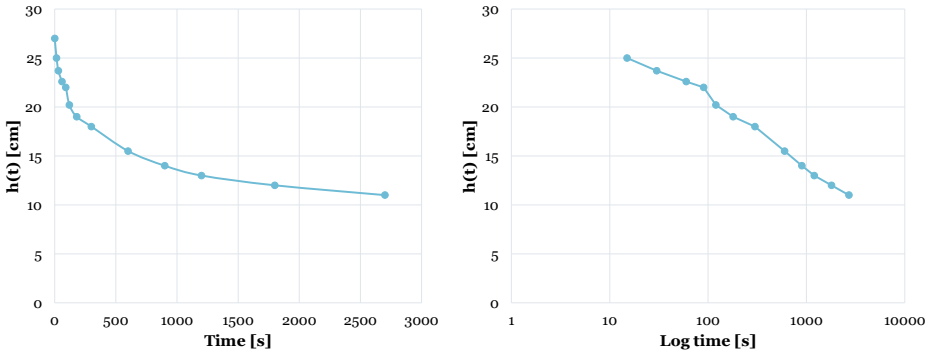

(b) Infiltration cropland (location 10) Myittha basin

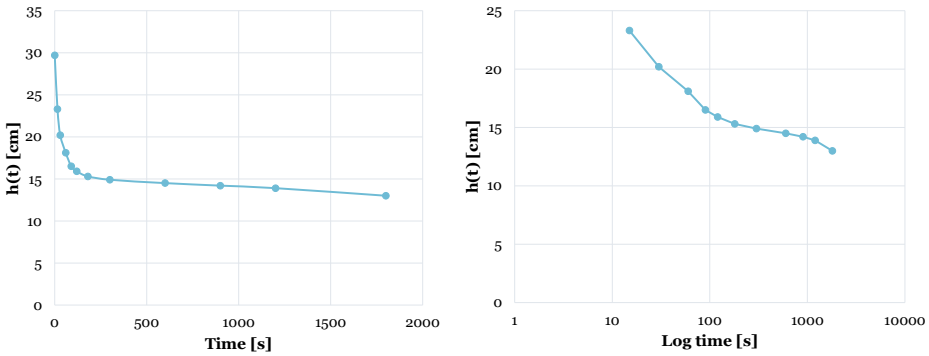

(c) Infiltration cropland (location 11) Myittha basin

Figure F.5: Infiltration experiments cropland Myittha

Table F.2: Saturated hydraulic conductivity K_s per field location in the Myittha basin

Location	Landcover	K_s [cm/s]
1	Deciduous forest	0,007348
2	Deciduous forest	0,006610
3	Deciduous forest	0,001021
4	Deciduous forest	0,002800
5	Mixed forest	0,000812
6	Mixed forest	0,000853
7	Mixed forest	0,000106
8	Mixed forest	0,000192
9	Cropland	0,000772
10	Cropland	0,000597
11	Cropland	0,000430

Again, these results are used to calibrate the model.

F.2. Sediment gradation

F.2.1. Myitnge

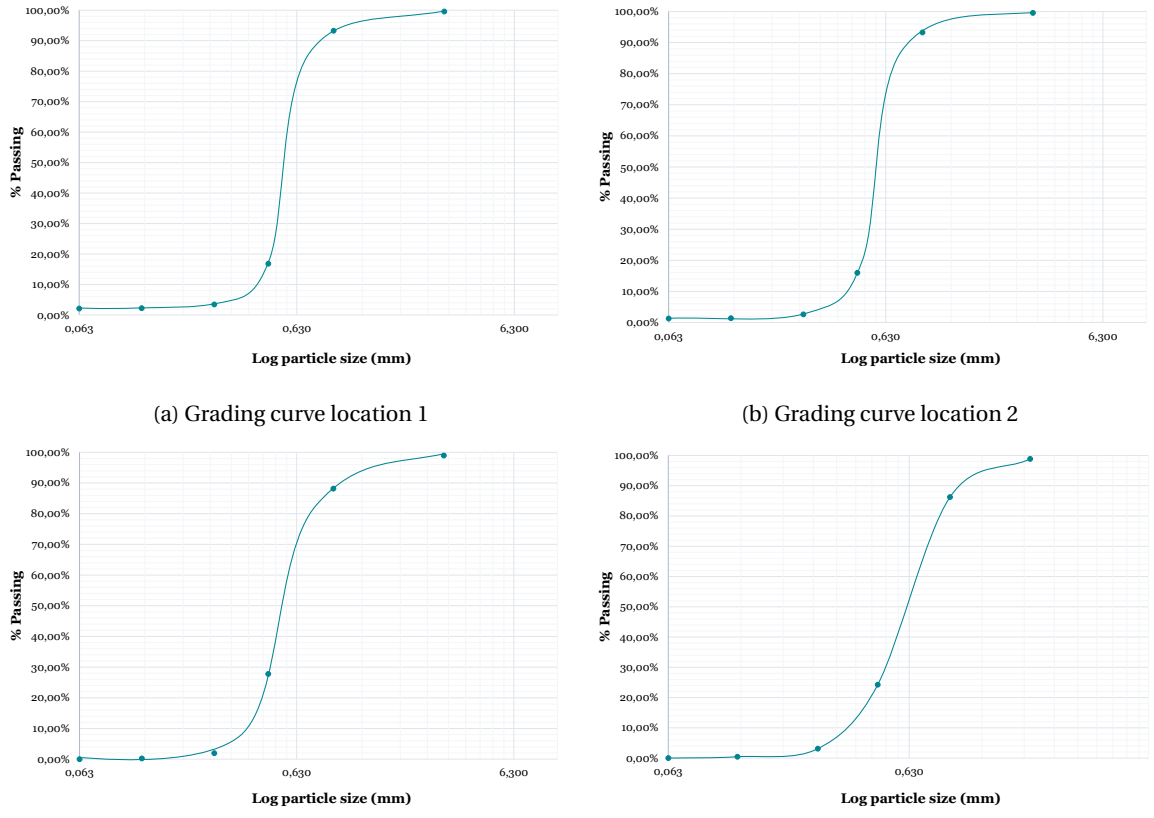

(a) Grading curve location 1

(b) Grading curve location 2

(c) Grading curve location 3

(d) Grading curve location 4

Figure F.6: Grading curves Myitnge

Figure F.6 shows that the soil samples taken from the Myitnge all seem uniformly graded. In other words, the particle-size distribution represents a type of soil in which most of the soil grains are the same size.

Table F.3: Diameter properties Myitnge sediment

Location ID	Type	Diameter (mm)				Uniformity coefficient	Gradation coefficient
		D90	D60	D30	D10		
1	Right bank	0.85	0.6	0.52	0.39	1.54	1.16
2	Right bank	0.85	0.6	0.51	0.4	1.50	1.08
3	Left bank	1	0.59	0.48	0.34	1.74	1.15
4	Left bank	1.3	0.66	0.51	0.34	1.94	1.16

F.2.2. Myittha

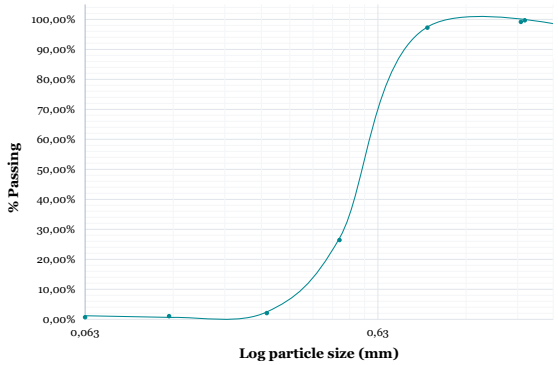

(a) Grading curve location 1

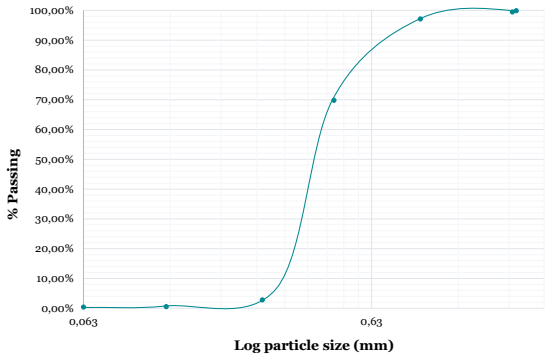

(b) Grading curve location 2

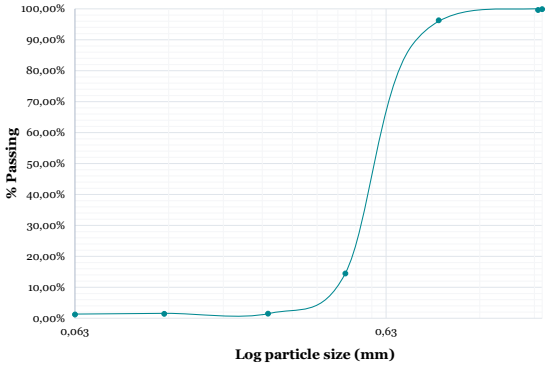

(c) Grading curve location 3

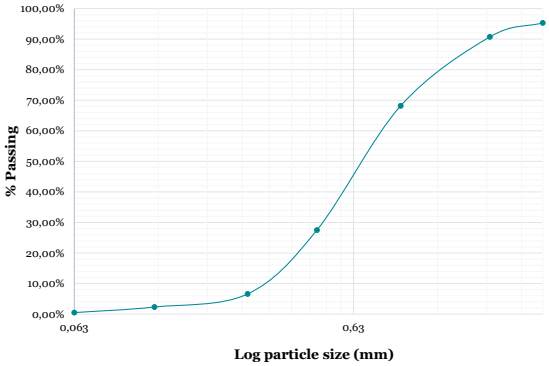

(d) Grading curve location 4

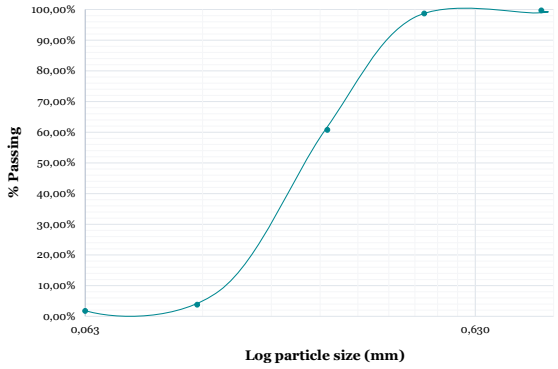

(e) Grading curve location 5

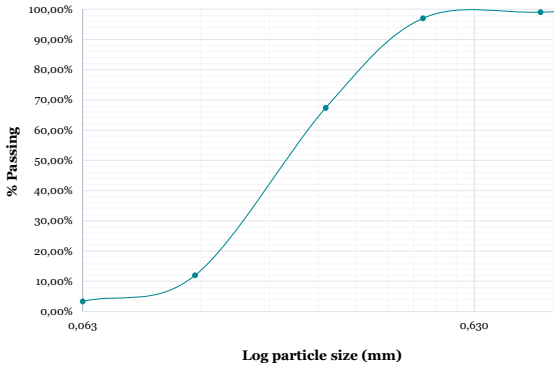

(f) Grading curve location 6

Figure F.7: Grading curves Myittha

Table F.4: Diameter properties Myittha sediment

Location ID	Type	Diameter (mm)				Uniformity coefficient	Gradation coefficient
		D90	D60	D30	D10		
1	Island	0.83	0.63	0.49	0.35	1.80	1.09
2	Right bank	0.69	0.42	0.33	0.29	1.45	0,89
3	Right bank	0.85	0.66	0.54	0.43	1.53	1.03
4	Left bank	1.9	0.78	0.48	0.3	2.60	0.98
5	Right bank	0.73	0.46	0.34	0.29	1.59	0.87
6	Right bank	0.73	0.42	0.32	0.25	1.68	0.98

G

Calibration and validation

G.1. Calibration Myitnge

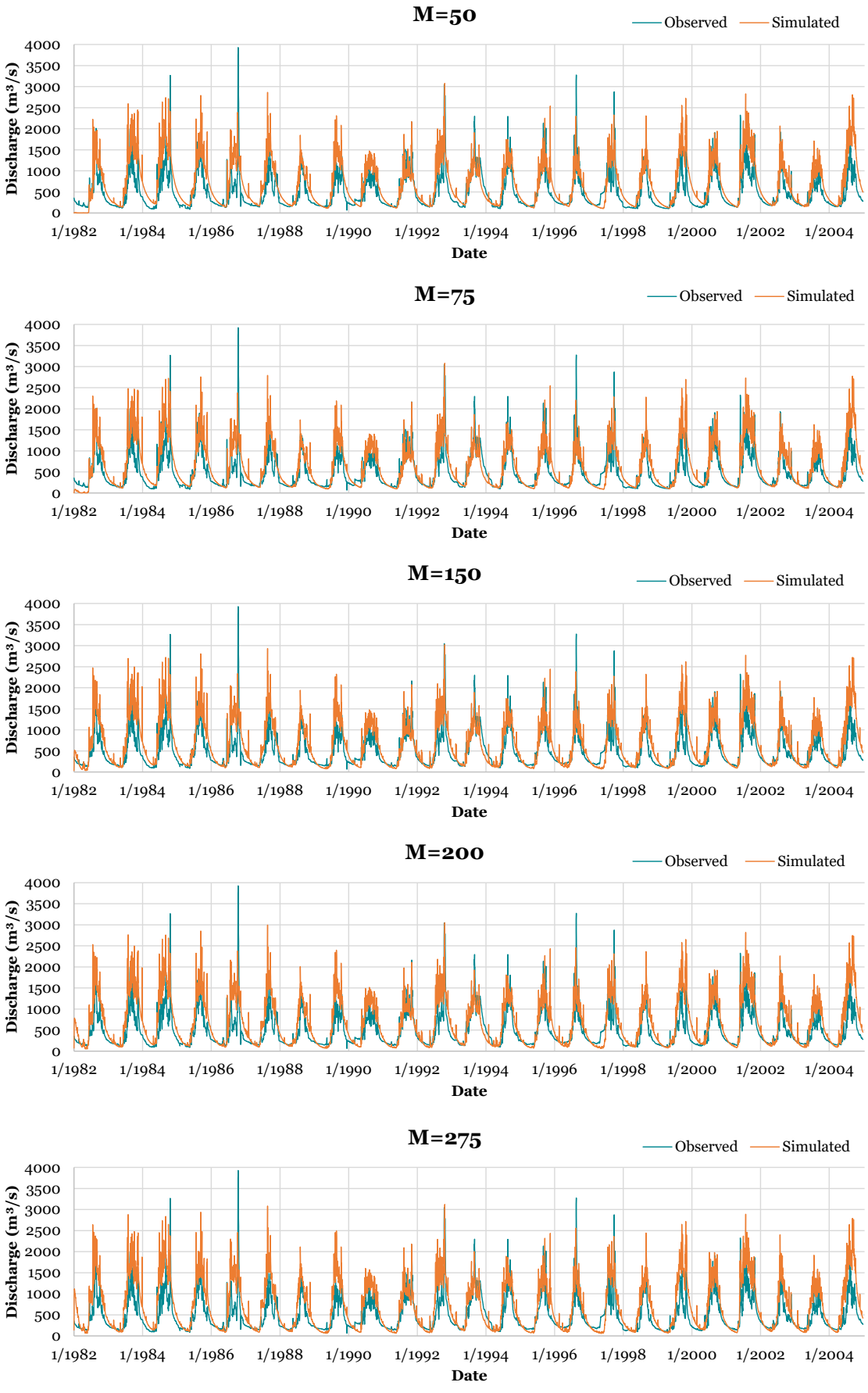

Figure G.1: Hydrographs for the calibration of the *M* parameter

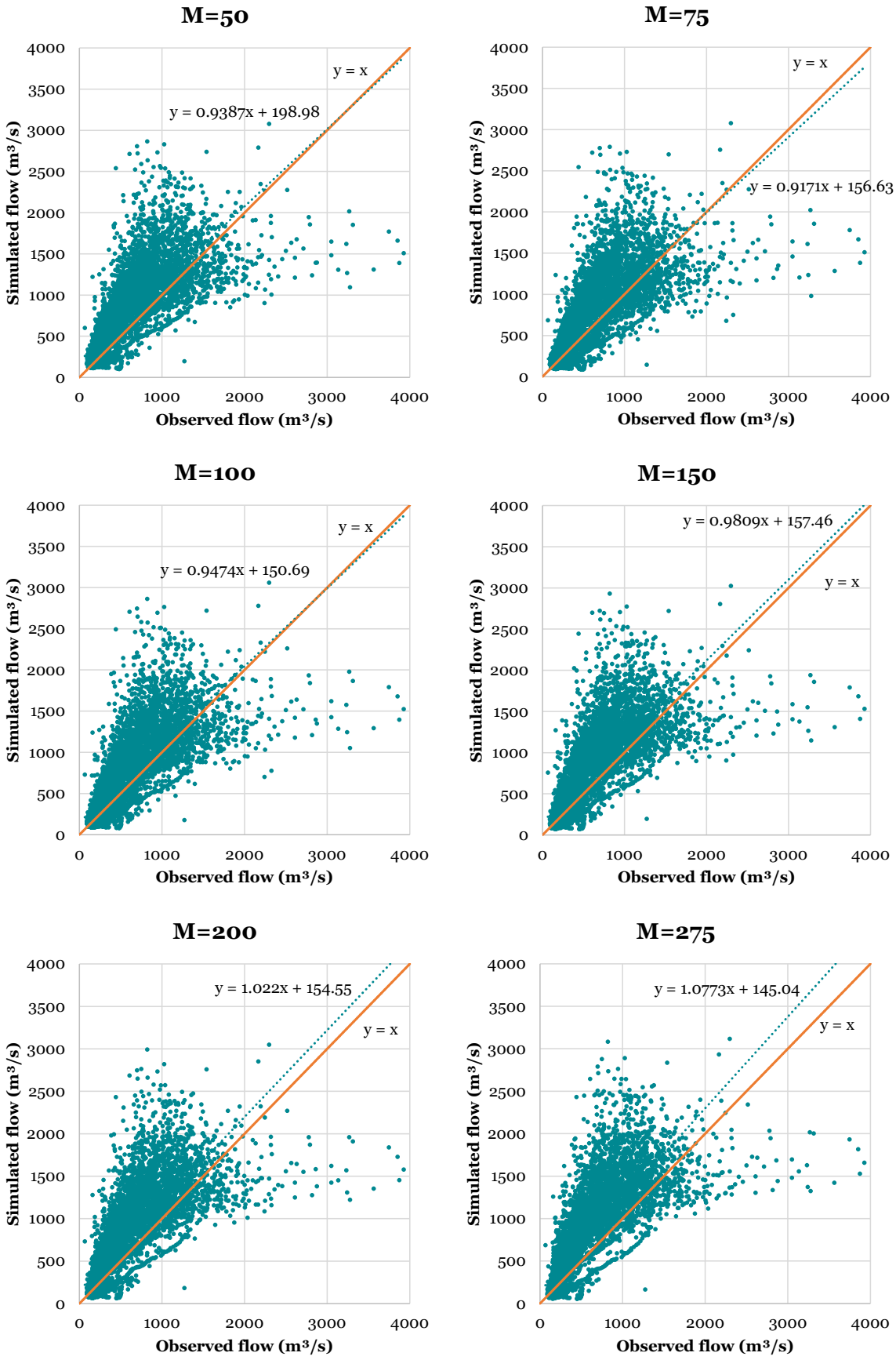

Figure G.2: Q-Q plots for the calibration of the *M* parameter

G.2. Calibration Myittha

centering

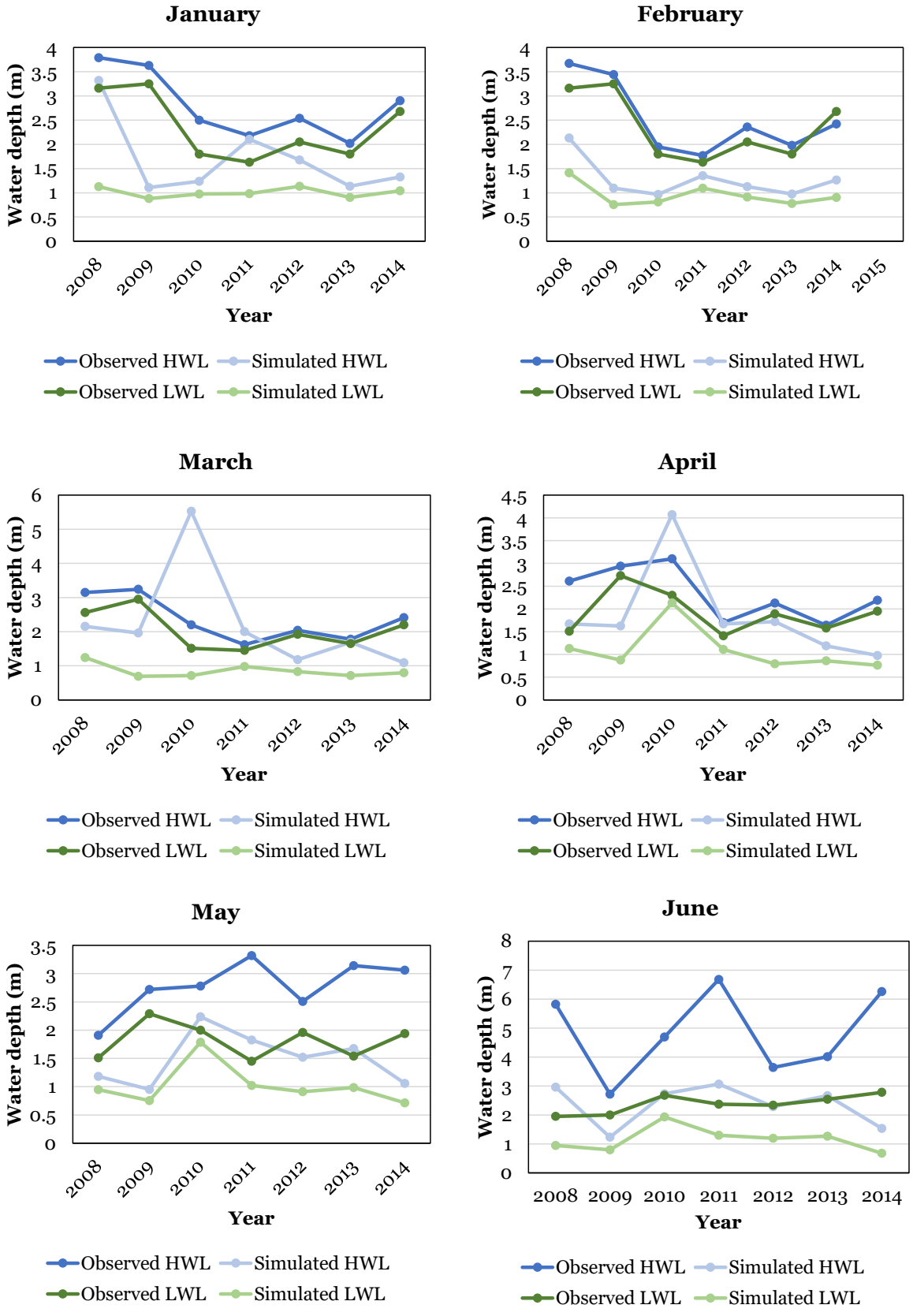

Figure G.3: Extreme water level simulations Myittha for alpha=120 (January - June)

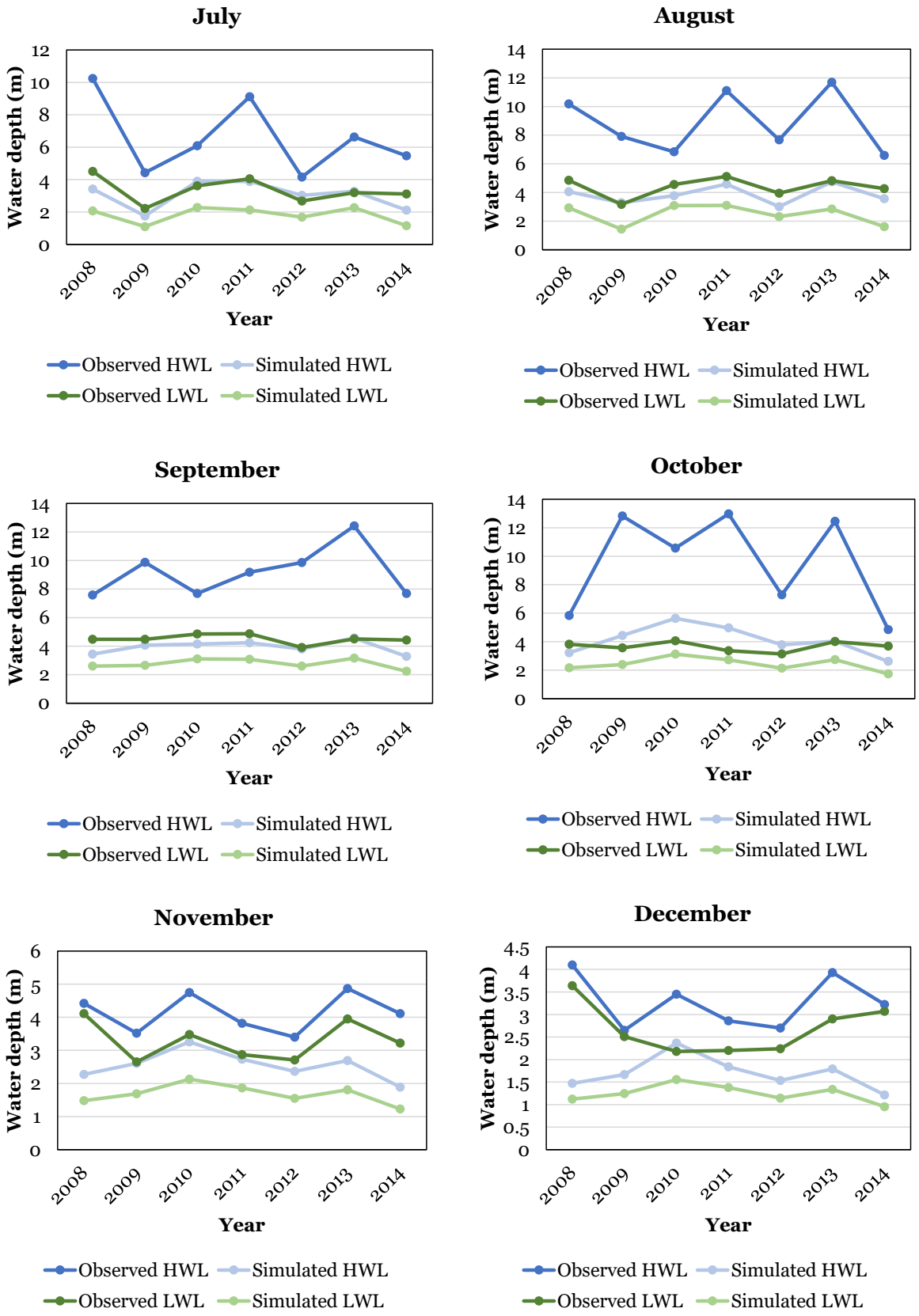

Figure G.4: Extreme water level simulations Myittha for alpha=120 (July - December)

H

Macroinvertebrates

H.1. Results of biomonitoring

River	Up/ downstream	Location	Date	Abundance		Taxa		Avg abundance		Avg taxa		Abundance	Taxa
				All	EPTO	All	EPTO	All	EPTO	All	EPTO	%EPTO	%EPTO
Myitnge	Upstream	1	nov-2016	107	101	15	11	89	84	11	9	95%	77%
	Upstream	2	nov-2016	70	67	7	6						
	Downstream	1	nov-2016	67	55	9	4	250	188	11	5	75%	48%
	Downstream	2	nov-2016	432	320	12	6						
Myitnge	Upstream	1	feb-2017	766	702	25	18	558	519	23	17	93%	73%
	Upstream	2	feb-2017	349	335	20	15						
	Downstream	1	feb-2017	171	24	14	5	476	376	16	8	79%	50%
	Downstream	2	feb-2017	781	728	18	11						
Shan	Upstream	1	dec-2016	228	227	20	19	228	227	20	19	100%	95%
	Downstream	1	dec-2016	53	52	10	9	89	88	12	11	99%	92%
	Downstream	2	dec-2016	125	124	14	13						
Shan	Upstream	1	mar-2017	431	423	30	23	431	423	30	23	98%	77%
	Downstream	1	mar-2017	33	31	7	6	260	244	14	12	94%	82%
	Downstream	2	mar-2017	487	457	21	17						

Figure H.1: Results of the biomonitoring during 2016-2017 on (tributaries of) the Myitnge river